Design and optimization of a modular prestressed relieving platform for deep-sea quay walls

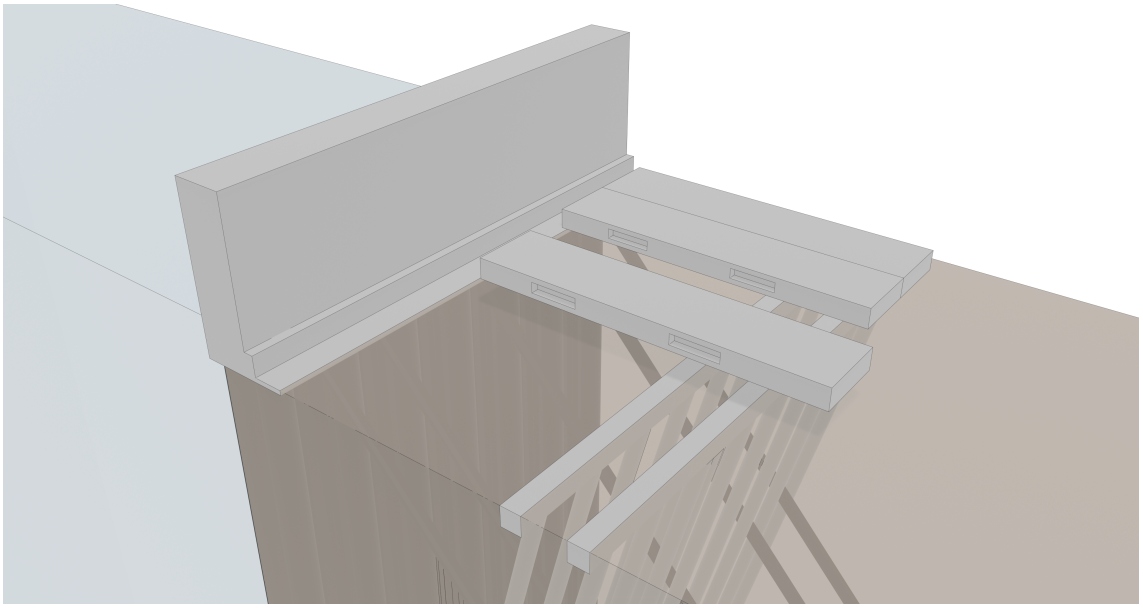

MSc Thesis

Liam Kokken

TU Delft

Royal HaskoningDHV
Enhancing Society Together

Port of Rotterdam

Design and optimization of a modular prestressed relieving platform for deep-sea quay walls

A study on the design of a prestressed, modular relieving platform for deep-sea quay walls, offering a lower-carbon and upgradeable alternative.

by

W.M.C. Kokken

to obtain the degree of Master of Science
in Civil Engineering

at the Delft University of Technology,
faculty of Civil Engineering and Geosciences,
to be defended publicly on Tuesday May 27, 2025.

Student number	5653134	
Date	20-05-2025	
Thesis committee	dr. S.C.B. Nunes	TU Delft, chair
	dr. ir. P.C.J. Hoogenboom	TU Delft, supervisor
	ir. C.M.P. 't Hart	Royal HaskoningDHV
	ir. D.T. Haarsma	Royal HaskoningDHV
	ir. W. Gall	Port of Rotterdam

Preface

This thesis concludes the Master's degree Civil Engineering at the Technische Universiteit Delft. In collaboration with Royal HaskoningDHV and the Port of Rotterdam, I investigated the possibilities of developing a prestressed and modular design for the relieving platform of deep-sea quay walls. The goal was to reduce material usage and enable an upgradeable quay wall. I would like to express my gratitude to everyone who helped me in completing my Master's Thesis over the past year.

First I want to thank my university supervisors Dr. Sandra Nunes and Dr. ir. Pierre Hoogenboom for their time, feedback and overall help with my master's thesis. Their insights into the theoretical aspects of prestressing and mechanics, along with their constructive feedback on the report, greatly contributed to the results of this thesis.

In addition, I would like to thank Royal HaskoningDHV and the Port of Rotterdam for the opportunity to work on this project, for the many valuable experiences I gained - from site visits to Christmas diners - and for sharing their extensive knowledge. In particular, I would like to thank my daily supervisors Marcel 't Hart and Douwe Haarsma from Royal Haskoning, for their time, patience and feedback that greatly contributed to my thesis from whom I have learned a great deal over the past year. And I want to thank Willem Gall from the Port of Rotterdam for his support, time and expertise regarding the specific complexities of port infrastructure.

Lastly, I would like to thank my family, friends and girlfriend for their support over the past year, without which I could not have completed this thesis and my master's degree.

Thank you!

Liam Kokken,
Delft, May 2025

Abstract

This thesis presents a prestressed and modular design for relieving platforms in deep-sea quay walls that reduces concrete usage, thereby lowering carbon emissions, and enabling future upgrades.

About 37% of the world's CO_2 emissions come from the built environment, making it a significant contributor. To address these issues the Port of Rotterdam has set sustainability goals, which include becoming climate neutral by the year 2050 and reducing CO_2 emissions from material consumption by 25% by the year 2030. This thesis has contributed to these goals by designing and optimizing a modular prestressed relieving platform for deep-sea quay walls, that has reduced material usage and carbon emissions. The focus lied on the relieving platform floor, creating a flexible and upgradable quay wall structure.

The application of post-tensioning has been investigated in the design of the relieving platform. Several different prestressing variants have been designed, parameterized and later optimized. In addition a parametric cross-section optimization has been performed by creating an opening around the neutral axis, that further reduced the concrete usage in the floor. A final design of the relieving platform floor using a total prestressing tendon area of 4.500 mm^2 per meter resulted in a minimum cross-section height of 890 mm and an embodied carbon reduction of 20%.

A prefabricated, modular solution has been designed that enables the upgrade of a quay wall structure by allowing for the relieving platform floor to be added at a later stage. The building sequence has been designed with a focus on efficiency. The modular design benefited from the weight reduction of 50% that resulted from the application of prestressing. Three main connections have been designed, for which several solutions have been proposed, namely: the module-to-module connection, the module-to-wall connection and the module-to-foundation pile connection. Particular attention is given to the placement of the prestressing anchor on the water side of the relieving platform, for which two alternative solutions have been proposed.

The findings of this thesis show that prestressing can play an important role in creating lightweight, lower-carbon and modular relieving platforms for deep-sea quay walls. It has allowed for a significant material reduction, crack control and weight reduction, facilitating the prefabrication of the floor. This design offers a flexible, upgradeable and lightweight alternative to traditional the relieving platform design.

Contents

Preface **iii**

Abstract **iv**

1 Introduction **1**
1.1 Project motivation . . . 1
1.2 Design objectives . . . 3
1.3 Scope . . . 4

2 Theoretical background **6**
2.1 Carbon emissions . . . 6
2.2 Quay walls . . . 6
2.3 Prestressing . . . 10
2.4 Prefabricated and modular design . . . 12

3 Methods **18**
3.1 Analytical model . . . 18
3.2 Cross-section resistance . . . 19
3.3 Carbon emissions . . . 23

4 Analysis of the SIF2 quay wall **26**
4.1 System analysis . . . 26
4.2 Quay wall design . . . 27
4.3 Analytical model . . . 37
4.4 Results . . . 39
4.5 Verification . . . 42

5 Prestressing **44**
5.1 Design . . . 44
5.2 Initial design variants . . . 47
5.3 Discussion . . . 53

6 Optimization **54**
6.1 Description . . . 54
6.2 Height reduction . . . 55
6.3 Height reduction: Increased shear resistance . . . 64
6.4 Cross-section . . . 68

7 Modular design **75**
7.1 Design . . . 75
7.2 Connections . . . 76
7.3 Building sequence . . . 82

8 Discussion **84**

9 Conclusion and recommendations **87**
9.1 Conclusion . . . 87
9.2 Recommendations . . . 89

References **91**

A Spring stiffness values **96**

B Analytical load cases **97**
B.1 Load cases . . . 97
B.2 Load combinations . . . 108

C Analytical results **112**
C.1 Load cases . . . 112
C.2 Resulting governing moments . . . 129
C.3 Resulting governing shear . . . 133

D Prestressing **137**
D.1 Initial prestressing variants . . . 137
D.2 Prestressing Property Calculations . . . 137

E Scripts **140**
E.1 Python: Initial analysis . . . 141
E.2 Maple: Moment resistance module . . . 144
E.3 Maple: Shear resistance module . . . 146
E.4 Maple: Crack width module . . . 147
E.5 Maple: Reinforcement properties module . . . 149
E.6 Maple: Solve ODE module . . . 150
E.7 Maple: Main Optimization module . . . 151
E.8 Maple: SLS compression zone height calculation - Rectangular cross-section 156
E.9 Maple: SLS compression zone height calculation - Cross-section opening . . 157
E.10 Maple: Tendon layout parameterization - Var 1/2 . . . 158
E.11 Maple: Tendon layout parameterization - Var 3 . . . 165

F Carbon calculations **171**
F.1 Carbon calculations . . . 171

G Verifications **179**
G.1 Model verification . . . 179
G.2 Resistance check modules . . . 184

H Calculations **195**
H.1 Chapter 4: Analytical results . . . 195
H.2 Chapter 6: Optimized results . . . 202
H.3 Chapter 8: Discussion . . . 223

1 Introduction

1.1 Project motivation

1.1.1 Quay walls

In recent decades, the urgency of reducing humanity's environmental impact has become increasingly clear. The built environment is a sector that is responsible for a large part of global emissions. It accounts for approximately 37% of the total CO_2 emissions (UN, 2024). This sector thus plays a key role in the transition to carbon neutrality. Carbon neutral means not contributing to the increase of greenhouse gasses in the atmosphere. The Port of Rotterdam has therefore set climate goals for the coming decades (Port of Rotterdam, 2022), one of which is to become climate neutral by the year 2050. One of the sub-goals is to lower the CO_2 emissions from material consumption for civil engineering projects by 25% by the year 2030. One of the main structures of these civil engineering projects being the quay walls.

Quay walls are an essential component of every port. A quay wall is an earth retaining structure that forms the transition between land and water. Its functions are to support the weight of soil and all facilities on land, and to facilitate the berthing of ships. The Port of Rotterdam is the largest port in Europe and one of the largest in the world. The high demand asks for the constant need for development and innovation. The most recent expansion of the port is the Maasvlakte 2, which is expected to be finished around the year 2035 (Figure 1).



Figure 1: Maasvlakte 2 (Source: Danny Cornelissen, PoR)

Quay walls in this new part of the port are relatively deep and robust in order to facilitate the largest ships currently in existence and ensuring the port remains future proof. There are many types of quay walls used in different ports across the world depending on their specific environment and requirements. This thesis will look into one specific quay wall type: a sheet pile wall with a relieving platform (Figure 2). These types of quay walls have four main components: a combi-wall consisting of steel sheets and piles, the anchors, the relieving platform and the foundation piles. The deeper a quay wall becomes and the heavier the imposed loads become the higher the horizontal loads on the wall will be. When the loads become too large it is no longer economically viable or even possible to keep increasing the combi-wall's cross-section to resist these loads. A solution to this lies in the addition of a relieving platform. A relieving platform reduces the amount of horizontal loads on the combi-wall, by transferring the loads directly into the subsoil. This is an effective solution which reduces the required cross-section thickness of the wall. The

downside however, is that these platforms require large amounts of concrete and reinforcement steel which significantly increases the CO_2 footprint of the structure. As can be seen in Figure 2 the relieving platform accounts for approximately half of the total CO_2 footprint of the quay wall. These high emissions will need to be reduced in order for the Port of Rotterdam to reach their goals of carbon neutrality.

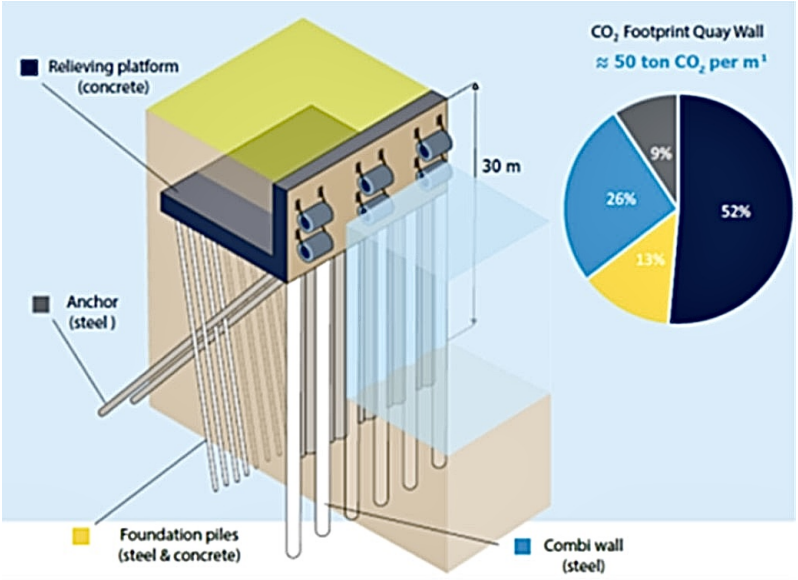

Figure 2: Quay wall footprint (Source: PoR)

1.1.2 Prestressing

A potential solution lies in the application of prestressing. Prestressing is a construction method that precompresses the concrete by placing tensioned steel rods or strands (tendons) in concrete elements. The compressive stress counteracts the effects of the tensile stresses in the concrete caused by for example bending moments. Concrete is particularly weak in tension, eventually leading to cracking. Prestressing therefore enhances the strength and durability of the concrete element, in turn allowing for more slender elements and consequently a reduction of concrete. This reduction will also lower the embodied carbon of the relieving platform and the quay wall. The downside however, is that it is often more expensive and complex than traditional reinforcement methods, and that the prestressing steel itself will also add to the embodied carbon. This trade-off has not yet been investigated for relieving platforms of deep sea quay walls. Prestressing has been widely applied in other fields within civil engineering however. For example in bridges and viaducts it has shown that the trade-off can be well worth it by creating more slender structures.

1.1.3 Prefabricated and modular design

Quay walls are build with a high level of strength to accommodate potential future changes, ensuring a future proof design. The typical technical lifespan of these types of structures is up to a 100 years. De Gijt & Toorn (2009) mentioned that the economical lifetime of a quay wall is however not necessarily the same as the technical and can often be much less. For this reason, investments in more flexible and future-proof structures may enable multiple economic lifetimes within the quay's technical lifespan. Zwakhals et al. (2012) has also emphasized the need for flexibility due to the many uncertainties in the future such as bigger ships, changing clients, changing legislation and changing technology. Zwakhals et al. (2012) defines flexibility as a system that can respond to changing conditions. Two types are distinct, namely passive and active flexibility. Passive refers to the attributes

that facilitate reuse without adaptation. Active refers to facilitating reuse with adaptation. Currently ensuring flexible and future proof designs for quay wall structures generally falls in the first category, namely passive flexibility. Quay walls are often overdimensioned, meaning they are designed with a higher capacity than is required to account for any future changes. However, incorporating active flexibility into the design could contribute to the sustainability goals and could reduce costs. Making the design upgradable prevents the need for overdimensioning of the quay wall, reducing material usage.

A method of creating a flexible, upgradable design is by the use of prefabricated and modular elements. Prefabricated means that the structural elements are fabricated in for example a factory instead of on-site. Modular refers to designing these prefabricated elements as standardized components, or modules, which can improve the efficiency of the construction process. Martins et al. (2023), Chippagiri et al. (2022) and Lan (2025) all mentioned an increased construction speed when using prefabricated construction methods compared to traditional construction methods. The prefabricated elements could reduce the downtime of the quay wall during the upgrade, which is an important consideration given that during the downtime the quay cannot be used which increases the costs.

1.2 Design objectives

Summarizing the problem, it can be said that:

- Human induced carbon emissions have caused a negative impact on the climate and pose a threat to many regions across the world. The built environment has a large contribution to these global emissions.
- Current relieving platforms in deep-sea quay walls are built using large amounts of reinforced concrete which cause significant carbon emissions.
- Quay walls are built for long life spans, but have the risk of becoming obsolete if future changes are not property taken into account. This often requires overdimensioning of the quay wall structures.

The main objectives of this thesis are:

- Investigating the application of prestressing in the floor of a relieving platform, with the aim of reducing material usage and carbon emissions.
- Designing an upgradable prefabricated and modular relieving platform, improving the flexibility of the quay wall.

The sub-objectives to achieve this are:

- Analyze the current quay wall structure.
- Creating and optimizing a prestressed design of the relieving platform floor.
- Exploring the connections required for the modular design.
- Create a construction sequence using the modular design, that allows for the later application of the floor of the relieving platform to the structure.

1.3 Scope

This thesis has focused on developing a modular design of the floor of a prestressed relieving platform for deep sea quay walls. The SIF2 quay wall in the Port of Rotterdam has been taken as a reference case for which the relieving platform has been redesigned. The design of all the other components of a quay wall are outside the scope of this thesis, which are the elements such as the combi wall, foundation piles and anchors. The general design includes the dimensions and cross-section of the relieving platform, the materials used, the reinforcement and prestressing layout and the modular design. The focus lies on developing an upgradable relieving platform, allowing for the addition of the floor at a later stage. For this reason the focus is on the floor and its connection to the wall. The wall itself has been for the most part be left outside of the scope of the thesis.

Prestressing

There are several parts that have been designed for a prestressed concrete element. Those that will be addressed in this thesis are:

- Determining the requirements for a post-tensioned, partially prestressed structure.
- Calculating the prestressing force required, resulting in the diameter and amount of strands needed to achieve this.
- Designing the tendon layout (eccentricities, drape and curvature), the amount of tendons and the exact prestressing load that together determine the loads exerted on the concrete element.

For the other required aspects of a prestressed design that have not been taken into account assumptions have been made.

Calculations: Analytical

To determine the structural properties of the relieving platform, analytical calculations has been made. A simplified 2D model of the relieving platform has been made. Documentation of the original design and calculations of the SIF2 quay wall have been used as reference and guidance (Schouten & van der Valk (2020) and Roelevink (2020)). The analytical model aims to come as close as possible to the original results in order to verify its accuracy. These calculations have looked into the loads and internal forces on the structure and give an insight into the governing cross-sections and reaction forces. The analytical model has also been used, to calculate the effect of prestressing on the structure. ULS and SLS checks are performed in order to evaluate the design. The performed checks are further elaborated in section 3.2.

Optimization

A parametric optimization has been performed to determine the optimal prestressing configuration to achieve a maximum amount of CO_2 reduction. The optimization searched for most slender floor cross-section height, while iterating through different variants of the prestressing design. The end goal of the optimization is minimizing embodied carbon, while the ULS and SLS criteria are met.

Cross-section analysis

After the optimal prestressing design and the minimal cross-section height have been found, a further analysis into the cross-section design has been performed. This analysis looked into the possibility of removing material from the cross-section around the neutral axis, which does not contribute much to the resistance of the cross-section. The goal was

to further achieve both weight and carbon reduction by removing as much as possible concrete.

Prefabricated and modular design

For the prefabricated and modular platform design the production process and the assembly of the modules on-site have been described. An investigation into the connections of modular concrete structures has been performed and applied to the design of the relieving platform. The main components that need to be designed for the concrete modules include its main shape and dimensions, its weight, materials used and the connections between the modules.

2 Theoretical background

2.1 Carbon emissions

Carbon emissions in the built environment can typically be assigned to several stages: material production, construction, use-life and end-of-life. Concrete and in particular cement are large contributors to the global greenhouse gas emissions. Globally the production of cement emits approximately 1.6 million metric tons of CO_2 (Global Carbon Project, 2023), which is around 6% of the total CO_2 emissions. The most used type of cement globally is Ordinary Portland Cement (OPC). The majority of CO_2 emissions in cement manufacturing originate from the pyroprocessing stage, accounting for approximately 85% (Imbabi et al., 2012). Pyroprocessing is the process of heating the raw materials, the main ones being limestone and clay, to temperatures around 1400-1600°C. The emissions of the pyroprocessing are partly caused by the energy required to reach these high temperatures and partly by the calcination process (around 50%). For this last mentioned process it is somewhat more difficult to reduce the CO_2 emissions since they are inherent to the chemical process. Alternatives to this type of cement exist that have lower carbon emissions, such as for example geopolymer (Nodehi & Taghvaee, 2021). This is however outside of the problem statement and scope of this thesis. This thesis will focus on the reduction of the material usage in quay walls altogether.

There are different types of chemical compounds that have a negative impact on the environment and the global climate. To measure the total impact of these different chemicals on the environment the CO_2eq (CBS, 2019), or carbon dioxide equivalent, is used as a measurement. It is a measure of the contribution of each of the chemicals base on their Global Warming Potential (GWP), recalculated in terms of the GWP of CO_2. The embodied carbon of a structural element is the amount of CO_2eq that is released during its production and assembly. The emissions of materials are estimated and collected in databases by several research institutes. It is required to know the embodied carbon of all components of a structure to estimate its total carbon footprint.

2.2 Quay walls

2.2.1 Types of quay walls

Quay walls used today can be divided into four general types: gravity quay walls, pile supported quay walls, sheet pile quay walls and sheet pile quay walls with relieving platforms (De Gijt, 2010).

- *Gravity quay walls*: The vertical forces, weight of the structure and the stability of the wall are achieved by the bearing stratum using only compressive stresses and are directly transferred to the subsoil (Figure 3a).
- *Pile supported quay wall*: Generally used if the soil conditions are poor and/or reclamation is very expansive. The stability and strength is derived from the piles (Figure 3b).
- *Sheet pile wall*: The loads are transferred via sheet pile wall to the subsoil. Stability is achieved by fixing an anchor to the top of the wall and in the soil. The anchor can be horizontal or diagonally placed (Figure 3c).
- *Sheet pile wall with relieving platform*: The strength and stability of this type of quay wall are also provided by the sheet pile wall and anchor. The difference is that the vertical loads are now also transferred by the relieving platform to the sheet pile wall and the foundation piles. This reduces forces generated on the front wall (Figure 3d).

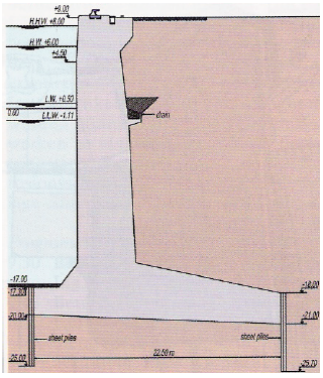

(a) Gravity quay wall (De Gijt, 2010)

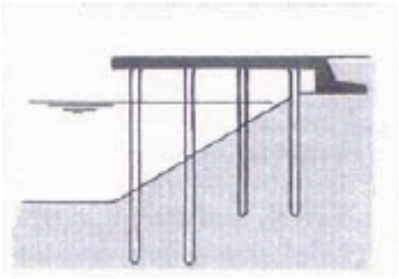

(b) Pile supported quay wall (De Gijt, 2010)

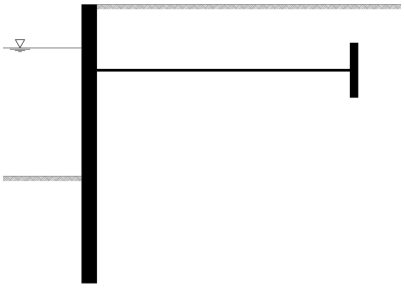

(c) Sheet pile wall

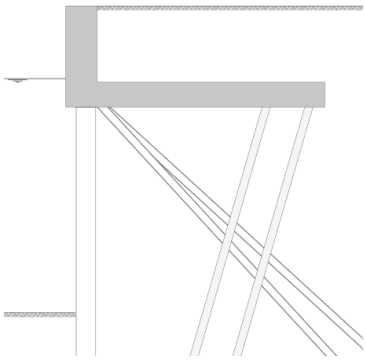

(d) Sheet pile wall with relieving platform

Figure 3: Quay wall general types

2.2.2 Combi-wall with relieving platform

The type of quay wall analyzed in this thesis is a combi-wall, which are metal piles together with a sheet wall, as main earth retaining structure and with a concrete L-shaped relieving platform. A general description of the components of this quay wall is given in Figure 4.

Combi wall

The combi wall is built up of long steel piles and steel sheets that are driven into the soil. The piles then transfer the loads into the subsoil. The combi wall functions as an earth retaining structure. Figure 5 shows an example of how the cross-section of a combi wall looks like. The higher the imposed loads and the deeper the wall becomes, the thicker the cross-section must be to resist the loads.

Anchorage

To help resist the horizontal forces and ensure stability anchorage is needed. Without anchorage, all the forces would need to be resisted by just the sheet pile wall and the resistance of the soil. These piles are diagonally driven into the soil and are connected to the relieving platform.

Relieving platform

A method of reducing the horizontal forces on the combi-wall is the use of a relieving platform. A relieving platform reduces the earth pressure on the wall by transferring the loads directly to the subsoil via foundation piles, as can be seen in Figure 4. The foundation piles are driven into the soil before the platform is cast. The deeper the relieving structure is placed, the more soil weight it will also carry. Currently these relieving platforms are

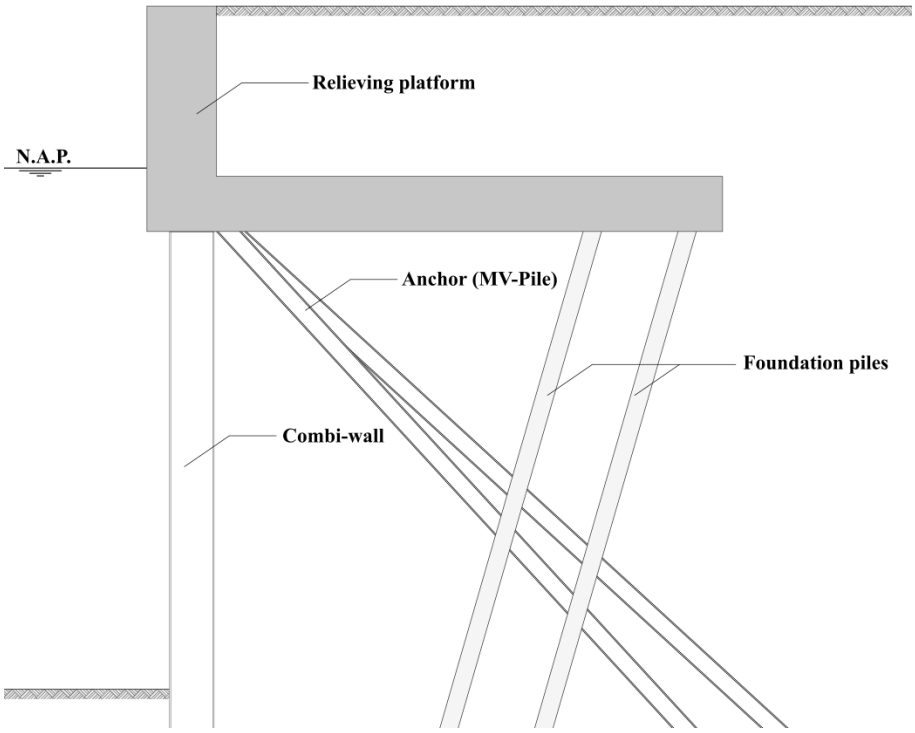

Figure 4: General design quay wall with relieving platform

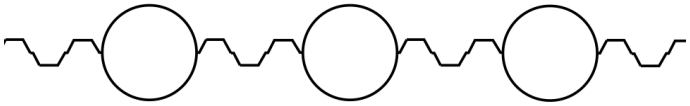

Figure 5: Combi wall cross-section example (adapted from Roelevink (2020))

constructed as reinforced cast-in-place concrete structures using large amounts of concrete and reinforcement steel. This is not desirable in terms of CO_2 emission reduction.

2.2.3 Loads on a quay wall

The main loads that act on this type of quay wall are listed below. It is of course not the task of the relieving platform alone to resist all of these forces, but since the platform is a component of a larger system an analysis cannot be done without taking all of them into account. The loads include:

- The terrain loads such as the cargo loads, infrastructure, traffic and more.
- Crane loads, from the cranes close to the quay loading and unloading the cargo.
- The surcharge loads in combination with the weight of the soil cause large horizontal earth pressures on the structure as well.
- The water pressure, which also includes those caused by the ships.
- Accidental collision forces of the ship and the quay.
- Mooring and berthing forces of the ship.

2.2.4 Quay wall literature and developments

Research about quay walls, specifically looking into several topics including flexible use and reducing CO_2 are described in this section.

Amaarouk et al. (2013) has looked into the development of a removable prefabricated diaphragm wall. This wall was designed as prefabricated concrete elements that are connected by vertical prestressing. It has been shown that the construction costs of the new design are higher compared to the cast-in-situ reference design, but became lower when maintenance and removal costs where included. The carbon footprint was shown to be almost equal, but when taking into account that there is a certain probability the prefabricated wall can be reused within its technical lifetime the prefabricated solution scored better.

In alignment with the goals of carbon reduction, the Port of Rotterdam has also been successful in applying geopolymer concrete in one of their quay walls in the 2e Petroleumhaven. By replacing regular concrete by geopolymer concrete the CO_2 emissions have been reduced by 50% (Port of Rotterdam, 2024). The use of geopolymer concrete had also been suggested by van Rhede van der Kloot (2019) in combination with precast elements as a potential improvement of the sustainability of quay walls. In addition, further research into alternative designs that reduce concrete and steel has also been recommended.

Sewcharan (2023) has also shown that CO_2 emissions of quay walls can be reduced by using different calculation methods. By using volume elements and non-linear calculation approaches, 2D and 3D numerical model had been made. These models were used to make an optimization either reducing the reinforcement or the concrete in the relieving platform. This resulted in an steel reduction of at most 23% and a concrete reduction of at most 22%. The CO_2 footprint of the relieving platform using these methods has been reduced to a maximum of 7% when the concrete was optimized and 15% when the reinforcement was optimized.

De Gijt (2010) has mentioned certain future developments expected in the quay wall design. Quay walls should take in to account the increase in size of ships and the increased demands for the quays. It is for example expected that ships will increase in size up to 500 meters. Looking into the alternative quay wall designs using new materials and improvements in the construction process should also be investigated. The possibilities of flexible, reusable quay wall structures was explored. De Gijt (2010) states that the idea of completely reusable quay walls are not viable when the costs are concerned. An adaptable, upgradable quay wall showed a better performance, but still with a 100% lower present value after 25 years compared to the conventional single use case. These costs estimates are however sensitive to many components, one of which being the technical possibilities at that time and the time frame considered for the cost analysis (De Gijt, 2010). Adaptable structures do therefore seem to have an advantage over reusable structures.

A flexible quay wall design was proposed by Buring (2013) that addressed the issue that the technical lifespan of a quay wall can be longer than the economical lifespan. Changing cargo requirements, vessels or economy can cause a different demands for a quay wall. Several variants had been explored, of which a caisson quay wall structure had been found to be optimal. A caisson structure is a large concrete, watertight retaining structure. The floating walls can be transported from manufacturer to the quay wall site and can be demounted in the case of changing demands. The proposed solution is shown in Figure 6.

Douairi & De Gijt (2013) has proposed several flexible and upgradable quay wall designs, to also address the difficulties in taking into account changing demands in the future. The proposed solutions include introducing land and/or side forces (such as an anchor), reduction of active pressure by relieving the sheet-pile (thus placing a relieving platform), building a new structure in front of the quay wall. Zwakhals et al. (2012) underscores the need for flexibility, while also noting the lack of practical examples in

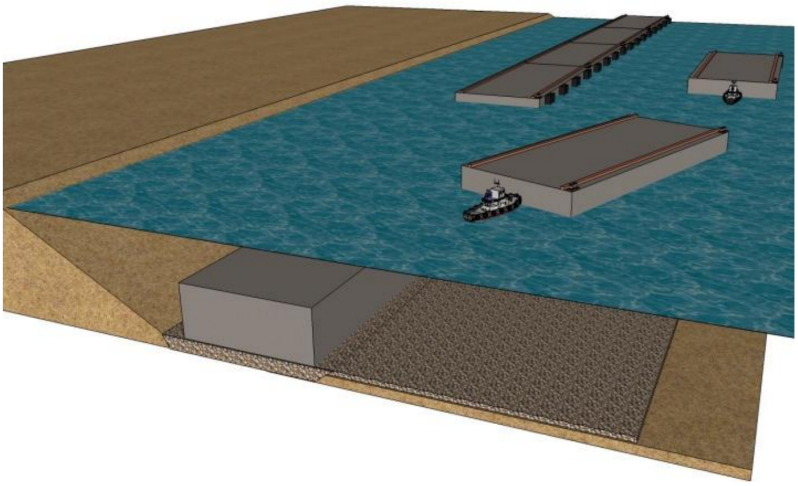

Figure 6: Proposed flexible quay wall structure by Buring (2013)

this specific field. This highlights the importance of further research into flexible and sustainable infrastructural solutions.

2.3 Prestressing

2.3.1 General principles

Prestressing can contribute to the previously mentioned problems and objectives by creating more slender cross-sections. Concrete is a material that is relatively weak in tension. One method to mitigate this weakness is by adding reinforcement that resists the tensile stresses. Another method is prestressing, which places a compressive stress on the concrete element (note prestressing can be seen as preloading) which will counteract the tensile stresses. This method has not been researched much in quay wall structures and therefore little to no case studies are available. This method has however been widely applied in other fields, such as for example in bridges and viaducts.

Figure 7 shows the general mechanical principle of how prestressing works. In the first diagram the stresses of a cross-section under the distributed load q are displayed. Because concrete is unable to handle the tensile stresses at the bottom cracking will occur. To counteract this, the prestressing force p is applied to the beam. The second diagram shows the compressive stresses in the concrete that result from prestressing. As can be seen, the combined result no longer has any tensile stresses in the bottom of the beam (Walraven & Braam, 2019).

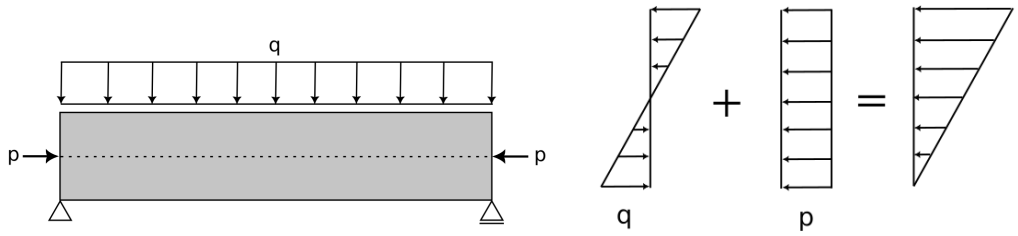

(a) Example prestressed beam (b) Prestressing stresses

Figure 7: Prestressing example

In addition to the axial stresses introduced by prestressing, the tendon can be designed in such a way it also imposes counteracting loads on the structure, this will be addressed in the next section. Whether prestressing can effectively be used to reduce the elements

cross-section depends on which failure mechanisms (cracking, deformation, shear, etc.) are governing. This will need to be investigated to assess whether prestressing can be a useful solution.

2.3.2 Loads

The general method of how prestressing is taken into account is by applying equivalent loads to the structure. Depending on the specific prestressing design, different forces are imposed on the structure. The figures below show what loads are placed on the structure in addition to the axial load P, based on the specific tendon layout.

By placing the the ends of the tendon at a distance e from the centroidal axis, an eccentric force P is applied on the element. This causes a bending moment P·e on the ends of the element.

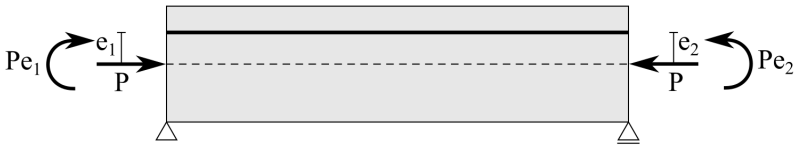

Figure 8: Prestressing equivalent loads: Eccentric

A kink in the tendon will cause an upwards force equal to 2· $\sin(\alpha/2)$. The use of a kink is only applicable in the design stage of a prestressed element. It is not possible to create a sudden change in angle and in reality a certain transition curve must be present with a certain minimum radius based on the thickness of the tendon.

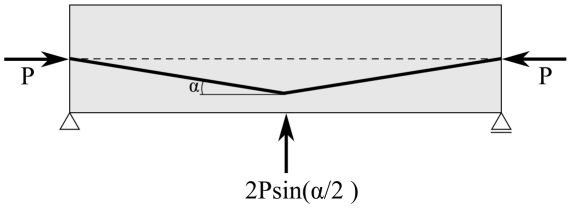

Figure 9: Prestressing equivalent loads: Kink

A curved tendon path will impose an distributed load on the element. This is often applied in prestressing designs as it can have a significant benefit to the structural element by counteracting the other imposed distributed loads,

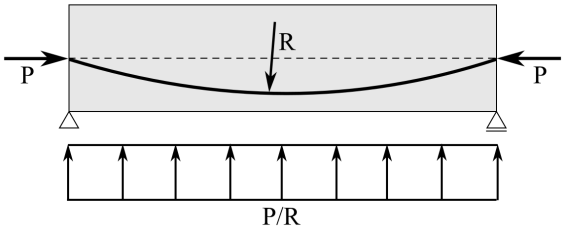

Figure 10: Prestressing equivalent loads: Curved

If a prestressing tendon is applied at the ends at an angle, the horizontal axial load is technically not equal to P, but to P· $\cos(\theta)$ (Figure 11). In addition the vertical component P· $\sin(\theta)$ is imposed on the structure. Often these forces are neglected and the horizontal component is simplified as P, since the angle θ is generally small.

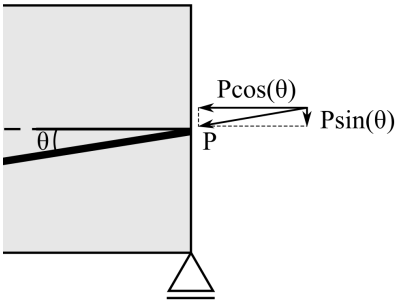

Figure 11: Prestressing equivalent loads: Angle ends

2.3.3 Prestressing methods

A distinction is made between fully, limited and partial prestressing. Full prestressing means that under SLS loads no tensile stresses are allowed in the concrete. For limited prestressing tensile stresses are allowed, but no cracking is allowed to form. For partial prestressing some cracking is allowed, which can lead to a more economical solution. For this reason, partial prestressing has been used for the design made in this thesis.

There are also two general methods of prestressing: pre-tensioning and post-tensioning. With pre-tensioning the steel tendons are stressed before the concrete is cast. The tendons are anchored and stressed within a formwork, in which the concrete is then cast. Once the concrete has hardened the tendons are released from the anchors and the stresses are transferred from the steel to the concrete by their bond. This method of prestressing is usually performed in a factory and is thus suitable for prefabricated elements. The size and flexibility of the design is more limited however, compared to post-tensioning.

Post-tensioning differs in that the tendons are stressed after the concrete has hardened. Ducts are placed in the concrete formwork before casting, in which the tendons will be placed once the concrete has hardened. The tendons are stressed using a jack and anchors are then placed on the ends of the tendons that hold them in place. These anchors transfer the stresses to the concrete element. In general, grout is inserted into the ducts after prestressing, to protect the tendon from corrosion. For the case of the relieving platform, grout will be needed to protect the tendon from the harsh environment. Post-tensioning can be used both for prefabricated elements as well as on-site. It has the benefit of having a more flexible design as well as enabling larger elements when constructed on-site. The main downsides are higher costs and a more labor intensive process to stress the tendons. While pre-tensioning only allows straight tendon paths, post-tensioning also allows curvatures.

Since prestressing is applied before all the loads are imposed on the structure, the phase where only the self-weight is imposed is important to keep into account. It is possible that the structure is be prestressed too much, causing cracking in cross-sections different from those that are critical during its use life.

2.4 Prefabricated and modular design

2.4.1 Background

In addition to the improved efficiency in the building process mentioned in Section 1.1.3, prefabricated construction methods also showed a reduction of the carbon emissions. Lyu et al. (2022) found that when comparing a precast, prestressed foundation pile to a cast-in-situ pile, the latter released 1,4 times more carbon than the former. A study by Jang et al. (2022) showed that when comparing a modular residential building to an equivalent, conventional residential building, that the modular building has a reduced carbon emission by approximately 38%. Another meta-analysis by Teng et al. (2018) showed an

average CO_2 reduction of 15,6% across 27 cases by using prefabricated elements, looking at residential, commercial and industrial buildings. It should be noted however, that these studies did not look at structures similar to that of a quay wall, but it shows the potential benefits that can be obtained.

A prefabricated and modular design will allow for more flexible construction. As mentioned in Section 1.1.3, the economical lifetime of a quay wall is not necessarily the same as the technical or usage lifetime. An upgradable quay wall could offer a solution. Modules can be added at a later stage when the requirements of a quay wall change, preventing an overuse of materials. In the design of a modular relieving platform there are several important considerations. One important and challenging aspect is the way the modules will be connected. The current L-shaped relieving platforms are constructed as one solid element with reinforcement steel that runs via the platform to the wall. In contrast, if the L-shaped platform would consist of separate modules there would be no similar solid connections. Several types of connections exist that could be used for the modules, but the applicability of these types must be investigated for this specific structure.

2.4.2 Construction

Another important consideration is the construction of the modules on-site. Relieving platforms are large structures that use a large amount of materials. A typical design of the floor of a relieving platform can have a length of around 15 m and a thickness of 1,75 m. When designing the modules the intended construction sequence needs to be kept in mind. The relieving platform could span the entire length with just one module, or alternatively by connecting several smaller modules together. This has implications for both the type of structural connections and the prestressing in the modules. There are also limitations, costs and higher CO_2 that go with the transport of such elements.

The weight and shape of the modules is also dependent on the regulations regarding transportation. In the Netherlands, for conventional transport without the need for any specific exemptions the maximum weight is 60 tonnes and the maximum length is 25,25 m (including the truck itself) (van Algemene Zaken, n.d.). For weights until a 100 tonnes, and a maximum size of 27,50 m x 3,50 m x 4,25 m (l x w x h) a yearly exception can be granted (RDW, n.d.). Anything above this will require special exemptions. A second consideration are the loads that can be carried by cranes on-site. Looking at the crane specifications from specific suppliers, it can be seen that loads up to a maximum of 700 tonnes are possible (Nederhoff, n.d.).

2.4.3 Connections of prefabricated concrete

Different types of connections exist that are typically used in precast concrete elements. Three general general classes that can be distinguished are dry, wet and hybrid connections (Chang et al., 2023).

Dry connections

Dry connections typically use mechanical fasteners and connectors. It has the benefit of having a faster construction speed. These types of connections can also be more easily demounted as compared to the other connection types.

Shear key
Shear keys are a type of connection that can transfer shear forces by creating two interlocking interfaces. An example of this can be seen in Figure 12. The advantage of such a connection is a straight forward application that does not require any mechanical fasteners. The use of cast-in-situ materials can also be prevented, however exactly matching

the sizes of the shear keys can prove difficult. Cast-in-situ concrete can be used to ensure a tight fit, but an alternative is to make use of match-casting. Match-casting is a type of casting where during the fabrication the modules and the connections are cast against each other, ensuring the shear key exactly fits in the opening of the other module.

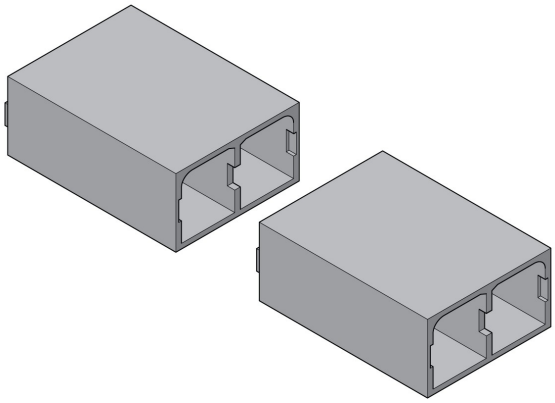

Figure 12: Shear key used in an immersed tunnel (*Handboek Tunnelbouw*, 2023)

Steel plates with bolts and/or mechanical joints
This type of dry connection utilizes pre-embedded steel plates and bolts to connect concrete elements. The connections can have construction speeds comparable to that of steel structures (Chang et al., 2023). The connections typically resist shear and axial loads, but can also be made to resist moments. An example of a steel plate connection using bolts and mechanical joints can be seen in Figures 13 and 14 respectively. However, since demountability is not a priority of the modules and that the connections will be placed under the soil exposed to harsh chemicals from the environment, dry connections using steel plates are not expected to be suitable for the application of this thesis.

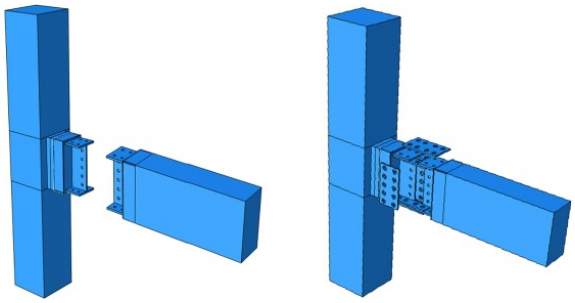

Figure 13: Bolted joint (Ye et al., 2021)

Dowels
Shear dowels have been widely applied in the construction of prefabricated concrete elements. Dowels are steel bars that resist the shear forces in a connection. The dowels protrude from one element into the other element. A typical beam to column connection with dowels can be seen in Figure 15. Due to the discontinuity of the longitudinal reinforcement the moment capacity of the joint is limited (Nie et al., 2025) and therefore this connection can be considered as a hinged connection only resisting horizontal and axial forces (Holly & Abrahoim, 2020). The dowel can be connected using mechanical fasteners, but also by grouting a duct within which the dowel is placed (technically making it a wet connection).

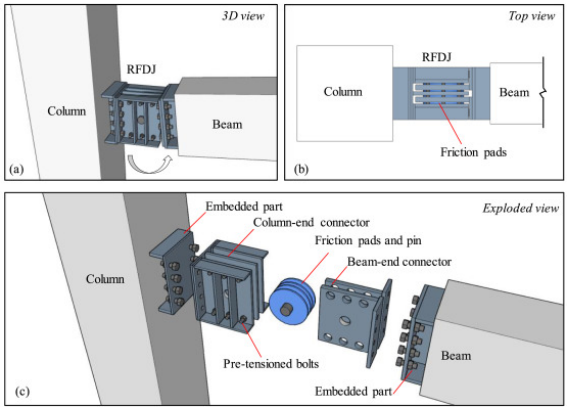

Figure 14: Mechanical joint (Yang et al., 2022)

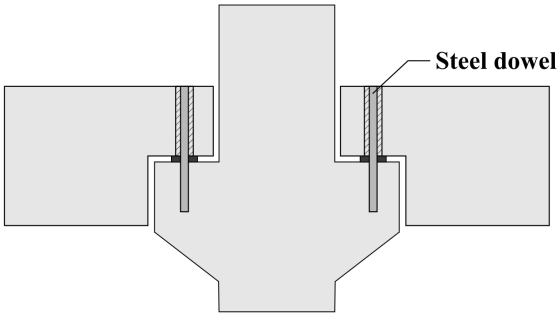

Figure 15: Shear dowel

Wet connections

Wet connections use cast-in-situ materials to connect different components (Chang et al., 2023). Typically the structural integrity of these types of connections is better and they do not have the same problems with stress concentrations that dry connections have. Another added benefit, is that the cast-in-situ materials also protect the steel within. Since the concrete is placed underground, within a harsh environment the exposure of steel directly to the chemicals is not desirable.

Cast-in-situ concrete
For hollow core slabs, a commonly used method involves casting concrete between two prefabricated elements. The connection is then made by the profile on the sides of the hollow core slabs and the cast-in-situ concrete. It is designed to resist only normal and shear forces. Figure 16 shows an example of this. This type of connection is usually intended as a continuous longitudinal hinge (Paolo & Giandomenico, 2012).

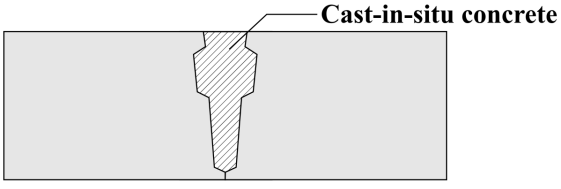

Figure 16: Cast-in-situ concrete connection

Protruding reinforcement bars
This type of connection can in addition to normal and shear forces also resist bending moments. By adding reinforcement bars that protrude into the joint and then casting concrete to form the connection. Figure 17 shows an example of such a connection between two concrete beams and a column (Holly & Abrahoim, 2020).

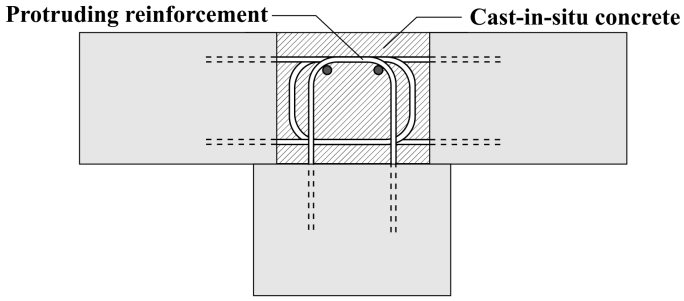

Figure 17: Protruding reinforcement

The reinforcement can either protrude from the precast element into the connection (as is shown in Figure 17). But it is also possible to post-install the reinforcement bars. This could be done by creating a hole in which the reinforcement can be placed (either on site or during manufacturing) and using an adhesive to create the bond between the reinforcement and the concrete element (Figure 18). Another method of post-installing the reinforcement is using a type of coupler (Figure 19) which are casted into the concrete elements.

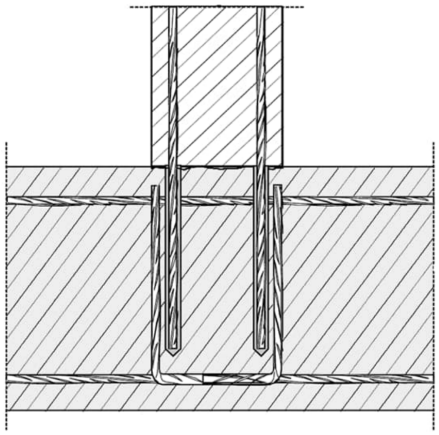

Figure 18: Example post-installed reinforcement using adhesive (Association of Consulting Engineers Singapore, 2025)

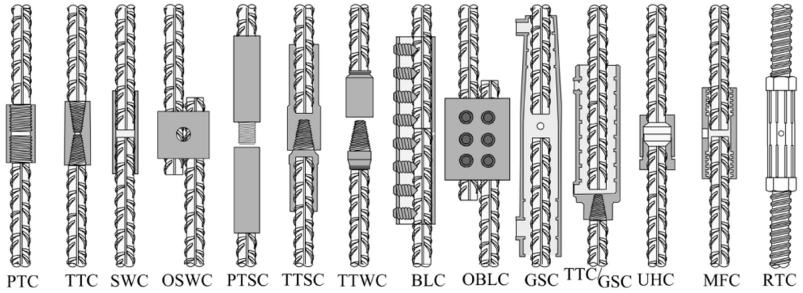

Figure 19: Example mechanical reinforcement couplers (Bompa & Elghazouli, 2017)

Notched connection
Another innovative type of connection mentioned in Nie et al. (2025) and originally suggested by Jiang et al. (2021) is the notched connection. Notches are formed in the prefabricated elements, in which reinforcement bars can be placed. The notches are then filled with concrete. This type of connection is suggested to have benefits in terms of preventing reinforcement congestion as well as an improved construction efficiency. Since one of the most important factors in the modular design is to create a fast and efficient construction process to reduce downtime, this could be a suitable option. However, the concrete elements must have the appropriate shape and space to accommodate such a connection.

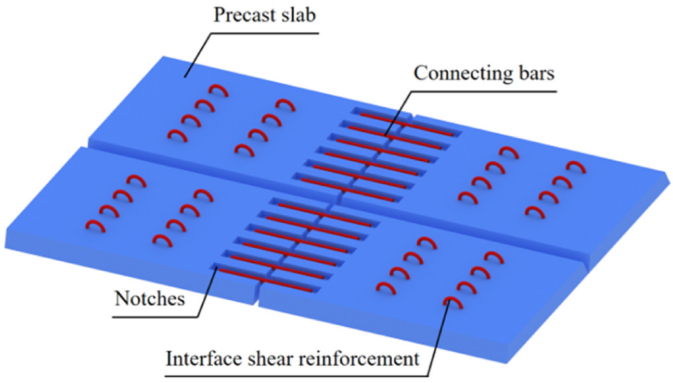

Figure 20: Notched connection (Nie et al., 2025)

Prestressed connection

In addition, prestressing itself can also be used to form a connection between two components. A common example of where this is applied is in segmented construction. A combination of prestressing, reinforcement and/or shear keys can be used to connect individual segments together. An example of this are box-girder bridges, that are constructed using individual prefabricated modules (Figure 21). Allowing for the prestressing tendon to run through multiple segments allows for prestressing loads that increase the strength of the connections and the total structure.
Tendons can be made continuous through the application of couplers. Another example of a prestressed, beam to column connection is shown in Figure 22.

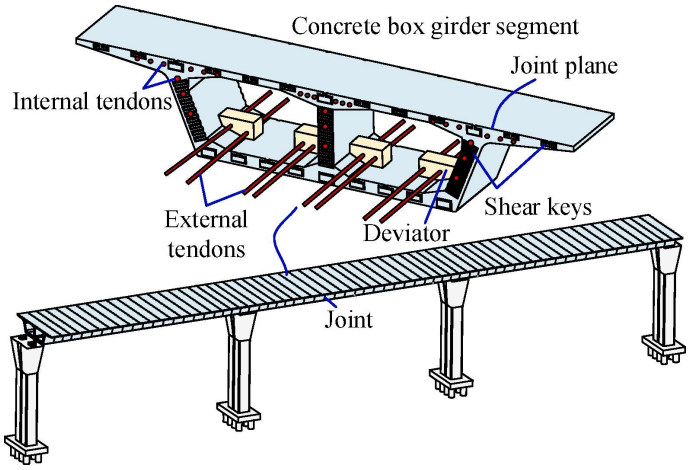

Figure 21: Example of a post-tensioned connection (Yan et al., 2020)

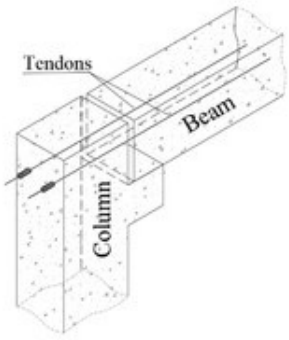

Figure 22: Example of a post-tensioned connection (Pekgokgoz & Yakut, 2024)

3 Methods

3.1 Analytical model

The analytical model of the structure will make use of Euler Bernoulli (EB) beams (Öchsner, 2021). Using the EB Beam Theory, the internal load and deformation behavior can be analyzed. The EB beam equation uses the assumption that plane sections remain plane during bending. This means that shear deformations are not taken into account (contrary to for example a Timoshenko beam).

Typically for elements where the length is larger than around 10 times the height, shear deformations are initially neglected (Öchsner, 2021). For such a case an EB beam would be suitable. The floor of a relieving platform can have a thickness to length ratio of 1,75 : 15,9, which is 1 : 9,1. However, the choice has been made to still use an EB beam model. The reason for this is the simplicity of the beam theory and the fact that one of the main objectives of the thesis is to explore the possibility of a more slender cross-section. This thus means that the optimized variants of the floor will be more slender, which in turn means that the more critical models (which are those with the most slender cross-section) can be accurately represented by EB beams.

The Euler Bernouilli beam equation for a static beam with a distributed load q is shown in Eq. (1).

$$EI\frac{\delta^4 w}{\delta x^4} = -q \tag{1}$$

Integrating this differential equation four times gives the general solution of the deflection $w(x)$ (Eq. (2)).

$$w(x) = \frac{1}{EI}(\frac{-qx^4}{24} + c_1\frac{x^3}{6} + c_2\frac{x^2}{2} + c_3x + c_4) \tag{2}$$

To determine the deflections and internal loads of the beam, the constants c_1 to c_4 have to be solved. To do this four boundary conditions are required per element. These boundary conditions represent imposed loads and supports on the nodes (the start and end) of the beam. Several different types of boundary conditions relevant to this thesis are shown below.

Imposing a displacement (in the y direction) on the structure at location x:

$$w(x) = 0 \tag{3}$$

Imposing a certain moment on location x. Can also be used to define free rotation when set to equal zero:

$$EI\frac{\delta^2 w(x)}{\delta x^2} = 0 \tag{4}$$

Spring support, which means displacements are allowed at the support but determined by a certain spring stiffness k:

$$EI\frac{\delta^3 w(x)}{\delta x^3} = k \cdot w(x) \tag{5}$$

Impose a certain rotation. Can also be used to set the rotation to zero for a clamped support:

$$\frac{\delta w(x)}{\delta x} = \varphi(x) \tag{6}$$

When a structure is modeled using EB beams, it typically consists of multiple elements connected to each other at nodes. Each of these elements represent a different segment of the structure. Multiple elements can be connected to each other by defining the interface conditions. These interface conditions specify how two elements influence each other at the connecting nodes. For every interface, two interface conditions are required. Similar to the boundary conditions, different properties can be defined. When defining a continuous element, the following interface conditions need to be defined:

The deflection of each element is equal in the interface point x:

$$w_1(x) = w_2(x) \tag{7}$$

The rotation of each element is equal in the interface point x:

$$\varphi_1(x) = \varphi_2(x) \tag{8}$$

The moments are equal in the interface point x:

$$EI\frac{\delta^2 w_1(x)}{\delta x^2} = EI\frac{\delta^2 w_2(x)}{\delta x^2} \tag{9}$$

And the shear forces are equal in the interface point x:

$$EI\frac{\delta^3 w_1(x)}{\delta x^3} = EI\frac{\delta^3 w_2(x)}{\delta x^3} \tag{10}$$

An external load or displacement can be added to any one of these interface conditions to represent an imposed load at the nodes. As can be seen in Eq. (1) a distributed load q can also be placed on an element. When the distributed load is intended to only be imposed on a certain part of an element, a piecewise function can be used as seen in the equation below. Here, an example is given where a distributed load q is placed on the element between x = 5 and x = 10.

$$EI\frac{\delta^4 w}{\delta x^4} = \begin{cases} 0 & x \leq 5 \\ -q & 5 \leq x \leq 10 \\ 0 & 10 \leq x \end{cases} \tag{11}$$

A simple EB beam can typically be solved analytically and by hand. However, when multiple beams are combined and more complicated loads are imposed (such as piecewise function above) solving it using computational methods becomes necessary. For this reason, the analytical model in this thesis will be solved using the software Maple. Maple is software that solves math problems, including these types of differential equations, using a programming language. The used model and its equations can be found in Appendix E.6. The Maple script can then later be used in the optimization loop as well.

3.2 Cross-section resistance

Several resistance checks have been checked, to evaluate whether the design is able to resist the imposed loads. Those resistance checks that are most important to give an to give an idea of the feasibility of the concept design will be used in this thesis. These are: the ULS bending moments resistance, ULS shear force resistance and the SLS crack widths.

ULS: Bending moment resistance

For the ULS bending moment resistance it is assumed that at failure the reinforcement steel is at its yield stress f_{yd}, the prestressing steel is at f_{pd} and the concrete is at the ultimate strain $\epsilon_{cu} = 3,5 \cdot 10^{-3}$. To calculate the moment resistance of the cross-section, the different forces present within the cross-section at bending need to be determined. The forces present can be seen in Figure 23. The compression zone height x_u represents the height of the cross-section that at bending is under compression. This value is needed for the calculation of the load N_c. Because the stresses resulting from the bending of the prestressing tendon $\Delta\sigma_p$ are dependent on the height of the compression zone x_u, but the height of the compressive zone is in its turn dependent on the stresses of the prestressing tendon, finding the exact value of the stresses and compression zone height becomes an iterative process. The correct value of the compression zone height is found when the horizontal force equilibrium is satisfied. The initial guess of x_u is calculated according to the formula below, which results from the initially assumed horizontal force equilibrium.

$$x_u = \frac{A_{sb} f_{yd} + A_p f_{pd} - N_{ed} - A_{st} f_{yd}}{\alpha f_{cd} b} \tag{12}$$

It needs to be checked whether assumptions about the stress of the reinforcement and prestressing steel at failure are correct and adjustments need to be made accordingly if required. Finally the bending moment resistance M_{Rd} is determined by looking at the moment equilibrium in the cross-section. Figure 23 shows the forces and strains within a specific cross-section.

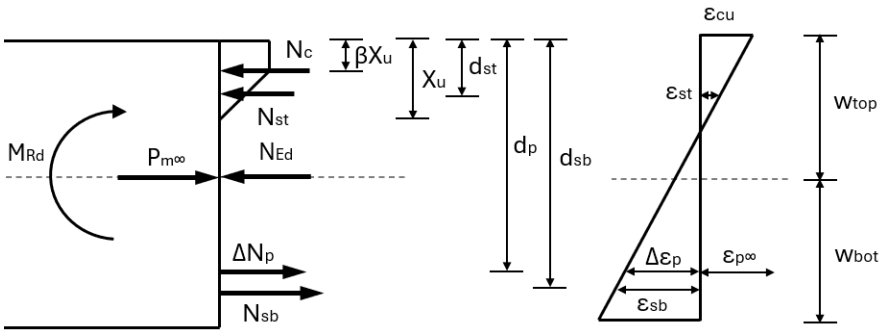

Figure 23: ULS Bending moment stresses and strains

The final moment resistance is then found by taking the moment equilibrium around the centroidal axis.

$$M_{Rd} = N_c \cdot (w_{top} - \beta \cdot x_u) + N_{st} \cdot (w_{top} - d_{st}) + \Delta N_p \cdot (d_p - w_{bot}) + N_{sb} \cdot (d_{sb} - w_{bot}) \tag{13}$$

where:

N_c	:	$= \alpha b x_u f_{cd}$ (for a rectangular compression zone $\alpha = 0,75$ and $\beta = 0,39$)
N_{st}	:	force in the top reinforcement
N_{sb}	:	force in the bottom reinforcement
ΔN_p	:	force in the prestressing tendon due to bending

In addition the rotational capacity at the location of the highest sagging moment is checked according to NEN-EN 1992-1-1, article 5.5. For this relieving platform with $f_{ck} \leq 50$ MPa, Eq. (14) is used to calculate this. The rotational capacity check limits the maximum height of the compression relative to the effective depth of the tensile reinforcement. It is used to ensure a ductile failure mechanism cross-section.

$$\delta \geq k_1 + k_2 x_u / d \tag{14}$$

The values k_1 and k_2 are values given by the NEN-EN 1992-1-1, Nation Annex, article 5.5. Even though $M_{Rd} >> M_{Ed}$ it can be the case that due to prestressing the rotational capacity is not sufficient. The prestressing is often designed for SLS rather than ULS. For this reason NEN-EN 1992-1-1, Nation Annex, article 6.1 allows for the use of fictitious reinforcement. This means fictitiously removing reinforcement to improve the rotational capacity, while ensuring that $M_{Rd} > M_{Ed}$.

ULS: Shear resistance

The ULS shear resistance will be checked according to NEN-EN 1992-1-1, article 6.2.2 (for cross-sections without shear reinforcement) and article 6.2.3 for cross-sections with shear reinforcement. The resistance of a cross-section without shear reinforcement is calculated according to the NEN-EN 1992-1-1, equation 6.2. The shear resistance equation is shown below (Eq. (15)).

$$V_{Rd,c} = [C_{Rd,c} k (100 \rho_l f_{ck})^{1/3} + k_1 \sigma_{cp}] b_w d \geq [0.035 k^{3/2} f_{ck}^{1/2} + k_1 \sigma_{cp}] b_w d \tag{15}$$

where:

k	:	$= 1 + \sqrt{\frac{200}{d}} \leq 2,0$
ρ_l	:	$= \frac{A_{sl}}{b_w d} \leq 0,02$
A_{sl}	:	Area of the longitudinal reinforcement within the tensile zone
ρ_{cp}	:	$N_{Ed}/A_c < 0,2 f_{cd}$
N_{Ed}	:	Normal force in the cross-section, including prestressing
A_c	:	Concrete cross-section area

The axial forces from prestressing have a positive effect on the shear resistance of the concrete, which is taken into account by σ_{cp}. A unity check is performed to check whether the shear resistance is higher than the design shear loads (Eq. (16)). If this check is satisfied, the specific cross-section does not require any shear reinforcement. If this check is not satisfied, shear reinforcement will be needed.

$$\frac{V_{Rd,c}}{V_{Ed}} < 1 \tag{16}$$

The shear resistance of cross-sections that require shear reinforcement $V_{Rd,s}$ can be calculated using NEN-EN 1992-1-1, article 6.2.3. The shear reinforcement will consist of vertical stirrups, meaning equation 6.8 from NEN-EN 1992-1-1 can be used. The shear resistance of the steel then is the smallest value of the Eq. (17) and (18) shown below.

$$V_{Rd,s} = \frac{A_{sw}}{s} z f_{ywd} cot(\theta) \tag{17}$$

$$V_{Rd,max} = \alpha_{cw} b_w z v_1 f_{cd} / (cot(\theta) + tan(\theta)) \tag{18}$$

where:

A_{sw}	:	area of the shear reinforcement
s	:	the center to center distance between the stirrups
z	:	internal lever arm, assumed to be $z = 0,9d$
f_{ywd}	:	yield strength of the shear reinforcement
θ	:	angle of the compression struts
v_1	:	Strength reduction factor for concrete cracked in shear (NEN-EN 1992-1-1, National Annex, article 6.2.3)
α_{cw}	:	A factor for the stresses in the compressed edge (NEN-EN 1992-1-1, National Annex, article 6.2.3)

When calculating the shear resistance, the effective depth of the prestressing steel in combination with the reinforcement steel needs to be determined. Only the prestressing tendons that lie within the tensile zone contribute to the shear resistance. However, since the prestressing tendon has a curved shape, it does not lie within the tensile zone of every cross-section. The compression zone height is calculated for every cross-section analyzed, from which will be determined whether the prestressing is located in the tensile zone. The formula for the ρ_l then becomes:

$$\rho_l = \frac{A_p + A_{sl}}{b_w \cdot d_{eff}} \tag{19}$$

The effective depth is then calculated using the formula:

$$d_{eff} = \frac{d_p A_p + d_{sl} A_{sl}}{A_p + A_s l} \tag{20}$$

For cross-sections where the prestressing steel is within the compression zone, A_p equals zero. A_{sl} is the longitudinal reinforcement in the tensile area.

The parameter b_w is the smallest web width of the cross-section. The prestressing ducts have an influence on the width of the cross-section. The width of b_w with prestressing ducts is defined according to the NEN-EN 1992-1-1, equation 6.16. If $\phi > b_w/8$, with ϕ being the outside diameter of the canal, then:

$$b_{w,nom} = b_w - 0.5 \sum \phi \tag{21}$$

If $\phi \leq b_w/8$, then $b_{w,nom} = b_w$.

SLS: Crack width control

The SLS check that will be performed is the calculation of the crack widths control. The deformations are not taken into account for this analysis. The reason for this is that using the analytical model only the longitudinal deformations can be determined, but these deformations can be relatively easily compensated for by the soil on top of the relieving platform. In addition the longitudinal deformations have less severe implications for the structure compared to transverse deformations, for example for potential rail tracks on top of the quay. These transverse deformations can however not be considered using this analysis. The crack widths will be calculated according to NEN-EN 1992-1-1, article 7.3.4.

The maximum allowable crack width is determined according to NEN-EN 1992-1-1, National Annex, table 7.1N. Together with the requirement of the ROK-0111 (Richtlijnen Ontwerp Kunstwerken, guidance for the design of infrastructural projects (Rijkswaterstaat, n.d.)) this results in a maximum crack-width of 0,2 mm if the prestressing duct is at a distance $>$ 200 mm from the outer edge and 0,1 mm if the distance $<$ 200 mm.

According to NEN-EN 1992-1-1, article 6.2.2, a prestressing tendon only contributes to the crack width control when within 150 mm of the outer edge. If the tendon is a greater distance, this means that A_p' in the effective reinforcement ratio Eq. (23) becomes zero.

Considering the design of the current cross-section (further elaborated in Section 4.3) the tendon is never within 150 mm from the outer edge. For this reason A_p does not contribute to the crack width control in Eq. (23).

$$w_k = S_{r,max}(\epsilon_{sm} - \epsilon_{cm}) \tag{22}$$

where:

$S_{r,max}$	:	the maximum crack distance
ϵ_{sm}	:	average strain in the reinforcement and prestressing steel
ϵ_{cm}	:	average concrete strain between the cracks

$$\epsilon_{sm} - \epsilon_{cm} = \frac{\sigma_s - k_t \frac{f_{ct,eff}}{\rho_{p,eff}}(1 + \alpha_e \rho_{p,eff})}{E_s} \tag{23}$$

where:

σ_s	:	stress in the tensile reinforcement steel, considering a cracked cross-section
α_e	:	the ratio E_s/E_{cm}
$\rho_{p,eff}$	:	$= A_s/A_{c,eff}$
$A_{c,eff}$	:	Effective area of concrete in tension, with height $h_{c,eff}$
$h_{c,eff}$	:	smallest of 2,5(h-d), (h-x)/3 and h/2
k_t	:	depends on the loading period, 0,6 for short term and 0,4 for long term loading

The σ_s is the stress at the depth of the reinforcement and will need to be determined for the moment equilibrium in the specific cross-section. Together with the horizontal force equilibrium two unknowns can be solved, namely the concrete strain at the top fiber ϵ_c and the compression zone height x_e. Similar to the shear force calculations, the shape of the tendon path also determines at which cross-sections the prestressing tendon is in the compressive or the tensile zone.

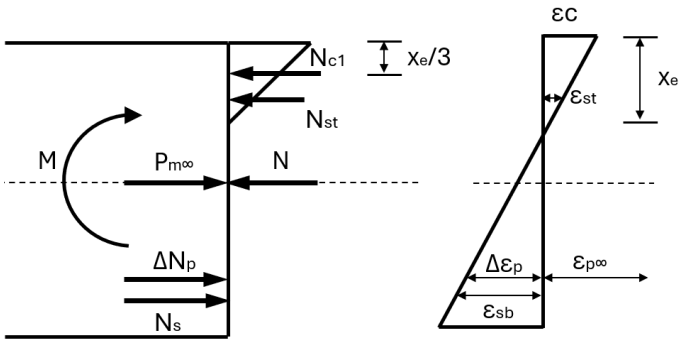

Figure 24: SLS moment equilibrium

$$S_{r,max} = k_3 c + k_1 k_2 k_4 \phi / \rho_{p,eff} \tag{24}$$

where:

3.3 Carbon emissions

One of the main objectives of this thesis is to reduce carbon emissions. For this an analysis looking into the embodied carbon of the structural elements has been made. According to the NEN-EN-ISO 14040 (a standard that describes the principles and framework of a

ϕ : reinforcement bar diameter
c : concrete cover on the longitudinal reinforcement
k_1 : = 0,8 (for high bonding strength)
k_2 : = 0,5 (for bending)
k_3 : = 3,4 (EN 1992-1-1, National Annex, article 7.3.4)
k_4 : = 0,425 (EN 1992-1-1, National Annex, article 7.3.4)

life cycle assessment (LCA)) the goal and scope are defined. The materials relevant to the CO_2 analysis are mentioned below, more details about the materials are mentioned in Sections 4.2.2 and 5.1.2.

Goal: To evaluate the reduction of material usage due to the prestressing in terms of CO_2 reduction.
Scope: Evaluating the embodied carbon of the relieving platform floor, by looking into the building phases A1-A3 (NEN-EN 15804). The materials have been chosen to be representative of the materials used in the relieving platforms in the Port of Rotterdam. The geographical location, common supplier of materials (if available) and properties have been chosen that match those of the current port structures.

The relieving platform analyzed in this thesis consists of the main materials: concrete, reinforcement steel, prestressing tendons and Expanded Polystyrene (EPS) used as remaining formwork for the cross-section opening. The CO_2eq values used for these materials are shown in Table 1.

Concrete
The GWP of concrete is based on the value of C35/45 concrete with CEMIII/B cement given by Nationale MilieuDatabase (NMD) (Milieudatabase, 2025). In addition, this value is compared to the report SGS Search Consultancy et al. (2019), made by NMD and reviewed by Betonhuis (a Dutch concrete industry association). Data provided by the NMD is divided into several categories (Verheul, 2023); namely category 1 being verified data owned by the manufacturer, category 2 being verified data owed by the industry and category 3 being untested, generic data which is not verified. For category 3 a markup factor of 30% is used, to account for the less accurate data. Milieudatabase (2025) gives a GWP of 194,3 kg CO_2eq per m^3, which compared to the GWP of 179,22 kg/m^3 from SGS Search Consultancy et al. (2019) seems to give a representative value. Milieudatabase (2025) also gives a specific value for C35/45 concrete with CEMIII/B cement which was also used for the specific reference case in this thesis (elaborated in Chapter 4). For this reason the used GWP value is 194,3 kg CO_2eq, with a markup factor of 30%, resulting in a final GWP of 252,59 kg CO_2eq .

Reinforcement steel
The embodied carbon of the reinforcement steel is based on two Environmental Product Declarations (EPD) of reinforcement steel in the Netherlands. Kamphorst (2022) gives a value of 954 kg CO_2eq per 1 ton of reinforcing steel and Nederland (2021) gives a value of 1.020 kg CO_2eq per 1 ton of reinforcing steel. The two EPD's are considered to be representative, given both their geographical scopes being The Netherlands. The value of Nederland (2021) will be used, since this EPD has taken into account a weighted average of all participating members of the Vereniging Wapeningstaal Nederland (VWN, a Dutch reinforcement steel industry association). This is considered to be more representative, compared to the value suggested by the NMD, which gives a GWP of 1.586 kg CO_2eq per ton (Milieudatabase, 2021b). The NMD data is also unverified category 3 data, for which the difference likely occurs to a more conservative estimation that was made by the NMD regarding the amount of secondary steel used in the product.

Prestressing steel
For the prestressing steel the value has been based on an EPD made by the Dutch company Nedri (SpanstaalBV, 2022). They also have a geographical scope in the Netherlands and therefore these values are considered to be representative of the prestressing steel in this thesis. The prestressing steel has a GWP value for phase A1-A3 of 1.830 kg CO2eq per ton. This is comparable to the category 3 data given by the NMD (Milieudatabase, 2021a) of 1.586 kg CO_2eq multiplied by 30%.
EPS
For the EPS used in the thesis to create the cross-section opening a GWP of 110,14 kg CO_2eq is used based on Milieudatabase (2020), for EPS with a density of 20 kg/m^3. This value includes the 30% markup value. There exists significantly less representative documentation and EPD's of this material. For this reason this value of the NMD will be used.

Table 1: GWP CO_2eq per material

Material	**CO_2eq**	
Concrete	252,59	kg/m^3
Reinforcement steel	1.020	kg/ton
Prestressing steel	1.830	kg/ton
EPS	110,14	kg/m^3

By determining the volume and weight of each of the components of the quay wall the total CO_2eq of the relieving platform can be determined. It is important to note that only the embodied carbon is investigated in the thesis. A full Life Cycle Analysis (LCA), including the transportation, the use phase and the end-of-life phase, would need to be analyzed to get a complete idea of the total environmental performance of the structure.

4 Analysis of the SIF2 quay wall

4.1 System analysis

4.1.1 Area analysis

The Port of Rotterdam is located in the province of Zuid-Holland, The Netherlands. Rotterdam is the second largest city of the Netherlands with around 600.000 inhabitants. It is the largest port of Europe, with a total area of approximately 12.500 hectares (Port of Rotterdam, n.d.). The port has expanded significantly since its origin, dating as far back as 1250. The latest part that has been added and is still under construction is the Maasvlakte 2. The specific quay wall that will be used as reference is also located in this area. The reference case is the SIF 2 quay wall, which is an extension of an existing deep sea quay wall for the offshore company Sif. The wall is located in the Arianahaven and has finished its construction in 2021. It is a quay wall that needs to handle very high loads that result from the manufacturing of the foundation piles of offshore wind turbines. Its location is shown in Figure 25.



(a) (b)

Figure 25: Sif quay wall location (Google, n.d.)

The port has a large socio-economic impact on the region and the country. The Port of Rotterdam Authority has around 1.300 employees. The total impact on the country is significantly larger however, generating over 500.000 jobs nation wide (direct and indirect) and providing an added value of over 60 billion euros to the Dutch economy. In 2023 the total cargo throughput was 438,8 million tonnes facilitating approximately 28.000 seagoing vessels and 90.000 inland vessels (Port of Rotterdam, n.d.). The port gives access to the largest ships currently in use with depths of more than 20 m.

A large part of the Maasvlakte 2 is already in use. Three large terminals: Euromax, APM Terminals and Rotterdam World Gateway are located in this area. Sif group is also one of the companies located in the new Maasvlakte 2 area. The Maasvlakte 2 is also built with sustainability in mind. Examples of this are the placement of a large amount of windmills and the reservation of 300 hectares of land area for sustainable industry (Port of Rotterdam, 2017).

The soil conditions in the port area vary a lot. Adequate tests need to be performed in order to get a good idea of the specific conditions at a location. The soil layers in this area mostly consist of a combination of fine and coarse sand and some clay layers at deeper levels below ground (20-30 m) (DINOloket, n.d.). The piles of the combi wall, the anchor and the foundation piles all require the subsoil layers to have adequate capacity. The Maasvlakte 2 consists of land that has been constructed on a massive scale. The total area is 2000 hectares and has expanded the Port of Rotterdam with approximately 20%. The companies Boskalis and Van Oord were responsible for its construction (Boskalis, n.d.). The sand used came from the deepening of the port and from some carefully selected

locations. The task of building the Sif quay wall was given to Van Hattum en Blankevoort and was completed at the end of 2021 (Port of Rotterdam, 2021).

4.2 Quay wall design

4.2.1 Geometry and Materials

Figure 26 and 27 show the main dimensions of the SIF 2 quay wall. The dimensions, loads, material properties and all other properties of the quay wall have been derived from the documentation of the quay wall design Roelevink (2020) and Schouten & van der Valk (2020). Only those values relevant to this thesis will be addressed in this chapter. The figures are also adapted from the documentation.

The quay wall is build in segments of 23 m. This analysis will look into one of these segments which is considered to be representative of the entire quay wall. The quay wall has been divided into a superstructure and a substructure. The superstructure consists of the relieving platform itself, including the wall and floor. The substructure includes the foundation piles, combi-wall, anchor and the resistance of the soil. The analysis in this thesis will only look into the superstructure. The loads resulting from the substructure are retrieved from the calculations made of the current design. A Plaxis model has been made in the original design of the quay wall, which gave the values for the interaction between the sub- and superstructure (Schouten & van der Valk, 2020).

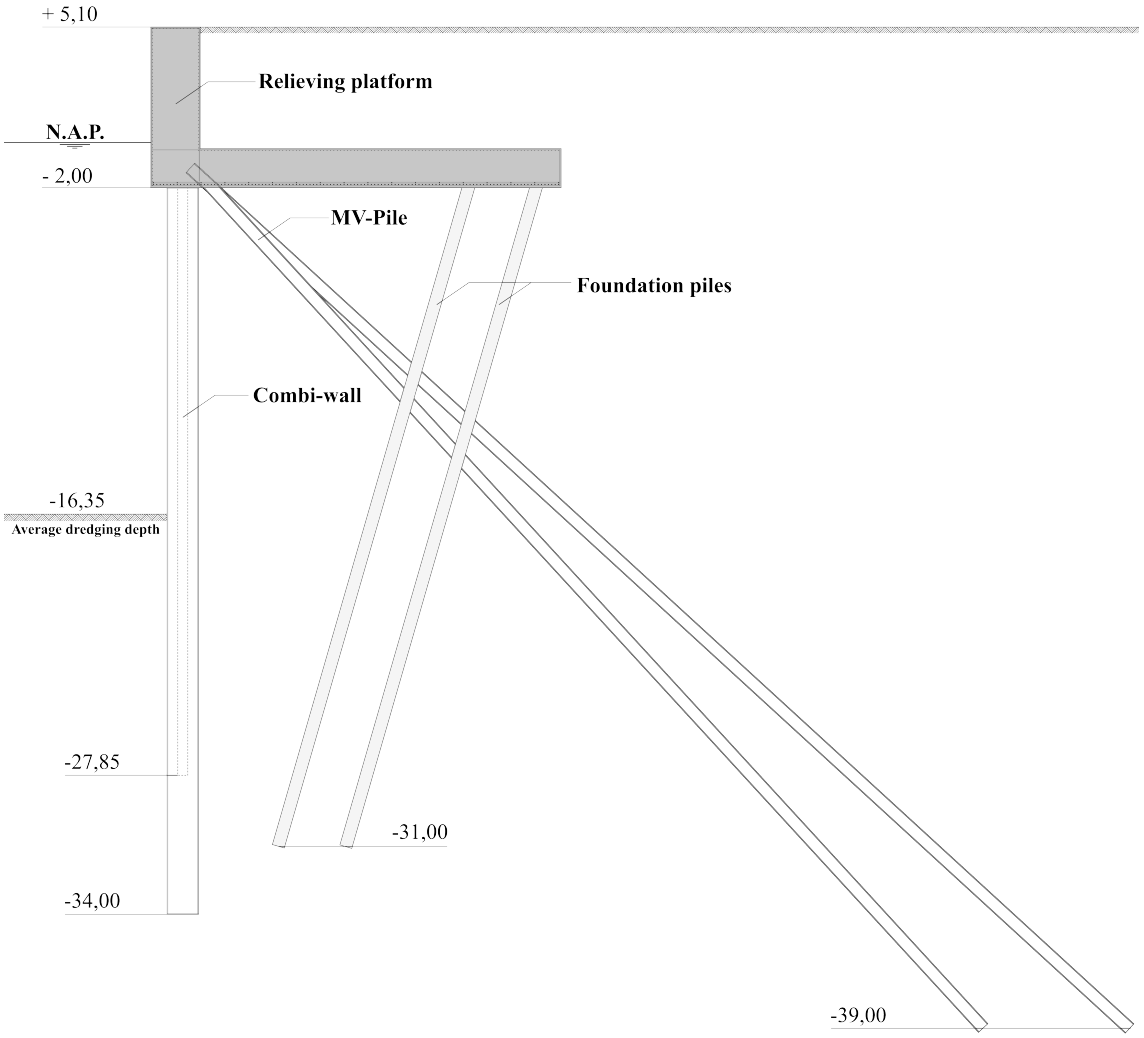

Figure 26: SIF2 Quay wall: Overal design

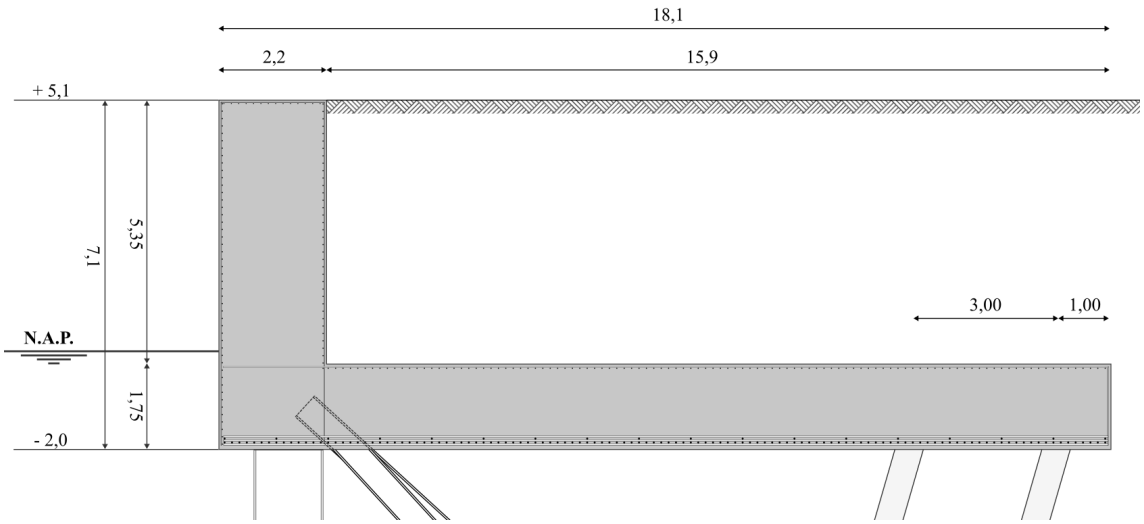

Figure 27: SIF2 Quay wall: Relieving platform side view

Relieving platform

The main geometrical properties of the relieving platform as show in Table 2. The top of the wall is at the level N.A.P. +5,10 m, the bottom of the floor at -2,00 m.

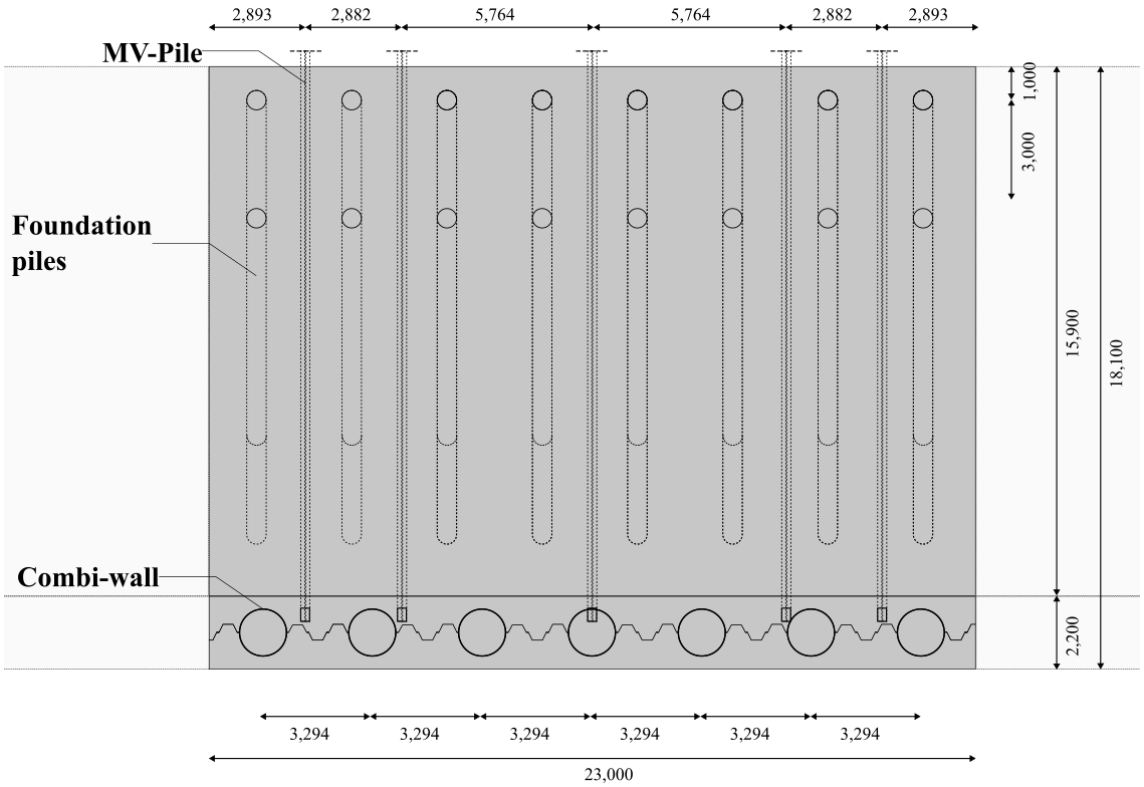

Figure 28: SIF2 Quay wall: Relieving platform top view

Table 2: Geometrical properties relieving platform

Component	Geometrical dimensions
Front wall	Height: 7,1 m, thickness: 2,2 m
Floor	Length: 15,9 m, thickness: 1,75 m

Combi wall

The piles used in the Sif quay wall have a diameter of 1.420 mm and are placed at a center to center distance of 3,294 m. This means that for each 23 m segment, there are a total of 7 steel piles. The average dredging depth next to the quay wall is 16,35 m. The depth of the sheet wall is 27,85 m and that of the steel piles is 34 m.

Anchorage

For this quay wall MV-piles with a HEB600 profile are used as anchors, which are long steel piles that are especially strong in tension. The center to center distance of these anchors alternate between 2,882 m and 5,764 m. The angles of the piles also alternate between 42,5° and 47,5°. This means a total of 5 MV-piles are located in each segment. The MV-piles are connected to the wall to provide stability to the wall. The anchor reaches a depth of NAP -39 m. In the calculations an angle of 45° has been used for every MV-pile as a simplification of the alternation angles.

Foundation piles

Within one 23 m segment there are two rows of 8 concrete foundation piles with diameter Ø610 mm. These piles are both placed on an angle with ratio 1:4 and reach a depth of NAP -31 m.

4.2.2 Materials

The main materials used in the relieving platform are displayed in the tables below.

Table 3: Concrete properties

Component	**Material properties**
Concrete class	C35/45
Characteristic compressive strength f_{ck}	35 N/mm^2
E-modulus E_{cm}	34.000 N/mm^2
Volumetric weight γ	25 kN/m^3
Linear expansion coefficient α	10^{-5} K^{-1}
Cement class	CEMIII/B

Table 4: Reinforcing steel properties

Component	**Material properties**
Steel class	B500B
Characteristic tensile strength f_{tk}	540 N/mm^2
Characteristic yield strength f_{yk}	500 N/mm^2
Design yield strength f_{yd}	435 N/mm^2

4.2.3 Cover and reinforcement

The reinforcement properties used in the SIF2 quay wall are displayed in the tables below and can be seen in Figure 29. The used concrete cover is also described in Table 6. It is a slightly simplified version of the reinforcement applied in the construction assuming constant reinforcement over length of the floor and not taking into account the lateral vertical reinforcement at the ends of the floor. This reinforcement layout is considered in the rest of this thesis.

Table 5: Environmental and construction classes (Schouten & van der Valk, 2020)

	Floor (bottom)	**Floor (top)**
Environmental class	XC4, XS3, XA2	XC4, XS3, XA2
Design life 100 years	+2	+ 2
Plate element	-1	-1
Construction class	S5	S5

Table 6: Concrete cover calculations (Schouten & van der Valk, 2020)

	Floor (bottom)		**Floor (top)**	
$\mathbf{C_{min;b}}$	40	mm	40	mm
$\mathbf{C_{min;dur}}$	45	mm	45	mm
$\mathbf{\Delta C_{dev}}$	10	mm	5	mm
$\mathbf{C_{nom}}$	55	mm	50	mm
$\mathbf{C_{applied}}$	**90**	**mm**	**85**	**mm**
$\mathbf{k_x}$	1,64	mm	1,70	mm

The k_x factor seen in Table 6 represents the ratio of applied and required concrete cover. The maximum crack width can be increased by this factor, which in this case was required since the crack widths would otherwise have been too large.

Table 7: Reinforcement layout longitudinal

Layer	Reinforcement		Depth	
1	ϕ25-150	mm	114	mm
2	ϕ40-150	mm	1464	mm
3	ϕ40-150	mm	1544	mm
4	ϕ40-150	mm	1624	mm

Table 8: Reinforcement layout transverse

Layer	Reinforcement		Depth	
1	ϕ25-150	mm	128	mm
2	ϕ40-1050	mm	1512	mm
3	ϕ32-150	mm	1588	mm

Table 9: Shear reinforcement layout

Layer	Reinforcement	
Shear	ϕ16-300 (4 legs per meter)	mm

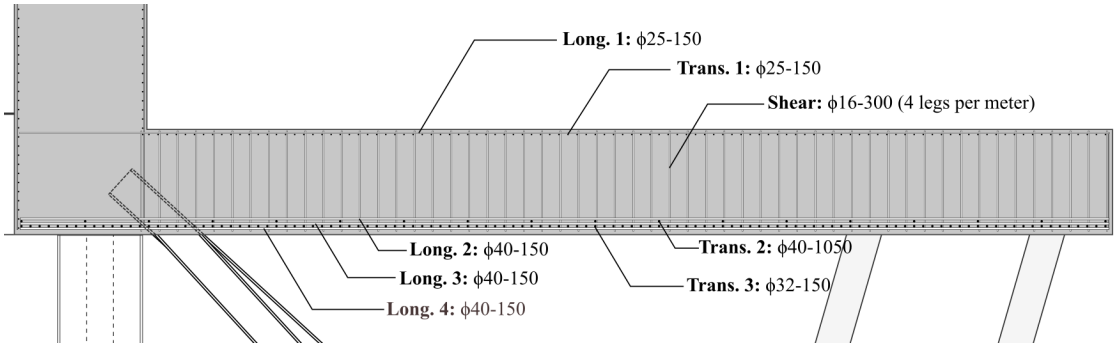

Figure 29: Relieving platform floor reinforcement

4.2.4 Current design: Loads

The load cases imposed on the superstructure of the SIF2 quay wall are described below. These load cases have been derived from the documentation of the original calculations. In addition, both a current and a future scenario are considered. This results in two sets of versions for certain load cases. This has been done to ensure a future proof design. The load cases are divided into the permanent loads cases (PL) and the varariable load cases (VL).

PL1 - Selfweight

The concrete used in the relieving platform has a density of 2.500 kg/m^3. The self-weight is calculated using this value for the entire structure, meaning differences caused by the reinforcement steel and other elements are neglected.

PL2 - Soil loads

These include those loads resulting from the weight of the soil. The loads cause a pressure both vertically and horizontally. Two different volumetric weights are considered:

- Dry soil Y_{dry} = 18 kg/m$_3$.
- Wet soil Y_{wet} = 20 kg/m$_3$.
- Soil pressure factor k_h = 0,5.

The water level relative to the top of the floor has been assumed to be at 0,5 m for SLS/ULS load cases and at 1,64 m for accidental load cases (not considered in this thesis).

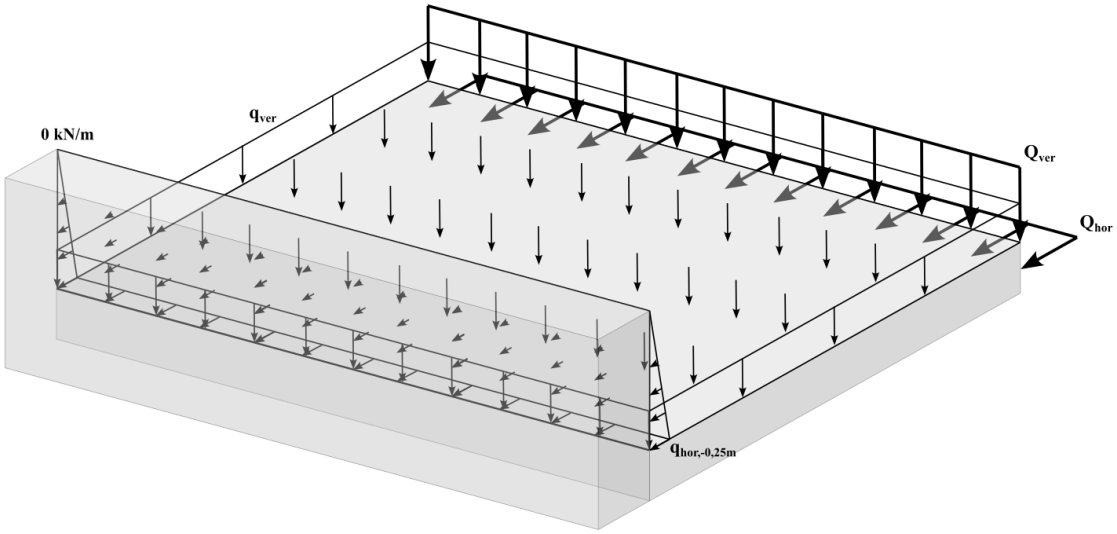

Figure 30: Load case PL2

PL3 - Geotechnical loads

For the current SIF2 quay wall, geotechnical calculations have been made in Plaxis (Schouten & van der Valk, 2020) which give values for the loads of the interaction between the sub- and superstructure. These loads are shown in Tables 10 and 11. The table gives the load for the ULS and SLS, and for a current and future scenario. Since the loads of the current scenario are considered to be on the high end for a quay wall, the future scenario looks at the effects of lower geotechnical loads.

Table 10: Geotechnical loads - Current - Loads per pile

	Combi-wall	**MV-Pile**	**Pile row 1**		**Pile row 2**	
	$\mathbf{F_{hor}}$ **kN**	$\mathbf{F_{axial}}$ **kN**	**M kNm**	$\mathbf{F_{hor}}$ **kN**	**M kNm**	$\mathbf{F_{hor}}$ **kN**
SLS	1.584	221	173	245	196	1.457
ULS	2.039	444	325	521	415	3.596

Table 11: Geotechnical loads - Future - Loads per pile

	Combi-wall	**MV-Pile**	**Pile row 1**		**Pile row 2**	
	$\mathbf{F_{hor}}$ **kN**	$\mathbf{F_{axial}}$ **kN**	**M kNm**	$\mathbf{F_{hor}}$ **kN**	**M kNm**	$\mathbf{F_{hor}}$ **kN**
SLS	1.239	176	132	184	138	1.014
ULS	1.463	317	216	354	251	2.158

PL4 - Shrinkage

Shrinkage was considered in the calculations of the current structure, but will be neglected in this thesis for simplicity reasons.

VL1 - Terrain loads - Current

The terrain loads include the weight of all equipment, storage, traffic and other infrastructure on top of the surface. A singular value is used to represent these components. The

current distributed terrain load used is a q_{ver} of 100 kN/m^2, with a horizontal coefficient k_h of 0,5. In addition, a part of the loads behind the floor as assumed to distribute via the soil to the edge of the floor at an angle of 24°. This results in a distributed line load $Q_{ver,floor} = q_{ver} \cdot 5,35 \cdot tan(24)$.

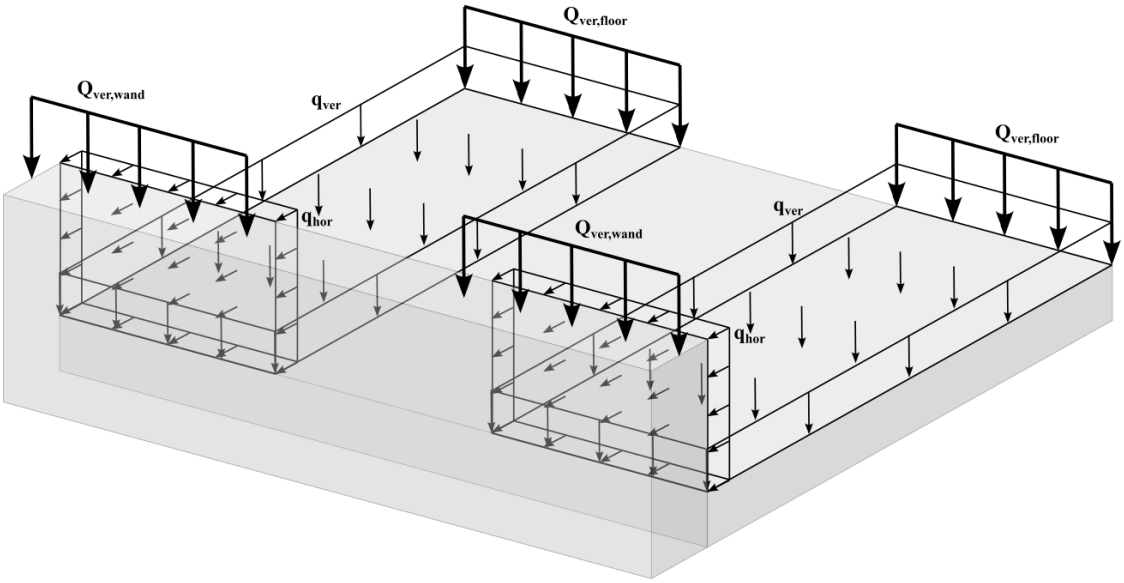

Figure 31: Load case VL1.1

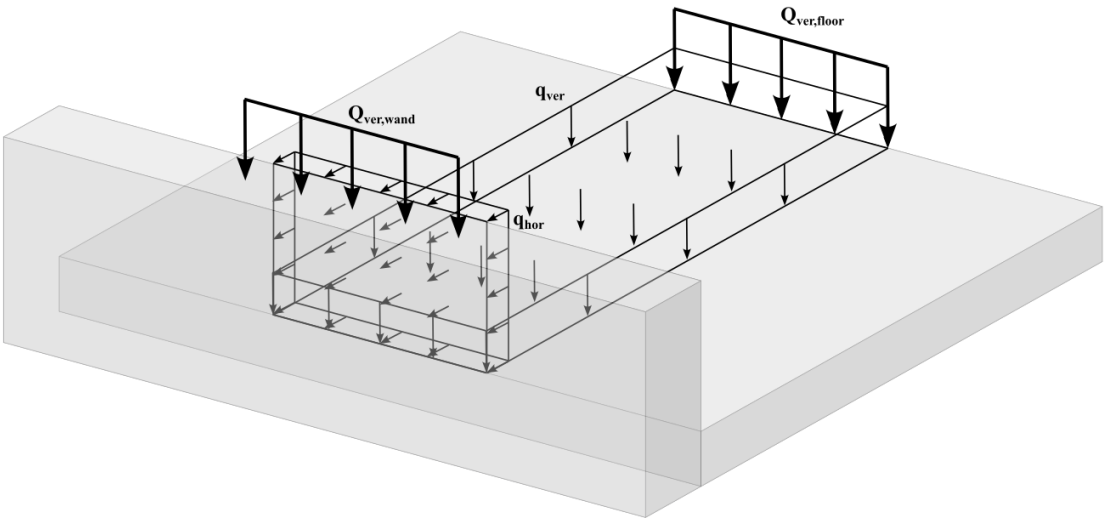

Figure 32: Load case VL1.2

VL2 - Terrain loads - Future

The future terrain load considered is a q_{ver} of 40 kN/m^2, with a horizontal coefficient k_h of 0,5. The future loads are lower, since the current use case of the quay wall, namely the offshore wind turbine foundation piles, impose higher loads than conventionally considered.

VL3 - Bollard loads - Current

The loads imposed by the ship on the bollards. Bollards are the short posts on top of the quay wall, which are used to attach the ship to when moored. The bollards are located on top of the wall of the relieving platform, with a center to center distance of 15,4 m. In

the current scenario, one bollard, per bollard position is considered. The maximum loads per bollard considered is 2.000 kN, which is imposed on a height of 0,5 m above the wall, also resulting in an additional moment.

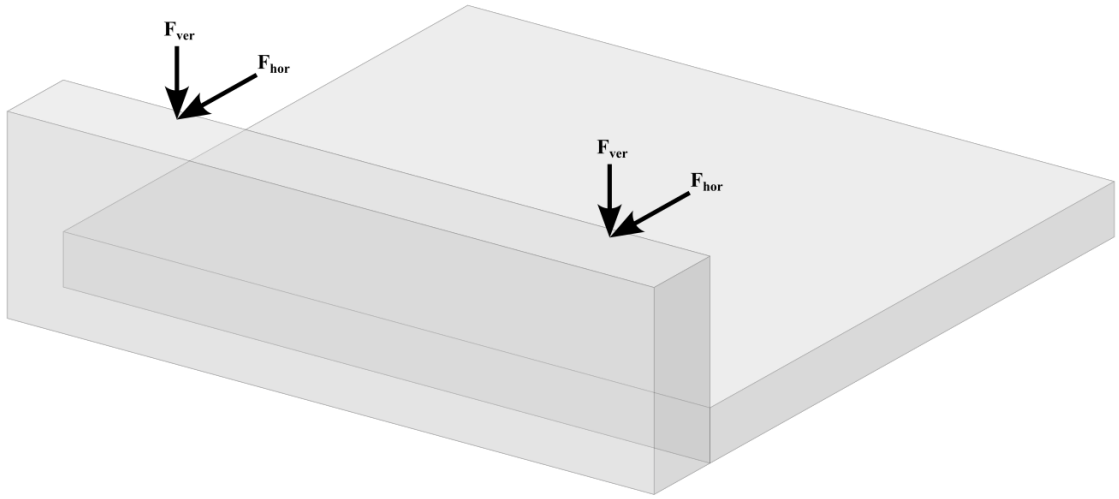

Figure 33: Load case VL3

VL4 - Bollard loads - Future

In the future scenario, two bollards per bollard position are considered, with a distance of 2,5 m between each bollard within one bollard position. The maximum load per bollard is still 2.000 kN, but in the case where both bollard pairs are being loaded at the same time, it is considered that one is loaded for a 100% and the other 70%. The loads are again both imposed at 0,5 m above the wall.

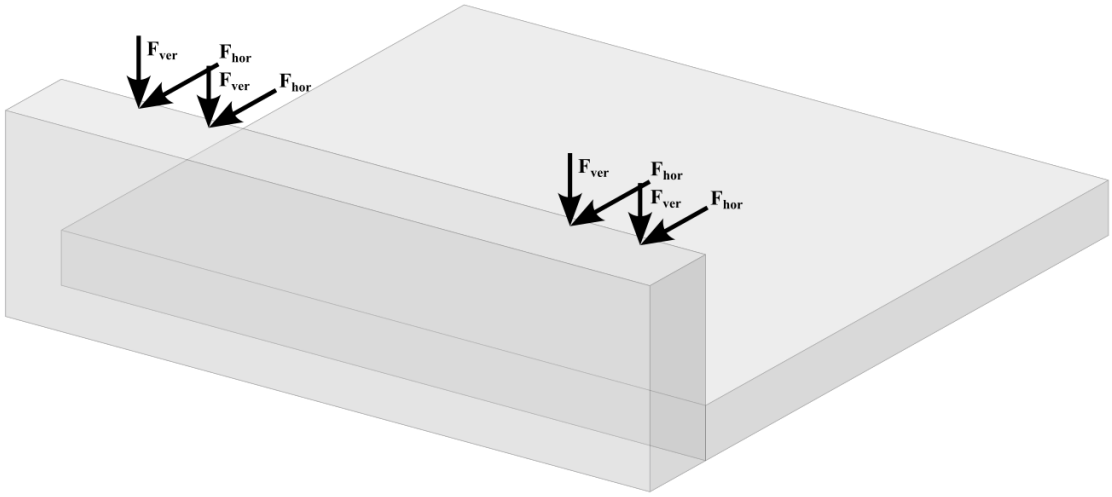

Figure 34: Load case VL4

VL5 - Impact loads

An impact load of 2.000 kN over a surface of 0,5 x 0,5 m on the top of the wall is considered. This load spreads to the center of the wall with a 1:1 ratio. This means that on the center of the wall, the load is spread over an area of:

- $h_{spread} = 0{,}5 + 0{,}5 \cdot 2{,}2 = 1{,}6$ m

- $b_{spread,edge} = 0{,}5 + 0{,}5 \cdot 2{,}2 = 1{,}6$ m
- $b_{spread,middle} = 0{,}5 + 2 \cdot 0{,}5 \cdot 2{,}2 = 2{,}7$ m

The figure shows three different variants of the load case that are considered, namely VL5.1, VL5.2 and VL5.3.

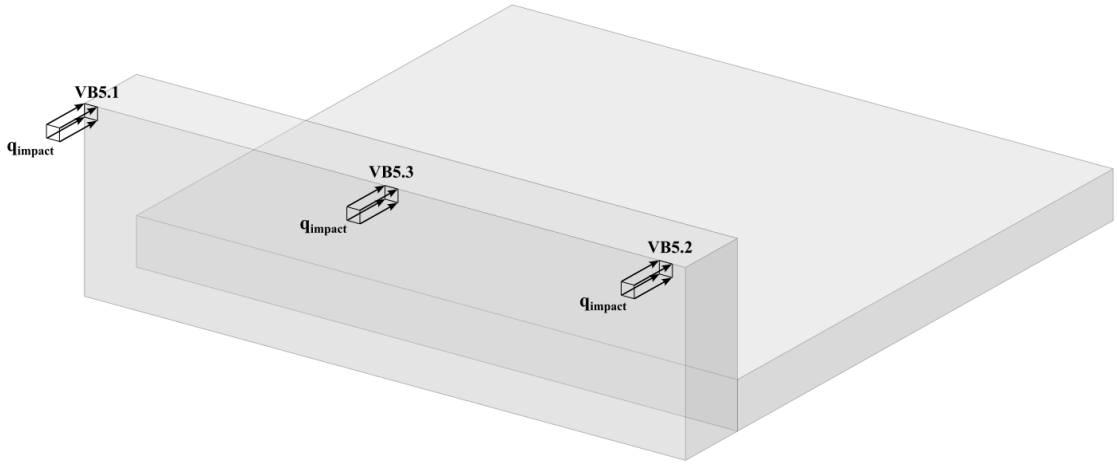

Figure 35: Load case VL5

VL6 - Collision loads

An impact load of 10.000 kN over a surface of 5 x 5 m on the top of the wall is considered. This load spreads to the center of the wall with a 1:1 ratio. This means that on the center of the wall, the load is spread over an area of:

- $h_{spread} = 5 + 0{,}5 \cdot 2{,}2 = 6{,}1$ m
- $b_{spread,edge} = 5 + 0{,}5 \cdot 2{,}2 = 6{,}1$ m
- $b_{spread,middle} = 5 + 2 \cdot 0{,}5 \cdot 2{,}2 = 7{,}2$ m

Again three different variants of the load case that are considered, namely VL6.1, VL6.2 and VL6.3.

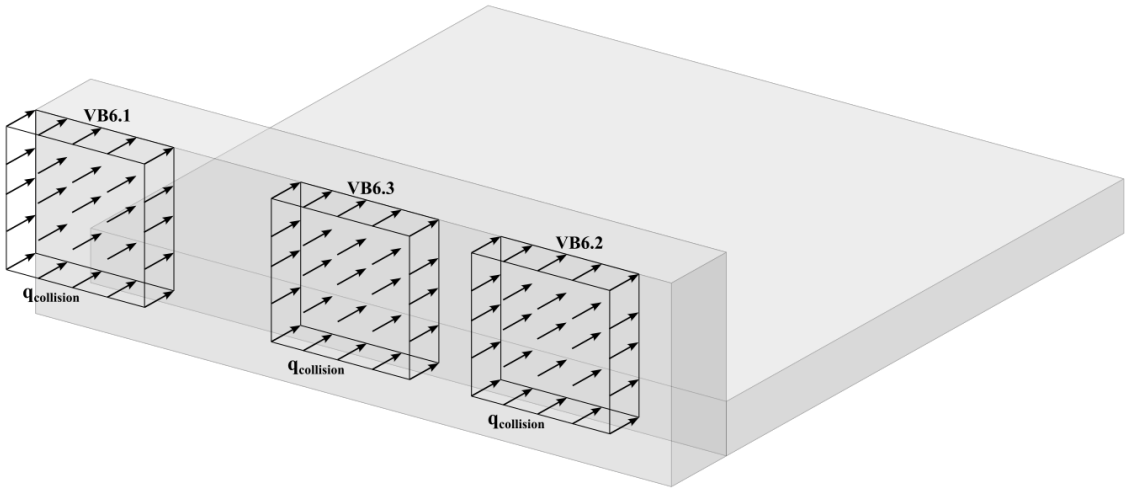

Figure 36: Load case VL6

VL7 - Crane loads - Future

In the current design of the quay wall, a rail crane is not needed. A future scenario where such a crane is included in the analysis. The crane loads are imposed at 3,0 m from front edge of the wall. The loads can be seen in Table 12. The distributed line load is assumed to include all different loading scenarios of the crane.

Table 12: Future crane loads

Vertical load		**Horizontal load**		**Moment**	
1.500	kN/m	225	kN/m	2.850	kN/m

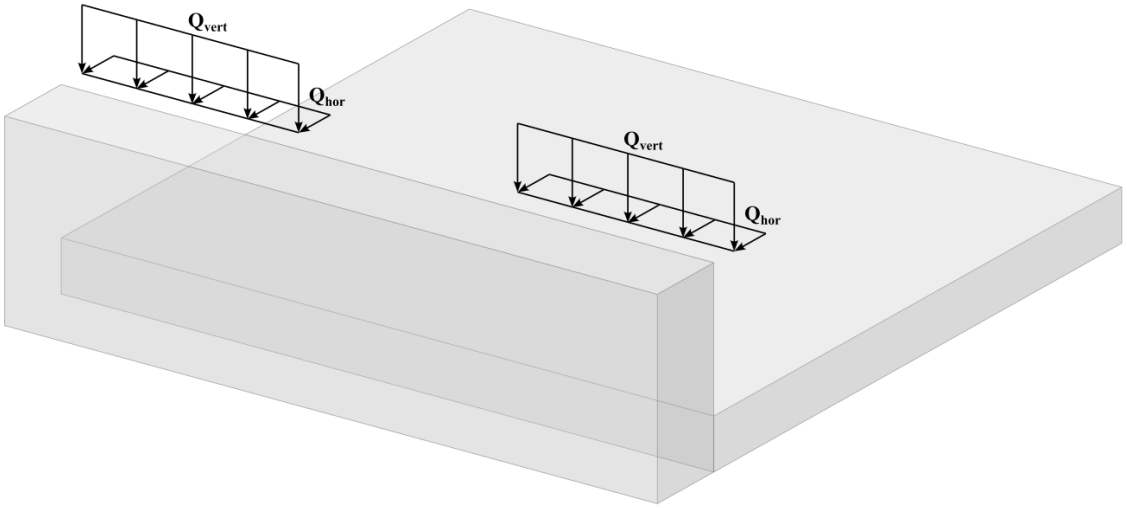

Figure 37: Load case VL7.1

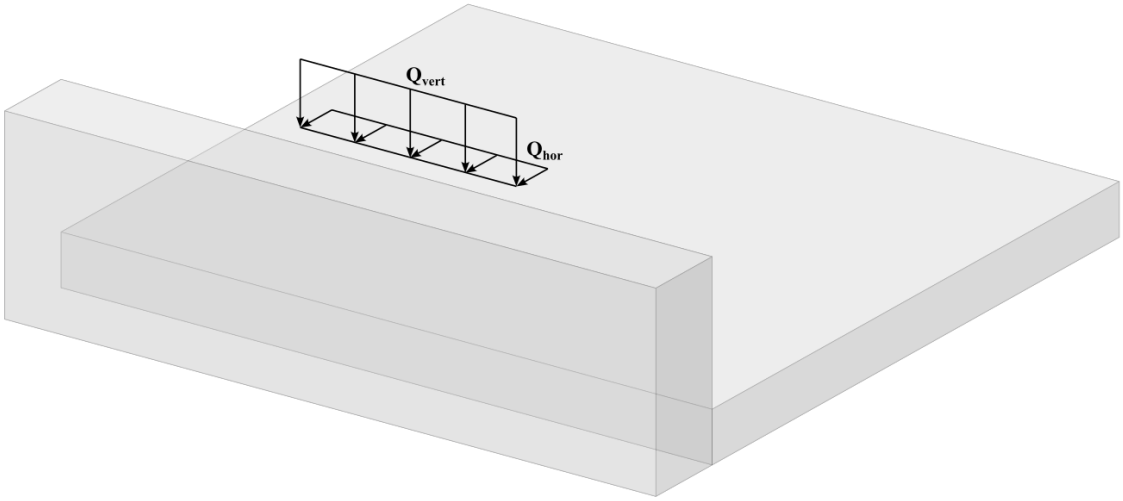

Figure 38: Load case VL7.2

4.3 Analytical model

In order to analyze the current structure and investigate the possibilities of applying prestressing to creating a more slender cross-section and designing a modular relieving platform an analytical model has been made. This analytical model is a simplification of the structure to a 2D EB beam model (Section 3.1). The 2D model will represent a single segment of the relieving platform of 23 m. This thesis will look into just the resistances and loads within the floor. The wall will for the most part be left outside of the scope of the thesis and is only considered for the loads imposed on the floor.

4.3.1 Geometry and supports

The geometry of the analytical model is shown in Figure 39. In this model the horizontal elements are considered to have a cross-section of 1.750 x 23.000 mm and the vertical element a cross-section of 2.200 x 23.000 mm. The material properties coincide with those mentioned in Section 4.2.

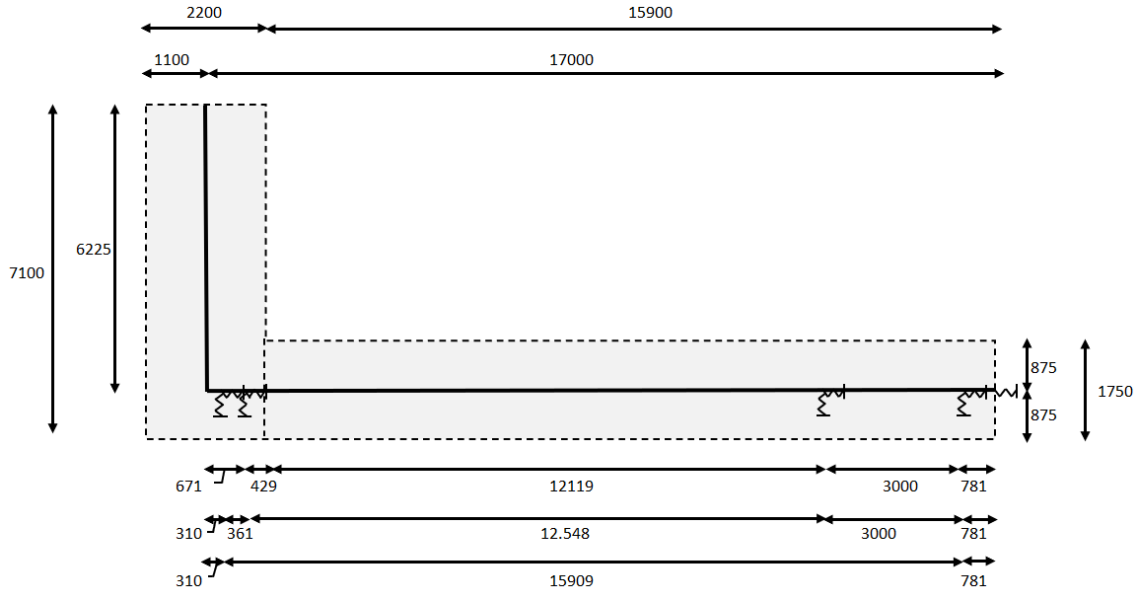

Figure 39: Analytical model 2D

This analytical model is further simplified to make the calculations (Figure 40). As can be seen, the simplified model removes the vertical element and the cantilevers at both ends. These removed elements are then added as loads to the simplified model instead, adding additional bending moments and forces to the sections A and D. The final analytical model now consists of four spring supports (A,B,C and D) with a horizontal and vertical component and three elements (respectively 1, 2 and 3).

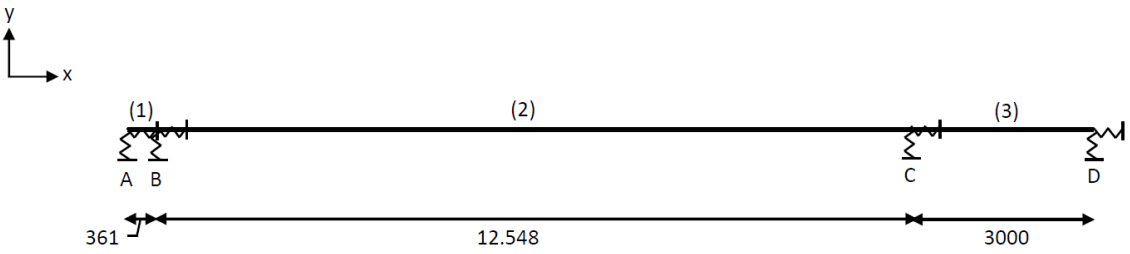

Figure 40: Simplified analytical model

The supports A through D are all springs with both a horizontal and vertical component. These springs respectively represent the combiwall, the anchor and the foundation

piles. The values of their stiffness represent the interaction between the substructure and the superstructure. The stiffnesses of each individual component are derived from the calculations that have been made in Plaxis (Schouten & van der Valk, 2020). The values that results from the Plaxis calculations are shown in Appendix A.

As can be seen these values have a upper and a lower bound, as well as a active and passive value. The upper and lower bound values represent a soil with a high and low stiffness respectively. In the analysis both cases have been taken into account, to determine which case results in the highest governing loads.

The springs have bi-linear, stepwise load displacement curves. To further simplify the system, only the initial passive stiffness values have been used. A spring over the entire length of the edge of the floor on the right end (Figure 39) represents the resistance of the soil. This spring only has a value for compression in horizontal direction. The table shows the axial and horizontal stiffness values in the local axis. To use these values for the simplified analytical model, the horizontal and vertical components of these stiffnesses are recalculated for the global axis. These stiffnesses are then also recalculated to represent a single spring stiffness for the entire 23 meter segment. This is done by multiplying the stiffness by the amount of piles at each spring location. The final spring horizontal and vertical stifnessess of the analytical supports are shown in Table 13 and 14.

Table 13: Spring constants analytical model, upper bound

	Support A	**Support B**	**Support C**	**Support D**	**Soil**
$\mathbf{k_H}$**[kN/m]**	21,56	625,88	514,41	534,13	7.743
$\mathbf{k_V}$**[kN/m]**	5.099,50	625,70	1.843,32	1.838,39	-

Table 14: Spring constants analytical model, lower bound

	Support A	**Support B**	**Support C**	**Support D**	**Soil**
$\mathbf{k_H}$**[kN/m]**	10,78	311,17	262,32	272,18	3.870
$\mathbf{k_V}$**[kN/m]**	2.549,75	311,08	942,29	939,83	-

4.3.2 Loads considered in the analytical model

Load cases

All the loads mentioned in 4.2.4 will need to be recalculated to suit the 2D elements. All the loads are calculated in terms of the loads seen in Figure 41. These calculations are shown in Appendix B.

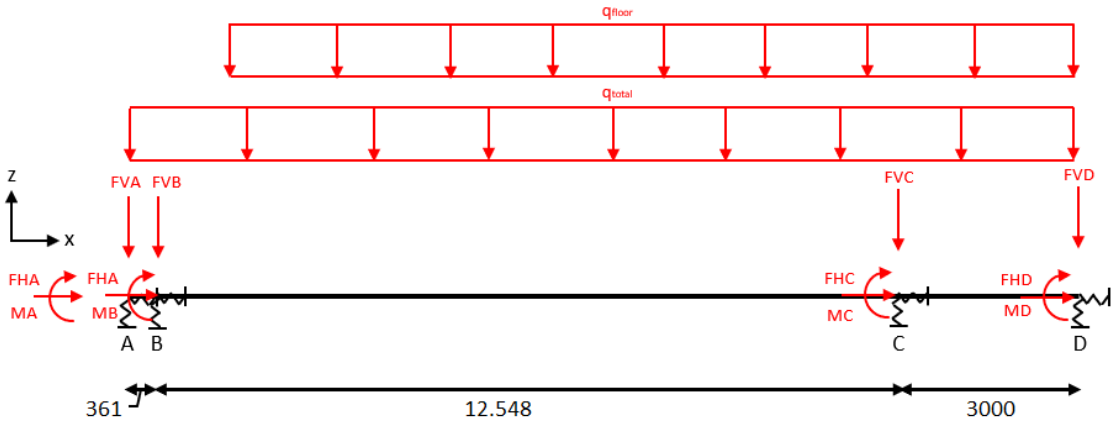

Figure 41: Analytical model loads

The normal forces in the elements are influenced by the horizontal spring stiffnesses, seen in Tables 13 and 14. They can be calculated by considering the springs as a parallel spring system. By summing all horizontal spring stiffnesses and then determining the contribution of each spring to the total, this ratio can be used to then calculate how much of the horizontal forces is taken by the specific springs. First the total horizontal stiffness $k_{H,total}$ is calculated by summing all the individual horizontal spring stiffnesses k_{HA} to k_{HD} of each support.

$$k_{H,total} = k_{HA} + k_{HB} + k_{HC} + k_{HD} \tag{25}$$

The total horizontal force $F_{H,total}$ is calculated by summing all the horizontal forces on each of the supports. From this the horizontal reaction forces R_{HA} to R_{HD} are calculated as the contribution of each spring stiffness to the total horizontal stiffness.

$$F_{Htotal} = F_{HA} + F_{HB} + F_{HC} + F_{HD} \tag{26}$$

$$R_{HA} = \frac{k_{HA}}{k_{total}} \cdot F_{Htotal} \tag{27}$$

$$R_{HB} = \frac{k_{HB}}{k_{total}} \cdot F_{Htotal} \tag{28}$$

$$R_{HC} = \frac{k_{HC}}{k_{total}} \cdot F_{Htotal} \tag{29}$$

$$R_{HD} = \frac{k_{HD}}{k_{total}} \cdot F_{Htotal} \tag{30}$$

The normal force within each element can then be calculated based on these values.

$$N_1 = R_{HA} - F_{HA} \tag{31}$$

$$N_2 = R_{HB} - F_{HB} + N_1 \tag{32}$$

$$N_3 = R_{HC} - F_{HC} + N_2 \tag{33}$$

Load combinations

The load combinations are shown in Appendix C. Within certain load cases, multiple variants exist. An example of this is the application of the terrain loads (VB1/2) in different locations, rather than only over the entire system. In the 3D model used for the original calculations, this has been done to create unfavorable load conditions also in the transverse direction. For the 2D model used in this analysis this does not always give the same result, since the loads in transverse direction are not taken into account.

To determine the governing load combinations, a Python script has been used (Appendix E Section E.1). This Python script uses the AnaStruct package (Vink, 2018), which allows for a basic structural analysis to be performed. The script is used to quickly iterate through all the different load combinations and return those that are governing. The governing load combinations that result from the python analysis will be further analyzed using Maple scripts.

4.4 Results

An initial analysis of the current relieving platform structure has been performed, according to the methods described in Chapter 3 and using the loads and properties described in this chapter.

The load combinations that where found to be governing are SLS load combination 1.3 and the ULS combination 3.12, both combinations using the lower bound of the spring stiffnesses. Table 15 shows the resulting loads of each combination and Table 16 shows the

load factors of each load combination. These are the load combinations that will be used in the analysis in the rest of the thesis. The values in this table are for one segment (of 23 m). In addition, it was found that the sum of the horizontal forces that are imposed on the structure all work in the negative x direction. This means that the spring at the right end of the floor representing the soil stiffness does not have an effect on the normal forces, since it only has a value for compression. This spring will not be further taken into account in the rest of the analysis.

Table 15: Governing load combinations (per 23 m segment)

	SLS 1.3	**ULS 3.12**	
$\mathbf{q_{total}}$	1.006	1.208	kN/m
$\mathbf{q_{floor}}$	3.381	6.127	kN/m
$\mathbf{M_A}$	-13.475	-39.123	kNm
$\mathbf{F_{VA}}$	10.717	17.414	kN
$\mathbf{F_{HA}}$	-17.314	-27.282	kN
$\mathbf{M_B}$	0	0	kNm
$\mathbf{F_{VB}}$	-5.151	-12.714	kN
$\mathbf{F_{HB}}$	-5.151	-12.714	kN
$\mathbf{M_C}$	-1.768	-3.552	kNm
$\mathbf{F_{VC}}$	0	0	kN
$\mathbf{F_{HC}}$	-1.384	-2.600	kN
$\mathbf{M_D}$	-7.504	-15.301	kNm
$\mathbf{F_{VD}}$	8.810	17.115	kN
$\mathbf{F_{HD}}$	-4.167	-6.439	kN

Table 16: Governing load combinations factors

	PL1	**PL2**	**PL3.1**	**PL3.2**	**PL4**	**VL1.1**	**VL1.2**	
SLS 1.3	1	1	1	-	1	0,5	0,5	
ULS 3.12	1,2	1,2	-	1	-	1,5	1,5	
	VL2.1	**VL2.2**	**VL3.1**	**VL3.2**	**VL3.3**	**VL4.1**	**VL4.2**	**VL4.3**
SLS 1.3	-	-	-	-	-	-	-	-
ULS 3.12	-	-	-	1,05	-	-	-	-
	VL5.1	**VL5.2**	**VL5.3**	**VL6.1**	**VL6.2**	**VL6.3**	**VL7**	**VL8**
SLS 1.3	-	-	-	-	-	-	-	-
ULS 3.12	-	1,05	-	-	-	-	-	-

Figure 42 shows the internal load and displacement diagrams of the initial model.

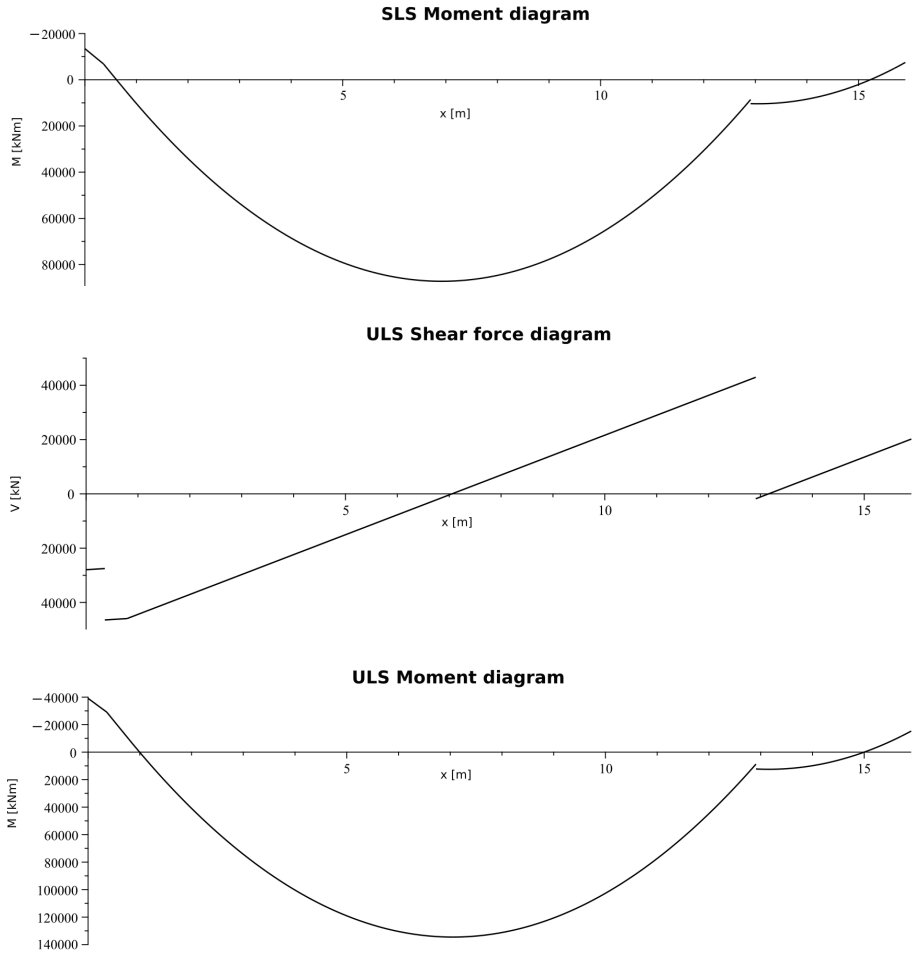

Figure 42: Analysis force diagrams (per 23 m)

The normal forces for each element calculated according to Section 4.3.2 are shown in Table 17.

Table 17: Normal forces in each element (per 1 m)

	Element 1	**Element 2**	**Element 3**	
ULS	1.159	938	398	kN
SLS	737	519	206	kN

The results of the resistance checks are shown in the tables below. The ULS bending moment has been checked at the largest sagging moment (1) and the largest hogging moment in the floor (2). The shear resistance has been calculated at the start of the floor (1) and the first row of foundation piles (2). The crack-widths have been calculated also at the location of the largest sagging moment (1) and the largest hogging moment (2).

Table 18: ULS Bending moment resistance (per 1 m)

Cross-section	**1**	**2**	
$\mathbf{M_{Ed}}$	5.848	-407	kNm
$\mathbf{N_{Ed}}$	938	398	kN
$\mathbf{M_{Rd}}$	14.260	2.199	kNm
u.c.	0,41	0,19	

Table 19: ULS Shear resistance (per 1 m)

Cross-section	**1**	**2**	
$\mathbf{V_{Ed}}$	1.793	1.522	kN
$\mathbf{N_{Ed}}$	938	938	kN
$\mathbf{V_{Rd,c}}$	383	383	kN
u.c.	4,68	3,98	
$\mathbf{V_{Rd,s}}$	2.001	2.001	kN
u.c.	0,90	0,76	

Table 20: Crack width check (per 1 m)

Cross-section	**1**	**2**	
M	3.793	-166	kNm
N	519	206	kN
w	0,25	0,14	mm
u.c.	0,76	0,40	

4.5 Verification

The analytical model has first been verified to ensure the model set up in Maple works accordingly. The results of this verification can be found in Appendix G Section G.1.

Since the analytical model has several simplifications compared to the original calculations, differences between the two models will inherently arise. Table 21 and 22 show the differences between the governing loads of the analytical model and those of original the 3D numerical SCIA model. In the original model a division was made between the floor and the wall. There are therefore separate values for the maximum loads in the floor and those in the walls. The loads mentioned below are only those of the floor. In the analytical model the floor starts at x = 0,79 m. This means that only the values of the forces after this are taken into account. It was found that the lower bound stiffness values gave the higher loads and also came closer to the results of the original models.

Table 21: Differences analytical and original model in the floor (SLS)

	Analytical		**Original**		**Difference**	
Positive moment M+	3.792	kNm	4.436	kNm	15	%
Negative moment M-	-166	kNm	-385	kNm	57	%
Normal force N	519	kN	830	kN	37	%

Table 22: Differences analytical and original model in the floor (ULS)

	Analytical		**Original**		**Difference**	
Positive moment M+	5.848	kNm	7.264	kNm	19	%
Negative moment M-	-407	kNm	-821	kNm	50	%
Shear force V	1.793	kN	2.068	kN	13	%
Normal force N	938	kN	1.795	kN	48	%

The differences have two main reasons, those stemming from the difference in the type of model used (2D to 3D) and those caused by the differences in applied loads. Because it is difficult to quantitatively evaluate the differences between the two models, the differences will only be described qualitatively. The model differences have been taken into account in the optimization of the relieving platform floor. This is further addressed in Section 6.2.1.

4.5.1 Model difference

- Inherent differences between 2D and 3D models.
- The supports in the analytical model would actually represent a line support in the 3D SCIA model, since a single support is taken for the entire width of the relieving platform. Whereas the supports of the SCIA model are individual point supports.
- The effects of the different support types can be seen in the governing moments for both SLS and ULS. The bending moments mid span are significantly closer to the original loads than negative moments are. This is caused by the fact that the negative loads are above the supports, which in the 3D model cause high concentrated loads. The expectation would be that the differences are bigger close to the supports compared to mid span, where the loads are inherently more evenly distributed.

4.5.2 Load differences

- One of the main differences in terms of the applied loads is that the unevenly distributed loads and point loads can have unfavorable effects in the transverse direction, while in the 2D model all loads are placed on the same location. There are no transverse loads.
- An example of this are the different versions of the terrain loads within one load case, that are applied on different parts of the floor to create an as unfavorable load case as possible. This cannot be done in the same way in the 2D model.
- The simplification of not taking into account temperature loads and shrinkage is also a contributor to the differences in the governing loads.

5 Prestressing

5.1 Design

5.1.1 Design choices

The type of prestressing this thesis will look into is post-tensioning. From the initial structural analysis it follows that the largest bending moments in the floor are for a large part caused by the high distributed loads of the selfweight, terrain and soil loads. It is therefore expected that a curved tendon path can give a large benefit to counteract these loads. The moment diagram also partly resembles that of a simply supported beam, the tendon path will also be designed accordingly. In addition, the goal is to create a relieving platform that can be added to the quay wall at a later stage in its use life. Only with post-tensioning can the wall be included in the prestressing, improving the connection between the floor and the wall. The main concept would then be to add ducts to the wall which are sealed off during the phase where the floor is not added, preventing corroding materials from entering the openings. Once the floor is added to the wall, these ducts are opened and the prestressing tendons are placed, running via the wall through the floor.

The prestressing will only be applied in x-direction (in the length of the floor). The largest loads on the structure are distributed in this direction and in addition, the intended modular design would from a practical view point not allow for the application of prestressing in the y-direction (to connect the modules to each other). Due to the way the relieving platforms are build next to each other, there is limited access and therefore also no possibility for prestressing in this direction.

The goal is to create a partially prestressed element. Partial prestressing means that the element allows limited cracking under SLS loading. This cracking should be limited to prevent the corrosion of the prestressing tendons and reinforcement steel. The reason this method is chosen, is because the main objective of this thesis is to reduce the carbon emissions of the floor. Partial prestressing gives a more lenient crack width requirement compared to full prestressing, which results in the possibility of a more economical solution to be found with less material usage.

Finding the optimal prestressing design is an iterative process. Initially multiple variants will be made using the current cross-section properties and reinforcement from which initial conclusions can be drawn. In Chapter 6 this design will be further optimized with the goal of finding a cross-section which uses as little concrete as possible.

5.1.2 Tendon layout

To counteract the mid span bending moments, a large distributed load is desired. To achieve this while limiting the required prestressing force and tendon diameter, an as small as possible radius is needed. A smaller radius (or a higher curvature) means a larger distributed load. The smallest possible radius of the tendon is based on the maximum height within which the tendon is allowed to be placed and the length of the tendon. The maximum height h_{max} is determined by the required concrete cover, the reinforcement present in the cross-section, the height of the cross-section itself and the movement of the tendon within the duct. The initially chosen prestressing tendons are bundled 7-wired strands. Their properties are displayed in Table 23.

In addition, there is also a minimum radius of the tendon (Eq. (34)) based on the diameter of the duct NEN 8670, article 7.4.1.2, Table 5. This results in a minimum radius of 3,5 m based on the duct diameter of 85 mm.

$$R \geq 40 \cdot \phi_{duct} \tag{34}$$

Figure 43 shows how the maximum tendon height is built up. With the values of the reinforcement of the original cross-section mentioned in Section 4.2.3, the calculations for

Table 23: Tendon properties (Tensacciai, n.d.)

Material property		
Prestressing steel grade	FeP 1860	
Strand type	7 wire	
Number of strands $n_{strands}$	15	strands
Tendon area	2.250	mm^2
Equivalent diameter	75,89	mm
Tensile strength	1.860	N/mm^2
Young's modulus E_p	195.000	N/mm^2
Characteristic ultimate resistance F_{pk}	4.185	kN
Duct diameter ϕ	85	mm
Duct thickness	0.6	mm

the maximum tendon height for the original cross-section with a height of 1.750 mm can be made.

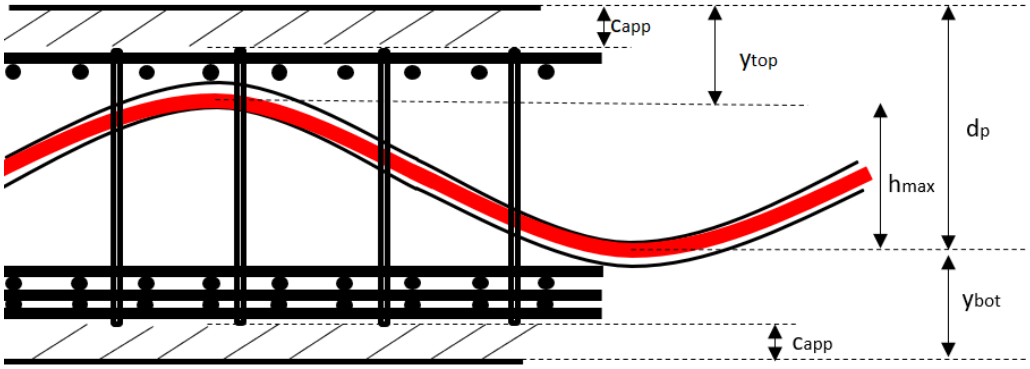

Figure 43: Maximum tendon height

$$y_{bot} = c_{app} + \phi_{stir} + \phi_{trans} + \phi_{long} + \phi_{duct} + t_{duct} + \phi_{eff}/2 \tag{35}$$
$$y_{bot} = 90 + 16 + (40 + 40) + (3 \cdot 40) + 85 + 0,6 + 75,89/2$$
$$y_{bot} = 353,65mm$$

$$y_{top} = c_{app} + \phi_{stir} + \phi_{trans} + \phi_{long} + \phi_{duct} + t_{duct} + \phi_{eff}/2 \tag{36}$$
$$y_{top} = 85 + 16 + 25 + 25 + 85 + 0,6 + 75,89/2$$
$$y_{top} = 198,65mm$$

$$h_{max} = h - y_{top} - y_{bot} \tag{37}$$
$$h_{max} = 1.198mm$$

The maximum tendon height is thus dependent on the height of the cross-section together with the reinforcement and concrete cover properties. Section 3.2 mentions that according to the ROK-0111 in the case where the cover is larger than 200 mm, the maximum allowable crack widths can be determined based on the first column of Table 7.1N of the NEN-EN 1992-1-1, National Annex, which means the same values as those for reinforced concrete can be used. In the case where the cover is smaller than 200 mm, the second column with the values specifically for prestressing has to be used. For this case, this means that on the bottom side the prestressing tendon always has a cover of that is greater than

200 mm, meaning the less strict requirements of w_{max} = 0,2 mm can be used. For the top of the relieving platform, depending on the exact tendon layout the cover can be less than 200 mm. In this case the maximum allowable crack widths becomes w_{max} = 0,1 mm. It thus needs to be checked whether the crack-width requirements are met, or if a larger distance from the top edge needs to be used.

The prestressing tendon needs a certain straight length at the anchors. This value is based on Rogowsky & Marti (1996) and determines the required straight length based on the characteristic ultimate resistance F_{pk}. This results in a length of 1 m.

It needs to be ensured that the ducts of the prestressing tendons are placed at a minimum distance from each other in the design according to NEN-EN 1992-1-1, article 8.10.1.3. Figure 44 shows the minimum distances that need to be present between them. Ideally the tendons are placed as low as possible, in order to achieve an as large as possible equivalent load. A maximum of 5 tendons can be placed next to each other per meter using this specific duct size.

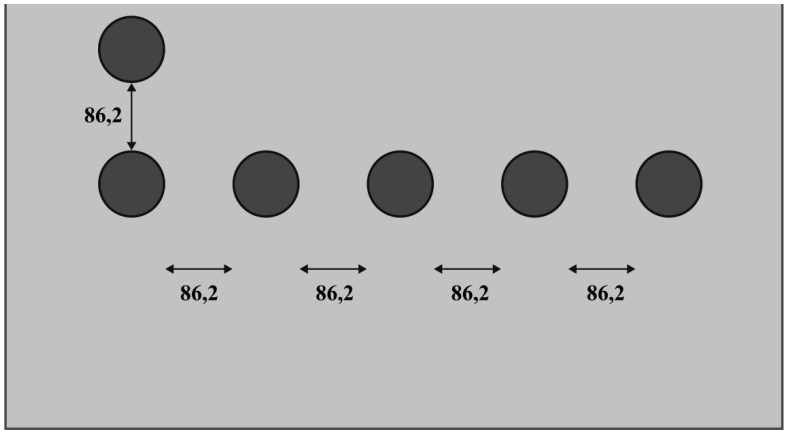

Figure 44: Prestressing ducts detailing

5.1.3 Prestressing force

In the case the prestressing tendon starts and ends at an angle, the horizontal force in the tendon is not equal to the applied prestressing force P, since the force has both a horizontal and vertical component (Section 2.3.2). In the analysis, as a simplification, the horizontal force due to prestressing is assumed to be equal to P. Since one of the objectives of the thesis is to reduce the cross-section height, as the height is reduced the difference between the horizontal component of the force P and the force P itself will also reduce. So when iterating towards the most optimal solution, this difference will reduce. The vertical component will be taken into account, since this gives an unfavorable load that can not be neglected.

Losses

The prestressing force used per tendon is based on the assumption that the total prestressing losses at $t = \infty$ is 20%. This includes both the immediate losses as well as the time dependent losses (shrinkage, creep and relaxation). The time dependent losses are estimated at 4%, based on Dieteren (2022).

The prestressing force is then calculated based on the prestressing tendon. The prestressing force applied will be iterated through in the analysis performed in Chapter 6, to find an optimal value. From the properties in Table 23 it can be seen that the area of one tendon is A_p = 2.250 mm^2. The applied force after all losses $P_{m,\infty}$ can then be calculated as 0,8 $\cdot P_{max}$. The value P_{max} can be calculated using $\sigma_{p,max}$ = 1.488 N/mm^2 according to NEN-EN 1992-1-1, article 5.10.2.1. This is then the prestressing force used for the initial

prestressing variants. When checking the effect of the prestressing force on the case before the other loads are applied (at t=0) the value for $P_{m,0}$ should be used instead, because this represents the prestressing force before time dependent losses. This can be calculated with $P_{m,0}$= 0,96·P_{max}. The prestressing forces per tendon are shown in the Table 24.

Table 24: Prestressing force per tendon

Time	**P_m**	
t = 0	3.214	kN
t = ∞	2.700	kN

5.2 Initial design variants

Several initial design variants are made to investigate the optimal prestressing layout for this specific structure. The initial designs will use the same cross-sectional properties as those used in the analysis of the current design of the relieving platform used in Chapter 4. The initial design variants are used to determine the effect of the prestressing loads on the structure and the resistance checks.

All the initial variants will apply one prestressing tendon (A_p = 4.500 mm^2) per meter, with the properties mentioned in Table 23. This means a prestressing force $P_{m,\infty}$ of 2.700 kN is applied. The specific equivalent loads are elaborated for each variant in the relevant sections and are shown in Appendix D Section D.1.

5.2.1 Variant 1

The first design variant will span a single curved tendon over the entire length of the relieving platform. Since the moment distribution found in the analysis of the current structure resembles that of a simply supported beam, it might be optimal to use one upwards distributed load over the entire cross-section. The loads imposed by this variant are shown in Figure 45.

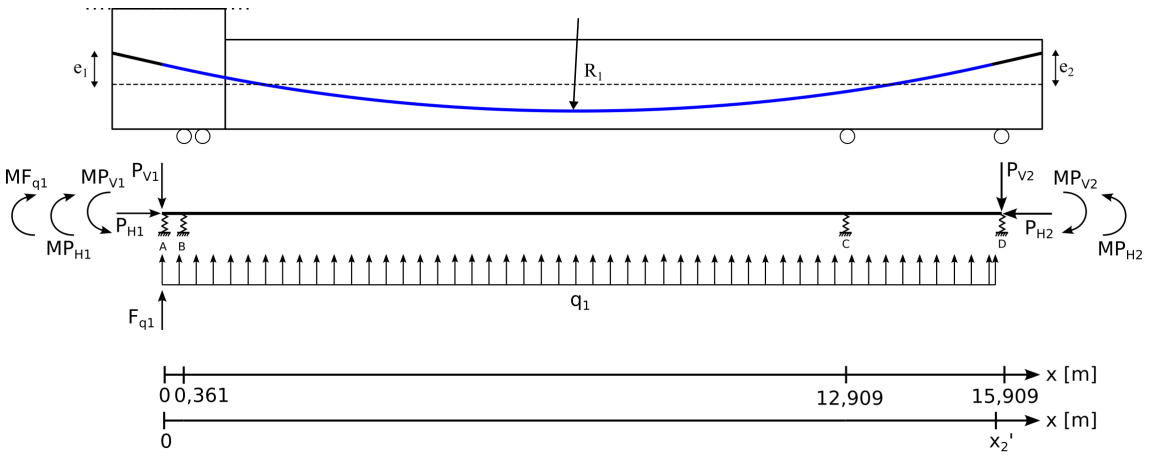

Figure 45: Initial prestressing - Var 1

Table 25: Variant 1: Main tendon properties

Floor thickness	1,75	m
R_1	36,22	m
e_1	0,61	m
e_2	0,61	m

Results

The results of this variant are shown in the figures below. As can be seen the shear forces and bending moment are all reduced significantly for both the ULS and SLS load combination. The governing loads in the floor for variant 1 are shown in Table 26 (starting from x = 0,790 m in the analytical model).

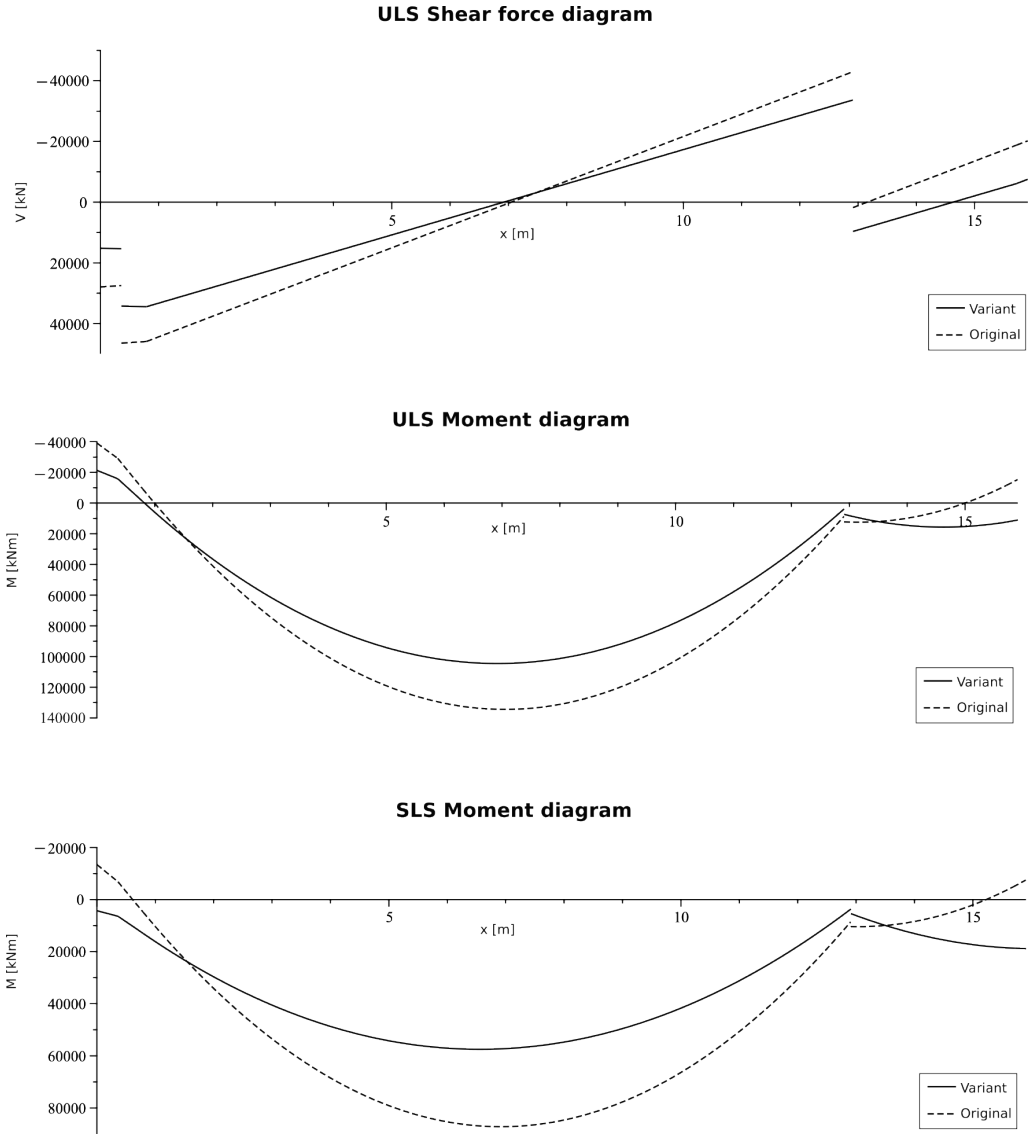

Figure 46: Prestressing variant 1 force diagrams

Table 26: Variant 1: Governing loads comparison (per 1 m)

	Initial		Variant 1		Reduction	
ULS V	1.793	kN	1.498	kN	16	%
ULS M+	5.848	kNm	4.544	kNm	22	%
ULS M-	-407	kNm	-	kNm	-	%
SLS M+	3.792	kNm	2.499	kNm	34	%
SLS M-	-166	kNm	-	kNm	-	%

5.2.2 Variant 2

The second design variant is shown in Figure 49. This prestressing design introduces two transition curves at each end of the relieving platform. The main curve will impose a higher distributed load over a shorter distance, as its radius decreases. This variant aims to investigate if applying a distributed load over a smaller part of the floor but with a higher value is more optimal compared to variant 1.

Since there are negative bending moments in the original structure on both ends of the floor, the downwards distributed loads caused by the two additional curves could also have a positive effect of countering these. In addition the shear forces shown to be present at the supports can be counteracted by the downwards force of these curves. Another expectation is that an upwards moment in section BC caused by the downwards distributed load in section CD has a positive effect. The behavior of the spring supports might influence this expectation.

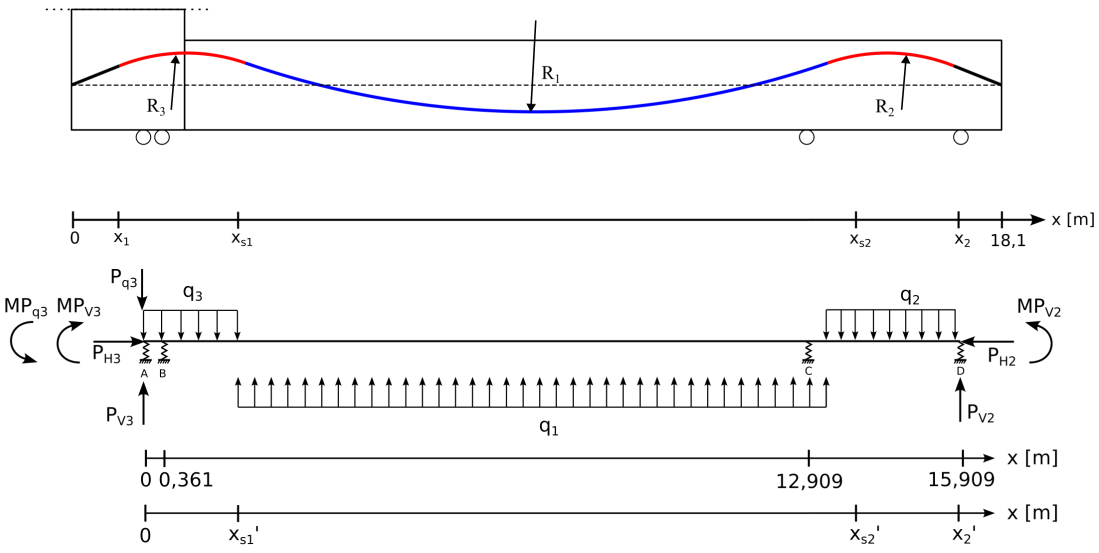

Figure 47: Initial prestressing - Var 2

Table 27: Variant 2: Main tendon properties

Floor thickness	1,75	m
R_1	17,31	m
R_2	3,5	m
R_3	3,5	m
e_1	0,00	m
e_2	0,00	m

Results

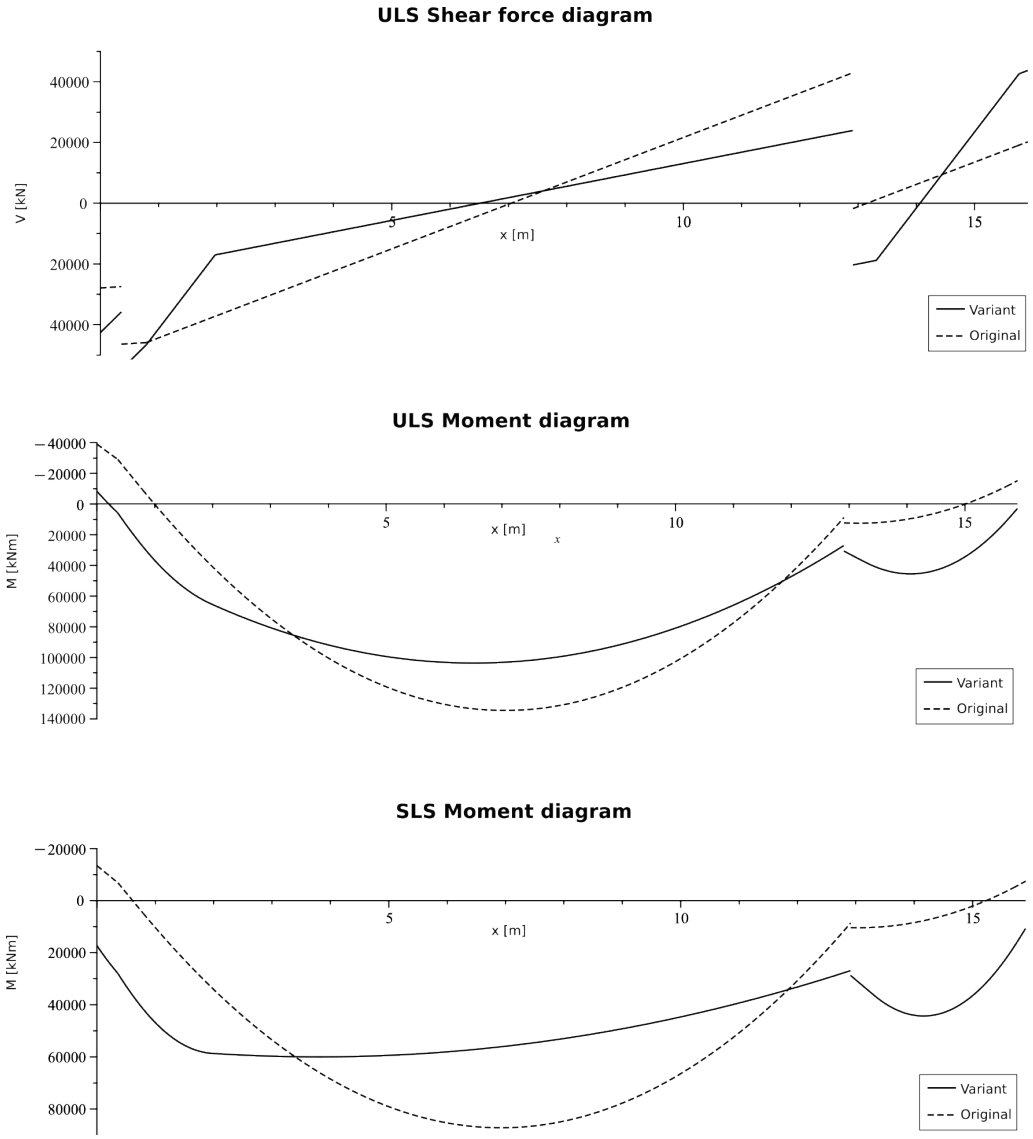

Figure 48: Prestressing variant 2 force diagrams

Table 28: Variant 2: Governing loads comparison (per 1 m)

	Initial		**Variant 1**		**Reduction**	
ULS V	1.793	kN	1.328	kN	26	%
ULS M+	5.848	kNm	4.506	kNm	23	%
ULS M-	-407	kNm	-	kNm	-	%
SLS M+	3.792	kNm	2.609	kNm	31	%
SLS M-	-166	kNm	-	kNm	-	%

5.2.3 Variant 3

A third variant is made based on the findings of the analysis of the current structure and the initial two variants. It was found that both in the original and prestressed structures, the shear resistance was governing. The crack-widths due to the reduction of the bending moments in combination with the compressive stress on the cross-section have been reduced so much that the unity checks now are far from that of the shear checks. This variant is a modification of the second variant, where the first transition curve R_3 is fixed to be above support A and B (the combi-wall and the anchor) and second transition curve R_2 is placed above support C (the first row of foundation piles). This is done to see if the largest shear forces can be further reduced by ensuring the downwards forces are transferred directly to the supports.

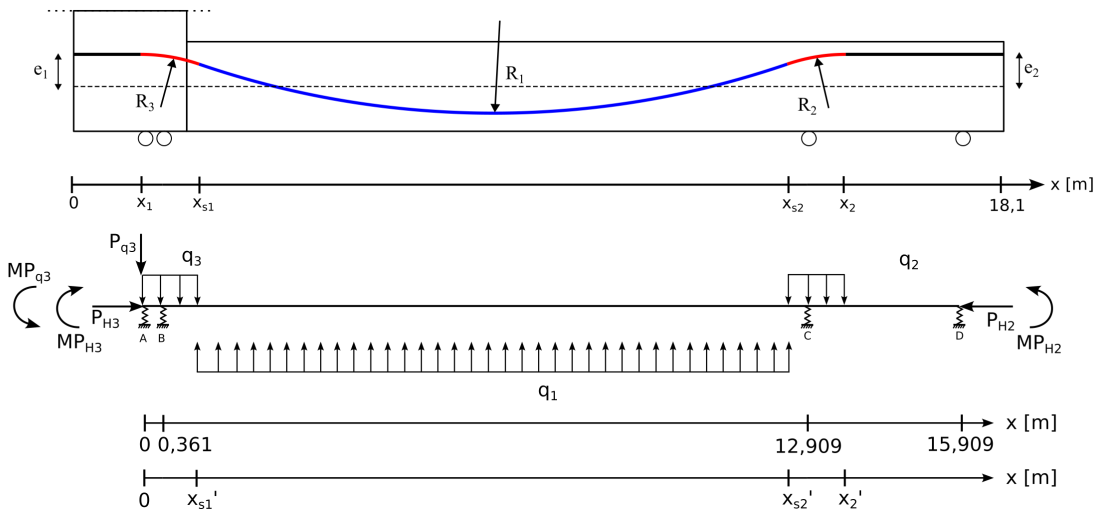

Figure 49: Initial prestressing - Var 3

Table 29: Variant 3: Main tendon properties

Floor thickness	1,75	m
R_1	17,85	m
R_2	3,5	m
R_3	3,5	m
e_1	0,63	m
e_2	0,63	m

Results

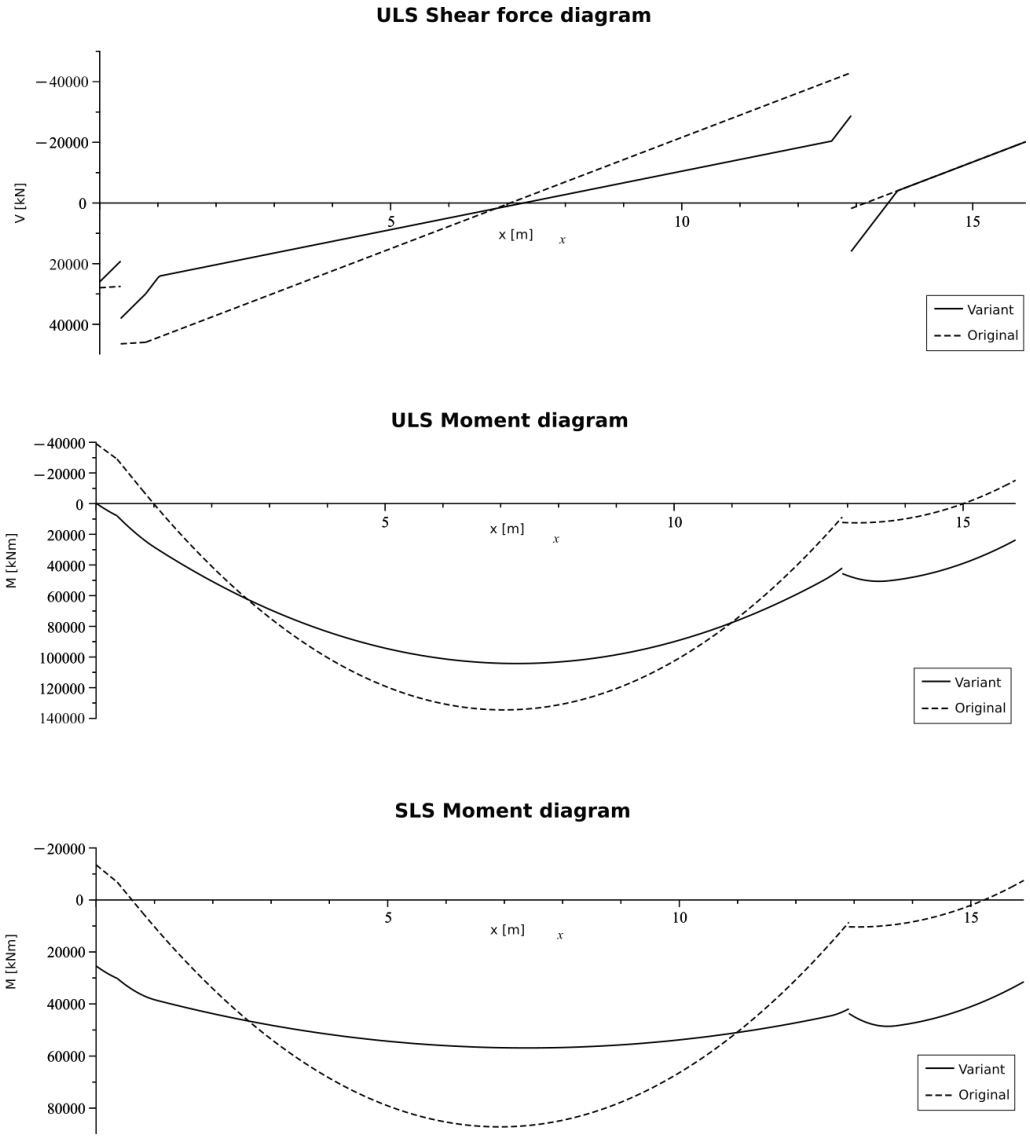

Figure 50: Prestressing variant 3 force diagrams

Table 30: Variant 3: Governing loads comparison

	Initial		Variant 1		Reduction	
ULS V	1.793	kN	980	kN	45	%
ULS M+	5.848	kNm	4.533	kNm	22	%
ULS M-	-407	kNm	-	kNm	-	%
SLS M+	3.792	kNm	2.473	kNm	35	%
SLS M-	-166	kNm	-	kNm	-	%

5.3 Discussion

The assumption that the downwards force caused by tendon curve R_2 in Variant 2 would provide a positive effect on the largest span BC seems not to be as beneficial as expected. There is no improvement of the largest bending moment mid span compared to the first variant. The main reason for this is most likely the spring supports. If one would compare a hinged support instead of spring supports, it is conceivable that curve R_2 would have been more beneficial. However, due to the downwards movement of the springs and their reaction forces, this is not the case.

The negative moments for all cases within the floor (starting from x = 0,790 m) are fully counteracted by the prestressing forces. These are positive initial findings in terms of the effectiveness of the prestressing variants and the prevention of large negative moments occurring due to the prestressing itself.

Variant 3 is shown the perform best in reducing the shear forces, which was intended for by its design. The shear forces can be reduced in two ways. First by the distributed prestressing load that counteracts the distributed imposed loads. Second by ensuring the transition curves are placed above the supports. This causes the downwards forces to be taken directly by the supports.

The findings give an initial idea of how the prestressing variants perform. The variants will be optimized and analyzed in the next chapter to find the prestressing design that gives the minimum slender height. The tendon layout as well as the prestressing force will varied, in order to find an optimal design.

6 Optimization

6.1 Description

The main objective of the thesis is to reduce carbon emissions by reducing material usage in the cross-section. This chapter describes the optimization that has been performed to achieve this. The first method (Section 6.2 and 6.3) is by creating a more slender cross-section. The prestressing forces have been shown in Section 5.2 to improve the cross-section resistance and reduce the crack-widths. This shows there is a margin to reduce the height. Once the cross-section height is reduced, the resistance of the cross-section and the forces due to prestressing change. Parametric optimization is used to find the lowest possible section height.

The second method (Section 6.4) is the removal of material from the cross-section. By creating an opening within the optimized floor of the first method, concrete around the neutral axis that does not contribute a significant amount to the resistance is removed. This will further reduce the material usage and in turn the carbon emissions. This second method is a manual approach, using the specific prestressing design and minimum height that results from the first optimization.

The prestressing variants of the analysis in Chapter 5 will be parametrized in order for them to be used in the optimization. For simplicity reasons, the tendon layout of the variants will be made dependent on two variables, namely the height of the cross-section h and the length of the main curve L_1. All the layout parameters such as the curve radii, the eccentricities and coordinates of the transition between two curves are then a result of these two parameters. Figures 51 to 53 show the boundaries of each variant within which they can vary. The optimization will in addition for the minimum possible height h, also look for the optimal L_1.

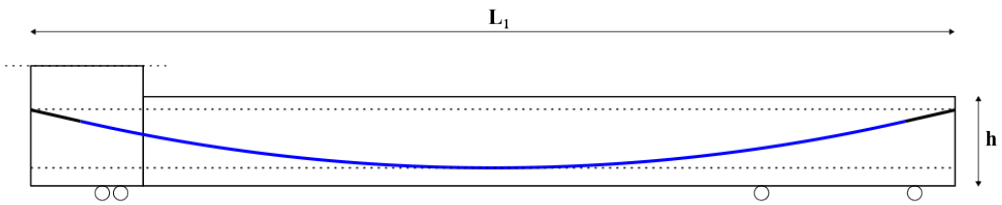

(a) Lower bound L_1 = 18,1 m

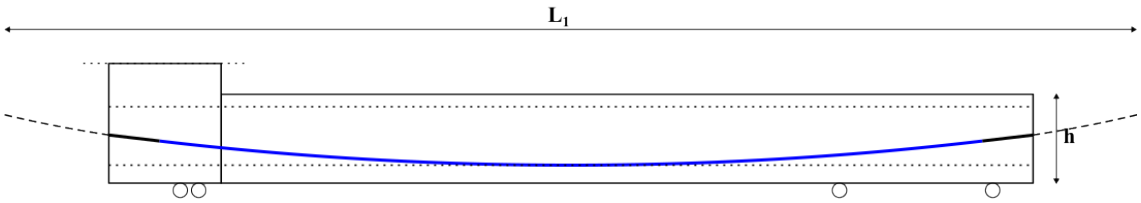

(b) Upper bound L_1 = 25,0 m

Figure 51: Variant 1 - L_1 parameter

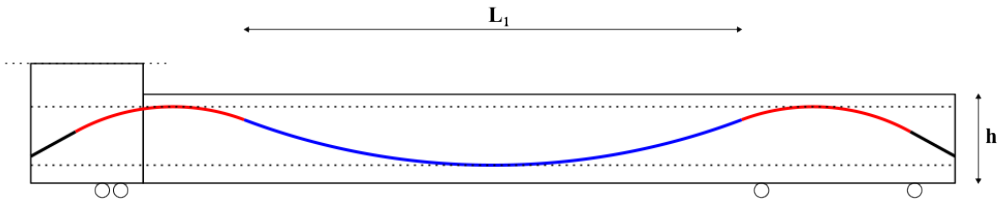

(a) Lower bound $L_1 = 11$ m

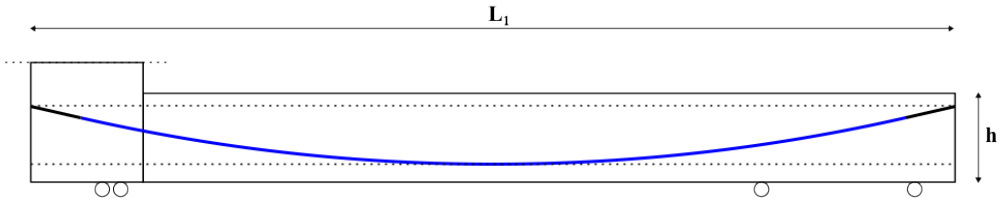

(b) Upper bound $L_1 = 18{,}1$ m

Figure 52: Variant 2 - L_1 parameter

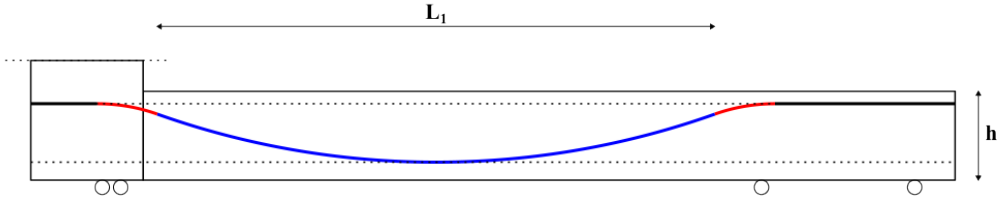

(a) Lower bound $L_1 = 12{,}0$ m

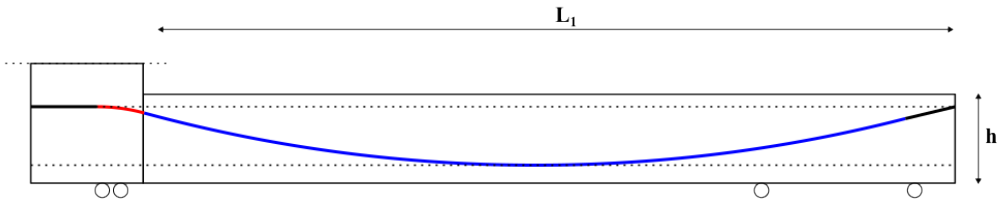

(b) Upper bound $L_1 = 16{,}2$ m

Figure 53: Variant 3 - L_1 parameter

6.2 Height reduction

6.2.1 Optimization method

The resistance checks, governing loads and prestressing properties in this chapter are all given per 1 m length. The flowchart below describes first optimization loop. A similar optimization approach has been used by Hanusaik (2021). Initially the cross-sectional properties of the current relieving platform are used. The starting height of the cross-section is that of 1.75 m (original design). L_1 increases iteratively within the given boundary of

each variant, as can be seen in the previous section. A_p is increased iteratively as well, starting from 0 tendons (current case $A_p = 0$ mm^2) and increasing with 1 tendon ($A_p =$ 2.250 mm2) at a time, consequently increasing the prestressing force applied. The height of the cross-section is decreased for the current L_1 and A_p until the resistance checks are no longer satisfied. At this point the prestressing tendon design is changed by going to the next L_1 step until the upper bound is reached. Once the maximum L_1 has been reached, the minimum height for a specific variant has been found as the tendon layout cannot change anymore. The amount of tendons are then increased and the process is repeated until the addition of more prestressing tendons no longer results in a lower cross-section height. The full flowchart is shown in Figure 54.

An analysis of the embodied carbon of each variant is then manually performed. This analysis will show which variant is optimal in terms of CO_2 reduction, since there will also be a trade-off between the addition of a tendon and the reduction in concrete it causes. The final optimal design is that with the largest embodied carbon reduction.

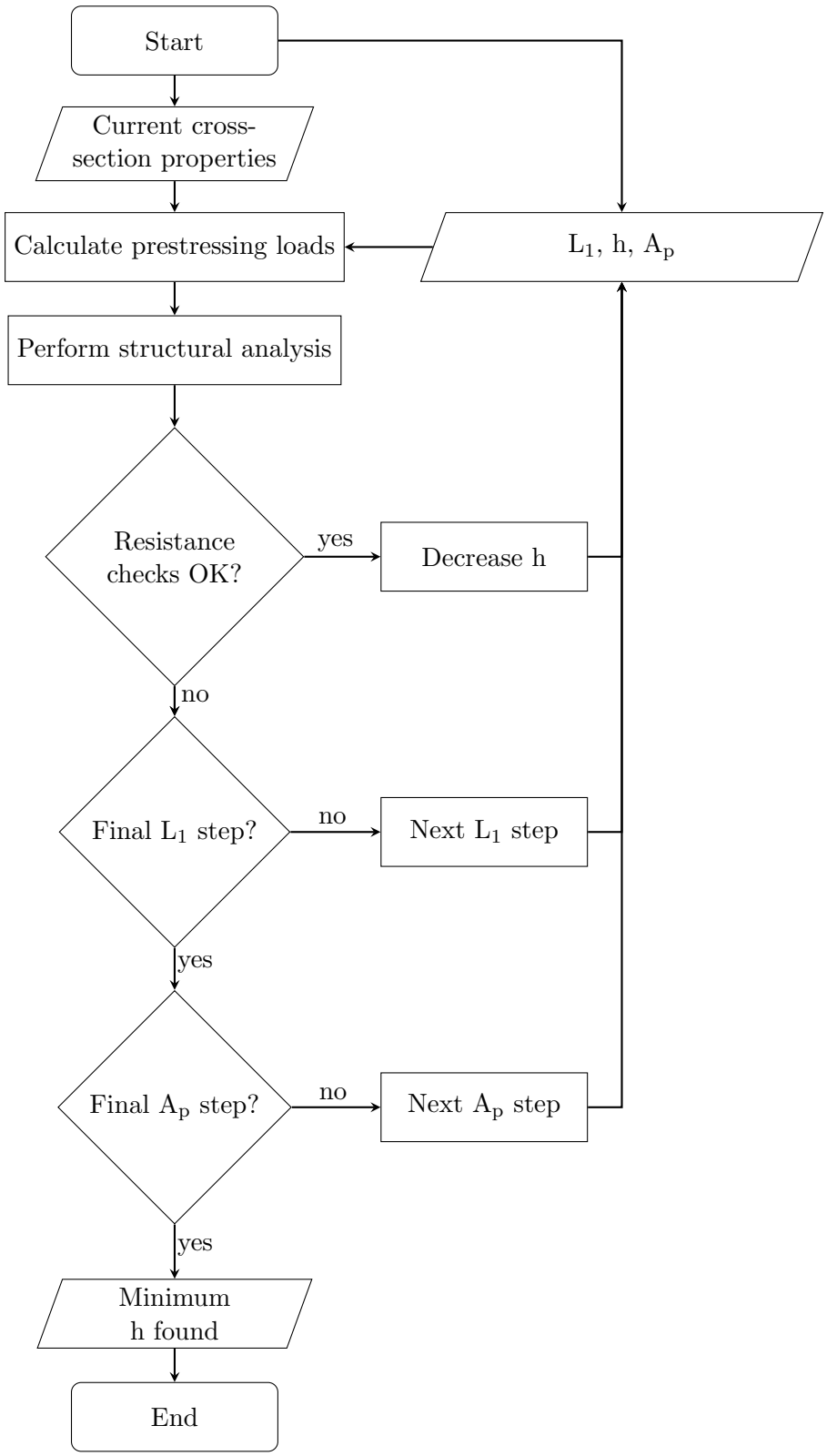

Figure 54: Optimization flowchart

Resistance checks

For the optimization Maple is used to calculate all the iterations, the loads, resistance checks and perform the structural analysis. The resistance checks are the same as those used in Chapters 4 and 5. The cross-sections analyzed in the optimization loop are:

- ULS, M_{Rd}: Moment resistance check at the maximum moment.

- ULS, R.C.: Rotational capacity check.
- ULS, V_{Rd1}: Shear resistance check in the floor at the interface with the wall.
- ULS, V_{Rd2}: Shear resistance check in the floor at the first row of foundation piles.
- SLS, w: The crack width at the maximum moment.

These checks where found to give a good estimate of the governing cross-sections. Afterwards, the optimal results will be further analyzed to ensure the design satisfies all requirements.

Reference case

As discussed in Section 4.5 the loads resulting from the analytical 2D model are lower than the loads resulting from the original calculations of the quay wall. This difference means that when using the 2D analytical loads, the resistance checks are inherently more favorable. Consequently, part of the reduction in the thickness of the floor is attributed to these differences in the modeling approach rather than solely to the effects of prestressing.

In order to make a fair comparison of the initial and final optimal solution, is was essential to determine the lowest possible cross-section height of the relieving platform floor using the 2D analytical loads. This has been done by using the same optimization loop as shown in Figure 54, but without including any prestressing (i.e. $A_p = 0$ mm^2). This has resulted in a minimum floor height of 1.640 mm (instead of 1.750 mm).

This outcome has been called the reference case. The reference case serves as the baseline for comparing the relative improvements in terms of floor height and embodied carbon reduction. By comparing the optimized solution with the reference case, the benefits of prestressing and the other optimization methods can be assessed.

6.2.2 Results

The results of the optimization are shown below for every tendon increase step. Tables 31 to 34 show the minimum floor height and the result of the unity checks of the optimum result for each variant. The respective prestressing designs of each variant, with a specific tendon parameter L_1 is shown in the figures below. The shear resistance checks V_{Rd1} and V_{Rd2} show if the concrete shear strength $V_{Rd,c}$ was high enough or if the shear reinforcement $V_{Rd,s}$ of the floor mentioned in Table 9 (Section 4.2.3) was required.

One tendon

Table 31: Optimization unity checks: 1 tendon

Variant	**h**		**M_{Rd}**	**R.C.**	**$V_{Rd\ 1}$**	**$V_{Rd\ 2}$**	**w**
Reference	1.640	mm	0,43	OK	$V_{Rd,s}$: 0,99	$V_{Rd,s}$: 1,00	0,81
1	1.570	mm	0,33	OK	$V_{Rd,s}$: 0,96	$V_{Rd,s}$: 0,88	0,27
2	1.330	mm	0,41	OK	$V_{Rd,s}$: 1,00	$V_{Rd,s}$: 0,98	0,44
3	1.250	mm	0,46	OK	$V_{Rd,s}$: 1,00	$V_{Rd,s}$: 0,99	0,48

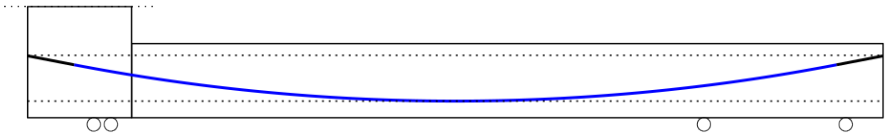

(a) Variant 1 - L_1 = 18,1 m, h = 1,57 m

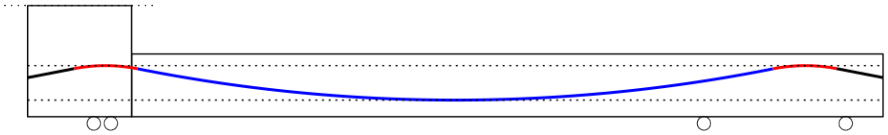

(b) Variant 2 - L_1 = 14,1 m, h = 1,33 m

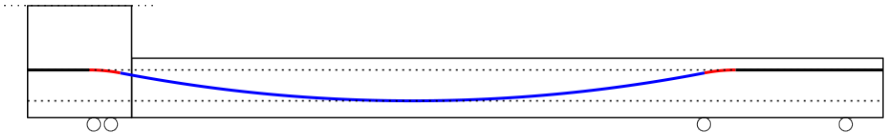

(c) Variant 3 - L_1 = 13,0 m, h = 1,25 m

Figure 55: Optimization results one tendon

Two tendons

Table 32: Optimization unity checks: 2 tendons

Variant	**h**		$\mathbf{M_{Rd}}$	**R.C.**	$\mathbf{V_{Rd\ 1}}$	$\mathbf{V_{Rd\ 2}}$	**w**
Reference	1.640	mm	0,43	OK	$V_{Rd,s}$: 0,99	$V_{Rd,s}$: 1,00	0,81
1	1.470	mm	0,29	OK	$V_{Rd,c}$: 0,81	$V_{Rd,s}$: 1,00	0,03
2	1.210	mm	0,46	OK	$V_{Rd,c}$: 0,98	$V_{Rd,c}$: 0,83	0,18
3	1.060	mm	0,60	OK	$V_{Rd,c}$: 0,87	$V_{Rd,c}$: 0,93	0,25

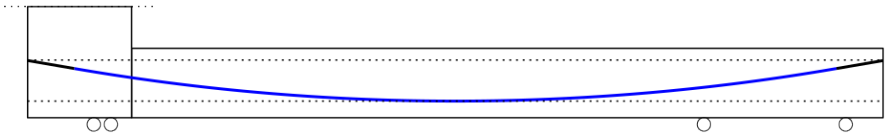

(a) Variant 1 - L_1 = 18,1 m, h = 1,47

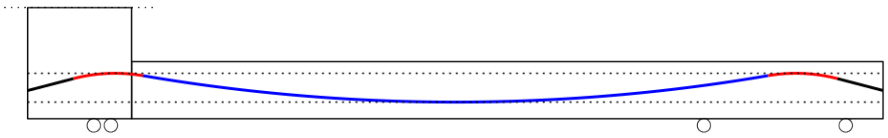

(b) Variant 2 - L_1 = 13,8 m, h = 1,21 m

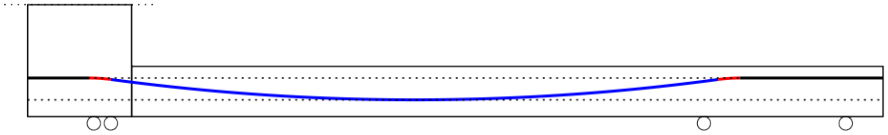

(c) Variant 3 - L_1 = 13,3 m, h = 1,06 m

Figure 56: Optimization results two tendons

Three tendons

Table 33: Optimization unity checks: 3 tendons

Variant	h		M_{Rd}	R.C.	$V_{Rd\ 1}$	$V_{Rd\ 2}$	w
Reference	1.640	mm	0,43	OK	$V_{Rd,s}$: 0,99	$V_{Rd,s}$: 1,00	0,81
1	1.320	mm	0,33	OK	$V_{Rd,c}$: 0,59	$V_{Rd,c}$: 1,00	0,01
2	1.090	mm	0,57	OK	$V_{Rd,c}$: 0,91	$V_{Rd,c}$: 1,00	0,16
3	1.040	mm	0,60	OK	$V_{Rd,c}$: 0,58	$V_{Rd,c}$: 0,99	0,06

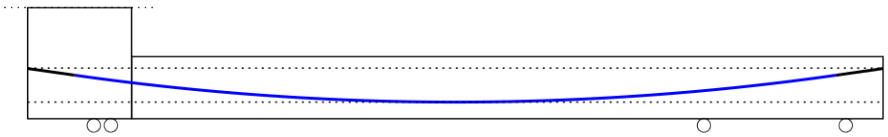

(a) Variant 1 - L_1 = 18,1 m, h = 1,32 m

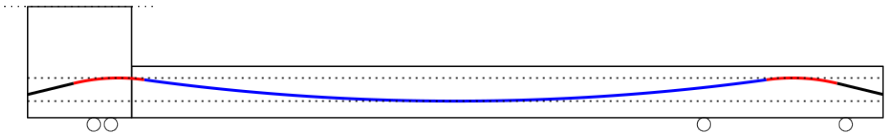

(b) Variant 2 - L_1 = 13,7 m, h = 1,09 m

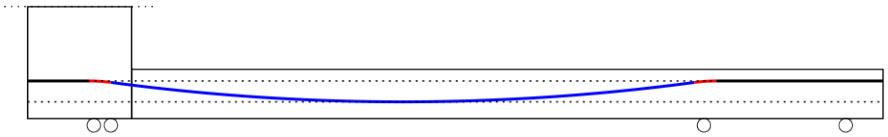

(c) Variant 3 - L_1 = 12,8 m, h = 1,04 m

Figure 57: Optimization results three tendons

Four tendons

Table 34: Optimization unity checks: 4 tendons

Variant	h		M_{Rd}	R.C.	$V_{Rd\ 1}$	$V_{Rd\ 2}$	w
Reference	1.640	mm	0,43	OK	$V_{Rd,s}$: 0,99	$V_{Rd,s}$: 1,00	0,81
1	1.200	mm	0,41	OK	$V_{Rd,c}$: 0,56	$V_{Rd,c}$: 1,00	0
2	1.110	mm	0,53	OK	$V_{Rd,c}$: 0,38	$V_{Rd,c}$: 1,00	0,15
3	1.120	mm	0,52	OK	$V_{Rd,c}$: 0,35	$V_{Rd,c}$: 0,98	0,16

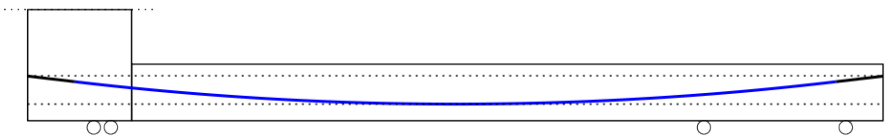

(a) Variant 1 - L_1 = 18,3 m, h = 1,20 m

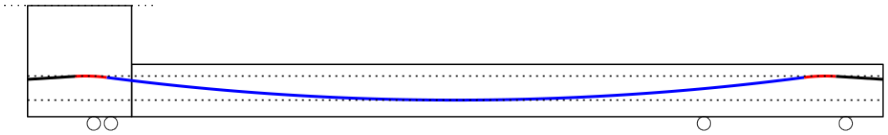

(b) Variant 2 - L_1 = 15,2 m, h = 1,11 m

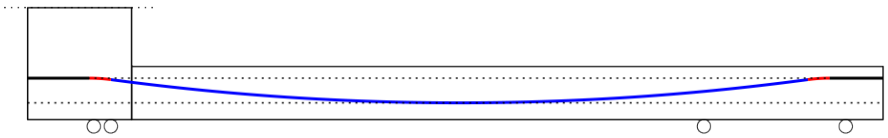

(c) Variant 3 - L_1 = 15,2 m, h = 1,12 m

Figure 58: Optimization results four tendons

Figure 59 shows the cross-section height of the variants for each number of prestressing tendons applied. All the variants start at the reference height (h = 1.640 mm). It can be seen that the largest height reduction is achieved in the first two steps. After that, the reduction reaches a limit at just above 1 m. It can be seen that the shear resistance of all the cross-sections is the governing check for all of the optimal solutions. The graphs also indicates which resistance check was governing (in this case either the concrete shear strength $V_{Rd,c}$ or the reinforcement steel strength $V_{Rd,s}$). The $V_{Rd,s}$ was lower than the $V_{Rd,c}$ for variant 2 and 3 after the application of 2 prestressing tendons.

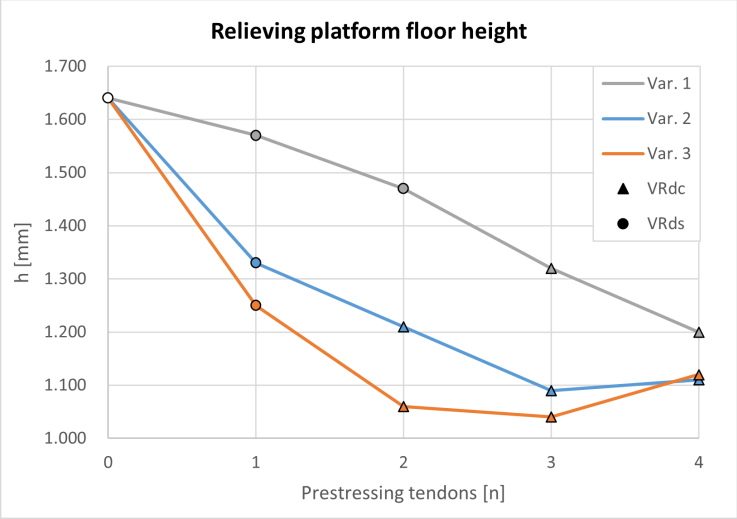

Figure 59: Relieving platform floor height optimization results

Carbon

The embodied carbon of the variants for each step is shown in Figures 60 and 61. The results show a strong decrease of the embodied carbon after the application of a single tendon. A minimum in terms of CO_2eq is reached with the application of two tendons. After that, the concrete reduction due to the reduced cross-section height is smaller than the increase of CO_2eq due to the addition of another tendon.

Table 35: Optimization embodied carbon variant 1

$n_{tendons}$	Concrete	Bending reinf.	Shear reinf.	Prestressing tendon	Total	
0	6.415	4.868	577	0	**11.859**	kg CO_2eq
1	6.124	4.868	553	587	**12.132**	kg CO_2eq
2	5.713	4.868	519	1.173	**12.273**	kg CO_2eq
3	5.102	4.868	468	1.759	**12.197**	kg CO_2eq
4	4.611	4.868	427	2.344	**12.250**	kg CO_2eq

Table 36: Optimization embodied carbon variant 2

$n_{tendons}$	Concrete	Bending reinf.	Shear reinf.	Prestressing tendon	Total	
0	6.415	4.868	577	0	**11.859**	kg CO_2eq
1	5.163	4.868	471	588	**11.089**	kg CO_2eq
2	4.672	4.868	430	1.175	**11.144**	kg CO_2eq
3	4.181	4.868	389	1.758	**11.196**	kg CO_2eq
4	4.251	4.868	396	2.344	**11.858**	kg CO_2eq

Table 37: Optimization embodied carbon variant 3

$n_{tendons}$	Concrete	Bending reinf.	Shear reinf.	Prestressing tendon	Total	
0	6.415	4.868	577	0	**11.859**	kg CO_2eq
1	4.842	4.868	444	588	**10.742**	kg CO_2eq
2	4.071	4.868	379	1.173	**10.490**	kg CO_2eq
3	3.981	4.868	372	1.758	**10.979**	kg CO_2eq
4	4.291	4.868	399	2.344	**11.902**	kg CO_2eq

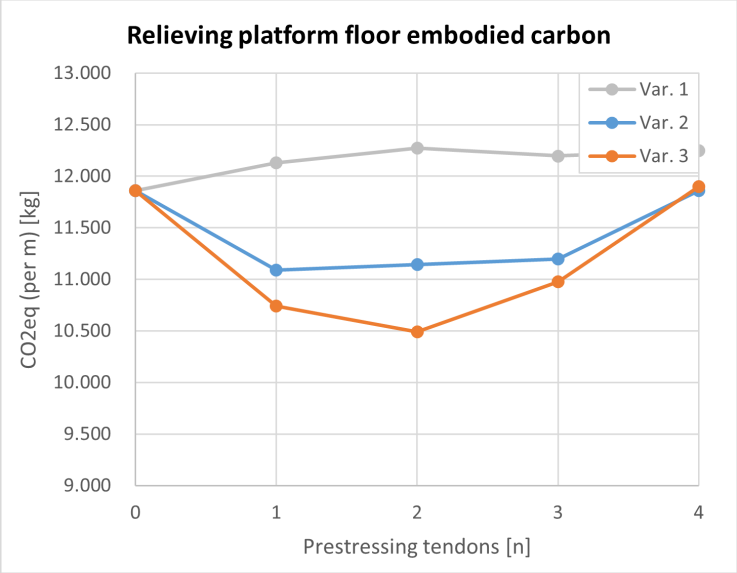

Figure 60: Embodied carbon variants

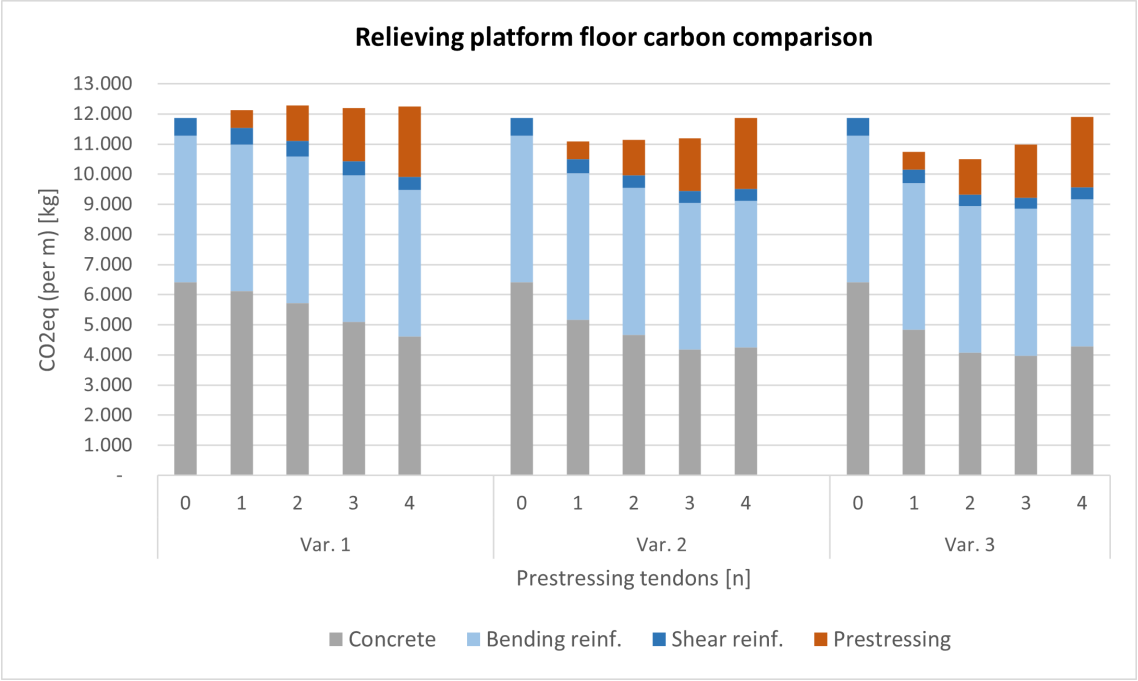

Figure 61: Embodied carbon: prestressing variants

Variant 3 using 2 prestressing tendons (A_p = 4.500 mm^2) can be seen to have the lowest amount of embodied carbon, with a reduction of 12% compared to the reference floor variant.

6.2.3 Discussion

The optimal solution has been found in the case where the shear forces are reduced the most and the $V_{Rd,c}$ has been increased the most. Specifically variant 3 performs well in terms of reducing the shear forces, as was intended in its design. For all the variants using 1 tendon, the shear reinforcement strength was governing. This means a prestressing force of 2.700 kN did not increase the compressive stress in the cross-sections enough for $V_{Rd,c}$ to satisfy the checks. Only after the application of 2 tendons (5.400 kN), did $V_{Rd,c}$ increase enough for variant 2 and 3 and after the application of 3 tendons (7.100 kN) for variant 1.

The reduction of shear forces is achieved twofold. On the one hand reducing the largest

distributed loads by creating an opposite distributed prestressing load that reduces the shear forces. On the other hand the placement of the transition curves close to or above the supports causes these loads to be directly transferred to the supports. It must be noted however that the optimization calculates the shear forces at the peaks, which is a very conservative value. This has been further explored in the next optimization analysis.

The prestressing has reduced the unity checks of the crack-widths for all the variants significantly compared to that of the reference case (0,81). For every additional tendon, the crack widths further reduced up until the application of 4 tendons. At this point the additional tendon for variant 3 actually increased the largest bending moments in the floor, causing the formation of larger cracks.

Variant 3 has the best performing prestressing design in terms of cross-section height and carbon reduction. This variant reduces the shear unity check by reducing the shear forces in the governing cross-sections the most. There seems to be an optimum in terms of carbon reduction around the application of 2 tendons (A_p=4.500 mm^2) for this variant. The graph displaying the height reduction in Figure 59 shows that the cross-section height keeps decreasing with the addition of an extra prestressing tendon (up until 3 tendons). However, the contribution of each additional tendon on the height reduction diminishes. Due to these diminishing effects, it can be seen that with the application of 3 or more tendons the embodied carbon increases again.

Variant 3 using 2 prestressing tendons is considered to give the optimal prestressing design. Given the shear force became governing, the next step was to investigate if increasing the shear reinforcement could further facilitate the reduction of the cross-section height and the embodied carbon of the floor.

6.3 Height reduction: Increased shear resistance

This optimization has looked into increasing the stirrup diameter and quantity for the optimal prestressing variant, with the goal of finding a more slender cross-section. The additional shear reinforcement is placed in the areas around the beginning of the floor and the first foundation pile (support C see Figure 40), since these are the locations with the highest shear loads. The current shear reinforcement used is $\phi 16 - 300$ mm, shown in Section 4.2.3. The diameter will initially be increased to 20 mm and the center to center (c.t.c.) distance between the stirrups will be iteratively decreased with increments of 50 mm. Figure 62 shows the location of additional shear reinforcement.

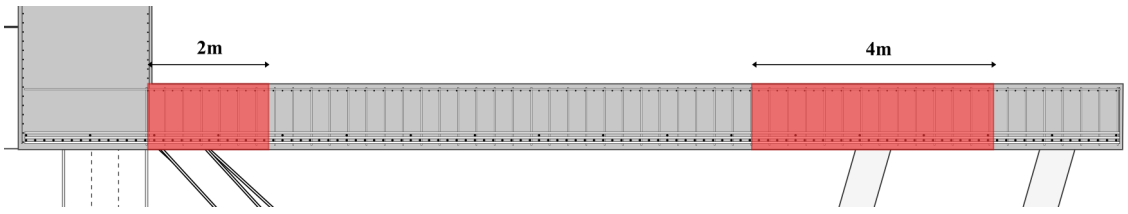

Figure 62: Regions with increased shear reinforcement

The same optimization Maple script from the previous section will be used, but now also iteratively (and manually) increasing the shear reinforcement.

6.3.1 Results

It became clear that the cross-section height can be further reduced by increasing the shear reinforcement. The optimization resulted in a minimum cross-section height of 860 mm. However, this height showed to be too small to satisfy the rotational capacity check. The shear reinforcement was increased to $\phi_{stir} 20 - 250$ mm, after which adding additional shear reinforcement did not improve the capacity any further. It was found that the minimum height that did satisfied the rotation capacity was 890 mm. This calculation can be found

in Appendix H Section H.2.1. Figure 63 shows the final optimal prestressing design. After that a more detailed analysis is performed, looking into additional cross-sections to ensure the final design has sufficient capacity.

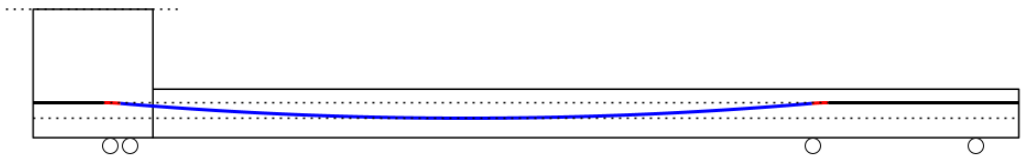

Figure 63: Final prestressed relieving platform - L_1 = 12,9 m, h = 0,89 m

Table 38: Minimum height unity checks: Two tendons, $\phi_{stir}20 - 250$ mm

Variant	**h**		**M_{Rd}**	**R.C.**	**$V_{Rd\ 1}$**	**$V_{Rd\ 2}$**	**w**
Reference	890	mm	0,90	OK	$V_{Rd,s}$: 0,76	$V_{Rd,s}$: 0,94	0,55

Final analysis

A more detailed analysis of the final prestressed variant that looks into additional resistance checks has been performed. The calculations can be found in Appendix H Section H.2.1. The bending moments in four different cross-sections have been checked. These are respectively the start of the floor (1), the point with the largest sagging moment (2) and left (3) and the right side (4) of the first row of foundation piles. For the bending moments above the supports, the moment is now calculated on the edge of the supports rather than at the peak in the middle of the support. The peak moments are higher at this location than they would realistically be, due to the fact that the supports are modeled as a point support. The results are shown in tables 39.

Table 39: ULS Moments resistance (per 1 m)

Cross-section	**M_{Ed}**		**M_{Rd}**		**u.c.**
1	526	kNm	4.376	kNm	0,12
2	3.635	kNm	4.038	kNm	0,90
3	-438	kNm	2.966	kNm	0,15
4	-457	kNm	3.133	kNm	0,15

The shear force checks are performed at the same location as those in the optimization, namely the start of the floor and the first row of foundation piles. As opposed to the shear check in the optimization loop which took the peak loads, the shear resistance was calculated more realistically at a distance 0,5·d from the edge of the supports. All loads within a distance 0,5·d from the support are considered to be directly transferred to the respective supports, based on the NEN-EN 1992-1-1, article 6.2.2. Three checks have been performed, one close to the interface of the floor and the wall (1), one on the left side (2) and one on the right side (3) of the first foundation pile. The results are shown in Table 40.

Table 40: ULS Shear resistance (per 1 m)

Check	**V_{Ed}**		**V_{Rd}**		**u.c.**
1	1.207	kN	$V_{Rd,s}$ 1.652	kN	0,73
2	1.262	kN	$V_{Rd,s}$ 1.652	kN	0,76
3	616	kN	$V_{Rd,c}$ 763	kN	0,67

The additional crack width calculations look into two cross-sections. The first cross-section is that with the maximum sagging moment under full SLS loading at (t = ∞)

and the second that where the cross-section is only loaded by selfweight and prestressing (t=0). At t=0, when the time-dependent losses have not yet occurred, the prestressing force is therefore at $P_{m,0} = 3.214$ kN (Section 5.1.3).

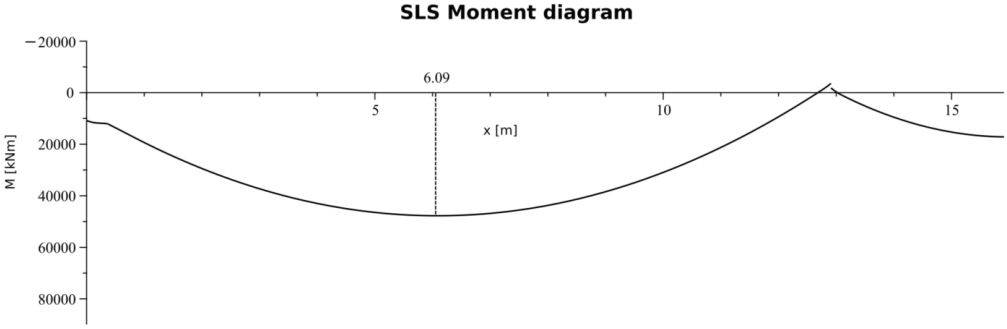

Figure 64: SLS: Bending moment diagram t=∞ (per 23 m)

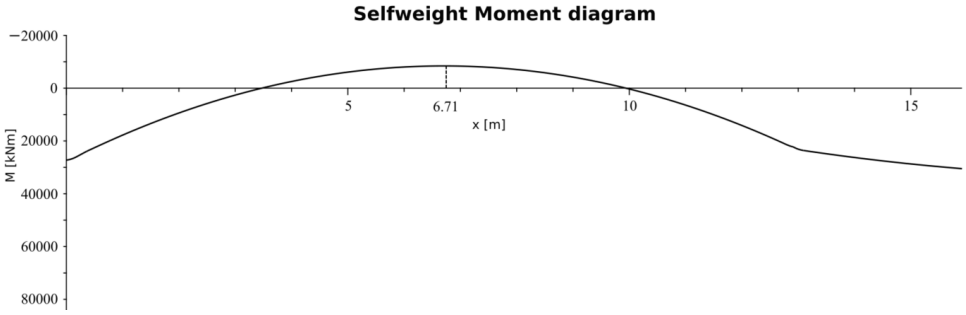

Figure 65: Selfweight: Bending moment diagram t=0 (per 23 m)

Table 41: SLS: Crack-widths (per 1 m)

Check	**M**		**w**		**w_{max}**		**u.c.**
t = ∞	2.076	kNm	0,182	mm	0,342	mm	0,53
t = 0	-338	kNm	0	mm	0,356	mm	0

Carbon

The embodied carbon of the floor is calculated again for the case with increased shear resistance. Figure 66 below shows the total embodied carbon per meter of the optimal prestressing design using an increased amount of shear reinforcement compared to the reference case and to the optimal prestressing design with the original amount of shear reinforcement. The reduction of the embodied carbon of the relieving platform floor reduced further from 12%, to 17% due to the increase of shear reinforcement.

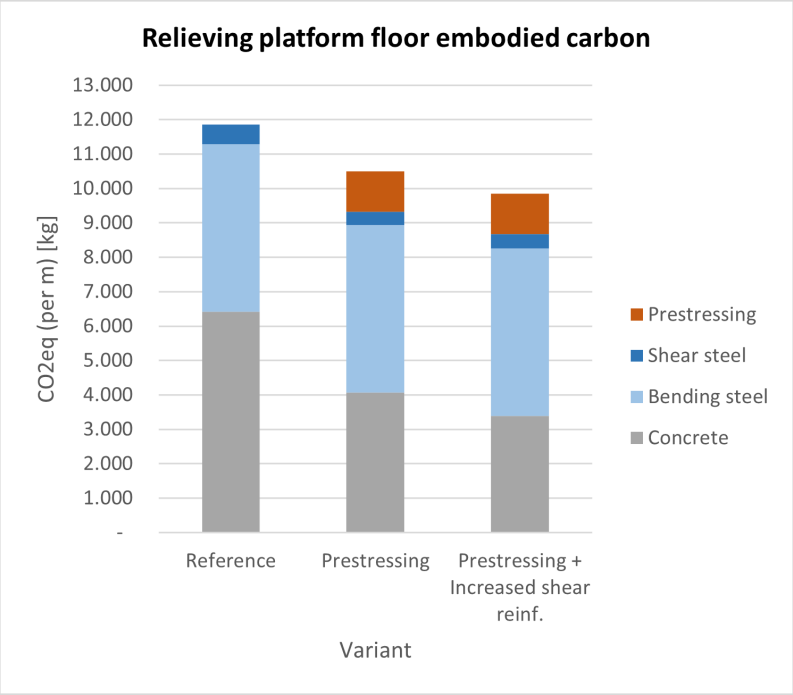

Figure 66: Embodied carbon: shear reinforcement $\phi 20 - 250$ mm

Table 42: Embodied carbon shear reinforcement $\phi 20 - 250$ mm

Case	Concrete	Bending	Shear reinf.	Prestr. reinf.	Total tendon	
Reference	6.415	4.898	577	0	**11.859**	kg CO_2eq
Prestressed	4.071	4.898	379	1.173	**10.490**	kg CO_2eq
Prestressed + shear	3.387	4.898	427	1.171	**9.853**	kg CO_2eq

6.3.2 Discussion

The optimization script using an increased shear reinforcement showed a further height reduction from 1.210 mm to 890 mm. The final more detailed analysis of the structure showed that the shear resistance now reaches a maximum unity check of 0,76. This suggests that using the shear reinforcement resulting from the optimization script of $\phi 20 - 250$ mm is more than is required. When recalculating the highest shear resistance check 2 from Table 40 but changing the shear reinforcement c.t.c. distance back to 300 mm this results in a unity check of 0,92. The diameter of the shear reinforcement could not be reduced. This implies using shear resistance of $\phi 20 - 300$ mm is sufficient.

The carbon is shown to further reduce by increasing the shear reinforcement. The shear reinforcement only has a small contribution to the total embodied carbon and is compensated for by the reduction of concrete.

Both crack width checks, at t = 0 and at t = ∞, are satisfied. The extra cover that has been applied to the original structure which was required to satisfy the crack width requirements (as mentioned in Section 4.2.3) used $k_x = 1{,}64$ (for the bottom of the floor), meaning the crack widths were allowed to be 1,64 times higher. The additional concrete cover applied could potentially be removed, because the crack-widths now remain below the original requirement of $w_{max} = 0{,}2$ mm (Table 41). If this were to be removed the reinforcement bars and prestressing tendon could move further outwards making them more effective in terms of resisting bending moments. This could potentially also improve the rotational capacity of the cross-section as d_{eff} becomes larger as well. If this is the case, the cross-section might be slightly further reduced in height although the differences are not expected to be very large. The next step of the optimization will be to look into creating a cross-section opening. The cover will at this point not be reduced since it might still be needed for this type of cross-section.

6.4 Cross-section

The next optimization that has been performed to reduce the material usage, is to look into the possibility of removing concrete around the neutral axis of the cross-section. This optimization has been manually performed, based on the results of the previous optimization. To create the cross-section opening, expanded polystyrene (EPS) will be used as remaining formwork. The use of this material will also contribute to the total embodied carbon.

6.4.1 Cross-section design

The additional shear reinforcement that will be used as mentioned in the previous section will be $\phi 20 - 300$ mm around the critical cross-sections. The height of the floor is 890 mm and the prestressing design of the last optimization will be used (Figure 63). The maximum size of the opening is based on the required concrete cover of the reinforcement. The outside of the floor is considered to still use the same cover properties as the original design, namely 85 mm for the top and 90 mm for the bottom. The cover for the inside of the opening will need to be determined. Leakage of corroding chemicals into the opening will need to be prevented by reducing the crack widths, according to NEN-EN 1992-3, article 7.3. The code defines tightness classes ranging from class 0 (leakage acceptable) to class 3 (no leakage acceptable). If class 1 to 3 are satisfied by the structure, this means that the cracks that are expected to run through the entire height of the flange are either small enough or none existent to prevent any intrusion of corroding liquids. If these requirements can be met, it means that the consequence class of the relieving platform changes to XC1. The concrete cover used then thus depends on the leakage requirements. Tables 43 to 45 give the required concrete cover properties for the inside of the opening for the case where the leakage tightness can be satisfied.

Table 43: Environmental and construction classes

	Inside opening
Environmental class	XC1
Design life 100 years	+2
Strength class ≥ C30/37	-1
Construction class	S5

Table 44: Concrete cover (horizontal)

	Bottom		**Top**	
$\mathbf{C_{min;b}}$	40	mm	25	mm
$\mathbf{C_{min;dur}}$	20	mm	20	mm
$\mathbf{\Delta C_{dev}}$	5	mm	5	mm
$\mathbf{C_{nom}}$	45	mm	30	mm
$\mathbf{C_{applied}}$	45	mm	30	mm

Table 45: Concrete cover (vertical)

	Stirrups		**Prestressing**	
$\mathbf{C_{min;b}}$	20	mm	76	mm
$\mathbf{C_{min;dur}}$	20	mm	30	mm
$\mathbf{\Delta C_{dev}}$	5	mm	5	mm
$\mathbf{C_{nom}}$	25	mm	81	mm
$\mathbf{C_{applied}}$	25	mm	81	mm

According to NEN-EN 1992-3, article 7.3, the crack width requirements for tightness class 1 are based on the hydrostatic pressure (h_D). The code defines the maximum crack width w_{k1}, which is 0,2 mm where $h_D/h \leq 5$ and 0,05 mm where $h_D/h \geq 35$, with h being the thickness of the containers (in the context of liquid storage). Intermediate values can be interpolated. The groundwater level used is based on Section 4.2.4. For the top part of the opening h_D = 0,5 m and h_f = 0,185 m, being the height of the top flange, which gives:

$$\frac{h_D}{h_f} = \frac{0,5}{0,185} = 2,7 \tag{38}$$

This thus means that the additional crack width requirement for leakage prevention for the interior part of the top flange becomes w_{k1} = 0,2 mm. For the bottom part of the floor h_D = 0,5 + 0,89 = 1,39 m and h_f = 0,355 m, being the height of the bottom flange, which gives:

$$\frac{h_D}{h_f} = \frac{1,39}{0,355} = 3,9 \tag{39}$$

The additional crack width requirement for leakage prevention for the interior part of the bottom flange then also becomes w_{k1} = 0,2 mm.

This finally gives the initial design as can be seen in Figure 67. The bending reinforcement will be kept the same as that in the original structure. The longitudinal reinforcement has a center to center distance of 150 mm, which means that for every 1 m section 6,67 bars are present. To ensure the same ratio is used, a three meter section is designed with a total of 20 reinforcement bars. The design of the cross-section is then based on keeping the shear reinforcement equally spaced. The maximum opening based on the required concrete cover has a width of 230 mm and a height of 350 mm. It will be investigated how large the opening can be based on the capacity required.

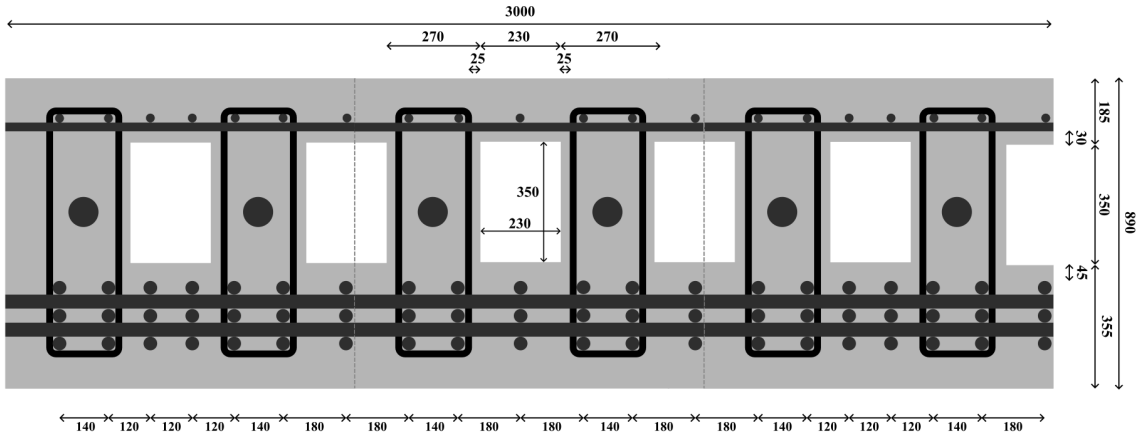

Figure 67: Cross-section with initial maximum opening

6.4.2 Resistance checks

To calculate the capacity of the cross-section, some changes need to be made to the methods described in Section 3.2.

ULS: MRd

In the case that the compression zone height x_u is larger than the height of the top flange, the compressive stress can no longer be determined using the assumed shape of the stress-strain relationship of concrete with $\alpha = 0,75$ and $\beta = 0,39$. Instead, the bending moment resistance will be determined by the moment equilibrium shown in Figure 68. When the compression zone height is larger than the size of the top flange, the compressive force is divided into two separate forces. An additional force F_{cdw} that represents the compressive force at the location of the web and F_{cdf} which represents the force in the top flange. These forces are determined using the factors $\eta = 1$ and $\lambda = 0{,}8$ according to NEN-EN 1992-1-1, article 3.1.7. The initial estimate for the compression zone height x_u can be determined using the original approach.

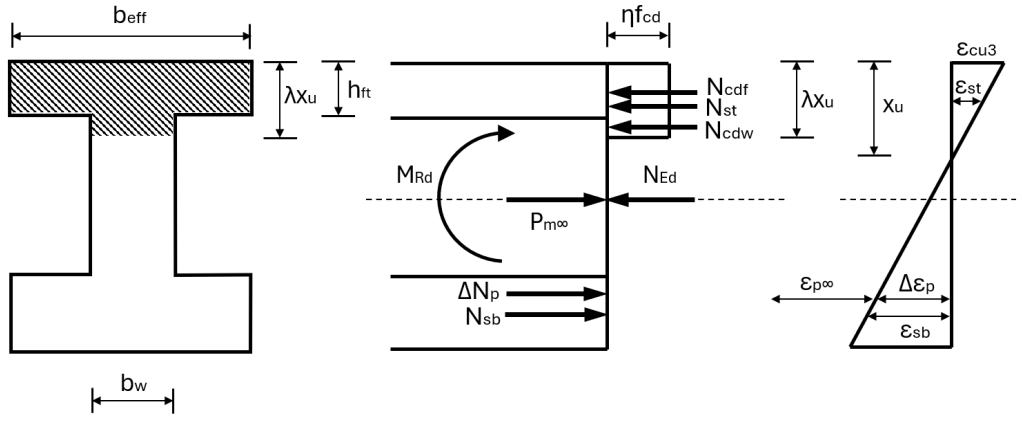

Figure 68: ULS Bending moment resistance

The horizontal force equilibrium becomes:

$$N_{cdf} + N_{cdw} + N_{Ed} + N_{st} = N_{sb} + \Delta N_p + P_{m\infty} \tag{40}$$

Which can be rewritten to calculate the first estimation of the compression zone height x_u. This height is then again found using an iterative process which looks for the x_u which gives the horizontal force equilibrium.

$$\eta f_{cd} h_f b_{eff} + \eta f_{cd}(\lambda x_u - h_f) b_w + N_{Ed} + A_{st} f_{yd} = A_{sb} f_{yd} + A_p(f_{pd} - \sigma_{pm\infty}) + A_p \sigma_{pm\infty} \quad (41)$$

$$x_u = \frac{-\eta f_{cd} h_f b_{eff} + \eta f_{cd} h_f b_w - N_{Ed} - A_{st} f_{yd} + A_{sb} f_{yd} + A_p f_{pd}}{\eta f_{cd} \lambda b_w} \quad (42)$$

The final moment resistance is then found by taking the moment equilibrium around the centroidal axis.

$$M_{Rd} = N_{c1} \cdot (c.a. - \frac{h_{ft}}{2}) + N_{c2} \cdot (c.a. - (\frac{\lambda x_u - h_{ft}}{2} + h_{ft})) + N_{st} \cdot e_{st} = N_{sb} \cdot e_{sb} + \Delta N_p \cdot e_p \quad (43)$$

With $e_{st} = c.a. - d_{st}$, $e_{sb} = c.a. - d_{sb}$ and $e_p = c.a. - d_p$

ULS: VRd

There are no changes to the methods mentioned in Section 3.2. Rather, the calculation of $b_{w,nom}$ as described will become more relevant since the width b_w is decreasing, changing the ratio with the duct size. If $\phi > b_w$ / 8, with $\phi = 86,2$ mm being the outside diameter of the canal, then:

$$b_{w,nom} = b_w - 0,5 \sum \phi \quad (44)$$

If $\phi \leq b_w/8$, then $b_{w,nom} = b_w$.

SLS: Crack width control

Similar to the changed bending moment resistance calculations, the crack width calculations also slightly changes to incorporate the thinner web. In the case the compression zone is larger than the height of the top flange, a second force N_{c2} is introduced that works in the opposite direction of the compressive force N_{c1}. This force represents the material that is not present in the cross-section and thus serves as a reduction force.

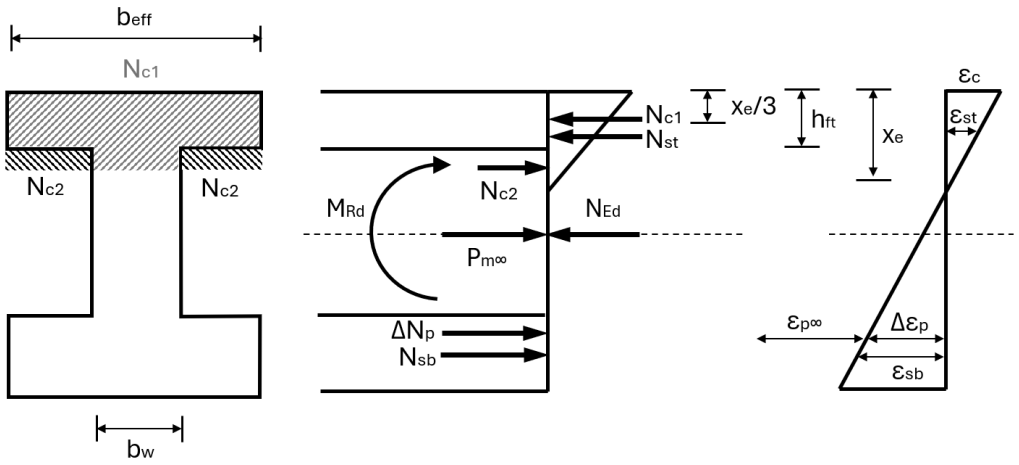

Figure 69: SLS opening moment equilibrium

6.4.3 Results

The cross-section with the maximum opening size is shown in Figure 72. The final opening size changed slightly compared to that shown in Figure 67 in order to satisfy the resistance checks. The opening now has a size of 200 x 345 mm.

The results of the analysis are shown in the tables below. The calculations can be found in Appendix H Section H.2.2.

Table 46: ULS Bending moments

Check	**MEd**		**MRd**		u.c.
1	497	kNm	4.308	kNm	0,12
2	3.534	kNm	3.650	kNm	0,97
3	-477	kNm	2.899	kNm	0,16
4	-488	kNm	3.058	kNm	0,16

Table 47: ULS Shear

Checks	**VEd**		**VRdc**		u.c.	**VRds**		u.c.
1	1.182	kN	653	kN	1,81	1.377	kN	0,86
2	1.241	kN	512	kN	2,42	1.345	kN	0,92
3	624	kN	530	kN	1,18	1.412	kN	0,44

Table 48: SLS: Crack-widths

Check	**M**		**w**		$\mathbf{w_{max}}$		**u.c.**
$t = \infty$	1.977	kNm	0,143	mm	0,2	mm	0,72
$t = 0$	-233	kNm	0	mm	0,2	mm	0

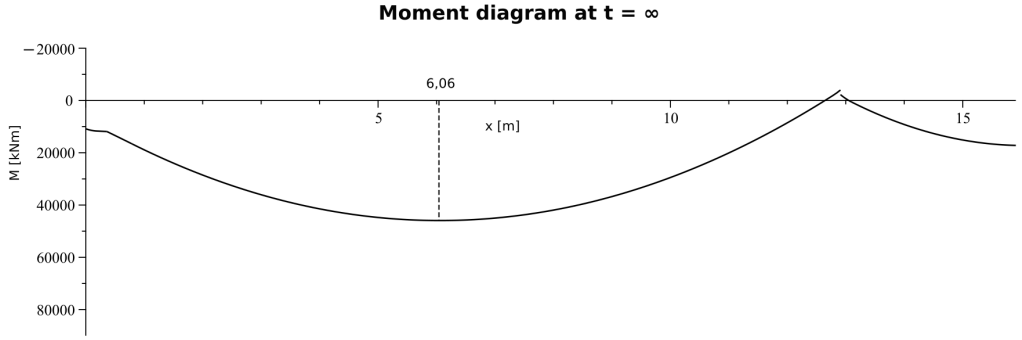

Figure 70: SLS: Bending moment diagram t=∞ (per 23 m)

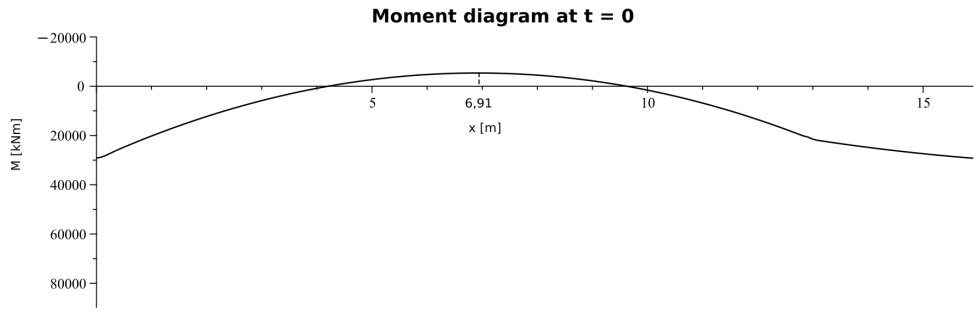

Figure 71: Selfweight: Bending moment diagram t=0 (per 23 m)

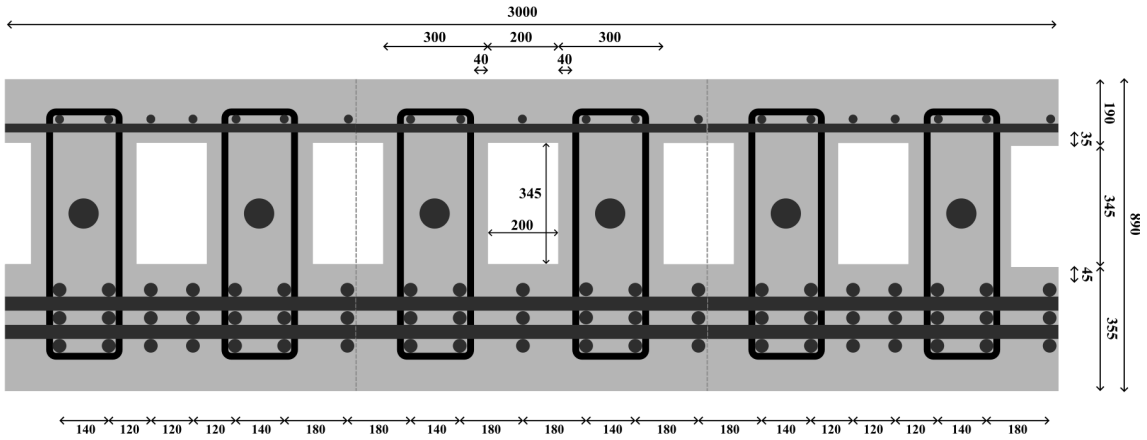

Figure 72: Final cross-section design

The results indicate that the crack width demand of 0,2 mm is satisfied and leakage is adequately prevented. The bending moment resistance has become governing in determining the maximum size of the cross-section opening.

Carbon

Table 49 shows the final comparison of the embodied carbon, comparing the final cross-section opening with the reference case, the optimized prestressing and the case with increased shear reinforcement. The total achieved embodied carbon reduction of the floor compared to the reference case is 20 % (-2.356 kg CO_2eq per meter).

Table 49: Embodied carbon CO_2eq final comparison

Cross-section	**Concrete**	**Bending**	**Shear reinf.**	**Prestr. reinf.**	**EPS tendon**	**Total**	
Reference	6.415	4.868	577	-	-	**11.859**	kg
Prestressing	4.071	4.868	379	1.173	-	**10.490**	kg
Prestr.+shear	3.387	4.868	427	1.171	-	**9.853**	kg
Prestr.+shear+opening	2.834	4.868	389	1.171	242	**9.504**	kg

Table 50: Weight reduction final comparison

Cross-section	**Weight**	
Reference	68.828	kg
Prestressing	46.077	kg
Prestr.+shear	39.351	kg
Prestr.+shear+opening	33.885	kg

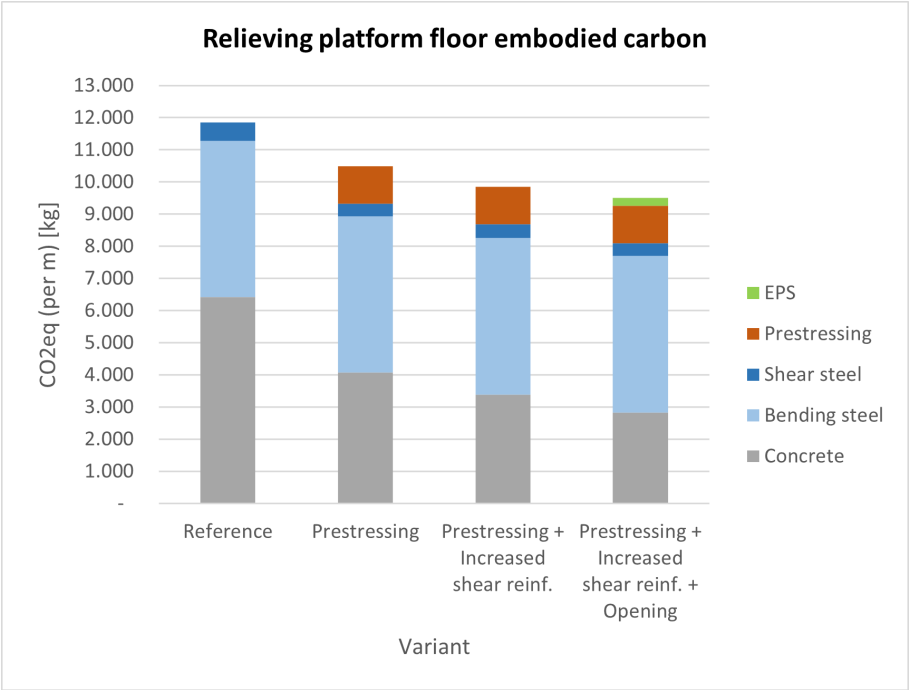

Figure 73: Embodied CO_2 final comparison

6.4.4 Discussion

The additional requirements regarding crack width to prevent leakage were satisfied. This means leakage of corroding materials into the opening can be prevented. This could only have been achieved by the use of prestressing, since the maximum crack width of the reference case was already at 0,266 mm (Section 6.2.2).

The EPS used as remaining formwork has a contribution of approximately 2,5% to the embodied carbon of the relieving platform floor. It does not however have a large contribution to the total weight of the module, which benefits the prefabricated design (around 0,1%). Exploring different methods of creating the opening in the cross-section could help further reduce the embodied carbon.

The total achieved embodied carbon reduction of the floor compared to the reference case is 20 % (-2.356 kg CO_2eq per meter). The largest part of the reduction can be attributed to the height reduction achieved by the application of prestressing (12%). The increase in shear reinforcement contributed approximately 5% additional reduction and the creation of a cross-section opening 3%.

It is important to note that the embodied carbon reduction is that of the relieving platform floor alone. Meaning that the percentage of total carbon reduction of the entire quay wall would be less. As mentioned in Section 1.1 the embodied carbon is estimated at 50 tonnes of CO_2eq per meter of sheet pile quay wall with relieving platform. Comparing this to the achieved reduction of 2.356 kg, the reduction of the embodied carbon of the total quay wall becomes approximately 5%. It must be noted however that this value only serves as a rough estimate, since the dimensions of the specific quay wall and underlying assumptions this specific value are not known.

The total weight reduction of the relieving platform floor achieved is approximately 50 %. The weight decreased from 69 tonnes to 34 tonnes. This is of great benefit for the prefabricated design of the relieving platform floor. Again the largest part of the weight reduction was achieved by the height reduction due to the initial application of prestressing.

7 Modular design

The results of the optimization showed benefits not only in terms of carbon reduction, but also in terms of weight reduction. This is an important benefit to the modular and prefabricated design. The weight per meter of the final optimized design compared to the reference variant (with h = 1.640 mm) are shown in the table below.

Table 51: Relieving platform floor weight (per 1 m)

	Reference		**Optimized**	
Weight	68.828	kg	33.917	kg

The goal is to create a modular building system, that enables the upgrade of a quay wall initially without a relieving platform floor at a later stage during its use life. An upgrade could be required when for example the future design of ships require deeper ports. A relieving platform might enable the deepening (given the combi-wall itself is already deep enough) by alleviating the additional forces that result from the deeper port. Another example is that the client using a specific quay changes to another client who has the need for heavier loads to be supported. One of the most important components of the modules is to create an efficient building process that increases construction speed and ensures a low downtime of a quay during the upgrade. The reduced weight of the modules has benefits for the construction and transportation, as well as the flexibility of the module shapes and sizes.

The modules need to resist the loads mentioned in Section 4.2.4. The type of connections used depends on the types of loads that the quay needs to resist. Unevenly spaced loads, such as point loads or locally distributed loads, will bring the need for different types of connections that can adequately transfer loads and therefore allow for a wider distribution of the loads.

With carbon reduction as one of the main goals, ensuring the modules work together in resisting the imposed loads is important. If the modules do not work together, each individual module will need to resist higher loads and in turn will need increase in size again. Adequate connections thus allow for the modules to stay as small as possible. The primary advantage of the upgradable floor system in terms of embodied carbon is that the floor is only installed when necessary. This means that for significant portions of a quay's lifespan, the floor may not be included, thereby avoiding the addition of a substantial amount of embodied carbon. Removing the floor results in an estimated carbon reduction of 25% (12,4 tonnes CO_2eq) for the entire sheet pile quay wall with a total CO_2 footprint of 50 tonnes (Section 1.1.1 Figure 2). However, as was mentioned this is rough estimate, given the underlying assumptions of the CO_2 are not known.

7.1 Design

The design of the modules is dependent on the transportation and construction limitations. The limitations regarding the transportation are mentioned in Section 2.4.2. The length of the floor is 15,9 m, the width shall be taken as 3 meters. This gives the general geometrical properties of one module as can be seen in Table 52. The weight of one such module, is then approximately 102 tonnes. This can be transported over land, but with the need of transport exemptions. The cranes mentioned in Section 2.4.2 have a capacity of up to 700 tonnes, which thus should not pose a problem.

The modules on the sides of a quay wall segment will need to be slightly different from the other modules. Quay walls are constructed in individual segments of, in the case of the SIF2 quay wall, 23 m. The segments are not monolithically connected to each other, but only by a shear key. The quay wall segments are not always of the same size and not always (like in this case) divisible by 3 m modules. Therefore the end modules must

Table 52: Geometrical properties of a module

Length	15,9	m
Width	3,0	m
Height	0,89	m
Weight	102	tonnes

be of variable size to facilitate the specific quay wall. An alternative would be to make these edge modules cast-in-situ instead, allowing for a single type of module to be used for a specific project and casting the variable end modules. This would however change the building process and require more on-site construction potentially slowing the speed.

7.2 Connections

From the results of the previous analysis design choices can be made regarding the types and locations of the connections. The connection type will be based on the literature described in Section 2.4.1. The modules will need to be connected to the wall and the substructure in a way that allows for the transfer of forces. Three connections can be distinct: the module to module connection, the module to wall connection and the module to foundation pile connection.

Demountable connections are as mentioned not going to be explored. The main goal of this modular design is to create an as efficient as possible construction process. Quay walls are built to last at least a 100 years and large parts of the quays of of the Port of Rotterdam have been in use for even longer than that. It is unlikely that after a 100 year period, such a module would be removed and be used for another quay wall for another period of this length.

7.2.1 Module to module

The modules can be considered to act as one way slabs, transferring the loads between the combi-wall and foundation piles. For this reason little load transfer in the lateral direction of the modules is expected. For evenly distributed loads, the modules could be designed to have no connection, since the loads themselves are already equally distributed over the modules. However, as can be seen in Section 4.2.4 there are several load cases with unevenly distributed or point loads, such as the collision loads and the bollard loads. The connections will therefore need to be designed to resist shear forces in both vertical and horizontal direction to transfer the loads through the modules.

Taking the impact loads as an example, Figure 74 shows how the loads are distributed through the wall to the modules. In order for the modules to work together in resisting these loads, a shear connection is required. If no shear connection would be present, each module will have to resist the loads directly imposed on it. This is undesirable, since this would require each individual module to have a higher resistance than they otherwise would have. This higher resistance means the dimensions of module need to increase which has a negative impact on the objective of the thesis to reduce material usage and carbon emissions.

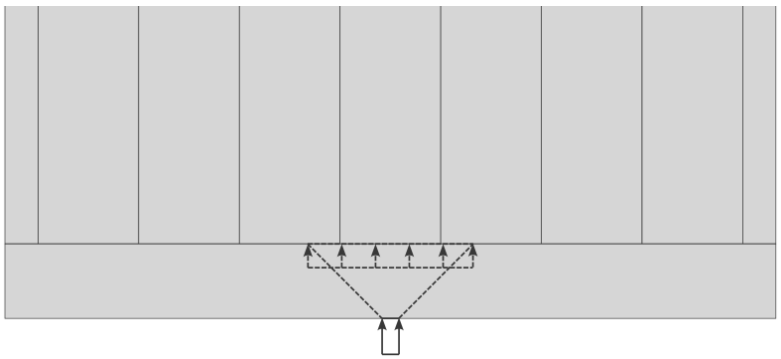

Figure 74: Example of horizontal loads distribution (impact loads)

The suggested connection will use a shear key, as shown in Figure 75. This connection is able to resist loads in both horizontal and vertical direction, ensuring stability and load distribution within the relieving platform. The same goes for any unevenly distributed or point loads in the vertical direction on top of the quay. In addition, this connection also benefits a fast building process. Making this type of connection for prefabricated elements exactly fit can proof difficult. To solve this, match-casting could be used, as mentioned in Section 2.4.3. Another option could be to apply grouting on-site, this does however increase the construction time and reduce the simplicity of the connection.

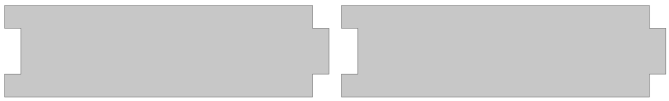

Figure 75: Module-to-module shear key

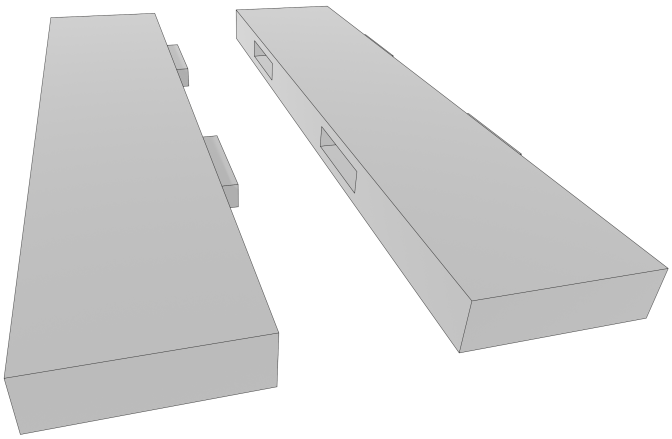

Figure 76: Module-to-module shear key 3D

7.2.2 Module to wall

The module to wall connection will need to resist bending moments, horizontal and axial forces in order for the loads to be transferred from the wall to the floor and the foundation piles. The foundation piles are a large contributor to the horizontal resistance of the relieving platform, due to their angled placement. The connection also needs to be able to resist moments for the floor and foundation piles to contribute to resisting the bending moments on the wall. Figure 77 shows a simplified schematic representation of a moment force in both directions. Figure 77a shows how the foundation piles can contribute and

Figure 77b shows how in addition the weight of the soil and the terrain loads can contribute to resisting the bending moments. The stability of the wall is dependent on this resistance.

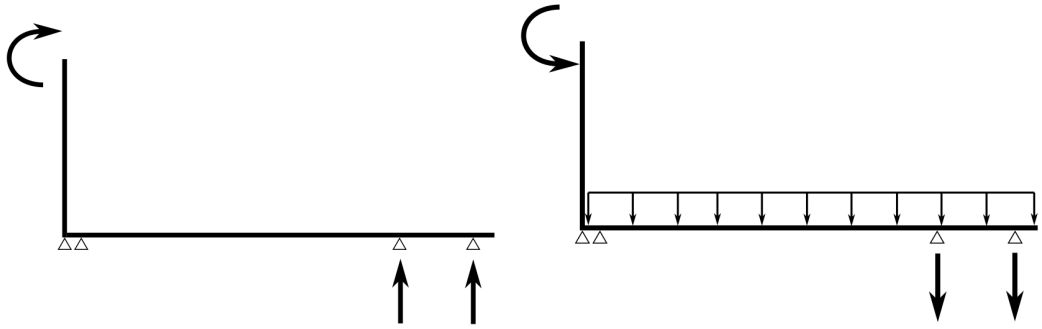

(a) Contribution of the piles (b) Contribution of the piles and the soil

Figure 77: Mechanical representation moment resistance modules

A corbel will be added to the bottom of the wall on top of which the module can be placed. The corbel serves two purposes, namely carrying the self-weight of the module during construction and ensuring there is enough room for the anchor. A wet connection will be made, by adding protruding reinforcement from the module and adding a type of reinforcement coupler in the wall. This allows for reinforcement to be installed within the connection after which in-situ concrete is added. It is important this connection is protected during the quay wall its use life when the floor is not installed yet. Possible methods are applying a waterproofing sealer or membrane that can be removed when the module is added to the wall. Vertical loads must be transferred via the relieving platform to the combi-wall and anchor. Figure 78 shows the suggested connection.

The prestressing tendon will run through the connection as well, contributing both to the moment resistance as well as the shear resistance of the connection. Similar to methods used in segmented construction, as mentioned in Section 2.4.3, the post-tensioning will be applied after the prefabricated module has been placed against the relieving platform wall. The type of anchorage used becomes an important design consideration, since the access from the water side of the wall is limited. Two alternative solutions to applying an anchor on the outside of the wall have been proposed.

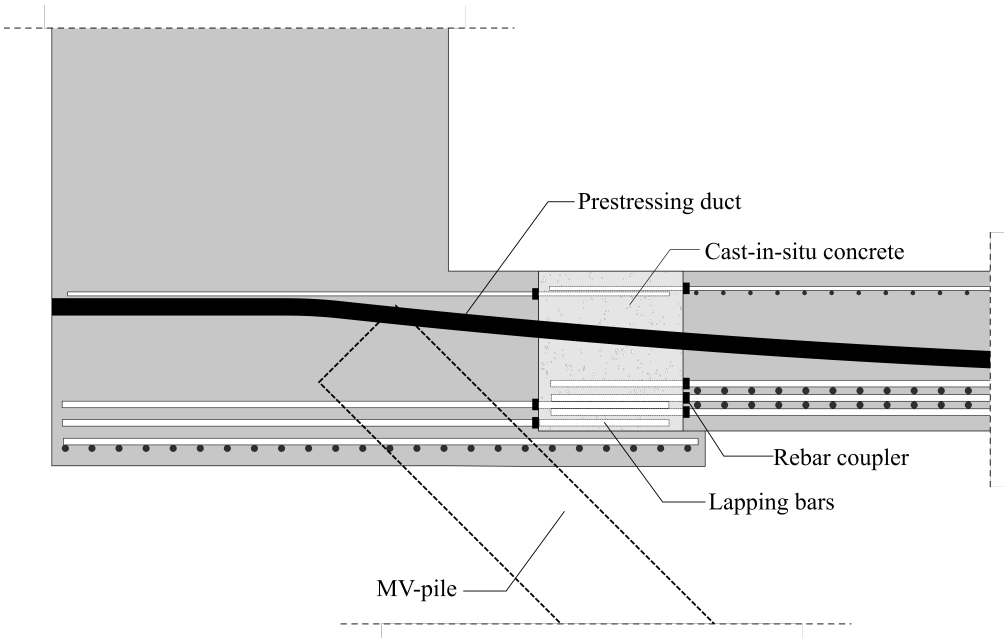

Figure 78: Suggested floor to wall connection

Solution 1: Looping anchorage

A solution can be to make use of looping anchorage. The tendons would loop through the wall, both starting and ending on the same side of the floor. This allows for both anchors of the prestressing tendon to be accessible. A looping duct should then be placed in the relieving platform wall during the initial construction, through which the prestressing tendon can be placed. The minimum radii of the loop is dependent on the thickness of the duct and is based on DIBt (2011) (European Technical Approval ETA-06/0022) and DYWIDAG (2021). For the tendon used in this thesis and defined in Table 23 (15, 7-wire strands with a total area of Ap = 2.250mm^2) the minimum radius would need to be 3,8m. To reduce the amount of overlapping looping ducts, some changes to the prestressing design could be made. One example is to reduce the c.t.c. distance (currently 0,5m) by placing multiple tendons above each other. Another option is to used tendons with a smaller thickness, for example taking 3 tendons each with 5 strands. This would reduce the minimum radius to 2,5 m. Figure 79 shows an example of looping anchors with c.t.c. of 1 m and radius of 3,8m.

This type of anchorage would however also have implications for the forces in the relieving platform resulting from prestressing, compared to the proposed prestressing design of Chapter 6. This should be held into account.

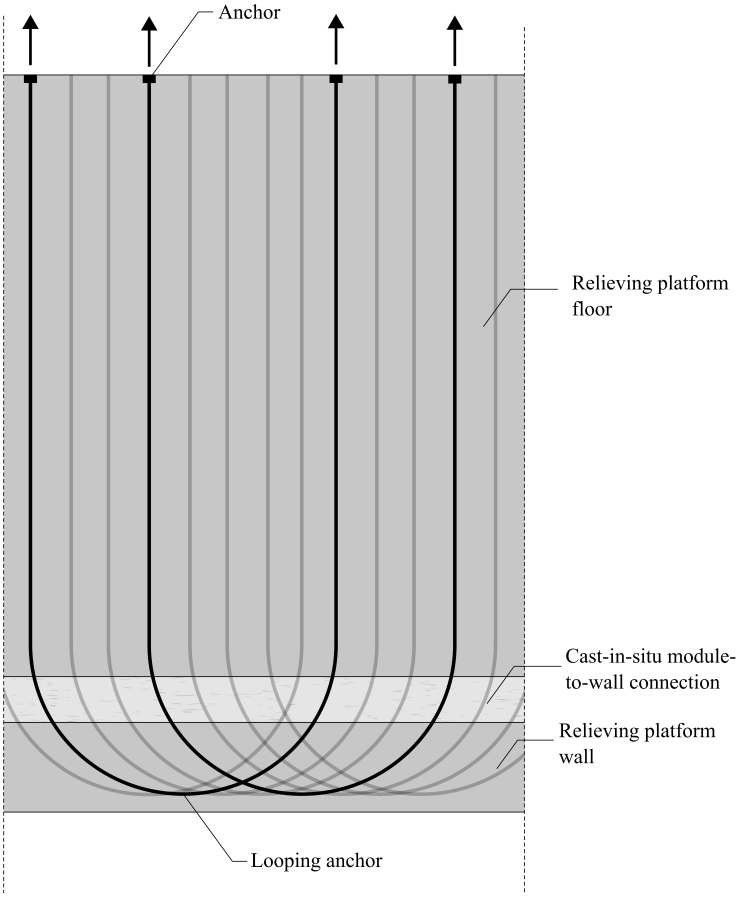

Figure 79: Solution 1: Looping anchorage

Solution 2: Prestressing only the floor

By prestressing the floor and wall together a stronger connection can be formed and in addition the prestressing can help resist the loads on the wall. However, from a practical point of view, prestressing only the floor might give a simpler solution. No anchor would need to be placed in the wall and instead can be already installed during manufacturing.

Prestressing the floor during manufacturing could also make the floor more robust during transportation and construction. The downside however is that there will be no contribution of the prestressing on the wall, that there are shear forces introduced in the floor not directly above the supports and that the connection between the wall and floor is not as strong. This could potentially however be compensated for by applying both additional shear reinforcement and longitudinal reinforcement in and near the connection.

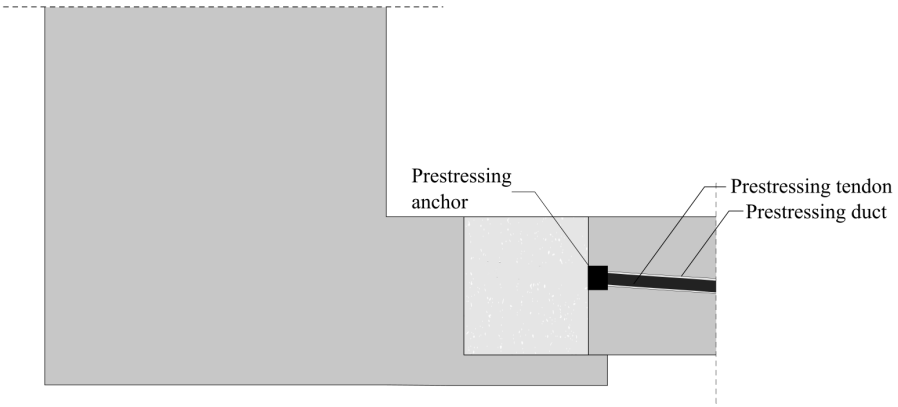

Figure 80: Solution 2: Only prestressing the floor

It is again important to take special care in water tightness and protecting the ducts from corroding materials at the location of the connection. The ducts and anchor needed for prestressing either need to be installed as the cast-in-situ concrete wall is being constructed or during the upgrade process. In the initial case the protection of the anchor and ducts is required to prevent corrosion.

After the addition of the lapping reinforcement and duct connectors, the concrete is casted into the connection. The prestressing itself can take place when the cast-in-situ concrete has hardened enough to reach a minimum strength. This should be possible after approximately 7 days.

7.2.3 Module to foundation piles

The foundation piles need to resist both vertical and horizontal loads. The first step of the design of this connection is to place a transverse beam on the foundation piles on top of which the modules can be placed. This beam transfers the loads from the modules to the foundation piles and facilitates the placement of the modules. In addition, the beam can also help mitigate the effects of slight misalignments and height differences in the foundation piles. This ensures the modules are all placed on the same level. The transverse beam can also be prefabricated and can be connected using the same approach as how the foundation piles are currently connected to the relieving platform, using protruding reinforcement bars.

The connections do not require the transfer of moments, because this would cause an increase in hogging moments above the supports of the continuous floor modules. This puts the upper flange under higher tensile stresses. Since the upper flange is both thinner and has a significantly lower amount of reinforcement it then comes at risk of excessive cracking.

The vertical forces can be directly transferred from the modules through the beam to the foundation piles. For the horizontal forces a connection is required. This connection needs to ensure the horizontal forces are transferred to the foundation piles. The foundation piles are placed at an angle, in order for them to resist horizontal forces when axially loaded. It is therefore important a connection is formed that transfers the horizontal forces from the relieving platform to the foundation piles, to ensure they become active. Two solutions are proposed.

Solution 1: Shear dowel

The first solution suggested is using steel shear dowels (Figure 81). A duct for the dowels will be installed in the foundation beam and in the module. The cross-section of the module will locally have to change in order for the ducts to be placed. The dowels will need to be placed on-site after the module has been installed, since the building sequence of the connections will not allow for protruding dowels from the beam or the modules. After installing the dowels, the ducts will be filled with grout to protect the steel dowel from corrosion. The installation and grouting should also be done after the prestressing has taken place. This prevents stresses in the connection caused by deformations of the concrete during prestressing.

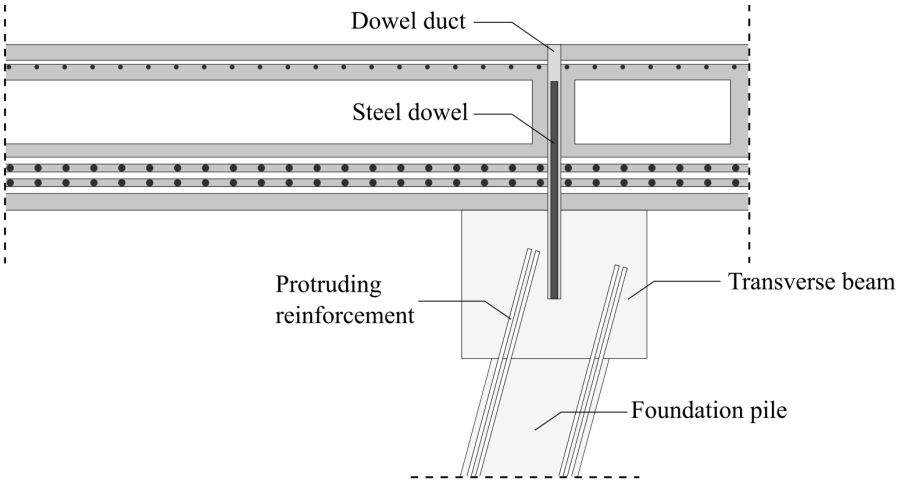

Figure 81: Solution 1: Shear dowel

Since no calculations have been made on this connection, the amount of shear dowels required to resist the loads will need to be held into account to justify this connection. If the amount of dowels required becomes too large for any practical purposes, the second solution might prove more suitable.

Solution 2: Shear key

Another solution is using a shear key. The benefit is that this connection will provide a higher strength, given proper reinforcement design. The suggested design is shown in Figure 82. The horizontal forces are then directly transferred via the transverse beam to the foundation piles. A downside however, is that it does require a significant increase in concrete and reinforcement steel. The reinforcement shown in Figure 82 is indicative and do not include the shear key. A more detailed design, including the placement of reinforcement in the shear key, must be developed. In addition this connection will also require some on-site actions to be taken, to ensure alignment and an adequate connection to be formed between the interface of the shear key and transverse beam.

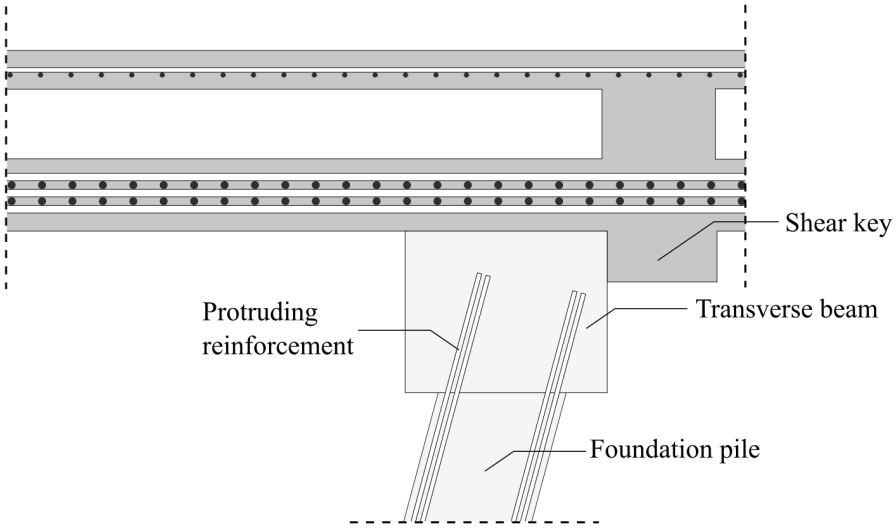

Figure 82: Solution 1: Shear key

7.3 Building sequence

The building sequence of the quay wall upgrade will be described in this section. As was mentioned the modular design aims to create an efficient and fast construction to reduce the downtime of the quay as much as possible. The steps of the building sequence are shown in Figure 83.

1. The initial case is a quay wall only containing a concrete wall supported by a steel sheet-pile wall and anchors.

2. The start of the upgrade will be by removing the infrastructure on top of the quay and excavating the soil to below the level of the concrete wall. This is done to ensure enough depth is reached to later place the substructure elements.

3. Construction of the foundation piles, using the same methods of the current foundation piles of quay walls.

4. Placing the transverse beams on top of the foundation piles. The connection between the transverse beams and the foundation piles is made using a wet connection, similar to the way foundation piles are conventionally connected to a relieving platform.

5. Placement of the modules on the corbel of the wall and the transverse beams. The modules have to be constructed from right to left (facing the water) to connect to floors to each other using the shear key connections. At this point the modules are only lying on the supports but the connections have not yet been formed.

6. Lapping reinforcement must be placed within the connection as well as duct couplers in which the prestressing tendon can run after the wall to module connections has been formed.

7. Casting concrete in the module-to-wall connection.

8. After a minimum period of 7 days the wet floor to wall connection has reached a minimum strength. The prestressing tendons can now be placed, prestressed and grouted.

9. In the case solution 1 of the module-to-pile connection (shear dowels) has been chosen: After the prestressing has been performed, the steel dowels can be placed in the floor to ensure a shear connection between the transverse beams and modules.

After this the ducts of the dowels can be grouted to protect the steel. For the second solution, this step includes the required on-site actions to ensure proper alignment and connection between the transverse beam and shear key.

10. Ensuring all other installations such as drainage are constructed. Thereafter the excavated soil can be placed back and the quay can be made ready for use again.

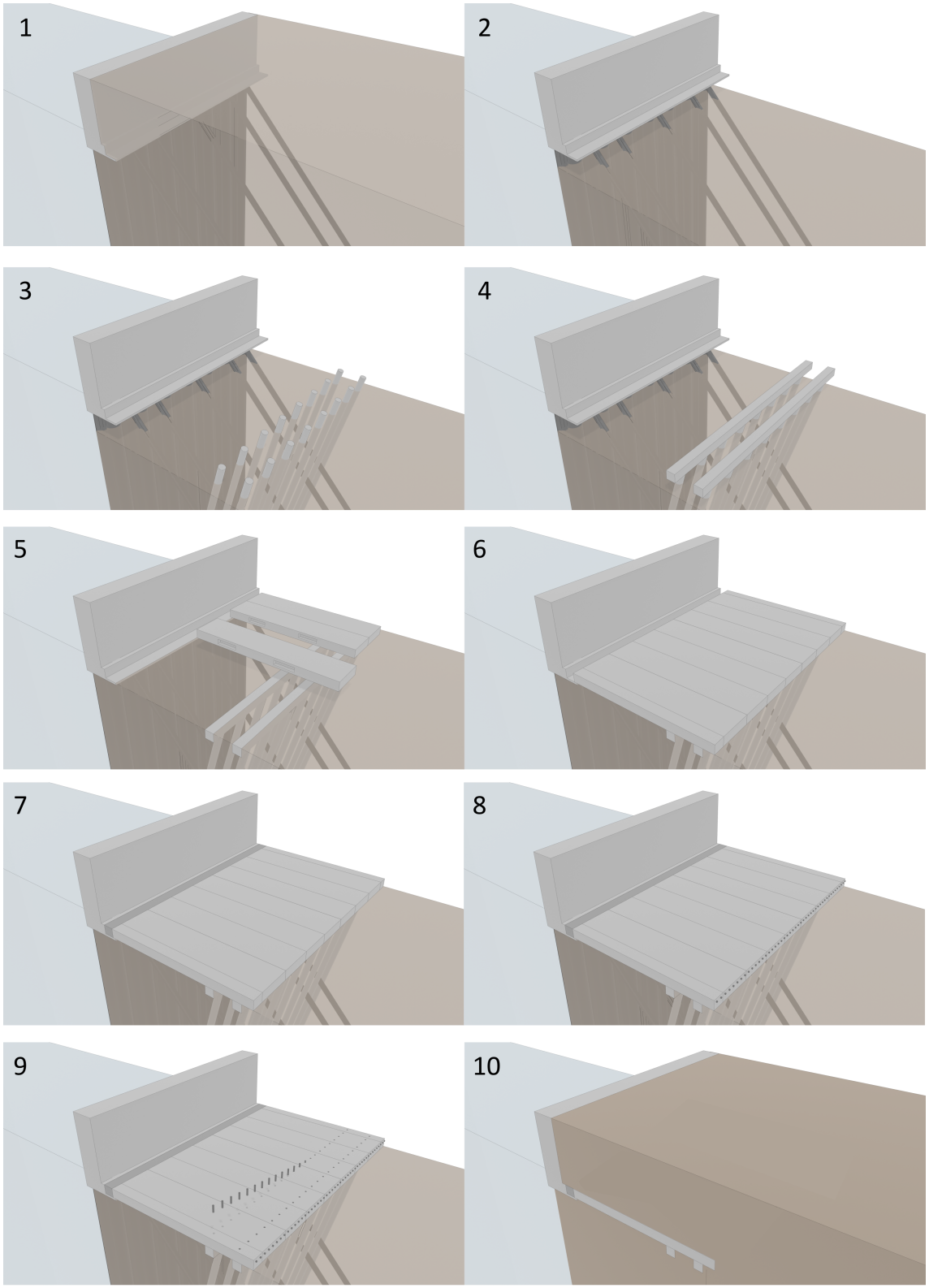

Figure 83: Building sequence

8 Discussion

Prestressing design method

The method of designing the prestressing layout has its limitations. A choice was made to use a tendon with an area A_p of 2.250 mm^2 and iteratively increase the amount of tendons within a one meter wide cross-section. This means that the tendon area and prestressing force are increased in large steps, respectively 2.250 mm^2 and 2.700 kN. This means many intermediate solutions have not been explored. In Chapter 5 different prestressing design variants have been analyzed. After this these prestressing designs were parametrized to be used in the optimization loop. The possible tendon layouts were within the boundaries of the parametrized layout scripts. The design choices of these scripts were made partly out of simplicity, to more quickly explore different design options. The use of L_1 for example, as the main parameter for the design meant all the other tendon layout parameters, such as curve radii, eccentricities and curve lengths had to be a result of this one parameter. This allowed for a simpler and more efficient Maple optimization code that could iterate through many variants and search for the optimal tendon layout. But this was at the cost of more flexible prestressing tendon variant designs. For all of these mentioned reasons, it is possible that there exist other tendon layouts that could potentially result in a more efficient prestressing design. However, it is not expected that there would be large differences with the final result in terms of height reduction, considering in the analysis performed in Section 6.3 showed eventually the rotational capacity check of the NEN-EN 1992-1-1, article 5.5 became governing, which could not be improved by changing the tendon layout. This method of optimization was mainly to explore the quantities and design options of the prestressing and what the effects are. In terms of embodied carbon, it is possible that there exists a design that uses a different layout and tendon design that would have lead to a slightly lower embodied carbon.

Governing load combinations

The load combinations used in the analysis have been based on a Python script using AnaStruct. Different combinations and variants within these combinations have been calculated in order to determine which specific load combination is governing. Two load combinations, one for SLS and one for ULS have been found, namely SLS 1.3 and SLS 3.12. These combinations were found to cause the largest bending moments. The shear forces were not the highest for these combinations, but only a negligible difference with the combinations that did give the highest shear loads. The final prestressing design has out of simplicity only considered these two load combinations. It is therefore possible that there exist load combinations for which this specific prestressing design is not exactly optimal. It is however not expected that the differences would cause a significant change in the required design.

Optimization shear forces

The optimization loop checked the shear force and bending moments at the peak loads above the supports. This was a too conservative and unrealistic value to use, since the analytical 2D model representing the supports as points causes high peak loads. In reality this is not the case, since every support also has a certain cross-sectional area. Shear forces within a distance 0,5·d from the edge of the support can be considered to directly transfer to the support. The bending moments can be taken at the edge of the support, rather than at the peak in the middle of the support. This caused the governing loads at the supports that were used in the optimization to be too high. However, looking at the final solution, it can be seen that the governing load has become the ULS bending moment at mid span. This implies that the optimization approach still resulted in an optimal solution, since the loads mid span do not suffer from the same inaccuracies as those above

the supports. It is therefore not expected that there will be a more slender cross-section height possible. The more detailed analysis of the final optimized solution also showed that the cross-sections above the supports no longer are governing (in particular after the increase of shear reinforcement).

Reference variant

The mentioned limitations of the optimization also has implications for the reference variant. As mentioned in Section 4.5 there are differences in the results of this 2D model and the original 3D model. These differences caused lower governing loads in the 2D analytical model. In the optimization analysis this was taken into account by creating a reference variant, that used the optimization loop to search for the lowest possible floor height without prestressing. This resulted in a floor height reduction from 1.750 to 1.640 mm. However, as mentioned the optimization loop took the maximum shear loads in the model, which were too conservative. This has led to the reference height being higher than it should be, which in turn means that the relative embodied carbon reduction will also be lower. To make a rough estimation of the difference a simplified approach is used, taking the relative difference of 13% between the shear forces of the original 3D model and the 2D model (Section 4.5) and using this to calculate an estimate for the reference height. This results in a floor height of 1.523 mm and a total relative embodied carbon reduction of 16% (instead of 20%).

Crack angle shear resistance

The crack angle used in the shear resistance calculations has been assumed at 39°, which was also used in the original calculations. This value has been kept the same throughout the different analysis performed. However, it can be seen in the shear resistance calculations (Appendix H) that the concrete strut strength $V_{Rd,max}$ is never reached and is approximately 2 times higher than the $V_{Rd,s}$. This indicates that a smaller angle could have been used. A smaller angle would increase $V_{Rd,s}$, since it causes more reinforcement bars to become active. This in turn could have meant the additional shear reinforcement used in Sections 6.3 and 6.4 would not have been required. A calculation is made looking at the final governing shear resistance calculation and is shown in Section H.3.1 of Appendix H This shows that the angle can be changed to 30°after which the $V_{Rd,max}$ becomes smaller than the $V_{Rd,s}$. The overall shear resistance then increased by 40 %, which is close to the difference between using shear reinforcement of $\phi 16 - 300$ mm and $\phi 20 - 300$ mm, which gave a 56% increase. Some additional shear reinforcement still is required, but the amount to which it was increased could be lower.

Embodied carbon: impact modular design

The final embodied carbon reduction (of 20%) shown in Section 6.4.3 will likely reduce due to the requirements of the prefabricated design defined in Chapter 7. The connections require an increase in the amount of materials needed compared to the design resulting from the optimization. Extra concrete is needed for the transverse foundation pile beam, the wet module-to-wall connection, the shear keys and the shear dowel to be placed. In addition the steel dowels themselves and the additional reinforcement required in the connections would also cause an increase in embodied carbon.

On the other hand, the effect prefabricated concrete elements can have in terms of embodied carbon reduction compared to more traditional in-situ concrete elements, as was mentioned in Section 2.4.1, has not been taken into account. The literature showed a reduction of embodied carbon ranging from 15,6% to 38%. This can have a significant positive effect in terms of the CO_2 emissions for the relieving platform as well.

Life Cycle Analysis

This thesis only looks at the embodied carbon of the relieving platform, the CO_2 resulting from other aspects such as transportation and construction are not taken into account. When the quay wall is being upgraded, there also will be an increase of carbon emissions that stem from the construction itself. This should also be held into account by performing a full Life Cycle Assessment (LCA) of the quay wall.

It is also important to note that all the embodied carbon reductions mentioned in this thesis are always based on many underlying assumptions of the EPD's, material databases and specific material usage of the reference case used. An LCA should also include a more in-depth evaluation of these aspects.

Geotechnical and soil loads

Two aspects that have not been taken into account are the changes of the geotechnical and the soil loads, caused by the weight and height reduction of the floor. The original geotechnical loads have been calculated using a Plaxis model by Schouten & van der Valk (2020). Here, the interaction between the sub- and superstructure has been calculated, which resulted in a set of loads placed on the superstructure. These loads will change as the weight of the floor decreases. In addition, the thinner floor also results in a change in the soil loads. The bottom of the floor is placed at the same height, meaning a larger amount of soil height needs to be carried.

Unity checks

The unity checks have all been checked until a maximum of 1,00. In practice, it often might be desirable to use a more conservative value. This could be the case in particular for the prefabricated modular design, where the modules could be made more robust to handle transportation and construction. This would again have implications for the floor thickness and the embodied carbon reduction.

Connection relieving platform wall and combi-wall

Another important consideration that needs to be taken into account is that the connection of the relieving platform wall with the combi-wall must be able to resist moments as well. This is needed to ensure stability of the quay wall during the situation when the floor is not yet added to the relieving platform. Examples of quay walls such as this exist, where only a concrete wall is placed on top of a sheet-pile wall. This connection provides a relevant example for reference.

9 Conclusion and recommendations

9.1 Conclusion

This thesis set out to explore two main objectives: first, the application of prestressing in the relieving platform of deep-sea quay walls to enable a more lightweight and lower embodied carbon design; second, the development of a prefabricated, modular relieving platform that allows for a upgradable quay wall and that could benefit from the weight reduction resulting from prestressing.

Prestressing

The results demonstrate that prestressing, in combination with an optimized cross-sectional geometry, significantly reduced material use in the floor slab. The prestressing led to a reduction of 12% reduction in embodied carbon compared to the reference design. By increasing the shear reinforcement in the critical areas in the floor and optimizing the cross-section geometry by creating a rectangular opening around the neutral axis, this was further reduced to 20%. These results reflect a 5% CO_2 reduction for the entire sheet pile quay wall. However, this is a rough estimate due to the unknown assumptions underlying the calculations for the entire sheet pile quay wall. Figure 84 shows the final results.

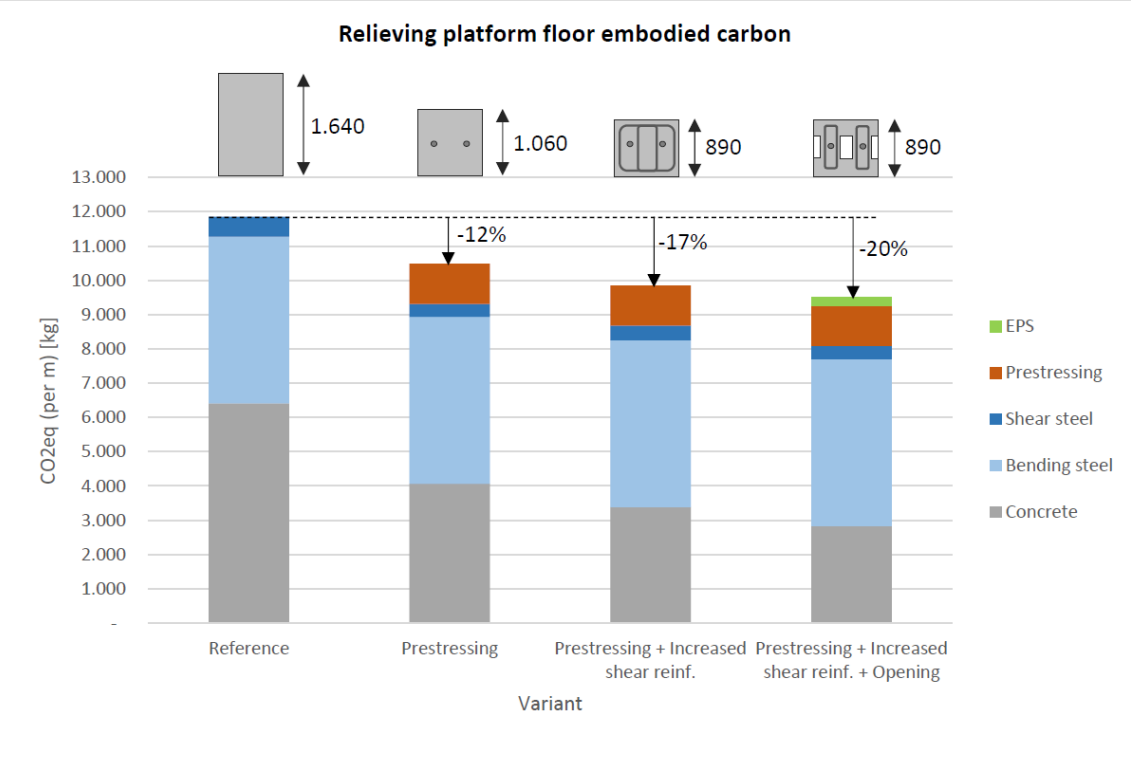

Figure 84: Embodied carbon reduction final results

The initial optimization resulted in a prestressing design that used 2 prestressing tendons (total area $A_p = 4.500$ mm^2), delivering a force after losses of 5.400 kN per meter achieving a minimum floor height of 1.060 mm. Beyond this, increasing the amount of prestressing tendons did not result in a lower embodied carbon of the floor. This is primarily due to the diminishing returns in height reduction with each additional tendon, which ultimately leads to an overall increase of the embodied carbon emissions, as the carbon increase of the tendons outweighs the savings achieved through concrete reduction.

The initial optimization with prestressing revealed that the shear capacity was governing in the design. To achieve a further height and embodied carbon reduction, the shear

reinforcement in the critical cross-sections was increased from $\phi 16-300$ to $\phi 20-300$ mm. This resulted in a final prestressing design shown in Figure 85 and a minimum height of the concrete relieving platform floor of 890 mm. Although the shear reinforcement caused a slight rise in carbon emissions, the reduction of concrete led to an additional net decrease in embodied carbon of 5%.

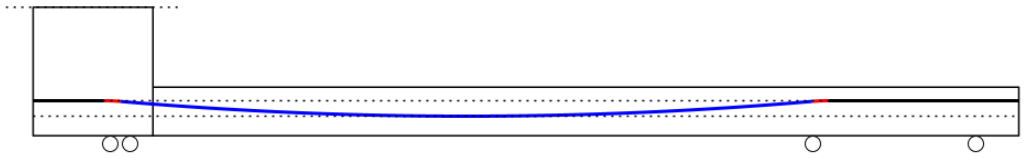

Figure 85: Final prestressing design - L_1 = 12,9 m, h = 0,89 m

Following the cross-section geometry optimization, an additional 3% embodied carbon reduction was achieved by creating a rectangular opening around the neutral axis. EPS was used as remaining formwork, which did have a small impact on the potential embodied carbon reduction (accounting for approximately 2,5% of the total embodied carbon of the relieving platform floor). The crack width reduction resulting from the prestressing played an important role in preventing leakage of corroding chemicals into the opening.

Modular design

The modular design also substantially benefited from prestressing, achieving an estimated 50% weight reduction. This has a positive impact on the transport logistics, ease of construction and the feasibility of using larger prefabricated modules. The primary advantage of the upgradable floor system in terms of embodied carbon is that the relieving platform floor is only installed when necessary. This means that for significant portions of a quay's lifespan, the floor may not be included, thereby avoiding the addition of a substantial amount of embodied carbon. Removing the floor results in an rough estimated carbon reduction of 25% (12,4 tonnes CO_2eq per meter), compared to a CO_2-footprint of 50 tonnes CO_2eq for the entire sheet pile quay wall. The modules have been designed with as 3 x 15,9 by 0,89 x elements, with a total weight per element of approximately 102 tonnes.

The module connections have been designed to align with the proposed building sequence. Three connections have been addressed: module-to-wall, module-to-module and module-to-foundation piles.

For the module-to-wall connection it was important to transfer shear forces, axial forces and bending moments. This was achieved through the use of a corbel and a wet joint using protruding reinforcement. For the module-to-module connection a shear key was proposed. This connection ensures the distribution of asymmetric loads (e.g. impact and bollard loads), allowing for the modules to remain slender and improving construction speed. For the module-to-foundation pile connection, two solutions have been proposed. A transverse beam is designed to be placed over the foundation piles, on top of which the modules can be placed. The first solution is making use of steel dowels, functioning as hinged supports to resist axial and shear loads. The second is adding a shear key, which is placed against the transverse beam.

Prestressing the relieving platform wall and the floor together can create a stronger connection. However, anchoring the tendons on the water side of the wall presents a challenge and is unpractical. Two alternative solutions have been proposed for the anchor placement. The first one is using looping reinforcement, which allows for access to the anchor from only one side of the floor. The second is to prestress only the floor. This simplifies the construction and if applied before transport can improve robustness. The downside is that this introduces shear forces in the floor not directly above the combi-wall and anchor, and that the module-to-wall connection has no benefit of the prestressing.

This can be mitigated through additional shear reinforcement in the floor and additional longitudinal reinforcement in the module to wall connection.

In conclusion, prestressing can play an important role in creating lightweight, lower-carbon and modular relieving platforms for deep-sea quay walls. It has allowed for a significant material reduction, crack control and weight reduction, facilitating the prefabrication of the floor. This design offers a flexible, upgradeable and lightweight alternative to traditional the relieving platform design.

9.2 Recommendations

In terms of prestressing the main recommendations are:

- The prestressing tendons should be designed with curvatures that reduce the largest bending moments in the structure, but care should also be taken to ensure the shear forces are reduced as much as possible. Placing the tendon transition curves directly above the supports ensures efficient load transfer.

- The number of tendons should be limited to the point at which the reduction of the embodied carbon from the decreased concrete use outweighs the additional embodied carbon introduced by the prestressing steel.

In terms of the prefabricated modular design:

- The module-to-module connection can be designed as a shear key, allowing for fast construction and the cooperation of the modules under unevenly distributed loads. The distribution of loads allows for the modules to remain slender.

- Introduce a transverse beam above the foundation piles to simplify module placement and counteract any misalignments of the foundation piles. The modules can then be connected using shear dowels or a shear key to transfer axial and horizontal loads.

- The module-to-wall connection is best suited as a wet connection that resists axial forces, shear forces, and bending moments. This maximizes the stability and strength benefits of the relieving platform. Special care should be taken for the prestressing anchor placement on the water side of the relieving platform.

Suggestions for future research:

- Expanding the current findings, which are based on a 2D analytical model, to a numerical 3D model. This can give a better understanding of the effects of prestressing on the relieving platform.

- Further investigating the connections of the modular design and the prestressing anchor placement. A more detailed investigation could give a better idea into the possibilities and limitations of the modular design.

- Exploring alternatives to EPS formwork for creating internal openings. Although lightweight, the material contributes to the embodied carbon and could be replaced with lower-impact materials or a different manufacturing method (e.g. slab extrusion).

- Performing a full life cycle analysis (LCA) to further evaluate the potential of both the prestressing and the modular, upgradeable design in terms of reduced CO_2 emissions.

- As has been suggested by van Rhede van der Kloot (2019) the prefabricated elements can be combined with geopolymer concrete. Geopolymer concrete has been successfully applied in the quay walls of the Port of Rotterdam and has shown to cause a significant CO_2 reduction. The effect of prestressing would need to be reevaluated for this.
- The prefabricated diaphragm wall using vertical prestressing suggested by Amaarouk et al. (2013) could be combined with the prefabricated floor modules of this thesis. This could allow for a completely modular quay wall, but would require additional investigation into the overall design and connections.

References

Amaarouk, A., de Gijt, J., & Braam, C. (2013). The feasibility of removable prefab diaphragm walls. In A. Djwantoro & H. Djwantoro (Eds.), *Proceedings of the 4th international conference of the euro-asia civil engineering forum, innovations in civil engineering for society and environment eacef 2013* (pp. 1–23). Institute for Research and Community Service. (EACEF 2013, the 4th international conference of the Euro-Asia civil engineering forum, Singapore ; Conference date: 26-06-2013 Through 28-06-2013)

Association of Consulting Engineers Singapore. (2025). *PRACTICAL GUIDE FOR POST-INSTALLED REINFORCEMENT*. Association of Consulting Engineers Singapore. Retrieved from https://www.aces.org.sg/wp-content/pdf/20250210%20Practical%20Guide%20for%20PIR_Final.pdf

Bompa, D., & Elghazouli, A. (2017). Ductility considerations for mechanical reinforcement couplers. *Structures*, *12*, 115-119. Retrieved from https://www.sciencedirect.com/science/article/pii/S2352012417300541 doi: https://doi.org/10.1016/j.istruc.2017.08.007

Boskalis. (n.d.). *Maasvlakte 2 rotterdam.* Retrieved Accessed: 2024-10-28, from https://nederland.boskalis.com/projecten/maasvlakte-2-rotterdam

Buring, P. (2013). *Flexible quay wall structures for container vessels* (Master's thesis, Delft University of Technology). Retrieved from https://resolver.tudelft.nl/uuid:31085c73-e1ee-4d6a-a915-40c9dbc564c9

CBS. (2019, 5). *CO2-equivalenten.* Retrieved from https://www.cbs.nl/nl-nl/nieuws/2019/19/uitstoot-broeikasgassen-licht-gedaald/co2-equivalenten

Chang, R., Zhang, N., & Gu, Q. (2023, 6). A Review on Mechanical and Structural Performances of Precast Concrete Buildings. *Buildings*, *13*(7), 1575. Retrieved from https://doi.org/10.3390/buildings13071575 doi: 10.3390/buildings13071575

Chippagiri, R., Bras, A., Sharma, D., & Ralegaonkar, R. V. (2022). Technological and sustainable perception on the advancements of prefabrication in construction industry. *Energies*, *15*(20). Retrieved from https://www.mdpi.com/1996-1073/15/20/7548 doi: 10.3390/en15207548

De Gijt, J. (2010). *A history of quay walls, techniques, types, costs and future* (Doctoral dissertation). doi: 10.13140/RG.2.2.12178.66249

De Gijt, J., & Toorn, A. (2009, 1). Future trends in quay wall design..

DIBt. (2011, 1). *European technical approval eta-06/0022* (Tech. Rep.). Retrieved from https://www.dibt.de/pdf_storage/2011/ETA-06%210022%288.03.01-34%2110%29e.pdf

Dieteren, G. (2022, 11). *RBK 1.2 Achtergrondrapport Beton.*

DINOloket. (n.d.). *Ondergrondmodellen kaart.* Retrieved Accessed: 2024-10-28, from https://www.dinoloket.nl/ondergrondmodellen/kaart

Douairi, M., & De Gijt, J. (2013, 05). Upgrading techniques for quay walls. *IABSE Symposium Report*, *99*. doi: 10.2749/222137813806474192

DYWIDAG. (2021, 3). *Dywidag bonded post-tensioning systems using strands* (Tech. Rep.). Retrieved from https://dywidag.com/downloads/bonded-post-tensioning-systems-using-strands/en

Global Carbon Project. (2023). *Carbon dioxide emissions from the manufacture of cement worldwide from 1960 to 2022.* Retrieved 2024-10-16, from https://www.statista.com/statistics/1299532/carbon-dioxide-emissions-worldwide-cement-manufacturing/

Google. (n.d.). *Location of the sif quay wall in the port of rotterdam.* Retrieved 2024-10-26, from https://maps.app.goo.gl/QtFHTuWUmMMLzw4M6

Handboek Tunnelbouw. (2023, 4). Retrieved 2025-05-05, from https://www.handboektunnelbouw.nl/ontwerpaspecten/ontwerpaspecten-definitieve-constructie/zink-sluit-en-mootvoegen-afgezonken-tunnels/tand-en-kraagconstructies/

Hanusaik, N. V. (2021). *Analysis and optimization of transverse post-tensioning in immersed tunnels* (Master's thesis, Delft University of Technology). Retrieved from https://resolver.tudelft.nl/uuid:4274c784-6f14-4bd5-94b0-9ac3524fc308

Holly, I., & Abrahoim, I. (2020, 3). Connections and Joints in Precast Concrete Structures. *Slovak Journal of Civil Engineering*, *28*(1), 49–56. Retrieved from https://doi.org/10.2478/sjce-2020-0007 doi: 10.2478/sjce-2020-0007

Imbabi, M. S., Carrigan, C., & McKenna, S. (2012). Trends and developments in green cement and concrete technology. *International Journal of Sustainable Built Environment*, *1*(2), 194-216. Retrieved from https://www.sciencedirect.com/science/article/pii/S2212609013000071 doi: https://doi.org/10.1016/j.ijsbe.2013.05.001

Jang, H., Ahn, Y., & Roh, S. (2022). Comparison of the embodied carbon emissions and direct construction costs for modular and conventional residential buildings in south korea. *Buildings*, *12*(1). Retrieved from https://www.mdpi.com/2075-5309/12/1/51 doi: 10.3390/buildings12010051

Jiang, Y., Chen, H., Nie, X., & Tao, M. (2021). Experimental study on bond and anchorage of steel bars in precast concrete structures with new-to-old concrete interface. *Engineering Structures*, *247*, 113086. Retrieved from https://www.sciencedirect.com/science/article/pii/S0141029621012232 doi: https://doi.org/10.1016/j.engstruct.2021.113086

Kamphorst, K. (2022, 10). *LCA van wapeningsstaal van Holterman Wapeningsstaal BV (A1-A3)* (Tech. Rep.).

Lan, S. (2025, 1). The Discourse and Investigation Regarding the Advancement of Prefabricated Concrete Building Technology. *Theoretical and Natural Science*, *79*(1), 139–144. Retrieved from https://doi.org/10.54254/2753-8818/2025.20097 doi: 10.54254/2753-8818/2025.20097

Lyu, F., Shao, H., & Zhang, W. (2022). Comparative analysis about carbon emission of precast pile and cast-in-situ pile. *Energy Reports*, *8*, 514-525. Retrieved from https://www.sciencedirect.com/science/article/pii/S235248472200659X (The 2021 7th International Conference on Advances in Energy Resources and Environment Engineering) doi: https://doi.org/10.1016/j.egyr.2022.03.101

Martins, R., do Carmo, R., Costa, H., & Júlio, E. (2023). A review on precast structural concrete walls and connections. *Advances in Structural Engineering*, *26*(14), 2600-2620. Retrieved from https://doi.org/10.1177/13694332231191073 doi: 10.1177/13694332231191073

Milieudatabase, S. N. (2020, 11). *Categorie 3 Milieuverklaring Ophoogmateriaal, EPS.* Retrieved from https://milieudatabase.nl/nl/viewer/milieuverklaring/nmd_36899/

Milieudatabase, S. N. (2021a, 9). *Categorie 3 Milieuverklaring Voorspanstaal (ligger).* Retrieved from https://milieudatabase.nl/nl/viewer/milieuverklaring/nmd_44995/

Milieudatabase, S. N. (2021b, 8). *Categorie 3 Milieuverklaring Wapeningsstaal.* Retrieved from https://milieudatabase.nl/nl/viewer/milieuverklaring/nmd_45791/

Milieudatabase, S. N. (2025, 2). *Categorie 3 Milieuverklaring Betonmortel C35/45 (o.b.v. CEM IIIB).* Retrieved from https://milieudatabase.nl/nl/viewer/milieuverklaring/nmd_201627/

Nederhoff. (n.d.). *Mobiele telescoopkranen - Kraanbedrijf Nederhoff.* Retrieved 2025-04-25, from https://www.nederhoff.nl/diensten/hijskranen/mobiele-telescoopkranen/

Nederland, V. W. (2021, 7). *EPD - wapeningsstaal voor toepassing in gewapende betonconstructies* (Tech. Rep.). Retrieved from https://www.wapned.nl/assets/uploads/files//1.1.00236.2021_MRPI-EPD_VWN_-_Vereniging_Wapeningsstaal_Nederland_Wapeningsstaal_voor_toepassing_in_gewapende_betonconstructies_FINAL_.pdf

Nie, X., Huang, D., Zhuang, L., Fan, J., & Deng, N. (2025). Precast concrete connections for alleviating reinforcement congestion: A state-of-the-art review. *Engineering Structures*, *331*, 119985. Retrieved from https://www.sciencedirect.com/science/article/pii/S0141029625003761 doi: https://doi.org/10.1016/j.engstruct.2025.119985

Nodehi, M., & Taghvaee, V. M. (2021, Jun). Alkali-activated materials and geopolymer: A review of common precursors and activators addressing circular economy. *Circular Economy and Sustainability*, *2*(1), 165–196. doi: 10.1007/s43615-021-00029-w

Paolo, N., & Giandomenico, T. (2012, 1). Design Guidelines for Connections of Precast Structures under Seismic Actions. *European Commission - Institute for the Protection and Security of the Citizen.* Retrieved from http://www.assobeton.it/ASSOBETON/gestsito_new.nsf/xsp/.ibmmodres/domino/OpenAttachment/assobeton/gestsito_new.nsf/801F35EA7CDFC12DC1257A83003BCF98/doc_allegati/Safecast_Regole_progettazione_connessioni_strutture_eng_2012_rev.pdf doi: 10.2777/37605

Pekgokgoz, R. K., & Yakut, I. (2024). Investigation of passive controlled post-tensioning system on the structural behaviour of precast reinforced concrete beam–column connections. *Buildings*, *14*(12). Retrieved from https://www.mdpi.com/2075-5309/14/12/3910 doi: 10.3390/buildings14123910

Port of Rotterdam. (n.d.). *Facts and figures.* Retrieved Accessed: 2024-10-28, from https://www.portofrotterdam.com/en/experience-online/facts-and-figures

Port of Rotterdam. (2017). *Maasvlakte 2 in 2035.*

Port of Rotterdam. (2021). *Nieuwe kademuur sif group gereed.* Retrieved Accessed: 2024-10-28, from https://www.portofrotterdam.com/nl/nieuws-en-persberichten/nieuwe-kademuur-sif-group-gereed

Port of Rotterdam. (2022). *Climate targets 2023.* Retrieved 2024-12-15, from https://www.portofrotterdam.com/sites/default/files/2023-11/climate-targets-2030-port-of-rotterdam-authority.pdf

Port of Rotterdam. (2024). *Geopolymeerbeton moet gemeengoed worden in haven rotterdam.* Retrieved 2025-04-21, from https://www.portofrotterdam.com/nl/nieuws-en-persberichten/geopolymeerbeton-moet-gemeengoed-worden-haven-rotterdam

RDW. (n.d.). *Aanvragen jaarontheffing.* Retrieved 2025-04-25, from https://www.rdw.nl/zakelijk/branches/exceptioneel-transport/ontheffing-aanvragen-voor-exceptioneel-transport/aanvragen-jaarontheffing

Rijkswaterstaat. (n.d.). *Richtlijnen Ontwerp Kunstwerken (ROK) versie 2.0* (Tech. Rep.). Retrieved from https://rok.rwskennisbron.nl/index.php/ROK

Roelevink, G. (2020, 5). *Maasvlakte-Offshore Center/kadeverlenging Sif - Definitief Ontwerp (DO).*

Rogowsky, D. M., & Marti, P. (1996). *DETAILING FOR POST-TENSIONED.*

Schouten, A., & van der Valk, R. (2020, 5). *Maasvlakte-Offshore Center/kadeverlenging Sif - DO Bovenbouw.*

Sewcharan, A. (2023). *A smarter design calculation for quay walls* (Master's thesis, Delft University of Technology). Retrieved from https://resolver.tudelft.nl/uuid:98fd32af-f757-4186-baf3-4d7e767d117b

SGS Search Consultancy, Diemel, V., Vroege, G.-J., & van Hövell, M. (2019, 9). *Ongetoetst LCA rapport voor betonmortel* (Tech. Rep.). Retrieved from https://milieudatabase.nl/nl/rapporten-tool/report/5/

SpanstaalBV, N. (2022, 1). *EPD - Prestressing steel (strand and wire) for application in prestressed concrete.* (Tech. Rep.). Retrieved from https://www.mrpi.nl/epd/prestressing-steel-strand-and-wire-for-application-in-prestressed-concrete/

Teng, Y., Li, K., Pan, W., & Ng, T. (2018). Reducing building life cycle carbon emissions through prefabrication: Evidence from and gaps in empirical studies. *Building and Environment*, *132*, 125-136. Retrieved from https://www.sciencedirect.com/science/article/pii/S0360132318300386 doi: https://doi.org/10.1016/j.buildenv.2018.01.026

Tensacciai. (n.d.). *Post-tensioning.* Retrieved from https://www.tensacciai.it/sites/default/files/technology/files/brochure/tensa-post-tensioning_0.pdf

UN. (2024). *Global status report for buildings and construction: Beyond foundations: Mainstreaming sustainable solutions to cut emissions from the buildings sector.* Nairobi.

van Algemene Zaken, M. (n.d.). *Veilig rijden in de vrachtwagen.* Retrieved 2025-04-25, from https://www.rijksoverheid.nl/onderwerpen/verkeersveiligheid/veilig-rijden-in-de-vrachtwagen

van Rhede van der Kloot, G. (2019). *Sustainability assessment of quay wall development in the port of rotterdam* (Master's thesis, Delft University of Technology). Retrieved from https://resolver.tudelft.nl/uuid:1b8b8008-3487-4bed-9702-691d65c69ce6

Verheul, L. (2023, 11). *Category 1, 2 and 3 data, what is the difference?* Retrieved from https://milieudatabase.nl/en/latest/news/category-1-2-and-3-data-what-is-the-difference/

Vink, R. (2018). *Anastruct.* Retrieved 2025-05-05, from https://anastruct.readthedocs.io/en/latest/index.html

Walraven, J., & Braam, C. (2019). *Cie3150/4160 prestressed concrete.*

Yan, W.-T., Han, B., Xie, H.-B., Li, P.-F., & Zhu, L. (2020). Research on numerical model for flexural behaviors analysis of precast concrete segmental box girders. *Engineering Structures*, *219*, 110733. Retrieved from https://www.sciencedirect.com/science/article/pii/S0141029619345286 doi: https://doi.org/10.1016/j.engstruct.2020.110733

Yang, C., Li, A., & Xie, L. (2022). Development of design method for precast concrete frame with dry-connected rotational friction dissipative beam-to-column joints. *Journal of Building Engineering*, *45*, 103563. Retrieved from https://www.sciencedirect.com/science/article/pii/S2352710221014212 doi: https://doi.org/10.1016/j.jobe.2021.103563

Ye, M., Jiang, J., Chen, H., Zhou, H., & Song, D. (2021). Seismic behavior of an innovative hybrid beam-column connection for precast concrete structures. *Engineering Structures*, *227*, 111436. Retrieved from https://www.sciencedirect.com/science/article/pii/S0141029620340372 doi: https://doi.org/10.1016/j.engstruct.2020.111436

Zwakhals, J., Taneja, P., & Ligteringen, H. (2012, 02). Quay wall design for an uncertain future. *Proc. Int.Conf. on Coastal Engineering in Developing Countries,*.

Öchsner, A. (2021). *Classical Beam Theories of Structural Mechanics*. Retrieved from https://doi.org/10.1007/978-3-030-76035-9 doi: 10.1007/978-3-030-76035-9

A Spring stiffness values

The spring stiffnesses of the substructure have been calculated in a Plaxis model by Schouten & van der Valk (2020) and are shown in the Tables 53 to 56.

Table 53: Horizontal springs

	Combiwand		**Palen rij 1**		**Palen rij 2**		
	Actief	**Passief**	**Actief**	**Passief**	**Actief**	**Passief**	
Berekend [MN/m²]	-0,5	0,7	-0,7	1,6	-0,9	2,2	*per meter*
Ondergrens veerwaarde [MN/m²]	-0,32	0,47	-0,46	1,13	-0,61	1,57	*per meter*
Bovengrens veerwaarde [MN/m²]	-0,64	0,94	-0,93	2,26	-1,22	3,14	*per meter*
h.o.h. [m]	3,294	3,294	2,88	2,88	2,88	2,88	
Ondergrens veerwaarde [MN/m]	-1,05	1,54	-1,33	3,25	-1,76	4,52	*per paal*
Bovengrens veerwaarde [MN/m]	-2,11	3,08	-2,67	6,51	-3,53	9,05	*per paal*

Table 54: Horizontal spring soil

	Grondveer	
	Passief	
Berekend [MN/m²]	23,5	*per meter*
Ondergrens veerwaarde [MN/m²]	16,61	*per meter*
Bovengrens veerwaarde [MN/m²]	33,23	*per meter*

Table 55: Vertical springs

	Combiwand		**Palen rij 1**		**Palen rij 2**		
	U [m]	**F [MN]**	**U [m]**	**F [MN]**	**U [m]**	**F [MN]**	
Berekend - stap 1	0,017	8,742	0,032	5,500	0,032	5,500	*per paal*
Berekend - stap 2	0,050	13,400	0,092	6,000	0,092	6,000	*per paal*
Berekend - stap 3	0,142	17,867					*per paal*
Ondergrens veerwaarde - stap 1	0,024	8,742	0,045	5,500	0,045	5,500	*per paal*
Ondergrens veerwaarde - stap 2	0,070	13,400	0,130	6,000	0,130	6,000	*per paal*
Ondergrens veerwaarde - stap 3	0,201	17,86					*per paal*
Bovengrens veerwaarde - stap 1	0,012	8,742	0,023	5,500	0,023	5,500	*per paal*
Bovengrens veerwaarde - stap 2	0,035	13,400	0,065	6,000	0,065	6,000	*per paal*
Bovengrens veerwaarde - stap 3	0,100	17,867					*per paal*

Table 56: Springs anchors

	Ankers		
	Actief	**Passief**	
Berekend [MN/m]	125	125	*per paal*
Ondergrens veerwaarde [MN/m]	88	88	*per paal*
Bovengrens veerwaarde [MN/m]	177	177	*per paal*

B Analytical load cases

B.1 Load cases

Load cases

	PB1	PB2	PB3.1	PB3.2	PB4	VB1.1	VB1.2	VB2.1	VB2.2	VB3.1	VB3.2	VB3.3
Basic												
q_selfweight	1.006	-	-	-	-	-	-	-	-	-	-	-
q_floor	-	2.231	-	-	-	1.533	767	613	307	-	-	-
MA	-3.098	-8.374	9.702	12.488	-	-15.607	-7.803	-6.243	-3.121	-26.900	-13.450	-13.450
FVA	8.187	-	-	-	-	3.373	1.687	1.349	1.349	-	-	-
FHA	-	-3.150	-11.088	-14.273	-	-4.102	-2.051	-1.641	-820	-4.000	-2.000	-2.000
MB	-	-	-	-	-	-	-	-	-	-	-	-
FVB	-	-	-5.151	-12.714	-	-	-	-	-	-	-	-
FHB	-	-	-5.151	-12.714	-	-	-	-	-	-	-	-
MC	-	-	-1.768	-3.552	-	-	-	-	-	-	-	-
FVC	-	-	-	-	-	-	-	-	-	-	-	-
FHC	-	-	-1.384	-2.600	-	-	-	-	-	-	-	-
MD	-307	-2.747	-1.960	-4.168	-	-3.319	-1.659	-1.325	-663	-	-	-
FVD	786	4.388	-	-	-	4.847	2.424	1.936	968	-	-	-
FHD	-	-2.599	-1.568	-3.320	-	-	-	-	-	-	-	-

	VB4.1	VB4.2	VB4.3	VB5.1	VB5.2	VB5.3	VB6.1	VB6.2	VB6.3	VB7
Basic										
q_selfweight	-	-	-	-	-	-	-	-	-	-
q_floor	-	-	-	-	-	-	-	-	-	-
MA	-45.730	-22.865	-22.865	10.847	10.851	10.851	31.750	31.750	31.750	22.641
FVA	-	-	-	-	-	-	-	-	-	-34.500
FHA	-6.800	-3.400	-3.400	1.999	2.000	2.000	10.000	10.000	10.000	-5.175
MB	-	-	-	-	-	-	-	-	-	-
FVB	-	-	-	-	-	-	-	-	-	-
FHB	-	-	-	-	-	-	-	-	-	-
MC	-	-	-	-	-	-	-	-	-	-
FVC	-	-	-	-	-	-	-	-	-	-
FHC	-	-	-	-	-	-	-	-	-	-
MD	-	-	-	-	-	-	-	-	-	-
FVD	-	-	-	-	-	-	-	-	-	-
FHD	-	-	-	-	-	-	-	-	-	-

Figure 86: Analytical load cases

PB1 - Self weight

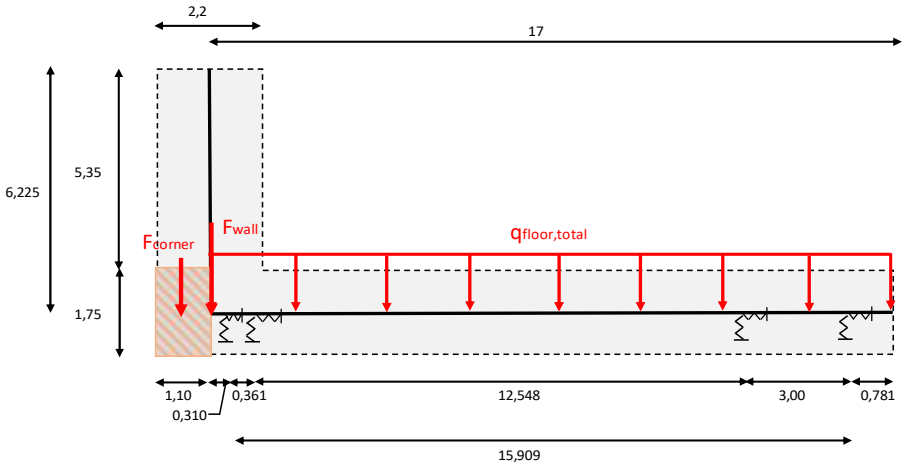

23 m segment

γ	25	kN/m3
F_{wall}	6.768	kN
F_{corner}	1.107	kN
$q_{floor,total}$	1.006	kN/m

Simplified model

q_{total}	: qfloor,total	1.006	kN/m
q_{floor}	-	0	kN/m
M_A	: Qcorner*(0,55+0,31) + Qwall*0,31 + 0,31*qfloor,total* 0,31/2	-3.098	kNm
F_{VA}	: Qwall + Qcorner + qfloor*0,31	8.187	kN
F_{HA}	-	0	kN
M_B	-	0	kNm
F_{VB}	-	0	kN
F_{HB}	-	0	kN
M_C	-	0	kNm
F_{VC}	-	0	kN
F_{HC}	-	0	kN
M_D	: qfloor*0,781*(0,5*0,781)	-307	kNm
F_{VD}	: qfloor*0,781	786	kN
F_{HD}	-	0	kN

PB2 - Soil loads

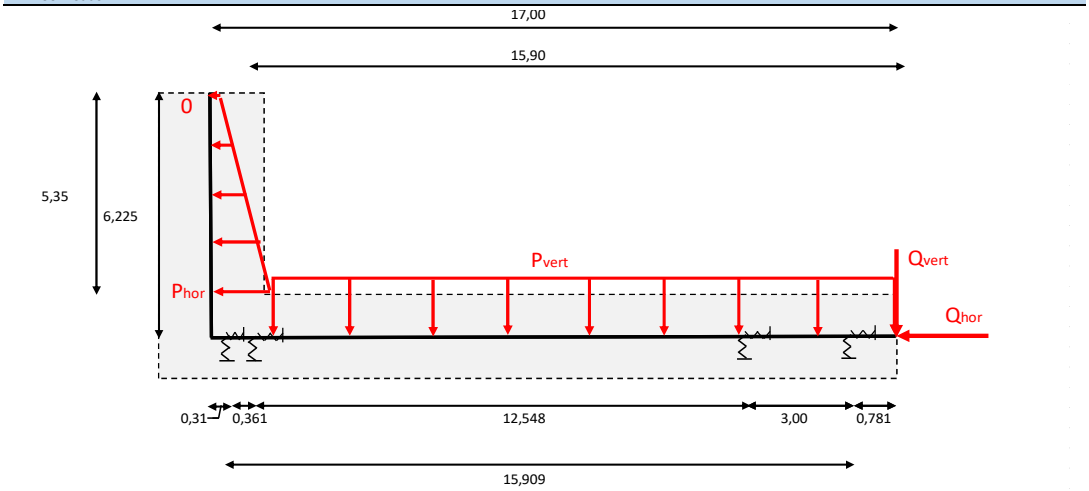

23 m segment

Pvert	97*23	2231	kN/m
Phor,-0,25m	51,2*23	1177,6	kN/m
Qhor	113*23	2599	kN
Qvert	115*23	2645	kN

Simplified model

q_{total}	-	0	kN/m
q_{floor}	: Pvert	2.231	kN/m
M_A	: ((6,225-5,350)+(5,350/3))*(5,350*Phor,-0,25m)/2	-8.374	kNm
F_{VA}	-	0	kN
F_{HA}	: -(5,350 * Phor,-0,25m*(1/2))	-3.150	kN
M_B	-	0	kNm
F_{VB}	-	0	kN
F_{HB}	-	0	kN
M_C	-	0	kNm
F_{VC}	-	0	kN
F_{HC}	-	0	kN
M_D	: 0,781*Pvert*0,5 + Qvert*0,781	-2.747	kNm
F_{VD}	: Qvert + 0,781* Pvert	4.388	kN
F_{HD}	: -Qhor	-2.599	kN

PB3.1/3.2 - Geotechnical loads BGT/UGT current scenario

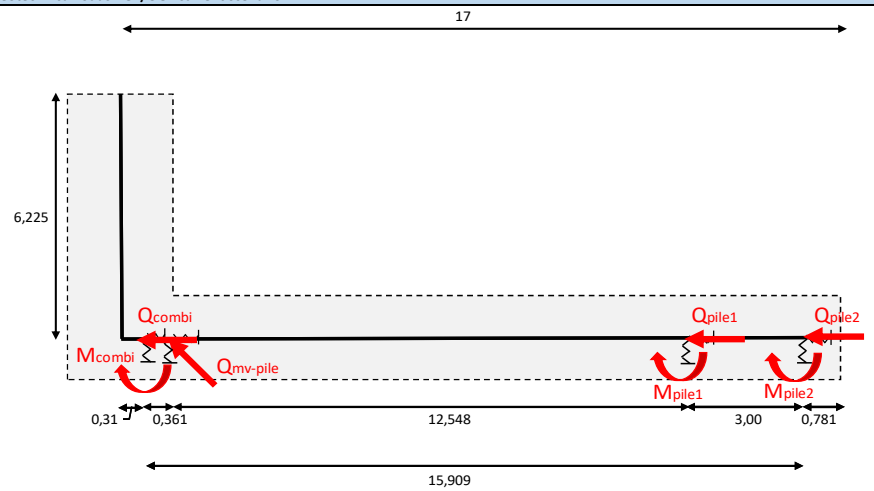

	BGT	UGT	23 m segment BGT	UGT		Amount	
Mcombi	1386		1784	9702	12488 kNm	7	
Mpile1	221		444	1768	3552 kNm	7	
Mpile2	245		521	1960	4168 kNm	8	
Qcombi	1584		2039	11088	14273 kN	7	
Qmv-pile	1457		3596	7285	17980 kN	5	45 [deg]
Qpile1	173		325	1384	2600 kN	8	
Qpile2	196		415	1568	3320 kN	8	

Simplified model (PB3.1)

q_{total}	-	0	kN/m
q_{floor}	-	0	kN/m
M_A	: Mcombi	9.702	kNm
F_{VA}	-	0	kN
F_{HA}	: -Qcombi	-11.088	kN
M_B	-	0	kNm
F_{VB}	: -cos(45) * Qmv-pile	-5.151	kN
F_{HB}	: -sin(45) * Qmv-pile	-5.151	kN
M_C	: Mpile1	-1.768	kNm
F_{VC}	-	-	kN
F_{HC}	: -Qpile1	-1.384	kN
M_D	: Mpile2	-1.960	kNm
F_{VD}	-	-	kN
F_{HD}	: -Qpile2	-1.568	kN

Simplified model (PB3.2)

q_{total}	-	0	kN/m
q_{floor}	-	0	kN/m
M_A	: Mcombi	12.488	kNm
F_{VA}	-	0	kN
F_{HA}	: -Qcombi	-14.273	kN
M_B	-	0	kNm
F_{VB}	: -cos(45) * Qmv-pile	-12.714	kN
F_{HB}	: -sin(45) * Qmv-pile	-12.714	kN
M_C	: Mpile1	-3.552	kNm
F_{VC}	-	-	kN
F_{HC}	: -Qpile1	-2.600	kN
M_D	: Mpile2	-4.168	kNm
F_{VD}	-	-	kN
F_{HD}	: -Qpile2	-3.320	kN

VB1 **Terrein belasting current**

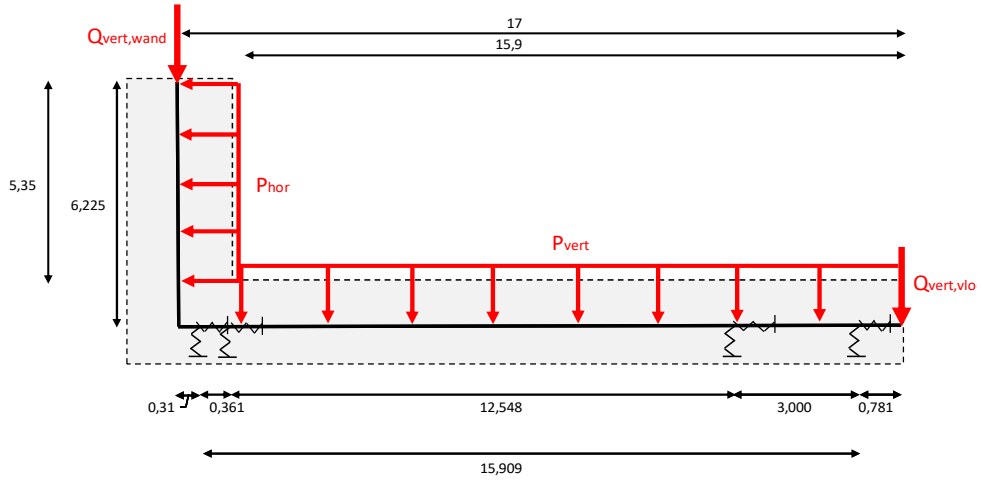

				VB1.1	VB1.2	
Pvert		100	kN/m2	1.533	767	kN/m
Phor	: Pvert*kh	50	kN/m2	767	383	kN/m
Qvert,wand	: Pvert*bkesp	220	kN/m	3.373	1.687	kN
Qvert,vloer	: Pvert*hgrond*tan24	238	kN/m	3.649	1.825	kN

Simplified model - VB1.1: 2/3 of the length

q_{total}	-	0	kN/m
q_{floor}	: Pvert	1.533	kN/m
M_A	: ((6,225-5,35)+(5,35/2))*(5,35)*Phor + 0.310*Qvert,wand	-15.607	kNm
F_{VA}	: Qvert,wand	3.373	kN
F_{HA}	: -5,35*Phor	-4.102	kN
M_B	-	0	kNm
F_{VB}	-	0	kN
F_{HB}	-	0	kN
M_C	-	0	kNm
F_{VC}	-	0	kN
F_{HC}	-	0	kN
M_D	: (1/2) * (0,781^2) * Pvert + 0,781 * Qvert,vloer	-3.319	kNm
F_{VD}	: 0,781*Pvert + Qvert,vloer	4.847	kN
F_{HD}	-	0	kN

Simplified model - VB1.2: 1/3 of the length

q_{total}	-	0	kN/m
q_{floor}	: Pvert	767	kN/m
M_A	: ((6,225-5,35)+(5,35/2))*(5,35)*Phor + 0.310*Qvert,wand	-7.803	kNm
F_{VA}	: Qvert,wand	1.687	kN
F_{HA}	: -5,35*Phor	-2.051	kN
M_B	-	0	kNm
F_{VB}	-	0	kN
F_{HB}	-	0	kN
M_C	-	0	kNm
F_{VC}	-	0	kN
F_{HC}	-	0	kN
M_D	: (1/2) * (0,781^2) * Pvert + 0,781 * Qvert,vloer	-1.659	kNm
F_{VD}	: 0,781*Pvert + Qvert,vloer	2.424	kN
F_{HD}	-	0	kN

VB2 **Terrein belasting future**

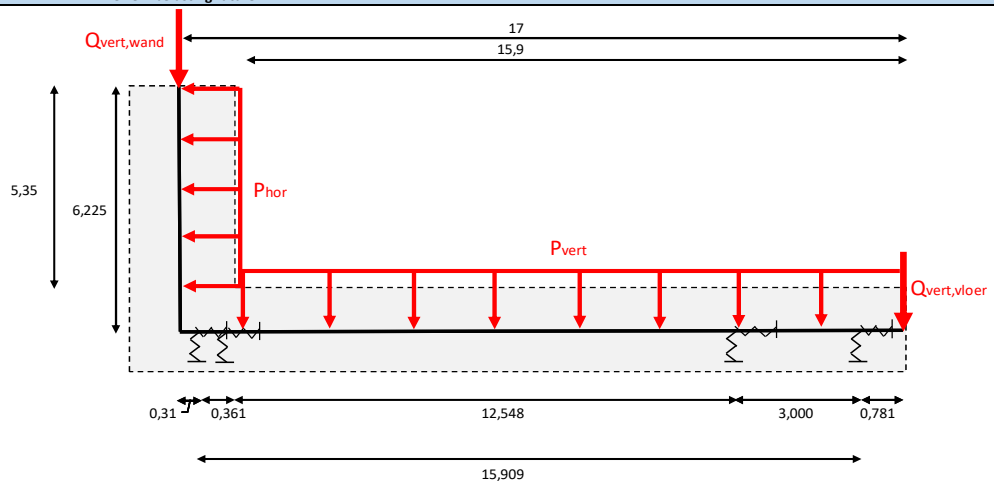

				VB2.1	VB2.2	
Pvert		40	kN/m2	613	307	kN/m
Phor	: Pvert*kh	20	kN/m2	307	153	kN/m
Qvert,wand	: Pvert*bkesp	88	kN/m	1.349	675	kN
Qvert,vloer	: Pvert*hgrond*tan24	95	kN/m	1.457	728	kN

Simplified model - VB2.1: 2/3 length

q_{total}	-	0	kN/m
q_{floor}	: Pvert	613	kN/m
M_A	: ((6,225-5,35)+(5,35/2))*(5,35)*Phor + 0.310*Qvert,wand	-6.243	kNm
F_{VA}	: Qvert,wand	1.349	kN
F_{HA}	: -5,35*Phor	-1.641	kN
M_B	-	0	kNm
F_{VB}	-	0	kN
F_{HB}	-	0	kN
M_C	-	0	kNm
F_{VC}	-	0	kN
F_{HC}	-	0	kN
M_D	: (1/2) * (0,781^2) * Pvert + 0,781 * Qvert,vloer	-1.325	kNm
F_{VD}	: 0,781*Pvert + Qvert,vloer	1.936	kN
F_{HD}	-	0	kN

Simplified model - VB2.2: 1/3 length

q_{total}	-	0	kN/m
q_{floor}	: Pvert	307	kN/m
M_A	: ((6,225-5,35)+(5,35/2))*(5,35)*Phor + 0.310*Qvert,wand	-3.121	kNm
F_{VA}	: Qvert,wand	1.349	kN
F_{HA}	: -5,35*Phor	-820	kN
M_B	-	0	kNm
F_{VB}	-	0	kN
F_{HB}	-	0	kN
M_C	-	0	kNm
F_{VC}	-	0	kN
F_{HC}	-	0	kN
M_D	: (1/2) * (1^2) * Pvert + 0,781 * Qvert,vloer	-663	kNm
F_{VD}	: 0,781*Pvert + Qvert,vloer	968	kN
F_{HD}	-	0	kN

VB3 **Bollard loads current**

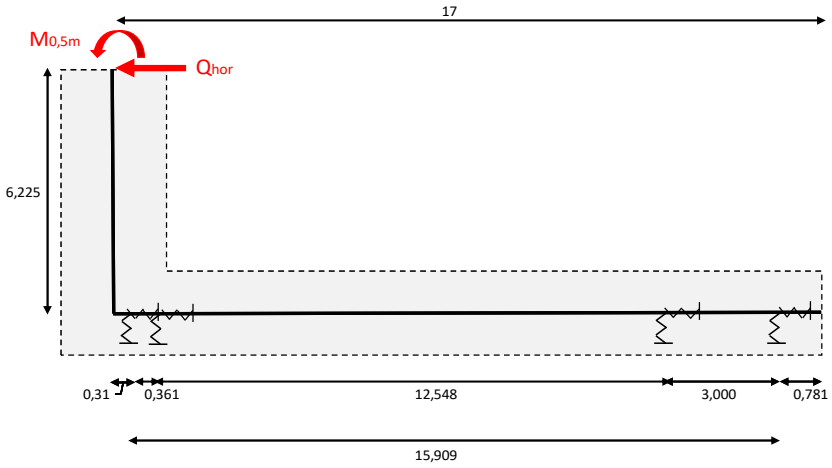

	23 m segment		
c.t.c. bollard pos.	15,4	m	(1 bollard per bollard position)
Load height	0,5	m	
VB3.1			
Qhor	4.000	kN	
M0,5m	2.000	kNm	
VB3.2 One right			
Qhor	2.000	kN	
M0,5m	1.000	kNm	
VB3.3 One mid			
Qhor	2.000	kN	
M0,5m	1.000	kNm	

Simplified model		***VB3.1***	***VB3.2***	***VB3.3***	
q_{total}	-	0	0	0	kN/m
q_{floor}	-	0	0	0	kN/m
M_A	: M0,5m + Qhor*6,225	-26.900	-13.450	-13.450	kNm
F_{VA}	-	0	0	0	kN
F_{HA}	: -Qhor	-4.000	-2.000	-2.000	kN
M_B	-	0	0	0	kNm
F_{VB}	-	0	0	0	kN
F_{HB}	-	0	0	0	kN
M_C	-	0	0	0	kNm
F_{VC}	-	0	0	0	kN
F_{HC}	-	0	0	0	kN
M_D	-	0	0	0	kNm
F_{VD}	-	0	0	0	kN
F_{HD}	-	0	0	0	kN

VB4 **Bollard loads future**

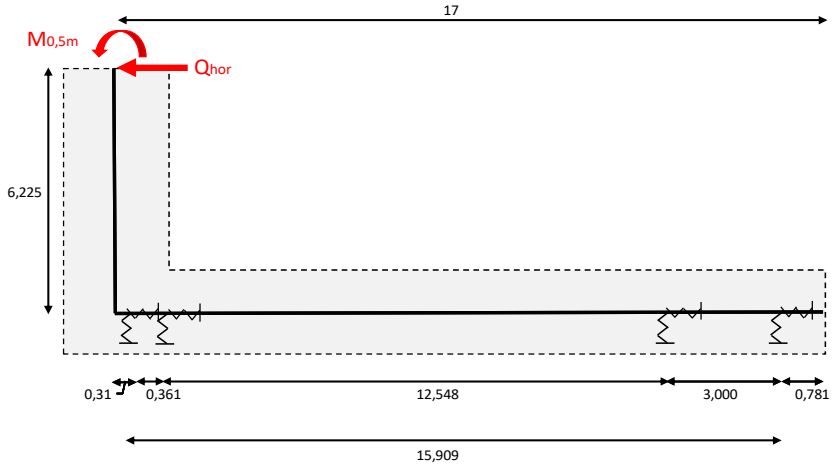

	23 m segment		
c.t.c. bollard pos.	15,4	m	(2 bollards per bollard position c.t.c 2,5m)
Load height	0,5	m	
VB4.1 Two			
Qhor	6.800	kN	
M0,5m	3.400	kNm	
VB4.2 One right			
Qhor	3.400	kN	
M0,5m	1.700	kNm	
VB4.3 One mid			
Qhor	3.400	kN	
M0,5m	1.700	kNm	

Simplified model		***VB4.1***	***VB4.2***	***VB4.3***	
q_{total}	-	0	0	0	kN/m
q_{floor}	-	0	0	0	kN/m
M_A	: M0,5m + Qhor*6,225	-45.730	-22.865	-22.865	kNm
F_{VA}	-	0	0	0	kN
F_{HA}	: -Qhor	-6.800	-3.400	-3.400	kN
M_B	-	0	0	0	kNm
F_{VB}	-	0	0	0	kN
F_{HB}	-	0	0	0	kN
M_C	-	0	0	0	kNm
F_{VC}	-	0	0	0	kN
F_{HC}	-	0	0	0	kN
M_D	-	0	0	0	kNm
F_{VD}	-	0	0	0	kN
F_{HD}	-	0	0	0	kN

VB5 **Collision loads**

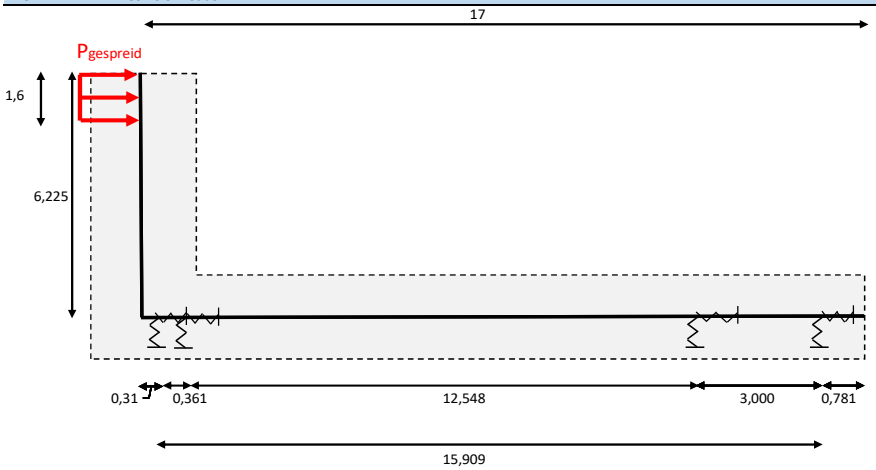

VB5.1			**23 m segment**		
$h_{gespreid}$	0,5	m			
$b_{gespreidrand}$	1,6	m			
Fmax	2000	kN			
VB5.1					
$P_{gespreid,rand}$	781	kN/m2	1249,6	kN/m	on 1,6 m from the top
VB5.2					
$P_{gespreid,rand}$	463	kN/m2	1250,1	kN/m	on 1,6 m from the top
VB5.3					
$P_{gespreid,rand}$	463	kN/m2	1250,1	kN/m	on 1,6 m from the top

There are als ecentric loads in the x-direction which are not taken into account in this model

Simplified model		***VB5.1***	***VB5.2***	***VB5.3***	
q_{total}	-	0	0	0	kN/m
q_{floor}	-	0	0	0	kN/m
M_A	: P * 1,6 * (6,225-1,6/2)	10.847	10.851	10.851	kNm
F_{VA}	-	0	0	0	kN
F_{HA}	: P * 1,6	1.999	2.000	2.000	kN
M_B	-	0	0	0	kNm
F_{VB}	-	0	0	0	kN
F_{HB}	-	0	0	0	kN
M_C	-	0	0	0	kNm
F_{VC}	-	0	0	0	kN
F_{HC}	-	0	0	0	kN
M_D	-	0	0	0	kNm
F_{VD}	-	0	0	0	kN
F_{HD}	-	0	0	0	kN

VB6 **Impact loads**

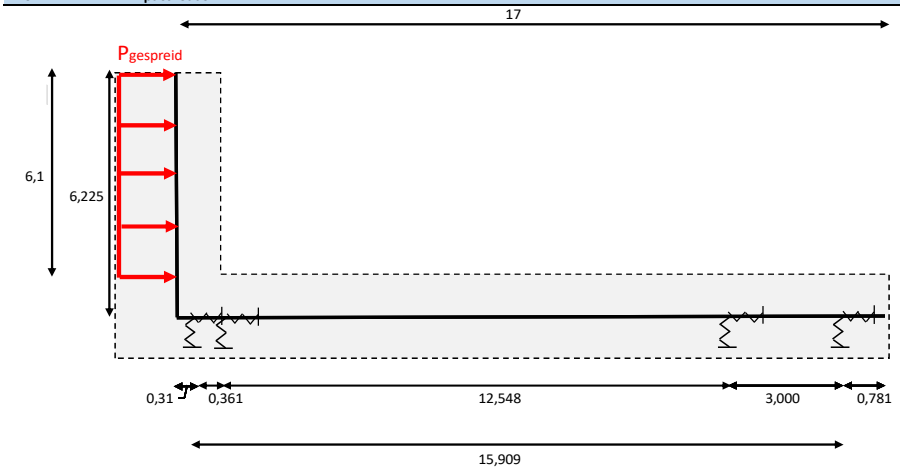

			23 m segment		
$h_{gespreid}$	6,1	m			
$b_{gespreidrand}$	7,2	m			
Fmax	10000	kN			
VB6.1					
$P_{gespreid,rand}$	269	kN/m2	1639,344	kN/m	on 1,6 m from the top
VB6.2					
$P_{gespreid,midden}$	228	kN/m2	1639,344	kN/m	on 1,6 m from the top
VB6.3					
$P_{gespreid,midden}$	228	kN/m2	1639,344	kN/m	on 1,6 m from the top

There are als ecentric loads in the x-direction which are not taken into account in this model

Simplified model		***VB6.1***	***VB6.2***	***VB6.3***	
q_{total}	-	0	0	0	kN/m
q_{floor}	-	0	0	0	kN/m
M_A	: P * 6,1* (6,225-6,1/2)	31.750	31.750	31.750	kNm
F_{VA}	-	0	0	0	kN
F_{HA}	: P * 6,1	10.000	10.000	10.000	kN
M_B	-	0	0	0	kNm
F_{VB}	-	0	0	0	kN
F_{HB}	-	0	0	0	kN
M_C	-	0	0	0	kNm
F_{VC}	-	0	0	0	kN
F_{HC}	-	0	0	0	kN
M_D	-	0	0	0	kNm
F_{VD}	-	0	0	0	kN
F_{HD}	-	0	0	0	kN

VB7 **Crane loads future**

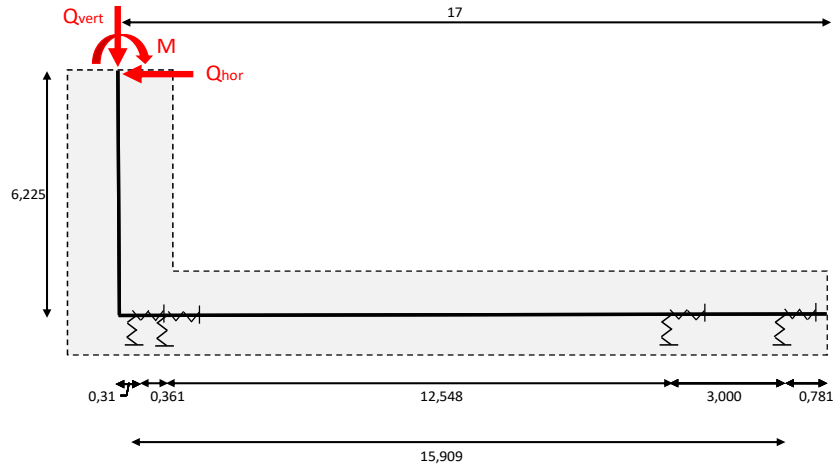

distance (centre)	1,9	m		
Qvert	1500	kN/m	**23 m segment**	
Qhor	225	kN/m	34.500	kN
M	2850	kNm/m	5.175	kN
			65.550	kNm

Simplified model		***VB7***	
qtotal	-	0	kN/m
qfloor	-	0	kN/m
MA	: -Qver * 0,31 - Qhor*6,225 + M	22.641	kNm
FVA	: -Qver	-34.500	kN
FHA	: -Qhor	-5.175	kN
MB	-	0	kNm
FVB	-	0	kN
FHB	-	0	kN
MC	-	0	kNm
FVC	-	0	kN
FHC	-	0	kN
MD	-	0	kNm
FVD	-	0	kN
FHD	-	0	kN

B.2 Load combinations

Load cases	PB1	PB2	PB3.1	PB3.2	PB4	VB1.1	VB1.2	VB2.1	VB2.2	VB3.1	VB3.2	VB3.3	VB4.1	VB4.2	VB4.3	VB5.1	VB5.2	VB5.3	VB6.1	VB6.2	VB6.3	VB7
BGT 1	1	1	1	0	1	0,5	0,5	0	0	0	0	0	0	0	0	0	0	0	0	0	0	0
BGT 1.1	1	1	1	0	1	0,5	0	0	0	0	0	0	0	0	0	0	0	0	0	0	0	0
BGT 1.2	1	1	1	0	1	0	0,5	0	0	0	0	0	0	0	0	0	0	0	0	0	0	0
BGT 1.3	1	1	1	0	1	0,5	0,5	0	0	0	0	0	0	0	0	0	0	0	0	0	0	0
BGT 2	1	1	1	0	1	0,3	0,3	0	0	0,3	0,3	0,3	0	0	0	0,3	0,3	0,3	0	0	0	0
BGT 2.1	1	1	1	0	1	0,3	0	0	0	0,3	0	0	0	0	0	0,3	0	0	0	0	0	0
BGT 2.2	1	1	1	0	1	0	0,3	0	0	0,3	0	0	0	0	0	0,3	0	0	0	0	0	0
BGT 2.3	1	1	1	0	1	0,3	0	0	0	0	0,3	0	0	0	0	0,3	0	0	0	0	0	0
BGT 2.4	1	1	1	0	1	0	0,3	0	0	0	0,3	0	0	0	0	0,3	0	0	0	0	0	0
BGT 2.5	1	1	1	0	1	0,3	0	0	0	0,3	0	0	0	0	0	0	0,3	0	0	0	0	0
BGT 2.6	1	1	1	0	1	0	0,3	0	0	0,3	0	0	0	0	0	0	0,3	0	0	0	0	0
BGT 2.7	1	1	1	0	1	0,3	0	0	0	0	0,3	0	0	0	0	0	0,3	0	0	0	0	0
BGT 2.8	1	1	1	0	1	0	0,3	0	0	0	0,3	0	0	0	0	0	0,3	0	0	0	0	0
BGT 2.9	1	1	1	0	1	0,3	0,3	0	0	0,3	0	0	0	0	0	0,3	0	0	0	0	0	0
BGT 2.10	1	1	1	0	1	0,3	0,3	0	0	0	0,3	0	0	0	0	0,3	0	0	0	0	0	0
BGT 2.11	1	1	1	0	1	0,3	0,3	0	0	0,3	0	0	0	0	0	0	0,3	0	0	0	0	0
BGT 2.12	1	1	1	0	1	0,3	0,3	0	0	0	0,3	0	0	0	0	0	0,3	0	0	0	0	0
BGT 3	1	1	1	0	1	0,3	0,3	0	0	0	0	0	0	0	0	0	0	0	0	0	0	0
BGT 3.1	1	1	1	0	1	0,3	0	0	0	0	0	0	0	0	0	0	0	0	0	0	0	0
BGT 3.2	1	1	1	0	1	0	0,3	0	0	0	0	0	0	0	0	0	0	0	0	0	0	0
BGT 3.3	1	1	1	0	1	0,3	0,3	0	0	0	0	0	0	0	0	0	0	0	0	0	0	0
BGT 4	1	1	1	0	1	0,3	0,3	0,5	0,5	0	0	0	0	0	0	0	0	0	0	0	0	0
BGT 4.1	1	1	1	0	1	0,3	0	0,5	0	0	0	0	0	0	0	0	0	0	0	0	0	0
BGT 4.2	1	1	1	0	1	0	0,3	0,5	0	0	0	0	0	0	0	0	0	0	0	0	0	0
BGT 4.3	1	1	1	0	1	0,3	0	0	0,5	0	0	0	0	0	0	0	0	0	0	0	0	0
BGT 4.4	1	1	1	0	1	0	0,3	0	0,5	0	0	0	0	0	0	0	0	0	0	0	0	0
BGT 4.5	1	1	1	0	1	0,3	0,3	0,5	0	0	0	0	0	0	0	0	0	0	0	0	0	0
BGT 4.6	1	1	1	0	1	0,3	0,3	0	0,5	0	0	0	0	0	0	0	0	0	0	0	0	0
BGT 4.7	1	1	1	0	1	0,3	0	0,5	0,5	0	0	0	0	0	0	0	0	0	0	0	0	0
BGT 4.8	1	1	1	0	1	0	0,3	0,5	0,5	0	0	0	0	0	0	0	0	0	0	0	0	0
BGT 4.9	1	1	1	0	1	0,3	0,3	0,5	0,5	0	0	0	0	0	0	0	0	0	0	0	0	0
BGT 5	1	1	1	0	1	0	0	0,3	0,3	0	0	0	0,3	0,3	0,3	0,3	0,3	0,3	0	0	0	0
BGT 5.1	1	1	1	0	1	0	0	0,3	0	0	0	0	0,3	0	0	0,3	0	0	0	0	0	0
BGT 5.2	1	1	1	0	1	0	0	0	0,3	0	0	0	0,3	0	0	0,3	0	0	0	0	0	0
BGT 5.3	1	1	1	0	1	0	0	0,3	0	0	0	0	0	0,3	0	0,3	0	0	0	0	0	0
BGT 5.4	1	1	1	0	1	0	0	0	0,3	0	0	0	0	0,3	0	0,3	0	0	0	0	0	0
BGT 5.5	1	1	1	0	1	0	0	0,3	0	0	0	0	0,3	0	0	0	0,3	0	0	0	0	0
BGT 5.6	1	1	1	0	1	0	0	0	0,3	0	0	0	0,3	0	0	0	0,3	0	0	0	0	0
BGT 5.7	1	1	1	0	1	0	0	0,3	0	0	0	0	0	0,3	0	0	0,3	0	0	0	0	0
BGT 5.8	1	1	1	0	1	0	0	0	0,3	0	0	0	0	0,3	0	0	0,3	0	0	0	0	0
BGT 5.9	1	1	1	0	1	0	0	0,3	0,3	0	0	0	0,3	0	0	0,3	0	0	0	0	0	0
BGT 5.10	1	1	1	0	1	0	0	0,3	0,3	0	0	0	0	0,3	0	0,3	0	0	0	0	0	0
BGT 5.11	1	1	1	0	1	0	0	0,3	0,3	0	0	0	0,3	0	0	0	0,3	0	0	0	0	0
BGT 5.12	1	1	1	0	1	0	0	0,3	0,3	0	0	0	0	0,3	0	0	0,3	0	0	0	0	0
BGT 6	1	1	1	0	1	0	0	0,3	0,3	0	0	0	0	0	0	0	0	0	0	0	0	0,6
BGT 6.1	1	1	1	0	1	0	0	0,3	0	0	0	0	0	0	0	0	0	0	0	0	0	0,6
BGT 6.2	1	1	1	0	1	0	0	0	0,3	0	0	0	0	0	0	0	0	0	0	0	0	0,6
BGT 6.3	1	1	1	0	1	0	0	0,3	0,3	0	0	0	0	0	0	0	0	0	0	0	0	0,6
BGT 7	1	1	1	0	1	0	0	0,3	0,3	0	0	0	0	0	0	0	0	0	0	0	0	0
BGT 7.1	1	1	1	0	1	0	0	0,3	0	0	0	0	0	0	0	0	0	0	0	0	0	0
BGT 7.2	1	1	1	0	1	0	0	0	0,3	0	0	0	0	0	0	0	0	0	0	0	0	0
BGT 7.3	1	1	1	0	1	0	0	0,3	0,3	0	0	0	0	0	0	0	0	0	0	0	0	0

Figure 87: Load combinations SLS

Load cases	PB1	PB2	PB3.1	PB3.2	PB4	VB1.1	VB1.2	VB2.1	VB2.2	VB3.1	VB3.2	VB3.3	VB4.1	VB4.2	VB4.3	VB5.1	VB5.2	VB5.3	VB6.1	VB6.2	VB6.3	VB7
UGT 1	1,35	1,35	0	1	0	1,05	1,05	0	0	1,05	1,05	1,05	0	0	0	1,05	1,05	1,05	0	0	0	0
UGT 1.1	1,35	1,35	0	1	0	1,05	0	0	0	1,05	0	0	0	0	0	1,05	0	0	0	0	0	0
UGT 1.2	1,35	1,35	0	1	0	0	1,05	0	0	1,05	0	0	0	0	0	1,05	0	0	0	0	0	0
UGT 1.3	1,35	1,35	0	1	0	1,05	0	0	0	0	1,05	0	0	0	0	1,05	0	0	0	0	0	0
UGT 1.4	1,35	1,35	0	1	0	0	1,05	0	0	0	1,05	0	0	0	0	1,05	0	0	0	0	0	0
UGT 1.5	1,35	1,35	0	1	0	1,05	0	0	0	1,05	0	0	0	0	0	0	1,05	0	0	0	0	0
UGT 1.6	1,35	1,35	0	1	0	0	1,05	0	0	1,05	0	0	0	0	0	0	1,05	0	0	0	0	0
UGT 1.7	1,35	1,35	0	1	0	1,05	0	0	0	0	1,05	0	0	0	0	0	1,05	0	0	0	0	0
UGT 1.8	1,35	1,35	0	1	0	0	1,05	0	0	0	1,05	0	0	0	0	0	1,05	0	0	0	0	0
UGT 1.9	1,35	1,35	0	1	0	1,05	1,05	0	0	1,05	0	0	0	0	0	1,05	0	0	0	0	0	0
UGT 1.10	1,35	1,35	0	1	0	1,05	1,05	0	0	0	1,05	0	0	0	0	1,05	0	0	0	0	0	0
UGT 1.11	1,35	1,35	0	1	0	1,05	1,05	0	0	1,05	0	0	0	0	0	0	1,05	0	0	0	0	0
UGT 1.12	1,35	1,35	0	1	0	1,05	1,05	0	0	0	1,05	0	0	0	0	0	1,05	0	0	0	0	0
UGT 2	0,9	0,9	0	1	0	1,05	1,05	0	0	1,05	1,05	1,05	0	0	0	1,05	1,05	1,05	0	0	0	0
UGT 2.1	0,9	0,9	0	1	0	1,05	0	0	0	1,05	0	0	0	0	0	1,05	0	0	0	0	0	0
UGT 2.2	0,9	0,9	0	1	0	0	1,05	0	0	1,05	0	0	0	0	0	1,05	0	0	0	0	0	0
UGT 2.3	0,9	0,9	0	1	0	1,05	0	0	0	0	1,05	0	0	0	0	1,05	0	0	0	0	0	0
UGT 2.4	0,9	0,9	0	1	0	0	1,05	0	0	0	1,05	0	0	0	0	1,05	0	0	0	0	0	0
UGT 2.5	0,9	0,9	0	1	0	1,05	0	0	0	1,05	0	0	0	0	0	0	1,05	0	0	0	0	0
UGT 2.6	0,9	0,9	0	1	0	0	1,05	0	0	1,05	0	0	0	0	0	0	1,05	0	0	0	0	0
UGT 2.7	0,9	0,9	0	1	0	1,05	0	0	0	0	1,05	0	0	0	0	0	1,05	0	0	0	0	0
UGT 2.8	0,9	0,9	0	1	0	0	1,05	0	0	0	1,05	0	0	0	0	0	1,05	0	0	0	0	0
UGT 2.9	0,9	0,9	0	1	0	1,05	1,05	0	0	1,05	0	0	0	0	0	1,05	0	0	0	0	0	0
UGT 2.10	0,9	0,9	0	1	0	1,05	1,05	0	0	0	1,05	0	0	0	0	1,05	0	0	0	0	0	0
UGT 2.11	0,9	0,9	0	1	0	1,05	1,05	0	0	1,05	0	0	0	0	0	0	1,05	0	0	0	0	0
UGT 2.12	0,9	0,9	0	1	0	1,05	1,05	0	0	0	1,05	0	0	0	0	0	1,05	0	0	0	0	0
UGT 3	1,2	1,2	0	1	0	1,5	1,5	0	0	1,05	1,05	1,05	0	0	0	1,05	1,05	1,05	0	0	0	0
UGT 3.1	1,2	1,2	0	1	0	1,5	0	0	0	1,05	0	0	0	0	0	1,05	0	0	0	0	0	0
UGT 3.2	1,2	1,2	0	1	0	0	1,5	0	0	1,05	0	0	0	0	0	1,05	0	0	0	0	0	0
UGT 3.3	1,2	1,2	0	1	0	1,5	0	0	0	0	1,05	0	0	0	0	1,05	0	0	0	0	0	0
UGT 3.4	1,2	1,2	0	1	0	0	1,5	0	0	0	1,05	0	0	0	0	1,05	0	0	0	0	0	0
UGT 3.5	1,2	1,2	0	1	0	1,5	0	0	0	1,05	0	0	0	0	0	0	1,05	0	0	0	0	0
UGT 3.6	1,2	1,2	0	1	0	0	1,5	0	0	1,05	0	0	0	0	0	0	1,05	0	0	0	0	0
UGT 3.7	1,2	1,2	0	1	0	1,5	0	0	0	0	1,05	0	0	0	0	0	1,05	0	0	0	0	0
UGT 3.8	1,2	1,2	0	1	0	0	1,5	0	0	0	1,05	0	0	0	0	0	1,05	0	0	0	0	0
UGT 3.9	1,2	1,2	0	1	0	1,5	1,5	0	0	1,05	0	0	0	0	0	1,05	0	0	0	0	0	0
UGT 3.10	1,2	1,2	0	1	0	1,5	1,5	0	0	0	1,05	0	0	0	0	1,05	0	0	0	0	0	0
UGT 3.11	1,2	1,2	0	1	0	1,5	1,5	0	0	1,05	0	0	0	0	0	0	1,05	0	0	0	0	0
UGT 3.12	1,2	1,2	0	1	0	1,5	1,5	0	0	0	1,05	0	0	0	0	0	1,05	0	0	0	0	0
UGT 4	0,9	0,9	0	1	0	1,5	1,5	0	0	1,05	1,05	1,05	0	0	0	1,05	1,05	1,05	0	0	0	0
UGT 4.1	0,9	0,9	0	1	0	1,5	0	0	0	1,05	0	0	0	0	0	1,05	0	0	0	0	0	0
UGT 4.2	0,9	0,9	0	1	0	0	1,5	0	0	1,05	0	0	0	0	0	1,05	0	0	0	0	0	0
UGT 4.3	0,9	0,9	0	1	0	1,5	0	0	0	0	1,05	0	0	0	0	1,05	0	0	0	0	0	0
UGT 4.4	0,9	0,9	0	1	0	0	1,5	0	0	0	1,05	0	0	0	0	1,05	0	0	0	0	0	0
UGT 4.5	0,9	0,9	0	1	0	1,5	0	0	0	1,05	0	0	0	0	0	0	1,05	0	0	0	0	0
UGT 4.6	0,9	0,9	0	1	0	0	1,5	0	0	1,05	0	0	0	0	0	0	1,05	0	0	0	0	0
UGT 4.7	0,9	0,9	0	1	0	1,5	0	0	0	0	1,05	0	0	0	0	0	1,05	0	0	0	0	0
UGT 4.8	0,9	0,9	0	1	0	0	1,5	0	0	0	1,05	0	0	0	0	0	1,05	0	0	0	0	0
UGT 4.9	0,9	0,9	0	1	0	1,5	1,5	0	0	1,05	0	0	0	0	0	1,05	0	0	0	0	0	0
UGT 4.10	0,9	0,9	0	1	0	1,5	1,5	0	0	1,05	0	0	0	0	0	0	1,05	0	0	0	0	0
UGT 4.11	0,9	0,9	0	1	0	1,5	1,5	0	0	0	1,05	0	0	0	0	1,05	0	0	0	0	0	0
UGT 4.12	0,9	0,9	0	1	0	1,5	1,5	0	0	0	1,05	0	0	0	0	0	1,05	0	0	0	0	0
UGT 5	1,2	1,2	0	1	0	1,05	1,05	0	0	1,5	1,5	1,5	0	0	0	1,5	1,5	1,5	0	0	0	0
UGT 5.1	1,2	1,2	0	1	0	1,05	0	0	0	1,5	0	0	0	0	0	1,5	0	0	0	0	0	0
UGT 5.2	1,2	1,2	0	1	0	0	1,05	0	0	1,5	0	0	0	0	0	1,5	0	0	0	0	0	0
UGT 5.3	1,2	1,2	0	1	0	1,05	0	0	0	0	1,5	0	0	0	0	1,5	0	0	0	0	0	0
UGT 5.4	1,2	1,2	0	1	0	0	1,05	0	0	0	1,5	0	0	0	0	1,5	0	0	0	0	0	0
UGT 5.5	1,2	1,2	0	1	0	1,05	0	0	0	1,5	0	0	0	0	0	0	1,5	0	0	0	0	0
UGT 5.6	1,2	1,2	0	1	0	0	1,05	0	0	1,5	0	0	0	0	0	0	1,5	0	0	0	0	0
UGT 5.7	1,2	1,2	0	1	0	1,05	0	0	0	0	1,5	0	0	0	0	0	1,5	0	0	0	0	0
UGT 5.8	1,2	1,2	0	1	0	0	1,05	0	0	0	1,5	0	0	0	0	0	1,5	0	0	0	0	0
UGT 5.9	1,2	1,2	0	1	0	1,05	1,05	0	0	1,5	0	0	0	0	0	1,5	0	0	0	0	0	0
UGT 5.10	1,2	1,2	0	1	0	1,05	1,05	0	0	0	1,5	0	0	0	0	1,5	0	0	0	0	0	0
UGT 5.11	1,2	1,2	0	1	0	1,05	1,05	0	0	1,5	0	0	0	0	0	0	1,5	0	0	0	0	0
UGT 5.12	1,2	1,2	0	1	0	1,05	1,05	0	0	0	1,5	0	0	0	0	0	1,5	0	0	0	0	0
UGT 6	0,9	0,9	0	1	0	1,05	1,05	0	0	1,5	1,5	1,5	0	0	0	1,5	1,5	1,5	0	0	0	0
UGT 6.1	0,9	0,9	0	1	0	1,05	0	0	0	1,5	0	0	0	0	0	1,5	0	0	0	0	0	0
UGT 6.2	0,9	0,9	0	1	0	0	1,05	0	0	1,5	0	0	0	0	0	1,5	0	0	0	0	0	0
UGT 6.3	0,9	0,9	0	1	0	1,05	0	0	0	0	1,5	0	0	0	0	1,5	0	0	0	0	0	0
UGT 6.4	0,9	0,9	0	1	0	0	1,05	0	0	0	1,5	0	0	0	0	1,5	0	0	0	0	0	0
UGT 6.5	0,9	0,9	0	1	0	1,05	0	0	0	1,5	0	0	0	0	0	0	1,5	0	0	0	0	0
UGT 6.6	0,9	0,9	0	1	0	0	1,05	0	0	1,5	0	0	0	0	0	0	1,5	0	0	0	0	0

UGT 6.7	0,9	0,9	0	1	0	1,05	0	0	0	0	1,5	0	0	0	0	0	1,5	0	0	0	0	0
UGT 6.8	0,9	0,9	0	1	0	0	1,05	0	0	0	1,5	0	0	0	0	0	1,5	0	0	0	0	0
UGT 6.9	0,9	0,9	0	1	0	1,05	1,05	0	0	1,5	0	0	0	0	0	1,5	0	0	0	0	0	0
UGT 6.10	0,9	0,9	0	1	0	1,05	1,05	0	0	0	1,5	0	0	0	0	1,5	0	0	0	0	0	0
UGT 6.11	0,9	0,9	0	1	0	1,05	1,05	0	0	1,5	0	0	0	0	0	0	1,5	0	0	0	0	0
UGT 6.12	0,9	0,9	0	1	0	1,05	1,05	0	0	0	1,5	0	0	0	0	0	1,5	0	0	0	0	0
UGT 7	1,35	1,35	0	1	0	0	0	1,05	1,05	0	0	0	1,05	1,05	1,05	1,05	1,05	1,05	0	0	0	0,9
UGT 7.1	1,35	1,35	0	1	0	0	0	1,05	0	0	0	0	1,05	0	0	1,05	0	0	0	0	0	0,9
UGT 7.2	1,35	1,35	0	1	0	0	0	0	1,05	0	0	0	1,05	0	0	1,05	0	0	0	0	0	0,9
UGT 7.3	1,35	1,35	0	1	0	0	0	1,05	0	0	0	0	1,05	0	0	0	1,05	0	0	0	0	0,9
UGT 7.4	1,35	1,35	0	1	0	0	0	0	1,05	0	0	0	1,05	0	0	0	1,05	0	0	0	0	0,9
UGT 7.5	1,35	1,35	0	1	0	0	0	1,05	0	0	0	0	0	1,05	0	1,05	0	0	0	0	0	0,9
UGT 7.6	1,35	1,35	0	1	0	0	0	0	1,05	0	0	0	0	1,05	0	1,05	0	0	0	0	0	0,9
UGT 7.7	1,35	1,35	0	1	0	0	0	1,05	0	0	0	0	0	1,05	0	0	1,05	0	0	0	0	0,9
UGT 7.8	1,35	1,35	0	1	0	0	0	0	1,05	0	0	0	0	1,05	0	0	1,05	0	0	0	0	0,9
UGT 7.9	1,35	1,35	0	1	0	0	0	1,05	1,05	0	0	0	1,05	0	0	1,05	0	0	0	0	0	0,9
UGT 7.10	1,35	1,35	0	1	0	0	0	1,05	1,05	0	0	0	1,05	0	0	0	1,05	0	0	0	0	0,9
UGT 7.11	1,35	1,35	0	1	0	0	0	1,05	1,05	0	0	0	0	1,05	0	1,05	0	0	0	0	0	0,9
UGT 7.12	1,35	1,35	0	1	0	0	0	1,05	1,05	0	0	0	0	1,05	0	0	1,05	0	0	0	0	0,9
UGT 8	0,9	0,9	0	1	0	0	0	1,05	1,05	0	0	0	1,05	1,05	1,05	1,05	1,05	1,05	0	0	0	0,9
UGT 8.1	0,9	0,9	0	1	0	0	0	1,05	0	0	0	0	1,05	0	0	1,05	0	0	0	0	0	0,9
UGT 8.2	0,9	0,9	0	1	0	0	0	0	1,05	0	0	0	1,05	0	0	1,05	0	0	0	0	0	0,9
UGT 8.3	0,9	0,9	0	1	0	0	0	1,05	0	0	0	0	0	1,05	0	0	1,05	0	0	0	0	0,9
UGT 8.4	0,9	0,9	0	1	0	0	0	0	1,05	0	0	0	0	1,05	0	0	1,05	0	0	0	0	0,9
UGT 8.5	0,9	0,9	0	1	0	0	0	1,05	0	0	0	0	1,05	0	0	1,05	0	0	0	0	0	0,9
UGT 8.6	0,9	0,9	0	1	0	0	0	0	1,05	0	0	0	1,05	0	0	1,05	0	0	0	0	0	0,9
UGT 8.7	0,9	0,9	0	1	0	0	0	1,05	0	0	0	0	0	1,05	0	0	1,05	0	0	0	0	0,9
UGT 8.8	0,9	0,9	0	1	0	0	0	0	1,05	0	0	0	0	1,05	0	0	1,05	0	0	0	0	0,9
UGT 8.9	0,9	0,9	0	1	0	0	0	0	1,05	0	0	0	1,05	0	0	1,05	0	0	0	0	0	0,9
UGT 8.10	0,9	0,9	0	1	0	0	0	0	1,05	0	0	0	1,05	0	0	0	1,05	0	0	0	0	0,9
UGT 8.11	0,9	0,9	0	1	0	0	0	0	1,05	0	0	0	0	1,05	0	1,05	0	0	0	0	0	0,9
UGT 8.12	0,9	0,9	0	1	0	0	0	0	1,05	0	0	0	0	1,05	0	0	1,05	0	0	0	0	0,9
UGT 9	1,2	1,2	0	1	0	0	0	1,5	1,5	0	0	0	1,05	1,05	1,05	1,05	1,05	1,05	0	0	0	0,9
UGT 9.1	1,2	1,2	0	1	0	0	0	1,5	0	0	0	0	1,05	0	0	1,05	0	0	0	0	0	0,9
UGT 9.2	1,2	1,2	0	1	0	0	0	0	1,5	0	0	0	1,05	0	0	1,05	0	0	0	0	0	0,9
UGT 9.3	1,2	1,2	0	1	0	0	0	1,5	0	0	0	0	0	1,05	0	0	1,05	0	0	0	0	0,9
UGT 9.4	1,2	1,2	0	1	0	0	0	0	1,5	0	0	0	0	1,05	0	0	1,05	0	0	0	0	0,9
UGT 9.5	1,2	1,2	0	1	0	0	0	1,5	0	0	0	0	1,05	0	0	1,05	0	0	0	0	0	0,9
UGT 9.6	1,2	1,2	0	1	0	0	0	0	1,5	0	0	0	1,05	0	0	1,05	0	0	0	0	0	0,9
UGT 9.7	1,2	1,2	0	1	0	0	0	1,5	0	0	0	0	0	1,05	0	0	1,05	0	0	0	0	0,9
UGT 9.8	1,2	1,2	0	1	0	0	0	0	1,5	0	0	0	0	1,05	0	0	1,05	0	0	0	0	0,9
UGT 9.9	1,2	1,2	0	1	0	0	0	1,5	1,5	0	0	0	1,05	0	0	1,05	0	0	0	0	0	0,9
UGT 9.10	1,2	1,2	0	1	0	0	0	1,5	1,5	0	0	0	1,05	0	0	0	1,05	0	0	0	0	0,9
UGT 9.11	1,2	1,2	0	1	0	0	0	1,5	1,5	0	0	0	0	1,05	0	1,05	0	0	0	0	0	0,9
UGT 9.12	1,2	1,2	0	1	0	0	0	1,5	1,5	0	0	0	0	1,05	0	0	1,05	0	0	0	0	0,9
UGT 10	0,9	0,9	0	1	0	0	0	1,5	1,5	0	0	0	1,05	1,05	1,05	1,05	1,05	1,05	0	0	0	0,9
UGT 10.1	0,9	0,9	0	1	0	0	0	1,5	0	0	0	0	1,05	0	0	1,05	0	0	0	0	0	0,9
UGT 10.2	0,9	0,9	0	1	0	0	0	0	1,5	0	0	0	1,05	0	0	1,05	0	0	0	0	0	0,9
UGT 10.3	0,9	0,9	0	1	0	0	0	1,5	0	0	0	0	0	1,05	0	0	1,05	0	0	0	0	0,9
UGT 10.4	0,9	0,9	0	1	0	0	0	0	1,5	0	0	0	0	1,05	0	0	1,05	0	0	0	0	0,9
UGT 10.5	0,9	0,9	0	1	0	0	0	1,5	0	0	0	0	1,05	0	0	1,05	0	0	0	0	0	0,9
UGT 10.6	0,9	0,9	0	1	0	0	0	0	1,5	0	0	0	1,05	0	0	1,05	0	0	0	0	0	0,9
UGT 10.7	0,9	0,9	0	1	0	0	0	1,5	0	0	0	0	0	1,05	0	0	1,05	0	0	0	0	0,9
UGT 10.8	0,9	0,9	0	1	0	0	0	0	1,5	0	0	0	0	1,05	0	0	1,05	0	0	0	0	0,9
UGT 10.9	0,9	0,9	0	1	0	0	0	1,5	1,5	0	0	0	1,05	0	0	1,05	0	0	0	0	0	0,9
UGT 10.10	0,9	0,9	0	1	0	0	0	1,5	1,5	0	0	0	1,05	0	0	0	1,05	0	0	0	0	0,9
UGT 10.11	0,9	0,9	0	1	0	0	0	1,5	1,5	0	0	0	0	1,05	0	1,05	0	0	0	0	0	0,9
UGT 10.12	0,9	0,9	0	1	0	0	0	1,5	1,5	0	0	0	0	1,05	0	0	1,05	0	0	0	0	0,9
UGT 11	1,2	1,2	0	1	0	0	0	1,05	1,05	0	0	0	1,5	1,5	1,5	1,5	1,5	1,5	0	0	0	0,9
UGT 11.1	1,2	1,2	0	1	0	0	0	1,05	0	0	0	0	1,5	0	0	1,5	0	0	0	0	0	0,9
UGT 11.2	1,2	1,2	0	1	0	0	0	0	1,05	0	0	0	1,5	0	0	1,5	0	0	0	0	0	0,9
UGT 11.3	1,2	1,2	0	1	0	0	0	1,05	0	0	0	0	0	1,5	0	0	1,5	0	0	0	0	0,9
UGT 11.4	1,2	1,2	0	1	0	0	0	0	1,05	0	0	0	0	1,5	0	0	1,5	0	0	0	0	0,9
UGT 11.5	1,2	1,2	0	1	0	0	0	1,05	0	0	0	0	1,5	0	0	1,5	0	0	0	0	0	0,9
UGT 11.6	1,2	1,2	0	1	0	0	0	0	1,05	0	0	0	1,5	0	0	1,5	0	0	0	0	0	0,9
UGT 11.7	1,2	1,2	0	1	0	0	0	1,05	0	0	0	0	0	1,5	0	0	1,5	0	0	0	0	0,9
UGT 11.8	1,2	1,2	0	1	0	0	0	0	1,05	0	0	0	0	1,5	0	0	1,5	0	0	0	0	0,9
UGT 11.9	1,2	1,2	0	1	0	0	0	1,05	1,05	0	0	0	1,5	0	0	1,5	0	0	0	0	0	0,9
UGT 11.10	1,2	1,2	0	1	0	0	0	1,05	1,05	0	0	0	1,5	0	0	0	1,5	0	0	0	0	0,9
UGT 11.11	1,2	1,2	0	1	0	0	0	1,05	1,05	0	0	0	0	1,5	0	1,5	0	0	0	0	0	0,9
UGT 11.12	1,2	1,2	0	1	0	0	0	1,05	1,05	0	0	0	0	1,5	0	0	1,5	0	0	0	0	0,9
UGT 12	0,9	0,9	0	1	0	0	0	1,05	1,05	0	0	0	1,5	1,5	1,5	1,5	1,5	1,5	0	0	0	0,9
UGT 12.1	0,9	0,9	0	1	0	0	0	1,05	0	0	0	0	1,5	0	0	1,5	0	0	0	0	0	0,9

UGT 12.2	0,9	0,9	0	1	0	0	0	0	1,05	0	0	0	1,5	0	0	1,5	0	0	0	0	0,9
UGT 12.3	0,9	0,9	0	1	0	0	0	1,05	0	0	0	0	0	1,5	0	0	1,5	0	0	0	0,9
UGT 12.4	0,9	0,9	0	1	0	0	0	0	1,05	0	0	0	0	1,5	0	0	1,5	0	0	0	0,9
UGT 12.5	0,9	0,9	0	1	0	0	0	1,05	0	0	0	0	1,5	0	0	1,5	0	0	0	0	0,9
UGT 12.6	0,9	0,9	0	1	0	0	0	0	1,05	0	0	0	1,5	0	0	1,5	0	0	0	0	0,9
UGT 12.7	0,9	0,9	0	1	0	0	0	1,05	0	0	0	0	0	1,5	0	0	1,5	0	0	0	0,9
UGT 12.8	0,9	0,9	0	1	0	0	0	0	1,05	0	0	0	0	1,5	0	0	1,5	0	0	0	0,9
UGT 12.9	0,9	0,9	0	1	0	0	0	1,05	1,05	0	0	0	1,5	0	0	1,5	0	0	0	0	0,9
UGT 12.10	0,9	0,9	0	1	0	0	0	1,05	1,05	0	0	0	1,5	0	0	0	1,5	0	0	0	0,9
UGT 12.11	0,9	0,9	0	1	0	0	0	1,05	1,05	0	0	0	0	1,5	0	1,5	0	0	0	0	0,9
UGT 12.12	0,9	0,9	0	1	0	0	0	1,05	1,05	0	0	0	0	1,5	0	0	1,5	0	0	0	0,9
UGT 13	1,2	1,2	0	1	0	0	0	1,05	1,05	0	0	0	1,05	1,05	1,05	1,05	1,05	1,05	0	0	1,5
UGT 13.1	1,2	1,2	0	1	0	0	0	1,05	0	0	0	0	1,05	0	0	1,05	0	0	0	0	1,5
UGT 13.2	1,2	1,2	0	1	0	0	0	0	1,05	0	0	0	1,05	0	0	1,05	0	0	0	0	1,5
UGT 13.3	1,2	1,2	0	1	0	0	0	1,05	0	0	0	0	0	1,05	0	0	1,05	0	0	0	1,5
UGT 13.4	1,2	1,2	0	1	0	0	0	0	1,05	0	0	0	0	1,05	0	0	1,05	0	0	0	1,5
UGT 13.5	1,2	1,2	0	1	0	0	0	1,05	0	0	0	0	1,05	0	0	1,05	0	0	0	0	1,5
UGT 13.6	1,2	1,2	0	1	0	0	0	0	1,05	0	0	0	1,05	0	0	1,05	0	0	0	0	1,5
UGT 13.7	1,2	1,2	0	1	0	0	0	1,05	0	0	0	0	0	1,05	0	0	1,05	0	0	0	1,5
UGT 13.8	1,2	1,2	0	1	0	0	0	0	1,05	0	0	0	0	1,05	0	0	1,05	0	0	0	1,5
UGT 13.9	1,2	1,2	0	1	0	0	0	1,05	1,05	0	0	0	1,05	0	0	1,05	0	0	0	0	1,5
UGT 13.10	1,2	1,2	0	1	0	0	0	1,05	1,05	0	0	0	1,05	0	0	0	1,05	0	0	0	1,5
UGT 13.11	1,2	1,2	0	1	0	0	0	1,05	1,05	0	0	0	0	1,05	0	1,05	0	0	0	0	1,5
UGT 13.12	1,2	1,2	0	1	0	0	0	1,05	1,05	0	0	0	0	1,05	0	0	1,05	0	0	0	1,5
UGT 14	0,9	0,9	0	1	0	0	0	1,05	1,05	0	0	0	1,05	1,05	1,05	1,05	1,05	1,05	0	0	1,5
UGT 14.1	0,9	0,9	0	1	0	0	0	1,05	0	0	0	0	1,05	0	0	1,05	0	0	0	0	1,5
UGT 14.2	0,9	0,9	0	1	0	0	0	0	1,05	0	0	0	1,05	0	0	1,05	0	0	0	0	1,5
UGT 14.3	0,9	0,9	0	1	0	0	0	1,05	0	0	0	0	0	1,05	0	0	1,05	0	0	0	1,5
UGT 14.4	0,9	0,9	0	1	0	0	0	0	1,05	0	0	0	0	1,05	0	0	1,05	0	0	0	1,5
UGT 14.5	0,9	0,9	0	1	0	0	0	1,05	0	0	0	0	1,05	0	0	1,05	0	0	0	0	1,5
UGT 14.6	0,9	0,9	0	1	0	0	0	0	1,05	0	0	0	1,05	0	0	1,05	0	0	0	0	1,5
UGT 14.7	0,9	0,9	0	1	0	0	0	1,05	0	0	0	0	0	1,05	0	0	1,05	0	0	0	1,5
UGT 14.8	0,9	0,9	0	1	0	0	0	0	1,05	0	0	0	0	1,05	0	0	1,05	0	0	0	1,5
UGT 14.9	0,9	0,9	0	1	0	0	0	1,05	1,05	0	0	0	1,05	0	0	1,05	0	0	0	0	1,5
UGT 14.10	0,9	0,9	0	1	0	0	0	1,05	1,05	0	0	0	1,05	0	0	0	1,05	0	0	0	1,5
UGT 14.11	0,9	0,9	0	1	0	0	0	1,05	1,05	0	0	0	0	1,05	0	1,05	0	0	0	0	1,5
UGT 14.12	0,9	0,9	0	1	0	0	0	1,05	1,05	0	0	0	0	1,05	0	0	1,05	0	0	0	1,5

Figure 88: Load combinations ULS

C Analytical results

C.1 Load cases

C.1.1 ULS Load Cases

```
UGT 1.1 (0)
[  1358.4375       4621.85       -36242.63587187  14593.859375
 -24933.03            0.         -12713.77992573 -12713.77992573
  -3552.              0.          -2600.         -11776.28109741
  12074.64960937  -6828.65      ]
UGT 1.2 (1)
[  1358.4375       3816.85       -28049.14462187  12822.859375
 -22779.655           0.         -12713.77992573 -12713.77992573
  -3552.              0.          -2600.         -10033.81771851
   9529.84335937  -6828.65      ]
UGT 1.3 (2)
[  1358.4375       4621.85       -22120.13587187  14593.859375
 -22833.03            0.         -12713.77992573 -12713.77992573
  -3552.              0.          -2600.         -11776.28109741
  12074.64960937  -6828.65      ]
UGT 1.4 (3)
[  1358.4375       3816.85       -13926.64462187  12822.859375
 -20679.655           0.         -12713.77992573 -12713.77992573
  -3552.              0.          -2600.         -10033.81771851
   9529.84335937  -6828.65      ]
UGT 1.5 (4)
[  1358.4375       4621.85       -36238.07887187  14593.859375
 -24932.19            0.         -12713.77992573 -12713.77992573
  -3552.              0.          -2600.         -11776.28109741
  12074.64960937  -6828.65      ]
UGT 1.6 (5)
[  1358.4375       3816.85       -28044.58762187  12822.859375
 -22778.815           0.         -12713.77992573 -12713.77992573
  -3552.              0.          -2600.         -10033.81771851
   9529.84335937  -6828.65      ]
UGT 1.7 (6)
[  1358.4375       4621.85       -22115.57887187  14593.859375
 -22832.19            0.         -12713.77992573 -12713.77992573
  -3552.              0.          -2600.         -11776.28109741
  12074.64960937  -6828.65      ]
UGT 1.8 (7)
[  1358.4375       3816.85       -13922.08762187  12822.859375
 -20678.815           0.         -12713.77992573 -12713.77992573
  -3552.              0.          -2600.         -10033.81771851
   9529.84335937  -6828.65      ]
UGT 1.9 (8)
[  1358.4375       5426.85       -44436.12712187  16364.859375
 -27086.405           0.         -12713.77992573 -12713.77992573
  -3552.              0.          -2600.         -13518.74447632
  14619.45585937  -6828.65      ]
UGT 1.10 (9)
[  1358.4375       5426.85       -30313.62712187  16364.859375
 -24986.405           0.         -12713.77992573 -12713.77992573
  -3552.              0.          -2600.         -13518.74447632
  14619.45585937  -6828.65      ]
UGT 1.11 (10)
[  1358.4375       5426.85       -44431.57012187  16364.859375
 -27085.565           0.         -12713.77992573 -12713.77992573
  -3552.              0.          -2600.         -13518.74447632
  14619.45585937  -6828.65      ]
UGT 1.12 (11)
[  1358.4375       5426.85       -30309.07012187  16364.859375
 -24985.565           0.         -12713.77992573 -12713.77992573
  -3552.              0.          -2600.         -13518.74447632
  14619.45585937  -6828.65      ]
UGT 2.1 (12)
[   905.625        3617.9        -31080.13328125  10909.90625
 -23515.494           0.         -12713.77992573 -12713.77992573
  -3552.              0.          -2600.         -10401.82965088
   9746.30390625  -5659.1       ]
UGT 2.2 (13)
[   905.625        2812.9        -22886.64203125   9138.90625
 -21362.119           0.         -12713.77992573 -12713.77992573
  -3552.              0.          -2600.          -8659.36627197
   7201.49765625  -5659.1       ]
UGT 2.3 (14)
```

```
[   905.625        3617.9        -16957.63328125  10909.90625
 -21415.494           0.         -12713.77992573 -12713.77992573
  -3552.              0.          -2600.         -10401.82965088
   9746.30390625  -5659.1       ]
UGT 2.4 (15)
[   905.625        2812.9         -8764.14203125   9138.90625
 -19262.119           0.         -12713.77992573 -12713.77992573
  -3552.              0.          -2600.          -8659.36627197
   7201.49765625  -5659.1       ]
UGT 2.5 (16)
[   905.625        3617.9        -31075.57628125  10909.90625
 -23514.654           0.         -12713.77992573 -12713.77992573
  -3552.              0.          -2600.         -10401.82965088
   9746.30390625  -5659.1       ]
UGT 2.6 (17)
[   905.625        2812.9        -22882.08503125   9138.90625
 -21361.279           0.         -12713.77992573 -12713.77992573
  -3552.              0.          -2600.          -8659.36627197
   7201.49765625  -5659.1       ]
UGT 2.7 (18)
[   905.625        3617.9        -16953.07628125  10909.90625
 -21414.654           0.         -12713.77992573 -12713.77992573
  -3552.              0.          -2600.         -10401.82965088
   9746.30390625  -5659.1       ]
UGT 2.8 (19)
[   905.625        2812.9         -8759.58503125   9138.90625
 -19261.279           0.         -12713.77992573 -12713.77992573
  -3552.              0.          -2600.          -8659.36627197
   7201.49765625  -5659.1       ]
UGT 2.9 (20)
[   905.625        4422.9        -39273.62453125  12680.90625
 -25668.869           0.         -12713.77992573 -12713.77992573
  -3552.              0.          -2600.         -12144.29302979
  12291.11015625  -5659.1       ]
UGT 2.10 (21)
[   905.625        4422.9        -25151.12453125  12680.90625
 -23568.869           0.         -12713.77992573 -12713.77992573
  -3552.              0.          -2600.         -12144.29302979
  12291.11015625  -5659.1       ]
UGT 2.11 (22)
[   905.625        4422.9        -39269.06753125  12680.90625
 -25668.029           0.         -12713.77992573 -12713.77992573
  -3552.              0.          -2600.         -12144.29302979
  12291.11015625  -5659.1       ]
UGT 2.12 (23)
[   905.625        4422.9        -25146.56753125  12680.90625
 -23568.029           0.         -12713.77992573 -12713.77992573
  -3552.              0.          -2600.         -12144.29302979
  12291.11015625  -5659.1       ]
UGT 3.1 (24)
[  1207.5          4977.2        -41544.794175    14883.875
 -26306.268           0.         -12713.77992573 -12713.77992573
  -3552.              0.          -2600.         -12811.6706543
  13479.796875    -6438.8       ]
UGT 3.2 (25)
[  1207.5          3827.2        -29839.806675    12353.875
 -23230.018           0.         -12713.77992573 -12713.77992573
  -3552.              0.          -2600.         -10322.43725586
   9844.359375    -6438.8       ]
UGT 3.3 (26)
[  1207.5          4977.2        -27422.294175    14883.875
 -24206.268           0.         -12713.77992573 -12713.77992573
  -3552.              0.          -2600.         -12811.6706543
  13479.796875    -6438.8       ]
UGT 3.4 (27)
[  1207.5          3827.2        -15717.306675    12353.875
 -21130.018           0.         -12713.77992573 -12713.77992573
  -3552.              0.          -2600.         -10322.43725586
   9844.359375    -6438.8       ]
UGT 3.5 (28)
[  1207.5          4977.2        -41540.237175    14883.875
 -26305.428           0.         -12713.77992573 -12713.77992573
```

```
  -3552.             0.          -2600.         -12811.6706543
  13479.796875    -6438.8       ]
UGT 3.6 (29)
[  1207.5          3827.2        -29835.249675    12353.875
 -23229.178           0.         -12713.77992573 -12713.77992573
  -3552.              0.          -2600.         -10322.43725586
   9844.359375    -6438.8       ]
UGT 3.7 (30)
[  1207.5          4977.2        -27417.737175    14883.875
 -24205.428           0.         -12713.77992573 -12713.77992573
  -3552.              0.          -2600.         -12811.6706543
  13479.796875    -6438.8       ]
UGT 3.8 (31)
[  1207.5          3827.2        -15712.749675    12353.875
 -21129.178           0.         -12713.77992573 -12713.77992573
  -3552.              0.          -2600.         -10322.43725586
   9844.359375    -6438.8       ]
UGT 3.9 (32)
[  1207.5          6127.2        -53249.781675    17413.875
 -29382.518           0.         -12713.77992573 -12713.77992573
  -3552.              0.          -2600.         -15300.90405273
  17115.234375    -6438.8       ]
UGT 3.10 (33)
[  1207.5          6127.2        -39127.281675    17413.875
 -27282.518           0.         -12713.77992573 -12713.77992573
  -3552.              0.          -2600.         -15300.90405273
  17115.234375    -6438.8       ]
UGT 3.11 (34)
[  1207.5          6127.2        -53245.224675    17413.875
 -29381.678           0.         -12713.77992573 -12713.77992573
  -3552.              0.          -2600.         -15300.90405273
  17115.234375    -6438.8       ]
UGT 3.12 (35)
[  1207.5          6127.2        -39122.724675    17413.875
 -27281.678           0.         -12713.77992573 -12713.77992573
  -3552.              0.          -2600.         -15300.90405273
  17115.234375    -6438.8       ]
UGT 4.1 (36)
[   905.625        4307.9        -38103.12578125  12427.90625
 -25361.244           0.         -12713.77992573 -12713.77992573
  -3552.              0.          -2600.         -11895.36968994
  11927.56640625  -5659.1       ]
UGT 4.2 (37)
[   905.625        3157.9        -26398.13828125   9897.90625
 -22284.994           0.         -12713.77992573 -12713.77992573
  -3552.              0.          -2600.          -9406.1362915
   8292.12890625  -5659.1       ]
UGT 4.3 (38)
[   905.625        4307.9        -23980.62578125  12427.90625
 -23261.244           0.         -12713.77992573 -12713.77992573
  -3552.              0.          -2600.         -11895.36968994
  11927.56640625  -5659.1       ]
UGT 4.4 (39)
[   905.625        3157.9        -12275.63828125   9897.90625
 -20184.994           0.         -12713.77992573 -12713.77992573
  -3552.              0.          -2600.          -9406.1362915
   8292.12890625  -5659.1       ]
UGT 4.5 (40)
[   905.625        4307.9        -38098.56878125  12427.90625
 -25360.404           0.         -12713.77992573 -12713.77992573
  -3552.              0.          -2600.         -11895.36968994
  11927.56640625  -5659.1       ]
UGT 4.6 (41)
[   905.625        3157.9        -26393.58128125   9897.90625
 -22284.154           0.         -12713.77992573 -12713.77992573
  -3552.              0.          -2600.          -9406.1362915
   8292.12890625  -5659.1       ]
UGT 4.7 (42)
[   905.625        4307.9        -23976.06878125  12427.90625
 -23260.404           0.         -12713.77992573 -12713.77992573
  -3552.              0.          -2600.         -11895.36968994
  11927.56640625  -5659.1       ]
```

```
UGT 4.8 (43)
[   905.625        3157.9        -12271.08128125   9897.90625
 -20184.154           0.         -12713.77992573 -12713.77992573
  -3552.              0.          -2600.          -9406.1362915
   8292.12890625  -5659.1       ]
UGT 4.9 (44)
[   905.625        5457.9        -49808.11328125  14957.90625
 -28437.494           0.         -12713.77992573 -12713.77992573
  -3552.              0.          -2600.         -14384.60308838
  15563.00390625  -5659.1       ]
UGT 4.10 (45)
[   905.625        5457.9        -49803.55628125  14957.90625
 -28436.654           0.         -12713.77992573 -12713.77992573
  -3552.              0.          -2600.         -14384.60308838
  15563.00390625  -5659.1       ]
UGT 4.11 (46)
[   905.625        5457.9        -35685.61328125  14957.90625
 -26337.494           0.         -12713.77992573 -12713.77992573
  -3552.              0.          -2600.         -14384.60308838
  15563.00390625  -5659.1       ]
UGT 4.12 (47)
[   905.625        5457.9        -35681.05628125  14957.90625
 -26336.654           0.         -12713.77992573 -12713.77992573
  -3552.              0.          -2600.         -14384.60308838
  15563.00390625  -5659.1       ]
UGT 5.1 (48)
[  1207.5          4287.2        -41745.864075    13365.875
 -25360.806           0.         -12713.77992573 -12713.77992573
  -3552.              0.          -2600.         -11318.13061523
  11298.534375    -6438.8       ]
UGT 5.2 (49)
[  1207.5          3482.2        -33552.372825    11594.875
 -23207.431           0.         -12713.77992573 -12713.77992573
  -3552.              0.          -2600.          -9575.66723633
   8753.728125    -6438.8       ]
UGT 5.3 (50)
[  1207.5          4287.2        -21570.864075    13365.875
 -22360.806           0.         -12713.77992573 -12713.77992573
  -3552.              0.          -2600.         -11318.13061523
  11298.534375    -6438.8       ]
UGT 5.4 (51)
[  1207.5          3482.2        -13377.372825    11594.875
 -20207.431           0.         -12713.77992573 -12713.77992573
  -3552.              0.          -2600.          -9575.66723633
   8753.728125    -6438.8       ]
UGT 5.5 (52)
[  1207.5          4287.2        -41739.354075    13365.875
 -25359.606           0.         -12713.77992573 -12713.77992573
  -3552.              0.          -2600.         -11318.13061523
  11298.534375    -6438.8       ]
UGT 5.6 (53)
[  1207.5          3482.2        -33545.862825    11594.875
 -23206.231           0.         -12713.77992573 -12713.77992573
  -3552.              0.          -2600.          -9575.66723633
   8753.728125    -6438.8       ]
UGT 5.7 (54)
[  1207.5          4287.2        -21564.354075    13365.875
 -22359.606           0.         -12713.77992573 -12713.77992573
  -3552.              0.          -2600.         -11318.13061523
  11298.534375    -6438.8       ]
UGT 5.8 (55)
[  1207.5          3482.2        -13370.862825    11594.875
 -20206.231           0.         -12713.77992573 -12713.77992573
  -3552.              0.          -2600.          -9575.66723633
   8753.728125    -6438.8       ]
UGT 5.9 (56)
[  1207.5          5092.2        -49939.355325    15136.875
 -27514.181           0.         -12713.77992573 -12713.77992573
  -3552.              0.          -2600.         -13060.59399414
  13843.340625    -6438.8       ]
UGT 5.10 (57)
[  1207.5          5092.2        -29764.355325    15136.875
```

```
 -24514.181           0.         -12713.77992573 -12713.77992573
  -3552.              0.          -2600.         -13060.59399414
  13843.340625    -6438.8       ]
UGT 5.11 (58)
[  1207.5          5092.2        -49932.845325    15136.875
 -27512.981           0.         -12713.77992573 -12713.77992573
  -3552.              0.          -2600.         -13060.59399414
  13843.340625    -6438.8       ]
UGT 5.12 (59)
[  1207.5          5092.2        -29757.845325    15136.875
 -24512.981           0.         -12713.77992573 -12713.77992573
  -3552.              0.          -2600.         -13060.59399414
  13843.340625    -6438.8       ]
UGT 6.1 (60)
[   905.625        3617.9        -38304.19568125  10909.90625
 -24415.782           0.         -12713.77992573 -12713.77992573
  -3552.              0.          -2600.         -10401.82965088
   9746.30390625  -5659.1       ]
UGT 6.2 (61)
[   905.625        2812.9        -30110.70443125   9138.90625
 -22262.407           0.         -12713.77992573 -12713.77992573
  -3552.              0.          -2600.          -8659.36627197
   7201.49765625  -5659.1       ]
UGT 6.3 (62)
[   905.625        3617.9        -18129.19568125  10909.90625
 -21415.782           0.         -12713.77992573 -12713.77992573
  -3552.              0.          -2600.         -10401.82965088
   9746.30390625  -5659.1       ]
UGT 6.4 (63)
[   905.625        2812.9         -9935.70443125   9138.90625
 -19262.407           0.         -12713.77992573 -12713.77992573
  -3552.              0.          -2600.          -8659.36627197
   7201.49765625  -5659.1       ]
UGT 6.5 (64)
[   905.625        3617.9        -38297.68568125  10909.90625
 -24414.582           0.         -12713.77992573 -12713.77992573
  -3552.              0.          -2600.         -10401.82965088
   9746.30390625  -5659.1       ]
UGT 6.6 (65)
[   905.625        2812.9        -30104.19443125   9138.90625
 -22261.207           0.         -12713.77992573 -12713.77992573
  -3552.              0.          -2600.          -8659.36627197
   7201.49765625  -5659.1       ]
UGT 6.7 (66)
[   905.625        3617.9        -18122.68568125  10909.90625
 -21414.582           0.         -12713.77992573 -12713.77992573
  -3552.              0.          -2600.         -10401.82965088
   9746.30390625  -5659.1       ]
UGT 6.8 (67)
[   905.625        2812.9         -9929.19443125   9138.90625
 -19261.207           0.         -12713.77992573 -12713.77992573
  -3552.              0.          -2600.          -8659.36627197
   7201.49765625  -5659.1       ]
UGT 6.9 (68)
[   905.625        4422.9        -46497.68693125  12680.90625
 -26569.157           0.         -12713.77992573 -12713.77992573
  -3552.              0.          -2600.         -12144.29302979
  12291.11015625  -5659.1       ]
UGT 6.10 (69)
[   905.625        4422.9        -26322.68693125  12680.90625
 -23569.157           0.         -12713.77992573 -12713.77992573
  -3552.              0.          -2600.         -12144.29302979
  12291.11015625  -5659.1       ]
UGT 6.11 (70)
[   905.625        4422.9        -46491.17693125  12680.90625
 -26567.957           0.         -12713.77992573 -12713.77992573
  -3552.              0.          -2600.         -12144.29302979
  12291.11015625  -5659.1       ]
UGT 6.12 (71)
[   905.625        4422.9        -26316.17693125  12680.90625
 -23567.957           0.         -12713.77992573 -12713.77992573
  -3552.              0.          -2600.         -12144.29302979
```

```
  12291.11015625  -5659.1       ]
UGT 7.1 (72)
[  1358.4375       3655.85       -25805.38387187 -18581.340625
 -29946.48            0.         -12713.77992573 -12713.77992573
  -3552.              0.          -2600.          -9682.80941772
   9017.66210938  -6828.65      ]
UGT 7.2 (73)
[  1358.4375       3333.85       -22527.98737187 -18581.340625
 -29085.13            0.         -12713.77992573 -12713.77992573
  -3552.              0.          -2600.          -8987.08187866
   8001.34960938  -6828.65      ]
UGT 7.3 (74)
[  1358.4375       3655.85       -25800.82687187 -18581.340625
 -29945.64            0.         -12713.77992573 -12713.77992573
  -3552.              0.          -2600.          -9682.80941772
   9017.66210938  -6828.65      ]
UGT 7.4 (75)
[  1358.4375       3333.85       -22523.43037187 -18581.340625
 -29084.29            0.         -12713.77992573 -12713.77992573
  -3552.              0.          -2600.          -8987.08187866
   8001.34960938  -6828.65      ]
UGT 7.5 (76)
[  1358.4375       3655.85        -1797.13387187 -18581.340625
 -26376.48            0.         -12713.77992573 -12713.77992573
  -3552.              0.          -2600.          -9682.80941772
   9017.66210938  -6828.65      ]
UGT 7.6 (77)
[  1358.4375       3333.85         1480.26262813 -18581.340625
 -25515.13            0.         -12713.77992573 -12713.77992573
  -3552.              0.          -2600.          -8987.08187866
   8001.34960938  -6828.65      ]
UGT 7.7 (78)
[  1358.4375       3655.85        -1792.57687187 -18581.340625
 -26375.64            0.         -12713.77992573 -12713.77992573
  -3552.              0.          -2600.          -9682.80941772
   9017.66210938  -6828.65      ]
UGT 7.8 (79)
[  1358.4375       3333.85         1484.81962813 -18581.340625
 -25514.29            0.         -12713.77992573 -12713.77992573
  -3552.              0.          -2600.          -8987.08187866
   8001.34960938  -6828.65      ]
UGT 7.9 (80)
[  1358.4375       3977.85       -29082.78037187 -17164.540625
 -30807.83            0.         -12713.77992573 -12713.77992573
  -3552.              0.          -2600.         -10378.53695679
  10033.97460938  -6828.65      ]
UGT 7.10 (81)
[  1358.4375       3977.85       -29078.22337187 -17164.540625
 -30806.99            0.         -12713.77992573 -12713.77992573
  -3552.              0.          -2600.         -10378.53695679
  10033.97460938  -6828.65      ]
UGT 7.11 (82)
[  1358.4375       3977.85        -5074.53037187 -17164.540625
 -27237.83            0.         -12713.77992573 -12713.77992573
  -3552.              0.          -2600.         -10378.53695679
  10033.97460938  -6828.65      ]
UGT 7.12 (83)
[  1358.4375       3977.85        -5069.97337187 -17164.540625
 -27236.99            0.         -12713.77992573 -12713.77992573
  -3552.              0.          -2600.         -10378.53695679
  10033.97460938  -6828.65      ]
UGT 8.1 (84)
[   905.625        2651.9        -20642.88128125 -22265.29375
 -28528.944           0.         -12713.77992573 -12713.77992573
  -3552.              0.          -2600.          -8308.35797119
   6689.31640625  -5659.1       ]
UGT 8.2 (85)
[   905.625        2329.9        -17365.48478125 -22265.29375
 -27667.594           0.         -12713.77992573 -12713.77992573
  -3552.              0.          -2600.          -7612.63043213
   5673.00390625  -5659.1       ]
UGT 8.3 (86)
```

```
[   905.625        2651.9          3369.92571875 -22265.29375
 -24958.104           0.         -12713.77992573 -12713.77992573
  -3552.              0.           -2600.          -8308.35797119
   6689.31640625  -5659.1       ]
UGT 8.4 (87)
[   905.625        2329.9          6647.32221875 -22265.29375
 -24096.754           0.         -12713.77992573 -12713.77992573
  -3552.              0.           -2600.          -7612.63043213
   5673.00390625  -5659.1       ]
UGT 8.5 (88)
[   905.625        2651.9        -20642.88128125 -22265.29375
 -28528.944           0.         -12713.77992573 -12713.77992573
  -3552.              0.           -2600.          -8308.35797119
   6689.31640625  -5659.1       ]
UGT 8.6 (89)
[   905.625        2329.9        -17365.48478125 -22265.29375
 -27667.594           0.         -12713.77992573 -12713.77992573
  -3552.              0.           -2600.          -7612.63043213
   5673.00390625  -5659.1       ]
UGT 8.7 (90)
[   905.625        2651.9          3369.92571875 -22265.29375
 -24958.104           0.         -12713.77992573 -12713.77992573
  -3552.              0.           -2600.          -8308.35797119
   6689.31640625  -5659.1       ]
UGT 8.8 (91)
[   905.625        2329.9          6647.32221875 -22265.29375
 -24096.754           0.         -12713.77992573 -12713.77992573
  -3552.              0.           -2600.          -7612.63043213
   5673.00390625  -5659.1       ]
UGT 8.9 (92)
[   905.625        2329.9        -17365.48478125 -22265.29375
 -27667.594           0.         -12713.77992573 -12713.77992573
  -3552.              0.           -2600.          -7612.63043213
   5673.00390625  -5659.1       ]
UGT 8.10 (93)
[   905.625        2329.9        -17360.92778125 -22265.29375
 -27666.754           0.         -12713.77992573 -12713.77992573
  -3552.              0.           -2600.          -7612.63043213
   5673.00390625  -5659.1       ]
UGT 8.11 (94)
[   905.625        2329.9          6642.76521875 -22265.29375
 -24097.594           0.         -12713.77992573 -12713.77992573
  -3552.              0.           -2600.          -7612.63043213
   5673.00390625  -5659.1       ]
UGT 8.12 (95)
[   905.625        2329.9          6647.32221875 -22265.29375
 -24096.754           0.         -12713.77992573 -12713.77992573
  -3552.              0.           -2600.          -7612.63043213
   5673.00390625  -5659.1       ]
UGT 9.1 (96)
[  1207.5          3597.2        -26893.746675   -19202.125
 -30212.268           0.         -12713.77992573 -12713.77992573
  -3552.              0.           -2600.          -9820.99682617
   9112.671875    -6438.8       ]
UGT 9.2 (97)
[  1207.5          3137.2        -22211.751675   -19202.125
 -28981.768           0.         -12713.77992573 -12713.77992573
  -3552.              0.           -2600.          -8827.1003418
   7660.796875    -6438.8       ]
UGT 9.3 (98)
[  1207.5          3597.2         -2880.939675   -19202.125
 -26641.428           0.         -12713.77992573 -12713.77992573
  -3552.              0.           -2600.          -9820.99682617
   9112.671875    -6438.8       ]
UGT 9.4 (99)
[  1207.5          3137.2          1801.055325   -19202.125
 -25410.928           0.         -12713.77992573 -12713.77992573
  -3552.              0.           -2600.          -8827.1003418
   7660.796875    -6438.8       ]
UGT 9.5 (100)
[  1207.5          3597.2        -26893.746675   -19202.125
 -30212.268           0.         -12713.77992573 -12713.77992573
```

```
  -3552.             0.          -2600.          -9820.99682617
   9112.671875    -6438.8       ]
UGT 9.6 (101)
[  1207.5          3137.2        -22211.751675   -19202.125
 -28981.768           0.         -12713.77992573 -12713.77992573
  -3552.              0.          -2600.          -8827.1003418
   7660.796875    -6438.8       ]
UGT 9.7 (102)
[  1207.5          3597.2         -2880.939675   -19202.125
 -26641.428           0.         -12713.77992573 -12713.77992573
  -3552.              0.          -2600.          -9820.99682617
   9112.671875    -6438.8       ]
UGT 9.8 (103)
[  1207.5          3137.2          1801.055325   -19202.125
 -25410.928           0.         -12713.77992573 -12713.77992573
  -3552.              0.          -2600.          -8827.1003418
   7660.796875    -6438.8       ]
UGT 9.9 (104)
[  1207.5          4057.2        -31575.741675   -17178.125
 -31442.768           0.         -12713.77992573 -12713.77992573
  -3552.              0.          -2600.          -10814.89331055
  10564.546875    -6438.8       ]
UGT 9.10 (105)
[  1207.5          4057.2        -31571.184675   -17178.125
 -31441.928           0.         -12713.77992573 -12713.77992573
  -3552.              0.          -2600.          -10814.89331055
  10564.546875    -6438.8       ]
UGT 9.11 (106)
[  1207.5          4057.2         -7567.491675   -17178.125
 -27872.768           0.         -12713.77992573 -12713.77992573
  -3552.              0.          -2600.          -10814.89331055
  10564.546875    -6438.8       ]
UGT 9.12 (107)
[  1207.5          4057.2         -7562.934675   -17178.125
 -27871.928           0.         -12713.77992573 -12713.77992573
  -3552.              0.          -2600.          -10814.89331055
  10564.546875    -6438.8       ]
UGT 10.1 (108)
[   905.625        2927.9        -23452.07828125 -21658.09375
 -29267.244           0.         -12713.77992573 -12713.77992573
  -3552.              0.          -2600.          -8904.69586182
   7560.44140625  -5659.1       ]
UGT 10.2 (109)
[   905.625        2467.9        -18770.08328125 -21658.09375
 -28036.744           0.         -12713.77992573 -12713.77992573
  -3552.              0.          -2600.          -7910.79937744
   6108.56640625  -5659.1       ]
UGT 10.3 (110)
[   905.625        2927.9           560.72871875 -21658.09375
 -25696.404           0.         -12713.77992573 -12713.77992573
  -3552.              0.          -2600.          -8904.69586182
   7560.44140625  -5659.1       ]
UGT 10.4 (111)
[   905.625        2467.9          5242.72371875 -21658.09375
 -24465.904           0.         -12713.77992573 -12713.77992573
  -3552.              0.          -2600.          -7910.79937744
   6108.56640625  -5659.1       ]
UGT 10.5 (112)
[   905.625        2927.9        -23452.07828125 -21658.09375
 -29267.244           0.         -12713.77992573 -12713.77992573
  -3552.              0.          -2600.          -8904.69586182
   7560.44140625  -5659.1       ]
UGT 10.6 (113)
[   905.625        2467.9        -18770.08328125 -21658.09375
 -28036.744           0.         -12713.77992573 -12713.77992573
  -3552.              0.          -2600.          -7910.79937744
   6108.56640625  -5659.1       ]
UGT 10.7 (114)
[   905.625        2927.9           560.72871875 -21658.09375
 -25696.404           0.         -12713.77992573 -12713.77992573
  -3552.              0.          -2600.          -8904.69586182
   7560.44140625  -5659.1       ]
```

```
UGT 10.8 (115)
[   905.625        2467.9          5242.72371875 -21658.09375
 -24465.904           0.         -12713.77992573 -12713.77992573
  -3552.              0.          -2600.          -7910.79937744
   6108.56640625  -5659.1       ]
UGT 10.9 (116)
[   905.625        3387.9        -28134.07328125 -19634.09375
 -30497.744           0.         -12713.77992573 -12713.77992573
  -3552.              0.          -2600.          -9898.59234619
   9012.31640625  -5659.1       ]
UGT 10.10 (117)
[   905.625        3387.9        -28129.51628125 -19634.09375
 -30496.904           0.         -12713.77992573 -12713.77992573
  -3552.              0.          -2600.          -9898.59234619
   9012.31640625  -5659.1       ]
UGT 10.11 (118)
[   905.625        3387.9         -4125.82328125 -19634.09375
 -26927.744           0.         -12713.77992573 -12713.77992573
  -3552.              0.          -2600.          -9898.59234619
   9012.31640625  -5659.1       ]
UGT 10.12 (119)
[   905.625        3387.9         -4121.26628125 -19634.09375
 -26926.904           0.         -12713.77992573 -12713.77992573
  -3552.              0.          -2600.          -9898.59234619
   9012.31640625  -5659.1       ]
UGT 11.1 (120)
[  1207.5          3321.2        -39782.112075   -19809.325
 -31634.256           0.         -12713.77992573 -12713.77992573
  -3552.              0.          -2600.          -9224.65893555
   8241.546875    -6438.8       ]
UGT 11.2 (121)
[  1207.5          2999.2        -36504.715575   -19809.325
 -30772.906           0.         -12713.77992573 -12713.77992573
  -3552.              0.          -2600.          -8528.93139648
   7225.234375    -6438.8       ]
UGT 11.3 (122)
[  1207.5          3321.2         -5478.102075   -19809.325
 -26533.056           0.         -12713.77992573 -12713.77992573
  -3552.              0.          -2600.          -9224.65893555
   8241.546875    -6438.8       ]
UGT 11.4 (123)
[  1207.5          2999.2         -2200.705575   -19809.325
 -25671.706           0.         -12713.77992573 -12713.77992573
  -3552.              0.          -2600.          -8528.93139648
   7225.234375    -6438.8       ]
UGT 11.5 (124)
[  1207.5          3321.2        -39782.112075   -19809.325
 -31634.256           0.         -12713.77992573 -12713.77992573
  -3552.              0.          -2600.          -9224.65893555
   8241.546875    -6438.8       ]
UGT 11.6 (125)
[  1207.5          2999.2        -36504.715575   -19809.325
 -30772.906           0.         -12713.77992573 -12713.77992573
  -3552.              0.          -2600.          -8528.93139648
   7225.234375    -6438.8       ]
UGT 11.7 (126)
[  1207.5          3321.2         -5478.102075   -19809.325
 -26533.056           0.         -12713.77992573 -12713.77992573
  -3552.              0.          -2600.          -9224.65893555
   8241.546875    -6438.8       ]
UGT 11.8 (127)
[  1207.5          2999.2         -2200.705575   -19809.325
 -25671.706           0.         -12713.77992573 -12713.77992573
  -3552.              0.          -2600.          -8528.93139648
   7225.234375    -6438.8       ]
UGT 11.9 (128)
[  1207.5          3643.2        -43059.508575   -18392.525
 -32495.606           0.         -12713.77992573 -12713.77992573
  -3552.              0.          -2600.          -9920.38647461
   9257.859375    -6438.8       ]
UGT 11.10 (129)
[  1207.5          3643.2        -43052.998575   -18392.525
```

```
 -32494.406          0.         -12713.77992573 -12713.77992573
  -3552.             0.          -2600.          -9920.38647461
   9257.859375    -6438.8       ]
UGT 11.11 (130)
[  1207.5          3643.2         -8762.008575   -18392.525
 -27395.606          0.         -12713.77992573 -12713.77992573
  -3552.             0.          -2600.          -9920.38647461
   9257.859375    -6438.8       ]
UGT 11.12 (131)
[  1207.5          3643.2         -8755.498575   -18392.525
 -27394.406          0.         -12713.77992573 -12713.77992573
  -3552.             0.          -2600.          -9920.38647461
   9257.859375    -6438.8       ]
UGT 12.1 (132)
[   905.625        2651.9        -36340.44368125 -22265.29375
 -30689.232          0.         -12713.77992573 -12713.77992573
  -3552.             0.          -2600.          -8308.35797119
   6689.31640625  -5659.1       ]
UGT 12.2 (133)
[   905.625        2329.9        -33063.04718125 -22265.29375
 -29827.882          0.         -12713.77992573 -12713.77992573
  -3552.             0.          -2600.          -7612.63043213
   5673.00390625  -5659.1       ]
UGT 12.3 (134)
[   905.625        2651.9         -2036.43368125 -22265.29375
 -25588.032          0.         -12713.77992573 -12713.77992573
  -3552.             0.          -2600.          -8308.35797119
   6689.31640625  -5659.1       ]
UGT 12.4 (135)
[   905.625        2329.9          1240.96281875 -22265.29375
 -24726.682          0.         -12713.77992573 -12713.77992573
  -3552.             0.          -2600.          -7612.63043213
   5673.00390625  -5659.1       ]
UGT 12.5 (136)
[   905.625        2651.9        -36340.44368125 -22265.29375
 -30689.232          0.         -12713.77992573 -12713.77992573
  -3552.             0.          -2600.          -8308.35797119
   6689.31640625  -5659.1       ]
UGT 12.6 (137)
[   905.625        2329.9        -33063.04718125 -22265.29375
 -29827.882          0.         -12713.77992573 -12713.77992573
  -3552.             0.          -2600.          -7612.63043213
   5673.00390625  -5659.1       ]
UGT 12.7 (138)
[   905.625        2651.9         -2036.43368125 -22265.29375
 -25588.032          0.         -12713.77992573 -12713.77992573
  -3552.             0.          -2600.          -8308.35797119
   6689.31640625  -5659.1       ]
UGT 12.8 (139)
[   905.625        2329.9          1240.96281875 -22265.29375
 -24726.682          0.         -12713.77992573 -12713.77992573
  -3552.             0.          -2600.          -7612.63043213
   5673.00390625  -5659.1       ]
UGT 12.9 (140)
[   905.625        2973.9        -39617.84018125 -20848.49375
 -31550.582          0.         -12713.77992573 -12713.77992573
  -3552.             0.          -2600.          -9004.08551025
   7705.62890625  -5659.1       ]
UGT 12.10 (141)
[   905.625        2973.9        -39611.33018125 -20848.49375
 -31549.382          0.         -12713.77992573 -12713.77992573
  -3552.             0.          -2600.          -9004.08551025
   7705.62890625  -5659.1       ]
UGT 12.11 (142)
[   905.625        2973.9         -5320.34018125 -20848.49375
 -26450.582          0.         -12713.77992573 -12713.77992573
  -3552.             0.          -2600.          -9004.08551025
   7705.62890625  -5659.1       ]
UGT 12.12 (143)
[   905.625        2973.9         -5313.83018125 -20848.49375
 -26449.382          0.         -12713.77992573 -12713.77992573
  -3552.             0.          -2600.          -9004.08551025
```

```
   7705.62890625  -5659.1       ]
UGT 13.1 (144)
[  1207.5          3321.2        -10500.174675   -40509.325
 -32578.968           0.        -12713.77992573 -12713.77992573
  -3552.              0.          -2600.          -9224.65893555
   8241.546875    -6438.8       ]
UGT 13.2 (145)
[  1207.5          2999.2         -7222.778175   -40509.325
 -31717.618           0.        -12713.77992573 -12713.77992573
  -3552.              0.          -2600.          -8528.93139648
   7225.234375    -6438.8       ]
UGT 13.3 (146)
[  1207.5          3321.2         13512.632325   -40509.325
 -29008.128           0.        -12713.77992573 -12713.77992573
  -3552.              0.          -2600.          -9224.65893555
   8241.546875    -6438.8       ]
UGT 13.4 (147)
[  1207.5          2999.2         16790.028825   -40509.325
 -28146.778           0.        -12713.77992573 -12713.77992573
  -3552.              0.          -2600.          -8528.93139648
   7225.234375    -6438.8       ]
UGT 13.5 (148)
[  1207.5          3321.2        -10500.174675   -40509.325
 -32578.968           0.        -12713.77992573 -12713.77992573
  -3552.              0.          -2600.          -9224.65893555
   8241.546875    -6438.8       ]
UGT 13.6 (149)
[  1207.5          2999.2         -7222.778175   -40509.325
 -31717.618           0.        -12713.77992573 -12713.77992573
  -3552.              0.          -2600.          -8528.93139648
   7225.234375    -6438.8       ]
UGT 13.7 (150)
[  1207.5          3321.2         13512.632325   -40509.325
 -29008.128           0.        -12713.77992573 -12713.77992573
  -3552.              0.          -2600.          -9224.65893555
   8241.546875    -6438.8       ]
UGT 13.8 (151)
[  1207.5          2999.2         16790.028825   -40509.325
 -28146.778           0.        -12713.77992573 -12713.77992573
  -3552.              0.          -2600.          -8528.93139648
   7225.234375    -6438.8       ]
UGT 13.9 (152)
[  1207.5          3643.2        -13777.571175   -39092.525
 -33440.318           0.        -12713.77992573 -12713.77992573
  -3552.              0.          -2600.          -9920.38647461
   9257.859375    -6438.8       ]
UGT 13.10 (153)
[  1207.5          3643.2        -13773.014175   -39092.525
 -33439.478           0.        -12713.77992573 -12713.77992573
  -3552.              0.          -2600.          -9920.38647461
   9257.859375    -6438.8       ]
UGT 13.11 (154)
[  1207.5          3643.2         10230.678825   -39092.525
 -29870.318           0.        -12713.77992573 -12713.77992573
  -3552.              0.          -2600.          -9920.38647461
   9257.859375    -6438.8       ]
UGT 13.12 (155)
[  1207.5          3643.2         10235.235825   -39092.525
 -29869.478           0.        -12713.77992573 -12713.77992573
  -3552.              0.          -2600.          -9920.38647461
   9257.859375    -6438.8       ]
UGT 14.1 (156)
[   905.625        2651.9         -7058.50628125 -42965.29375
 -31633.944           0.        -12713.77992573 -12713.77992573
  -3552.              0.          -2600.          -8308.35797119
   6689.31640625  -5659.1       ]
UGT 14.2 (157)
[   905.625        2329.9         -3781.10978125 -42965.29375
 -30772.594           0.        -12713.77992573 -12713.77992573
  -3552.              0.          -2600.          -7612.63043213
   5673.00390625  -5659.1       ]
UGT 14.3 (158)
```

```
[   905.625        2651.9         16954.30071875 -42965.29375
 -28063.104           0.         -12713.77992573 -12713.77992573
  -3552.              0.          -2600.          -8308.35797119
   6689.31640625  -5659.1       ]
UGT 14.4 (159)
[   905.625        2329.9         20231.69721875 -42965.29375
 -27201.754           0.         -12713.77992573 -12713.77992573
  -3552.              0.          -2600.          -7612.63043213
   5673.00390625  -5659.1       ]
UGT 14.5 (160)
[   905.625        2651.9         -7058.50628125 -42965.29375
 -31633.944           0.         -12713.77992573 -12713.77992573
  -3552.              0.          -2600.          -8308.35797119
   6689.31640625  -5659.1       ]
UGT 14.6 (161)
[   905.625        2329.9         -3781.10978125 -42965.29375
 -30772.594           0.         -12713.77992573 -12713.77992573
  -3552.              0.          -2600.          -7612.63043213
   5673.00390625  -5659.1       ]
UGT 14.7 (162)
[   905.625        2651.9         16954.30071875 -42965.29375
 -28063.104           0.         -12713.77992573 -12713.77992573
  -3552.              0.          -2600.          -8308.35797119
   6689.31640625  -5659.1       ]
UGT 14.8 (163)
[   905.625        2329.9         20231.69721875 -42965.29375
 -27201.754           0.         -12713.77992573 -12713.77992573
  -3552.              0.          -2600.          -7612.63043213
   5673.00390625  -5659.1       ]
UGT 14.9 (164)
[   905.625        2973.9        -10335.90278125 -41548.49375
 -32495.294           0.         -12713.77992573 -12713.77992573
  -3552.              0.          -2600.          -9004.08551025
   7705.62890625  -5659.1       ]
UGT 14.10 (165)
[   905.625        2973.9        -10331.34578125 -41548.49375
 -32494.454           0.         -12713.77992573 -12713.77992573
  -3552.              0.          -2600.          -9004.08551025
   7705.62890625  -5659.1       ]
UGT 14.11 (166)
[   905.625        2973.9         13672.34721875 -41548.49375
 -28925.294           0.         -12713.77992573 -12713.77992573
  -3552.              0.          -2600.          -9004.08551025
   7705.62890625  -5659.1       ]
UGT 14.12 (167)
[   905.625        2973.9         13676.90421875 -41548.49375
 -28924.454           0.         -12713.77992573 -12713.77992573
  -3552.              0.          -2600.          -9004.08551025
   7705.62890625  -5659.1       ]
```

C.1.2 SLS Load Cases

```
BGT 1.1 (0)
[  1006.25         2997.66666667  -9573.55297917   9873.22916667
 -16288.91333333      0.          -5151.27290094  -5151.27290094
  -1768.              0.          -1384.          -6673.82548014
   7597.7265625   -4167.        ]
BGT 1.2 (1)
[  1006.25         2614.33333333  -5671.89047917   9029.89583333
 -15263.49666667      0.          -5151.27290094  -5151.27290094
  -1768.              0.          -1384.          -5844.081014
   6385.9140625   -4167.        ]
BGT 1.3 (2)
[  1006.25         3381.         -13475.21547917  10716.5625
 -17314.33            0.          -5151.27290094  -5151.27290094
  -1768.              0.          -1384.          -7503.56994629
   8809.5390625   -4167.        ]
BGT 2.1 (3)
[  1006.25         2691.         -11268.26457917   9198.5625
 -16068.772           0.          -5151.27290094  -5151.27290094
  -1768.              0.          -1384.          -6010.02990723
   6628.2765625   -4167.        ]
BGT 2.2 (4)
[  1006.25         2461.          -8927.26707917   8692.5625
 -15453.522           0.          -5151.27290094  -5151.27290094
  -1768.              0.          -1384.          -5512.18322754
   5901.1890625   -4167.        ]
BGT 2.3 (5)
[  1006.25         2691.          -7233.26457917   9198.5625
 -15468.772           0.          -5151.27290094  -5151.27290094
  -1768.              0.          -1384.          -6010.02990723
   6628.2765625   -4167.        ]
BGT 2.4 (6)
[  1006.25         2461.          -4892.26707917   8692.5625
 -14853.522           0.          -5151.27290094  -5151.27290094
  -1768.              0.          -1384.          -5512.18322754
   5901.1890625   -4167.        ]
BGT 2.5 (7)
[  1006.25         2691.         -11266.96257917   9198.5625
 -16068.532           0.          -5151.27290094  -5151.27290094
  -1768.              0.          -1384.          -6010.02990723
   6628.2765625   -4167.        ]
BGT 2.6 (8)
[  1006.25         2461.          -8925.96507917   8692.5625
 -15453.282           0.          -5151.27290094  -5151.27290094
  -1768.              0.          -1384.          -5512.18322754
   5901.1890625   -4167.        ]
BGT 2.7 (9)
[  1006.25         2691.          -7231.96257917   9198.5625
 -15468.532           0.          -5151.27290094  -5151.27290094
  -1768.              0.          -1384.          -6010.02990723
   6628.2765625   -4167.        ]
BGT 2.8 (10)
[  1006.25         2461.          -4890.96507917   8692.5625
 -14853.282           0.          -5151.27290094  -5151.27290094
  -1768.              0.          -1384.          -5512.18322754
   5901.1890625   -4167.        ]
BGT 2.9 (11)
[  1006.25         2921.         -13609.26207917   9704.5625
 -16684.022           0.          -5151.27290094  -5151.27290094
  -1768.              0.          -1384.          -6507.87658691
   7355.3640625   -4167.        ]
BGT 2.10 (12)
[  1006.25         2921.          -9574.26207917   9704.5625
 -16084.022           0.          -5151.27290094  -5151.27290094
  -1768.              0.          -1384.          -6507.87658691
   7355.3640625   -4167.        ]
BGT 2.11 (13)
[  1006.25         2921.         -13607.96007917   9704.5625
 -16683.782           0.          -5151.27290094  -5151.27290094
  -1768.              0.          -1384.          -6507.87658691
   7355.3640625   -4167.        ]
BGT 2.12 (14)
```

```
[  1006.25         2921.          -9572.96007917   9704.5625
 -16083.782           0.          -5151.27290094  -5151.27290094
  -1768.              0.          -1384.          -6507.87658691
   7355.3640625   -4167.        ]
BGT 3.1 (15)
[  1006.25         2691.          -6452.22297917   9198.5625
 -15468.58            0.          -5151.27290094  -5151.27290094
  -1768.              0.          -1384.          -6010.02990723
   6628.2765625   -4167.        ]
BGT 3.2 (16)
[  1006.25         2461.          -4111.22547917   8692.5625
 -14853.33            0.          -5151.27290094  -5151.27290094
  -1768.              0.          -1384.          -5512.18322754
   5901.1890625   -4167.        ]
BGT 3.3 (17)
[  1006.25         2921.          -8793.22047917   9704.5625
 -16083.83            0.          -5151.27290094  -5151.27290094
  -1768.              0.          -1384.          -6507.87658691
   7355.3640625   -4167.        ]
BGT 4.1 (18)
[  1006.25         2997.66666667  -9573.55297917   9873.22916667
 -16288.91333333      0.          -5151.27290094  -5151.27290094
  -1768.              0.          -1384.          -6672.62756348
   7596.19322917  -4167.        ]
BGT 4.2 (19)
[  1006.25         2767.66666667  -7232.55547917   9367.22916667
 -15673.66333333      0.          -5151.27290094  -5151.27290094
  -1768.              0.          -1384.          -6174.78088379
   6869.10572917  -4167.        ]
BGT 4.3 (20)
[  1006.25         2844.33333333  -8012.88797917   9873.22916667
 -15878.74666667      0.          -5151.27290094  -5151.27290094
  -1768.              0.          -1384.          -6341.32873535
   7112.23489583  -4167.        ]
BGT 4.4 (21)
[  1006.25         2614.33333333  -5671.89047917   9367.22916667
 -15263.49666667      0.          -5151.27290094  -5151.27290094
  -1768.              0.          -1384.          -5843.48205566
   6385.14739583  -4167.        ]
BGT 4.5 (22)
[  1006.25         3227.66666667 -11914.55047917  10379.22916667
 -16904.16333333      0.          -5151.27290094  -5151.27290094
  -1768.              0.          -1384.          -7170.47424316
   8323.28072917  -4167.        ]
BGT 4.6 (23)
[  1006.25         3074.33333333 -10353.88547917  10379.22916667
 -16493.99666667      0.          -5151.27290094  -5151.27290094
  -1768.              0.          -1384.          -6839.17541504
   7839.32239583  -4167.        ]
BGT 4.7 (24)
[  1006.25         3151.         -11134.21797917  10547.89583333
 -16699.08            0.          -5151.27290094  -5151.27290094
  -1768.              0.          -1384.          -7003.9263916
   8080.1515625   -4167.        ]
BGT 4.8 (25)
[  1006.25         2921.          -8793.22047917  10041.89583333
 -16083.83            0.          -5151.27290094  -5151.27290094
  -1768.              0.          -1384.          -6506.07971191
   7353.0640625   -4167.        ]
BGT 4.9 (26)
[  1006.25         3381.         -13475.21547917  11053.89583333
 -17314.33            0.          -5151.27290094  -5151.27290094
  -1768.              0.          -1384.          -7501.77307129
   8807.2390625   -4167.        ]
BGT 5.1 (27)
[  1006.25         2415.         -14108.06757917   8591.3625
 -16170.472           0.          -5151.27290094  -5151.27290094
  -1768.              0.          -1384.          -5411.8951416
   5754.8515625   -4167.        ]
BGT 5.2 (28)
[  1006.25         2323.         -13171.66857917   8591.3625
 -15924.372           0.          -5151.27290094  -5151.27290094
```

```
  -1768.             0.          -1384.          -5213.11584473
   5464.4765625   -4167.        ]
BGT 5.3 (29)
[  1006.25         2415.          -7248.56757917   8591.3625
 -15150.472           0.          -5151.27290094  -5151.27290094
  -1768.              0.          -1384.          -5411.8951416
   5754.8515625   -4167.        ]
BGT 5.4 (30)
[  1006.25         2323.          -6312.16857917   8591.3625
 -14904.372           0.          -5151.27290094  -5151.27290094
  -1768.              0.          -1384.          -5213.11584473
   5464.4765625   -4167.        ]
BGT 5.5 (31)
[  1006.25         2415.         -14106.76557917   8591.3625
 -16170.232           0.          -5151.27290094  -5151.27290094
  -1768.              0.          -1384.          -5411.8951416
   5754.8515625   -4167.        ]
BGT 5.6 (32)
[  1006.25         2323.         -13170.36657917   8591.3625
 -15924.132           0.          -5151.27290094  -5151.27290094
  -1768.              0.          -1384.          -5213.11584473
   5464.4765625   -4167.        ]
BGT 5.7 (33)
[  1006.25         2415.          -7247.26557917   8591.3625
 -15150.232           0.          -5151.27290094  -5151.27290094
  -1768.              0.          -1384.          -5411.8951416
   5754.8515625   -4167.        ]
BGT 5.8 (34)
[  1006.25         2323.          -6310.86657917   8591.3625
 -14904.132           0.          -5151.27290094  -5151.27290094
  -1768.              0.          -1384.          -5213.11584473
   5464.4765625   -4167.        ]
BGT 5.9 (35)
[  1006.25         2507.         -15044.46657917   8996.1625
 -16416.572           0.          -5151.27290094  -5151.27290094
  -1768.              0.          -1384.          -5610.67443848
   6045.2265625   -4167.        ]
BGT 5.10 (36)
[  1006.25         2507.          -8184.96657917   8996.1625
 -15396.572           0.          -5151.27290094  -5151.27290094
  -1768.              0.          -1384.          -5610.67443848
   6045.2265625   -4167.        ]
BGT 5.11 (37)
[  1006.25         2507.         -15043.16457917   8996.1625
 -16416.332           0.          -5151.27290094  -5151.27290094
  -1768.              0.          -1384.          -5610.67443848
   6045.2265625   -4167.        ]
BGT 5.12 (38)
[  1006.25         2507.          -8183.66457917   8996.1625
 -15396.332           0.          -5151.27290094  -5151.27290094
  -1768.              0.          -1384.          -5610.67443848
   6045.2265625   -4167.        ]
BGT 6.1 (39)
[  1006.25         2415.           9941.34902083 -12108.6375
 -17835.28            0.          -5151.27290094  -5151.27290094
  -1768.              0.          -1384.          -5411.8951416
   5754.8515625   -4167.        ]
BGT 6.2 (40)
[  1006.25         2323.          10877.74802083 -12108.6375
 -17589.18            0.          -5151.27290094  -5151.27290094
  -1768.              0.          -1384.          -5213.11584473
   5464.4765625   -4167.        ]
BGT 6.3 (41)
[  1006.25         2507.           9004.95002083 -11703.8375
 -18081.38            0.          -5151.27290094  -5151.27290094
  -1768.              0.          -1384.          -5610.67443848
   6045.2265625   -4167.        ]
BGT 7.1 (42)
[  1006.25         2415.          -3643.02597917   8591.3625
 -14730.28            0.          -5151.27290094  -5151.27290094
  -1768.              0.          -1384.          -5411.8951416
   5754.8515625   -4167.        ]
```

```
BGT 7.2 (43)
[  1006.25         2323.          -2706.62697917   8591.3625
 -14484.18            0.          -5151.27290094  -5151.27290094
  -1768.              0.          -1384.          -5213.11584473
   5464.4765625   -4167.        ]
BGT 7.3 (44)
[  1006.25         2507.          -4579.42497917   8996.1625
 -14976.38            0.          -5151.27290094  -5151.27290094
  -1768.              0.          -1384.          -5610.67443848
   6045.2265625   -4167.        ]
```

C.2 Resulting governing moments

The governing moments for each element resulting from the Python Anastruct analysis are shown below. The governing load cases used in this thesis are ULS 3.12 (index = 35) and SLS 1.2 (index = 2). The bending moments are given per 23 m relieving platform segment and are expressed in kNm.

C.2.1 ULS

	Element 1	Element 2	Element 3	Element 4
0	36242.635872	29047.437040	-101807.114457	11776.281097
1	28049.144622	22408.765280	-89752.808059	10033.817719
2	22120.135872	15321.543977	-108328.779671	11776.281097
3	13926.644622	8682.872217	-96342.838153	10033.817719
4	36238.078872	29043.008016	-101809.196707	11776.281097
5	28044.587622	22404.336256	-89754.890309	10033.817719
6	22115.578872	15317.114953	-108330.949702	11776.281097
7	13922.087622	8678.443193	-96345.008184	10033.817719
8	44436.127122	35686.108800	-113861.420855	13518.744476
9	30313.627122	21960.215737	-120314.721190	13518.744476
10	44431.570122	35681.679776	-113863.503105	13518.744476
11	30309.070122	21955.786713	-120316.891221	13518.744476
12	31080.133281	26568.201412	-73832.120538	10401.829651
13	22886.642031	19929.529652	-61777.814140	8659.366272
14	16957.633281	12842.308349	-80349.762457	10401.829651
15	8764.142031	6203.636588	-68363.820938	8659.366272
16	31075.576281	26563.772388	-73834.202789	10401.829651
17	22882.085031	19925.100627	-61779.896391	8659.366272
18	16953.076281	12837.879324	-80351.932488	10401.829651
19	8759.585031	6199.207564	-68365.990969	8659.366272
20	39273.624531	33206.873172	-85886.426936	12144.293030
21	25151.124531	19480.980109	-92339.484153	12144.293030
22	39269.067531	33202.444148	-85888.509187	12144.293030
23	25146.567531	19476.551084	-92341.566404	12144.293030
24	41544.794175	33911.315244	-102814.379111	12811.670654
25	29839.806675	24427.498444	-85593.941399	10322.437256
26	27422.294175	20185.422181	-109276.104759	12811.670654
27	15717.306675	10701.605381	-92153.331161	10322.437256
28	41540.237175	33906.886220	-102816.461361	12811.670654
29	29835.249675	24423.069420	-85596.023650	10322.437256
30	27417.737175	20180.993157	-109278.274790	12811.670654
31	15712.749675	10697.176357	-92155.501192	10322.437256
32	53249.781675	43395.132044	-120034.816822	15300.904053
33	39127.281675	29669.238981	-126487.874039	15300.904053
34	53245.224675	43390.703020	-120036.899072	15300.904053
35	39122.724675	29664.809957	-126489.956289	15300.904053
36	38103.125781	32258.491492	-84164.383165	11895.369690
37	26398.138281	22774.674692	-66943.945454	9406.136292
38	23980.625781	18532.598429	-90623.426616	11895.369690
39	12275.638281	9048.781628	-73500.653018	9406.136292
40	38098.568781	32254.062468	-84166.465415	11895.369690
41	26393.581281	22770.245667	-66946.027704	9406.136292
42	23976.068781	18528.169404	-90625.596647	11895.369690
43	12271.081281	9044.352604	-73502.823049	9406.136292
44	49808.113281	41742.308292	-101384.820876	14384.603088
45	49803.556281	41737.879268	-101386.903127	14384.603088
46	35685.613281	28016.415229	-107837.878093	14384.603088
47	35681.056281	28011.986204	-107839.960344	14384.603088
48	41745.864075	35242.211780	-89189.007775	11318.130615
49	33552.372825	28603.540020	-77126.886878	9575.667236
50	21570.864075	15633.793118	-98444.545774	11318.130615
51	13377.372825	8995.121358	-86458.604255	9575.667236
52	41739.354075	35235.884603	-89191.857018	11318.130615
53	33545.862825	28597.212842	-77129.861521	9575.667236
54	21564.354075	15627.465941	-98447.645818	11318.130615
55	13370.862825	8988.794181	-86461.704299	9575.667236
56	49939.355325	41880.883540	-101262.436866	13060.593994
57	29764.355325	22272.464878	-110454.152841	13060.593994
58	49932.845325	41874.556363	-101265.286109	13060.593994
59	29757.845325	22266.137701	-110457.127484	13060.593994
60	38304.195681	33589.388028	-70601.101207	10401.829651
61	30110.704431	26950.716268	-58527.672115	8659.366272
62	18129.195681	13980.969366	-79791.867631	10401.829651
63	9935.704431	7342.297606	-67805.926112	8659.366272
64	38297.685681	33583.060850	-70603.950449	10401.829651
65	30104.194431	26944.389090	-58530.521358	8659.366272
66	18122.685681	13974.642189	-79794.967675	10401.829651
67	9929.194431	7335.970428	-67809.026156	8659.366272
68	46497.686931	40228.059788	-82674.530298	12144.293030
69	26322.686931	20619.641126	-91804.156895	12144.293030

```
70   46491.176931  40221.732610  -82677.379541  12144.293030
71   26316.176931  20613.313949  -91807.131539  12144.293030
72   25805.383872  19279.366560  -89295.208027   9682.809418
73   22527.987372  16651.638448  -84434.065504   8987.081879
74   25800.826872  19274.937535  -89297.290277   9682.809418
75   22523.430372  16647.209424  -84436.147754   8987.081879
76   -4054.651648 -16632.652792 -100629.484429   9682.809418
77   -6682.379759 -18375.142965  -95843.604413   8987.081879
78   -4059.080672 -16636.929557 -100631.742241   9682.809418
79   -6686.808783 -18379.419730  -95845.862224   8987.081879
80   29082.780372  21962.465481  -94079.950705  10378.536957
81   29078.223372  21958.036457  -94082.032955  10378.536957
82    5074.530372 -14833.427436 -105358.554340  10378.536957
83    5069.973372 -14837.704200 -105360.724371  10378.536957
84   20642.881281  16800.130931  -61320.214108   8308.357971
85   17365.484781  14172.402820  -56459.071585   7612.630432
86   -6538.316300 -15294.584174  -72737.812500   8308.357971
87   -9166.044412 -17037.074347  -67951.932484   7612.630432
88   20642.881281  16800.130931  -61320.214108   8308.357971
89   17365.484781  14172.402820  -56459.071585   7612.630432
90   -6538.316300 -15294.584174  -72737.812500   8308.357971
91   -9166.044412 -17037.074347  -67951.932484   7612.630432
92   17365.484781  14172.402820  -56459.071585   7612.630432
93   17360.927781  14167.973796  -56461.153836   7612.630432
94   -9161.615387 -17032.797583  -67949.674672   7612.630432
95   -9166.044412 -17037.074347  -67951.932484   7612.630432
96   26893.746675  20729.023412  -84104.160854   9820.996826
97   22211.751675  16975.126110  -77159.671536   8827.100342
98    2880.939675 -14671.603012  -95403.879958   9820.996826
99   -6363.321122 -17160.874688  -88566.908506   8827.100342
100  26893.746675  20729.023412  -84104.160854   9820.996826
101  22211.751675  16975.126110  -77159.671536   8827.100342
102   2880.939675 -14671.603012  -95403.879958   9820.996826
103  -6363.321122 -17160.874688  -88566.908506   8827.100342
104  31575.741675  24562.021871  -90939.507537  10814.893311
105  31571.184675  24557.592847  -90941.589788  10814.893311
106   7567.491675 -12097.004309 -102181.723527  10814.893311
107   7562.934675 -12101.281074 -102183.893558  10814.893311
108  23452.078281  19076.199659  -65454.164908   8904.695862
109  18770.083281  15322.302358  -58509.675590   7910.799377
110  -4262.247572 -13776.706090  -76807.926798   8904.695862
111  -8016.144874 -16265.977766  -69970.955346   7910.799377
```

C.2.2 SLS

	Element 1	Element 2	Element 3	Element 4
0	9573.552979	-6188.689926	-76285.818415	6673.825480
1	5671.890479	-8297.009603	-70578.227216	5844.081014
2	13475.215479	7229.234383	-81993.409615	7503.569946
3	11268.264579	6219.735380	-69426.359554	6010.029907
4	8927.267079	-4620.461260	-66001.804834	5512.183228
5	7233.264579	-7142.334692	-71347.815572	6010.029907
6	4892.267079	-8407.326499	-67923.260852	5512.183228
7	11266.962579	6218.469944	-69426.979563	6010.029907
8	8925.965079	-4621.683192	-66002.424843	5512.183228
9	7231.962579	-7143.556625	-71348.435580	6010.029907
10	4890.965079	-8408.548431	-67923.880861	5512.183228
11	13609.262079	8116.498740	-72850.914274	6507.876587
12	9574.262079	-5877.342886	-74772.370291	6507.876587
13	13607.960079	8115.233304	-72851.534282	6507.876587
14	9572.960079	-5878.564819	-74772.990300	6507.876587
15	6452.222979	-7875.345668	-71719.745456	6010.029907
16	4111.225479	-9140.337474	-68295.190736	5512.183228
17	8793.220479	-6610.353862	-75144.300175	6507.876587
18	9573.552979	-6188.814463	-76286.938863	6672.627563
19	7232.555479	-7453.806269	-72862.384143	6174.780884
20	8012.887979	-7018.571689	-73985.339003	6341.328735
21	5671.890479	-8283.563495	-70560.784283	5843.482056
22	11914.550479	5964.672916	-79711.493583	7170.474243
23	10353.885479	-5753.579882	-77409.893722	6839.175415
24	11134.217979	5345.575709	-78552.532410	7003.926392
25	8793.220479	-6597.032290	-75127.977690	6506.079712
26	13475.215479	7242.339069	-81977.087129	7501.773071
27	14108.067579	9433.945037	-62638.853478	5411.895142
28	13171.668579	8683.165577	-61249.955614	5213.115845
29	7248.567579	-6009.593915	-65894.002964	5411.895142
30	6312.168579	-6507.448250	-64513.043048	5213.115845
31	14106.765579	9432.679602	-62639.448406	5411.895142
32	13170.366579	8681.900141	-61250.550543	5213.115845
33	7247.265579	-6010.815848	-65894.622973	5411.895142
34	6310.866579	-6508.670183	-64513.663057	5213.115845
35	15044.466579	10200.544729	-64005.922814	5610.674438
36	8184.966579	-5495.529527	-67253.359092	5610.674438
37	15043.164579	10199.279294	-64006.517743	5610.674438
38	8183.664579	-5496.751460	-67253.979101	5610.674438
39	-14749.072786	-22971.329346	-75437.577639	5411.895142
40	-15499.852247	-23469.183681	-74089.376653	5213.115845
41	-13982.473095	-22457.264959	-76764.624316	5610.674438
42	3643.025979	-9393.410557	-67610.952061	5411.895142
43	2706.626979	-9891.264893	-66229.992145	5213.115845
44	4579.424979	-8879.346170	-68970.308189	5610.674438

C.3 Resulting governing shear

The governing shear forces for each element resulting from the Python Anastruct analysis are shown below. The governing load cases used in this thesis are ULS 3.12 (index = 35) and SLS 1.2 (index = 2). ULS 3.12 does not give the highest shear loads, but is close to the highest. For simplicity reasons, this thesis has considered ULS 3.12 to be governing for both shear and moments. The shear loads are given per 23 m relieving platform segment and are expressed in kN.

C.3.1 ULS

	Element 1	Element 2	Element 3	Element 4
0	-20176.496594	-37642.842400	-37060.072686	13061.341781
1	-15869.517414	-32488.529265	-31905.759550	11632.218067
2	-19077.862424	-36542.924675	36514.951853	13036.050095
3	-14770.883245	-31388.611540	31913.469638	11606.926381
4	-20176.142090	-37642.487483	-37059.717768	13061.333620
5	-15869.162911	-32488.174347	-31905.404633	11632.209906
6	-19077.507920	-36542.569757	36515.306771	13036.041934
7	-14770.528741	-31388.256622	31913.824556	11606.918220
8	-24483.475773	-42797.155536	-42214.385821	14490.465495
9	-23384.841603	-41697.237810	41116.434068	14465.173809
10	-24483.121270	-42796.800618	-42214.030903	14490.457334
11	-23384.487100	-41696.882893	41116.788985	14465.165648
12	-12661.891495	-28637.600286	-28249.087143	10036.312924
13	-8354.912316	-23483.287151	-23094.774007	8607.189210
14	-11563.257325	-27537.682560	27671.432025	10011.021238
15	-7256.278146	-22383.369425	23069.949810	8581.897524
16	-12661.536991	-28637.245368	-28248.732225	10036.304763
17	-8354.557812	-23482.932233	-23094.419090	8607.181049
18	-11562.902822	-27537.327643	27671.786943	10011.013077
19	-7255.923642	-22383.014507	23070.304728	8581.889363
20	-16968.870674	-33791.913421	-33403.400278	11465.436637
21	-15870.236505	-32691.995696	-32303.482553	11440.144951
22	-16968.516171	-33791.558504	-33403.045360	11465.428476
23	-15869.882001	-32691.640778	-32303.127635	11440.136790
24	-21363.324667	-39059.077716	-38541.060192	13277.962012
25	-15210.497268	-31695.773237	-31177.755713	11236.356707
26	-20264.690497	-37959.159991	37511.239523	13252.670326
27	-14111.863098	-30595.855512	30937.693502	11211.065021
28	-21362.970163	-39058.722799	-38540.705275	13277.953851
29	-15210.142764	-31695.418320	-31177.400795	11236.348546
30	-20264.335994	-37958.805073	37511.594441	13252.662165
31	-14111.508595	-30595.500594	30938.048420	11211.056859
32	-27516.152066	-46422.382196	-45904.364671	15319.567317
33	-26417.517896	-45322.464470	-44804.446946	15294.275631
34	-27515.797563	-46422.027278	-45904.009754	15319.559156
35	-26417.163393	-45322.109552	-44804.092028	15294.267470
36	-16353.587934	-33055.582973	-32667.069830	11261.276107
37	-10200.760535	-25692.278494	-25303.765351	9219.670802
38	-15254.953765	-31955.665248	31615.559638	11235.984421
39	-9102.126366	-24592.360769	25042.013617	9194.379116
40	-16353.233431	-33055.228056	-32666.714913	11261.267946
41	-10200.406032	-25691.923577	-25303.410433	9219.662641
42	-15254.599261	-31955.310330	31615.914555	11235.976260
43	-9101.771862	-24592.005851	25042.368534	9194.370955
44	-22506.415334	-40418.887452	-40030.374309	13302.881412
45	-22506.060830	-40418.532535	-40030.019392	13302.873251
46	-21407.781164	-39318.969727	-38930.456584	13277.589726
47	-21407.426661	-39318.614809	-38930.101666	13277.581565
48	-18233.611006	-35203.734384	-34685.716859	12065.936249
49	-13926.631827	-30049.421248	-29531.403724	10636.812535
50	-16664.133621	-33632.423347	33475.865867	12029.805269
51	-12357.154442	-28478.110212	28874.383652	10600.681555
52	-18233.104573	-35203.227358	-34685.209834	12065.924590
53	-13926.125393	-30048.914223	-29530.896699	10636.800877
54	-16663.627188	-33631.916322	33476.372892	12029.793610
55	-12356.648008	-28477.603186	28874.890677	10600.669897
56	-22540.590186	-40358.047519	-39840.029995	13495.059963
57	-20971.112801	-38786.736482	-38268.718958	13458.928983
58	-22540.083752	-40357.540494	-39839.522969	13495.048304
59	-20970.606367	-38786.229457	-38268.211933	13458.917324
60	-13223.874274	-29200.239640	-28811.726497	10049.250344
61	-8916.895094	-24045.926505	-23657.413362	8620.126630
62	-11654.396889	-27628.928604	27580.185981	10013.119364
63	-7347.417709	-22474.615468	22978.703767	8583.995650
64	-13223.367840	-29199.732615	-28811.219472	10049.238685
65	-8916.388661	-24045.419480	-23656.906337	8620.114972
66	-11653.890455	-27628.421579	27580.693007	10013.107705
67	-7346.911276	-22474.108443	22979.210792	8583.983992
68	-17530.853453	-34354.552776	-33966.039633	11478.374058
69	-15961.376068	-32783.241739	-32394.728596	11442.243078

```
70  -17530.347020 -34354.045751 -33965.532607  11478.362399
71  -15960.869635 -32782.734714 -32394.221571  11442.231419
72  -18322.808181 -31480.593609 -30897.823894  12042.005452
73  -16523.172762 -29417.102008 -28834.332294  11454.140335
74  -18322.453678 -31480.238691 -30897.468976  12041.997291
75  -16522.818259 -29416.747091 -28833.977376  11454.132174
76  -16455.130093 -29610.733475  31740.188633  11999.009586
77  -14655.494674 -27547.241875  29901.362093  11411.144469
78  -16454.775590 -29610.378557  31740.543550  11999.001425
79  -14655.140171 -27546.886957  29901.717011  11411.136308
80  -19969.061855 -33540.904853 -32958.135138  12598.111263
81  -19968.707351 -33540.549935 -32957.780221  12598.103102
82  -18101.383767 -31671.044720  33582.195528  12555.115396
83  -18101.029263 -31670.689802  33582.550446  12555.107235
84  -10808.203083 -22475.351494 -22086.838351   9016.976595
85   -9008.567664 -20411.859894 -20023.346751   8429.111478
86   -8940.170491 -20605.136443  22897.023722   8973.972567
87   -7140.535072 -18541.644842  21058.197183   8386.107450
88  -10808.203083 -22475.351494 -22086.838351   9016.976595
89   -9008.567664 -20411.859894 -20023.346751   8429.111478
90   -8940.170491 -20605.136443  22897.023722   8973.972567
91   -7140.535072 -18541.644842  21058.197183   8386.107450
92   -9008.567664 -20411.859894 -20023.346751   8429.111478
93   -9008.213160 -20411.504976 -20022.991833   8429.103316
94   -7140.889575 -18541.999760  21057.842265   8386.115611
95   -7140.535072 -18541.644842  21058.197183   8386.107450
96  -17294.749426 -30246.190314 -29728.172789  11523.935754
97  -14723.841685 -27298.345170 -26780.327646  10684.128444
98  -15426.716834 -28375.975262  30370.203651  11480.931727
99  -12855.809093 -25428.130119  27743.308595  10641.124417
100 -17294.749426 -30246.190314 -29728.172789  11523.935754
101 -14723.841685 -27298.345170 -26780.327646  10684.128444
102 -15426.716834 -28375.975262  30370.203651  11480.931727
103 -12855.809093 -25428.130119  27743.308595  10641.124417
104 -19646.540389 -33189.492091 -32671.474567  12318.372627
105 -19646.185885 -33189.137174 -32671.119649  12318.364465
106 -17778.862300 -31319.631958  33001.287156  12275.376760
107 -17778.507797 -31319.277040  33001.642074  12275.368599
108 -12285.012694 -24242.695571 -23854.182427   9507.249849
109  -9714.104952 -21294.850427 -20906.337284   8667.442539
110 -10416.980102 -22372.480519  24474.523766   9464.245822
111  -7846.072361 -19424.635376  21847.628709   8624.438512
```

C.3.2 SLS

	Element 1	Element 2	Element 3	Element 4
0	-15432.572285	-24124.119337	24831.029758	8582.947936
1	-13381.629819	-21669.684511	22639.847751	7902.412835
2	-17483.514751	-26578.554163	27022.211765	9263.483038
3	-14166.473498	-22535.664379	22702.991249	8047.144802
4	-12935.908018	-21063.003483	21388.282045	7638.823741
5	-13852.578021	-22221.402172	23017.253456	8039.918606
6	-12622.012541	-20748.741276	21702.544252	7631.597545
7	-14166.372211	-22535.562974	22703.092654	8047.142470
8	-12935.806731	-21062.902078	21388.383450	7638.821409
9	-13852.476734	-22221.300767	23017.354861	8039.916274
10	-12621.911254	-20748.639871	21702.645657	7631.595213
11	-15397.038978	-24008.325275	24017.700453	8455.465863
12	-15083.143501	-23694.063068	24331.962660	8448.239667
13	-15396.937691	-24008.223870	24017.801858	8455.463531
14	-15083.042214	-23693.961663	24332.064066	8448.237335
15	-13791.818312	-22160.571476	23078.084152	8038.519855
16	-12561.252832	-20687.910580	21763.374948	7630.198794
17	-15022.383792	-23633.232372	24392.793356	8446.840916
18	-15432.717880	-24124.287116	24830.861978	8583.267916
19	-14202.152400	-22651.626221	23516.152774	8174.946855
20	-14575.748633	-23141.672069	23955.230293	8303.332146
21	-13345.183153	-21669.011173	22640.521089	7895.011085
22	-16663.283360	-25596.948012	26145.571182	8991.588977
23	-15806.314112	-24614.332964	25269.939497	8711.653207
24	-16216.648201	-25105.387709	25708.008119	8848.080207
25	-14986.082721	-23632.726813	24393.298915	8439.759145
26	-17447.213680	-26578.048605	27022.717323	9256.401268
27	-13129.335947	-21208.539062	-20776.857792	7567.468191
28	-12615.154398	-20618.970033	-20187.288763	7399.506729
29	-12595.713636	-20674.293309	21219.518199	7555.183657
30	-12081.532088	-20084.724281	20694.139187	7387.222195
31	-13129.234660	-21208.437657	-20776.756387	7567.465859
32	-12615.053112	-20618.868628	-20187.187358	7399.504397
33	-12595.612349	-20674.191904	21219.619604	7555.181326
34	-12081.430801	-20084.622876	20694.240592	7387.219864
35	-13599.694139	-21797.199417	-21365.518147	7726.355565
36	-13066.071828	-21262.953665	21745.805883	7714.071032
37	-13599.592852	-21797.098012	-21365.416742	7726.353233
38	-13065.970542	-21262.852260	21745.907288	7714.068700
39	-13499.422437	-19381.938947	22511.872561	7988.414443
40	-12985.240889	-18792.369919	21986.493549	7820.452981
41	-13969.780630	-19970.599303	23038.160245	8147.301817
42	-12315.227093	-20393.479069	21500.332439	7548.726569
43	-11801.045545	-19803.910040	20974.953428	7380.765107
44	-12785.585285	-20982.139424	22026.620124	7707.613944

D Prestressing

D.1 Initial prestressing variants

The equivalent prestressing loads of the 3 initial variants are shown in the tables below.

Table 57: Variant 1: Prestressing loads (per 23 m segment)

q_1	1.714	kN/m
P_{V1}	13.843	kN
P_{H1}	60.537	kN
P_{V2}	13.843	kN
P_{H2}	60.537	kN
P_{q1}	-746	kN
M_{PV1}	-19.519	kNm
M_{PV2}	-10.812	kNm
M_{PH1}	37.115	kNm
M_{PH2}	37.115	kNm
M_{Pq1}	-162	kNm

Table 58: Variant 2: Prestressing loads (per 23 m segment)

q_1	3.588	kN/m
q_2	17.743	kN/m
q_3	17.743	kN/m
P_{V1}	-23.143	kN
P_{H1}	57.627	kN
P_{V2}	-23.143	kN
P_{H2}	57.627	kN
P_{q3}	8.553	kN
M_{PV1}	32.631	kNm
M_{PV2}	18.075	kNm
M_{Pq3}	2.012	kNm

Table 59: Variant 3: Prestressing loads (per 23 m segment)

q_1	6.958	kN/m
q_2	35.486	kN/m
q_3	35.486	kN/m
P_{H1}	124.200	kN
P_{H2}	124.200	kN
P_{q3}	3.903	kN
M_{PH1}	77.917	kNm
M_{PH2}	77.917	kNm
M_{Pq3}	215	kNm

D.2 Prestressing Property Calculations

This section describes how the tendon layout was parameterized to be used in the Maple optimization. The scripts used is shown in Appendix E section E.10 and E.11.

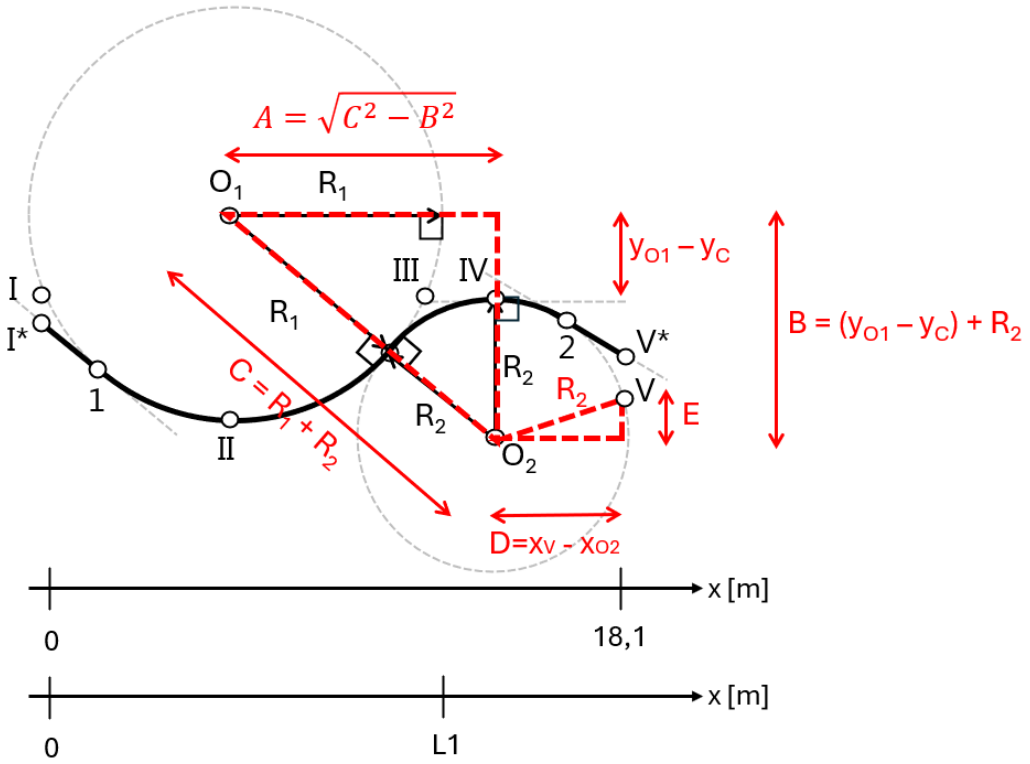

Figure 89: Radii calculation details

D.2.1 Transition curve radii

The calculations of the radius and location of the transition curve, are based on:

- The radius R_1 and the location of the center of (x_{O1},y_{O1}).
- The point IV on the top of the transition curve being fixed on the top edge of the prestressing tendon bound, meaning y_{IV} = hmax.
- The x-coordinate x_V is equal to 18,1 m, as this point is on the right edge of the relieving platform.
- The y-coordinate y_V, which is the point where the transition curve intersects with the edge of the relieving platform, does not become less than 0. Once this coordinate reaches 0, the radius R_2 will start increasing while the point V stays fixed.

Then using these properties together with the properties of two intersection circles (shown in Figure 89), the center of curve 2 (x_{O2},y_{O2}) and R_2 can be calculated. The same method is used for the transition curve on the other side, but using a mirrored approach.

D.2.2 Linear segment

Figure 90 shows the variables used to calculate the linear segment at the end of each curve. The main calculation is made using the property of lines that are tangent to a circle. The line from the center point O1 to the intersection point (x_1,y_1) and the tangent line are perpendicular to each other. This means two triangles can be drawn as shown in Figure 90, that have the same proportions. Then using the known variables, the P_1 and Q_1 values can be calculated. The values for P_1 and Q_1 can then be used to determine the coordinate of point I* (x_{I*},y_{I*}) and of the intersection point 1 (x_1,y_1). The known variables used are:

- The length of the diagonal edge of the small triangle is equal to 1 m (being the linear segment).

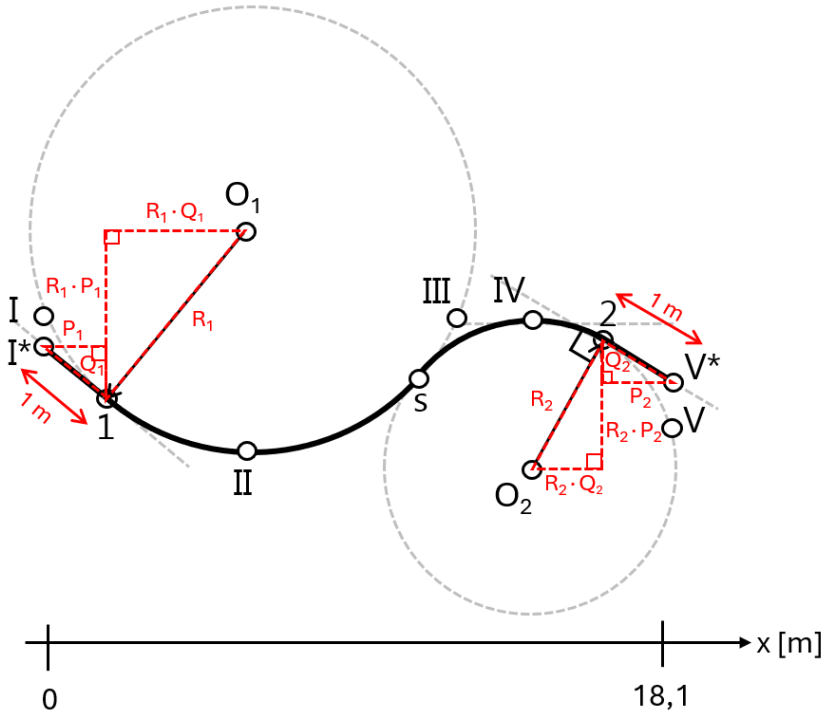

Figure 90: Radii calculation straight length

- The length of the diagonal edge of the large triangle is equal to R_1 (radius of circle 1).
- The x-coordinate x_I is equal to zero, as this point is located at the start of the relieving platform.
- The coordinates of the center of circle 1.

The same method is used for the linear segment on the other side and for the case where there is also a transition curve on the left side.

D.2.3 Prestressing variants

For variant 1 of section 5.2 there is only one curve, namely curve 1. This curve is centered at the middle of the relieving platform, meaning x_{O2} is at 18,1/2 = 9,05 m. The height of the curve center point is at $y_{O2} = R_1$. The parameter L_1 then varies between the case where the end points of the curve, point I and point V, are at the top boundary hmax and the case where these points are at the middle of the floor. The Maple script is shown in section E.10.

Variant 2 also has the main curve 1 centered around the middle of the relieving platform. The variant starts from the point where point I and V are at the edges at the top boundary, but then varies by making L_1 smaller introducing two transition curves on each side. The Maple script is shown in section E.10.

Variant 3 uses the same transition curves as variant 2 does, but the only difference is that now the left transition curve 3, is fixed above the first two supports, respectively the combi wall and the anchor. This means that the center of the main curve XO1 is now no longer in the middle of the relieving platform. Rather the point is in the middle of the length L1. The Maple script is shown in section E.11.

E Scripts

The scripts made in Python and Maple are included in this appendix.

E.1 Python: Initial analysis

```
import pandas as pd
import numpy as np
import scipy as sp
import matplotlib.pyplot as plt
import anastruct as ast
from anastruct import SystemElements
```

Structure geometry

```
ss = SystemElements()

#Defining system parameters

#Spring constants
kA = 5100*1000 #kN/m
kB = 626*1000  #kN/m
kC = 1843*1000 #kN/m
kD = 1838*1000 #kN/m

#Defining nodes and elements
ss.add_element(location=[[0, 0], [0.361, 0]], EA=None, EI=1.102*10**8)
ss.add_element(location=[[0.361, 0], [0.790, 0]], EA=None, EI=1.102*10**8)
ss.add_element(location=[[0.790, 0], [12.909, 0]], EA=None, EI=1.102*10**8)
ss.add_element(location=[[12.909, 0], [15.909, 0]], EA=None, EI=1.102*10**8)

#Defining the supports
ss.add_support_spring(node_id=1,translation=2,k=kA)
ss.add_support_spring(node_id=2,translation=2,k=kB)
ss.add_support_spring(node_id=4,translation=2,k=kC)
ss.add_support_spring(node_id=5,translation=2,k=kD)
```

```
#Applying the loads
def SolveStructure(loads,show=False):

    #Loads
    q_selfweight = -loads[0] #kN/m
    q_floor = -loads[1] #kN/m
    q_total = q_selfweight + q_floor #kN/m

    MA = -loads[2]    #kNm
    FVA = -loads[3]   #kN
    FHA = loads[4]   #kN
    MB = -loads[5]    #kNm
    FVB = -loads[6]   #kN
    FHB = loads[7]   #kN
    MC = loads[8]    #kNm
    FVC = -loads[9]   #kN
    FHC = loads[10]  #kN
    MD = loads[11]   #kNm
    FVD = -loads[12]  #kN
    FHD = loads[13]  #kN

    #Distributed
    ss.q_load(element_id=[1,2], q=q_selfweight)
    ss.q_load(element_id=[3, 4], q=q_total)

    #Support A
    ss.moment_load(node_id=1, Ty=MA)
    ss.point_load(node_id=1, Fy=FVA)

    #Support B
    #ss.moment_load(node_id=3, Ty=MB)
    ss.point_load(node_id=2, Fy=FVB)

    #Support C
    ss.moment_load(node_id=4, Ty=MC)
    #ss.point_load(node_id=4, Fy=FVC)

    #Support D
    ss.moment_load(node_id=5, Ty=MD)
    ss.point_load(node_id=5, Fy=FVD)

    ss.solve()

    if show:
        ss.show_structure(scale=0.6)
        ss.show_bending_moment(scale=0.6)
        ss.show_displacement(scale=0.6)
        ss.show_reaction_force(scale=0.6)

    max_m = []
    ele_result_m = ss.get_element_result_range('moment','both')
    for ele in ele_result_m:
        max_m.append(max(ele,key=abs))

    return max_m
```

```
loads_basic = pd.read_excel("Loads basic.xlsx")
```

ULS Loads

```
loads_combinations_UGT = pd.read_excel("UGT Load Combinations.xlsx")
loads_basic_np = loads_basic.to_numpy()
loads_combinations_UGT_np = loads_combinations_UGT.to_numpy()
```

```
UGT_loads = np.zeros((14,loads_combinations_UGT_np.shape[0]))
n=0
for UGT_n in range(loads_combinations_UGT_np.shape[0]):
    if(UGT_n % 12 == 0):
        n +=1
    print(f'UGT {n}.{UGT_n %12 +1} ({UGT_n})')
    for case_n in range(22):
       #print(loads_combinations_np[UGT_n,case_n])
       UGT_loads[:,UGT_n] += loads_basic_np[:,case_n]*loads_combinations_UGT_np[UGT_n,case_n]
    print(UGT_loads[:,UGT_n])
```

Solve structure

```
Max_moments = []
for i in range(112):
    Max_moments.append(SolveStructure(UGT_loads[:,i]))
```

```
df_UGT = pd.DataFrame(Max_moments, columns=['Element 1', 'Element 2', 'Element 3', 'Element 4'])
```

```
df_UGT
```

SLS loads

```
loads_combinations_BGT = pd.read_excel("BGT Load Combinations.xlsx")
loads_combinations_BGT_np = loads_combinations_BGT.to_numpy()
```

```
BGT_names = ["BGT 1.1", "BGT 1.2","BGT 1.3", "BGT 2.1", "BGT 2.2", "BGT 2.3", "BGT 2.4", "BGT 2.5", "BGT 2.6", "BGT 2.7",
```

```
BGT_loads = np.zeros((14,loads_combinations_BGT_np.shape[0]))

for BGT_n in range(loads_combinations_BGT_np.shape[0]):
    print(f'{BGT_names[BGT_n]} ({BGT_n})')
    for case_n in range(22):
       BGT_loads[:,BGT_n] += loads_basic_np[:,case_n]*loads_combinations_BGT_np[BGT_n,case_n]
    print(BGT_loads[:,BGT_n])
```

Solve structure

```
Max_moments = []
for i in range(loads_combinations_BGT_np.shape[0]):
    Max_moments.append(SolveStructure(BGT_loads[:,i]))

df_BGT = pd.DataFrame(Max_moments, columns=['Element 1', 'Element 2', 'Element 3', 'Element 4'])

df_BGT
```

E.2 Maple: Moment resistance module

```
ULS_MRd  := module ()
# This module is used to calculate the ULS Bending Moment resistance

     export  MRdCheck , CheckHorForceEq  ,PrestressingStrains  ;

     CheckHorForceEq  :=proc(sigmapu_ ,sigmapminf_ ,Nst,Nsb,xu_,b_,Ned_,Pminf_,Ap_)
          # Check the horizontal force equilibrium, considered to be equal (within a range of 50.000, otherwise iterations would need to be too small.
          # If there is no equilibrium, define the change to the compression zone height (dx is positive
          # or negative depending on which part is larger)
          local  dx:
          local  DeltaNp :=Ap_*(sigmapu_ -sigmapminf_ ):
          local  Nc := -0.75*xu_*b_*35/1.5:
          #print(  DeltaNp + Nsb + Nst + Nc + Pminf_ - Ned_):
          #print(  DeltaNp,Nsb,Nst,Nc, Pminf_, Ned_):
          if xu_  < 0 then
               dx :=10:
               return false, dx:
          elif  DeltaNp  + Nsb  + Nst  + Nc  + Pminf_  - Ned_  > 50000   then
               dx:=1:

               return  false,dx:
          elif    DeltaNp  + Nsb  + Nst  + Nc  + Pminf_  - Ned_  < -50000  then
               dx:=-1:
               return  false,dx:
          else
               return  true:
          end if:
     end proc:

     PrestressingStrains   := proc(xu_, dp_, dsb_, dst_, sigmapminf_ )
          # Calculate the strain of the prestressing tendon and the reinforcement, based on the calculated compression zone height xu
          local  Ep,epsiloncu ,epsilonst ,epsilonsb ,epsilonpinf ,Deltaepsilonp  ,epsilonp ;
          Ep := 195000 ;
          epsiloncu  := -0.0035 : # Assumption for the concrete strain at failure
          epsilonst  := (xu_ - dst_)/xu_*epsiloncu ;
          epsilonsb  := (xu_ - dsb_)/xu_*epsiloncu ;
          epsilonpinf  := sigmapminf_ /Ep;
          Deltaepsilonp  :=  (xu_ - dp_)/xu_*epsiloncu ;
          epsilonp  := epsilonpinf  + Deltaepsilonp  ;
          return  epsilonp ,epsilonst ,epsilonsb ;
     end proc:

     MRdCheck :=proc(h_,Ap_,dp_,Ned_,M_,props,printVar :=false)
          # Calculate the MRd. Due to the application of prestressing, finding the correct compression zone height xu becomes an iterative process.
          local  cnom, cappb, cappt, Asb_, ysb, phisb, Ast_, yst, phist, phistir, fyd, Es, Asb, dsb, Ast, dst, Ap, dp, M, Ned, fck, fcd, fpk, fp0_1k, fpd, sigmapu , epsilonuk ,
Ep, sigmapminf , Pminf , b, alpha , xu, HorEq , epsilonp , epsilonst , epsilonsb , sigmast , sigmasb , dx, deff , delta , f, rotCap , DeltaNp , Nc, Nst, Nsb, MRd;

          cnom  := props[1]:
          cappb  := props[2]:
          cappt  := props[3]:
          Asb_  := props[4]:
          ysb  := props[5]:
          phisb  := props[6]:
          Ast_  := props[7]:
          yst  := props[8]:
          phist  := props[9]:
          phistir  := props[10]:

          fyd:=435:
          Es:=200000 :

          if M_ > 0 then
               Asb:=Asb_:
               dsb:=h_ -ysb:

               Ast:=Ast_:
               dst:=yst:

               Ap:=Ap_:
               dp:=dp_:
               M:=M_:
          elif M_ < 0 then
               Asb:=Ast_:
               dsb:=h_ -yst:

               Ast:=Asb_:
               dst:=ysb:

               Ap:=Ap_:
               dp:=h_ - dp_:
               M:=-M_:
          end if:

          Ned:=Ned_:

          fck:=35:
          fcd:=(fck)/(1.5):
          fpk:=1860:
          fp0_1k  :=0.9*fpk:
          fpd:=fp0_1k/(1.1):
          sigmapu :=fpd:
          epsilonuk :=0.035 :

          Ep:=195000 :
          sigmapminf :=1200 :
          Pminf :=sigmapminf *Ap:

          b:=1000 :
          alpha :=0.75 :

          xu:=((Asb*fyd)+Ap*(fpd-sigmapminf )+sigmapminf *Ap - Ned - Ast*fyd)/((alpha*fcd*b)):
```

```
#`Check the horizontal force equilibirum ===================================`
     HorEq:=false:
     while HorEq = false do
          #Finding the compression zone height
          #f:=((fpk/(1.1)-sigmapminf)*Ap+fyd*Asb)/(Ap+Asb):
          epsilonp:=PrestressingStrains  (xu,dp,dsb,dst,sigmapminf)[1]:
          epsilonst:=PrestressingStrains  (xu,dp,dsb,dst,sigmapminf)[2]:
          epsilonsb:=PrestressingStrains  (xu,dp,dsb,dst,sigmapminf)[3]:

          sigmast:=min(max(epsilonst*Es,-fyd),fyd):
          sigmasb:=min(max(epsilonsb*Es,-fyd),fyd):

          if epsilonp>fpd/(Ep) then
               sigmapu:=fpd+((epsilonp-fpd/(Ep))/(epsilonuk-fpd/(Ep)))*(1691-fpd):
          else
               sigmapu:=epsilonp*Ep:
          end if:
          if CheckHorForceEq (sigmapu,sigmapminf,Ast*sigmast,Asb*sigmasb,xu,b,Ned_,Pminf,Ap)[1]=false then
               HorEq:=false:
               dx:=CheckHorForceEq (sigmapu,sigmapminf,Ast*sigmast,Asb*sigmasb,xu,b,Ned_,Pminf,Ap)[2]:
               xu:=xu + dx:

          else
               HorEq:=true:
          end if:
     end do:

     # Check if the prestressing tendon is within the tensile zone or not. This changes the
     if xu < dp then
          deff := (Ap*dp + Asb*dsb)/(Ap + Asb);
     else
          deff := dsb;
     end if:

     #Rotational capacity check
     delta := 1; #No redestribution
     f:=((fpk/(1.1)-sigmapminf)*Ap+fyd*Asb)/(Ap+Asb):
     if xu/deff < delta - f/(500 + f) then
          rotCap := true;
     else
          rotCap := false;
     end if;

     # Calculating the final MRd
     #epsilonst := PrestressingStrains(xu, dp, dsb, dst, sigmapminf)[2];
#    epsilonsb := PrestressingStrains(xu, dp, dsb, dst, sigmapminf)[3];
     DeltaNp := (sigmapu - sigmapminf)*Ap;
     Nc := -0.75*xu*b*fcd;
     Nst := Ast*sigmast;
     Nsb := Asb*sigmasb;
     MRd := -(Nc*(h_/2 - 0.39*xu) + DeltaNp*(h_/2 -dp) + Nsb*(h_/2-dsb) + Nst*(h_/2 - dst));
     print("MRd:", MRd, "kN");

     # Print statements
     if printVar then
          print("Asb, dsb, Ast, dst,Ap,dp,Ned"   , Asb, dsb, Ast, dst, Ap, dp, Ned);
          print("deff:", deff);
          print("xu:", xu);
          print("Nc:", Nc);
          print("Nst:", Nst);
          print("Nsb:", Nsb);
          print("DeltaNp:", DeltaNp);
          if rotCap = true then
               print("Rotational capacity Ok"  );
          else
               print("Rotational capacity not OK"  );
          end if:
     end if;

     if  M/(MRd)>1 then
          print("[ULS MRd] bending moment resistance, u.c.:"    ,M/(MRd)):
          return [false,xu]:
     else
          print("[ULS MRd] bending moment resistance, u.c.:"    ,M/(MRd)):
     return [true,xu]:
     end if:
end proc;

end module:
```

E.3 Maple: Shear resistance module

```
ULS_Shear :=module ()

     export   ShearResistanceNoRein  , ShearResistanceWithRein  ,CheckShear :

     ShearResistanceNoRein  :=proc(h_,b_,d_,f_ck,kl_,sigma_cp ,Ap_,Asl_,printVar )
          #Calculating the VRdc
          local k_ := 1 + sqrt(200/d_);
          local Ac := d_*b_;
          local rhol :=  (Asl_ + Ap_)/Ac;
          local kl := 0.15;

          local vmin := evalf(0.035*k_^(3/2)*sqrt(f_ck) + kl*sigma_cp );
          local vRdc := evalf(0.12*k_*(100*rhol*f_ck)^(1/3) + kl*sigma_cp );

          if printVar  then
              print("&sigma;_cp:" , sigma_cp );
              print("&rho;l: " , rhol);
              print("Asl_: " , Asl_);
              print("vmin " , vmin);
              print("vRdc " , vRdc);
              print("d_:", d_);
          end if;
          return max(vmin, vRdc);
     end proc:

     ShearResistanceWithRein  :=proc(b_,d_,f_ck,sigma_cp ,M,h_,N_,M_,phistir ,Sstir ,printVar )
          #Calculating VRds
          local phi_bgl , A_sw, c_bgl, s, z, fyd, theta_, vl, alpha_cw , fctd, VRds, VRdmax;

          phi_bgl  := phistir;
          A_sw := 4*(phi_bgl/2)^2*Pi;
          c_bgl := 90;
          s := Sstir;
          z := 0.9*d_;
          fyd := 435;
          theta_ := 39;
          vl := 0.6*(1 - f_ck/250);
          alpha_cw := 1 + sigma_cp/(f_ck/1.5);
          fctd := 1.5;


          VRds := evalf(A_sw*z*fyd*cot(theta_*Pi/180)/s);
          VRdmax := evalf(alpha_cw*b_*z*vl*f_ck/1.5/(cot(theta_*Pi/180) + tan(theta_*Pi/180)));
          if printVar  then
              print("VRds " , VRds);
              print("VRdmax " , VRdmax);
          end if:

          return min(evalf(VRds), VRdmax):
     end proc:

     CheckShear :=proc(h_,VEd,N,Ap,M_,d_p,props,xu,printVar :=false)
          local cnom, cappb, cappt, Asb, ysb, phisb, Ast, yst, phist, phistir, Sstir, d_sl, A_sl, d_p_, b_, Ap_, P_minf, d_, f_ck, CRdc, sigma_cp , VRd;

          cnom := props[1]:
          cappb := props[2]:
          cappt := props[3]:
          Asb := props[4]:
          ysb := props[5]:
          phisb := props[6]:
          Ast := props[7]:
          yst := props[8]:
          phist := props[9]:
          phistir := props[10]:
          Sstir := props[11]:

          #Check whether the moment is positive or negative, this changes which reinforcement is used.
          if M_<0 then
               d_sl:=h_-yst:
               A_sl:=Ast:
               d_p_ :=h_-d_p:
          else
               d_sl:=h_ - ysb:
               A_sl:=Asb:
               d_p_:=d_p:
          end if:

          b_ := 1000;
          Ap_ := Ap;
          P_minf := 1200*Ap_;
          # Assumption that only the prestressing below (1/2)h contributes to the shear resistance
          if xu < d_p_ then
              d_ := evalf((A_sl*d_sl + Ap_*d_p_)/(A_sl + Ap_));
          else
              d_ := d_sl;
              Ap_ := 0;
          end if:

          f_ck := 35;
          CRdc := 0.18/1.5;

          sigma_cp := min((P_minf - N)/(b_*h_), 0.2*f_ck/1.5);

          VRd:=evalf(ShearResistanceNoRein  (h_,b_,d_,f_ck,kl,sigma_cp ,Ap_,A_sl,printVar )*b_*d_):

          if VEd/(VRd)>=1 then
               print("[ULS VRd,c] Without shear reinforcement u.c.:"     ,VEd/(VRd)):
               VRd:=ShearResistanceWithRein  (b_,d_,f_ck,sigma_cp ,M_,h_,N,M_,phistir ,Sstir ,printVar ):
               print("[ULS VRd,s] With shear reinforcement u.c.:"     ,VEd/(VRd));
          else
               print("[ULS VRd,c] Without reinforcement u.c.:"     ,VEd/(VRd)):
               print("[ULS VRd,s] With reinforcement u.c.:"    ,VEd/(ShearResistanceWithRein  (b_,d_,f_ck,sigma_cp ,M_,h_,N,M_,phistir ,Sstir ,printVar ))):
          end if:

          if printVar  then
               print("dP: ",d_p_):
               end if:

          return VEd/(VRd):
     end proc:

end module:
```

E.4 Maple: Crack width module

```
SLS_CrackWidths :=module ()

     export EffReinforcement ,EffArea , XiPrestressing , CompressionZoneHeight , SLSCheck :

     EffReinforcement :=proc(A_s_,A_p_, xi_1_, Ac_eff_);
          #Calculating the effective reinforcement
          local rhop_eff_:=(A_s_+A_p_*xi_1_)/(Ac_eff_):
          return rhop_eff_:
     end proc:

     EffArea := proc(h_, d_, x_, b_)
          local hc_eff;
          hc_eff := min(2.5*(h_ - d_), 1/3*h_ - 1/3*x_, 1/2*h_);
          return b_*hc_eff;
     end proc:

     XiPrestressing := proc(phi_s_, phi_p_)
          local xi_, xi_1_; xi_ := 0.5;
          if 0 < phi_p_ then
               xi_1_ := sqrt(xi_*phi_s_/phi_p_);
          else xi_1_ := 0;
          end if;
          return xi_1_;
     end proc:

     CompressionZoneHeight :=proc(h_,b_,P_minf_,M_,N_,d_st_,d_sb_,d_p_,E_cm_,E_s_,E_p_,xi_1_,A_st_,A_sb_,A_p_)
          #Calculating the compression zone height from the equllibrium of forces and moments
          local epsilon_st , epsilon_sb , Deltaepsilon_p , N_c, N_st, N_sb, DeltaN_p , varphi , f_ck, f_cd, E_c, eq1, eq2, e_1, e_2, e_3, e_4, sol_x, x_sol, epsilon_c_sol , x,
epsilon_c ;
          epsilon_st :=epsilon_c *(x-d_st_)/(x):
          epsilon_sb :=epsilon_c *(d_sb_-x)/(x):
          Deltaepsilon_p :=epsilon_c *(d_p_-x)/(x):
          N_c :=(E_c*epsilon_c )*x*b_*17/2:
          N_st:=epsilon_st *E_s_*A_st_:
          N_sb:=epsilon_sb *E_s_*A_sb_:
          DeltaN_p := xi_1_*Deltaepsilon_p *E_p_*A_p_:
          varphi:=1.4:
          f_ck:=35: f_cd:=f_ck/(1.5):
          E_c:=(E_cm_)/((1+varphi));

          eq1:=P_minf_-N_+DeltaN_p - N_st- N_c+N_sb=0:
          eq2:=M_=N_c*e_1+N_st*e_2- N_sb *e_3+N_*((h_)/(2))-P_minf_*((h_)/(2))-DeltaN_p *e_4:
          e_1:=h_-x/(3):e_2:=h_-d_st_:e_3:=h_-d_sb_:e_4:=h_-d_p_:
          sol_x:=solve({eq1,eq2,0 < x, x < 5000,epsilon_c >0},{x,epsilon_c }): assign(sol_x):
          x_sol:=x:
          epsilon_c_sol :=epsilon_c :
          x:='x':
          epsilon_c :=epsilon_c :
          return x_sol,epsilon_c_sol :
     end proc:

     SLSCheck :=proc(Ap_,d_p_,h_,M_,N_,props,printVar:=false)
          local E_p, E_cm, E_s, alpha_e, k1, k2, k3, k4, cnom, cappb, cappt, Asb, ysb, phisb, Ast, yst, phist, phistir, d_sb, d_st, d_p, A_st, A_sb, phi_sb, M, kx, c, d_first,
A_p, b_, phi_p, sigma_pminf, P_minf_, xi_1, CompressionZone , x_, epsilon_c , d_eff, phi_eq, Ac_eff, rhop_eff, kt, f_ctm, Deltaepsilon_p , Deltasigma_p , sr_max,
epsilonsm_epsiloncm , w_, wmax, uc_SLS;


          E_p:=195000:
          E_cm:=34000:
          E_s:=200000:
          alpha_e:=E_p/(E_cm):
          k1:=0.8:
          k2:=0.5:
          k3:=3.4:
          k4:=0.425:

          cnomb:=props[1]:cappb:=props[2]:cappt:=props[3]:Asb:=props[4]:ysb:=props[5]:phisb:=props[6]:Ast:=props[7]:yst:=props[8]:phist:=props[9]:phistir:=props[10]:cnomt:=
props[12]:
          if M_ > 0 then
               d_sb:=h_-ysb:
               d_st:=yst:
               d_p:=d_p_: #`Calculated in the prestressing properties`
               A_st:=Ast: A_sb:=Asb: phi_sb:=phisb: M:=M_:
               kx := cappb/cnomb;
               c := cappb + phistir : # The cover on the longitudinal reinforcement
               d_first := h_ - (cappb + phistir + phisb/2):
          else
               d_sb:=h_-yst: #`The top reinforcement, but in the case of a negative moment`
               d_st:=ysb: #`The bottom reinforcement, but in the case of a negative moment`
               d_p:=h_-d_p_: #`Calculated in the prestressing properties`
               A_st:=Asb:
               A_sb:=Ast:
               phi_sb:=phist:
               M:=-M_: #`Make it positive, since the cross-section is turned around`
               kx := cappt/cnomt;
               c := cappt + phistir : # The cover on the longitudinal reinforcement
               d_first := h_ - (cappt + phistir + phist/2):
          end if:

          A_p := Ap_;
          b_ := 1000;
          phi_p := evalf(1.6*sqrt(A_p));
          sigma_pminf := 1200;
          P_minf_ := sigma_pminf*A_p;
          xi_1 := XiPrestressing(phi_sb, phi_p);
```

```
1
2           CompressionZone   := CompressionZoneHeight  (h_, b_, P_minf_, M, N_, d_st, d_sb, d_p, E_cm, E_s, E_p, xi_1, A_st, A_sb, A_p);
3           x_ := CompressionZone [1];
4           epsilon_c  := CompressionZone [2];
5
6           d_eff  := A_sb*d_sb*1/A_sb;
7           phi_eq  := phi_sb;
8           Ac_eff  := EffArea (h_, d_eff, x_, b_);
9           rhop_eff  := EffReinforcement  (A_sb, 0, xi_1, Ac_eff);
10
11          kt  := 0.4;
12          f_ctm  := 3.2;
13          Deltaepsilon_p   :=  (d_first  - x_)*epsilon_c /x_;
14          Deltasigma_p   := Deltaepsilon_p *E_p;
15
16          sr_max  := k3*c + k1*k2*k4*phi_eq /rhop_eff ;
17          epsilonsm_epsiloncm   := max((Deltasigma_p  - kt*f_ctm*(alpha_e*rhop_eff  + 1)/rhop_eff )/E_p, 0.6*Deltasigma_p /E_p);
18          w_  := evalf (epsilonsm_epsiloncm  *sr_max);
19          wmax  := 0.2*kx;
20          uc_SLS  := w_/wmax;
21
22          if printVar   then
23               print("x: ",x_):
24               print("&epsilon;_c: "  ,epsilon_c ):
25               print("Ac_eff: " ,evalf (Ac_eff)):
26               print("&rho;p_eff: " ,evalf (rhop_eff )):
27               print("d_p: " ,evalf (d_p)):
28               print("d_st: " ,evalf (d_st)):
29               print("d_sb: " ,evalf (d_sb)):
30               print("d_eff: " ,evalf (d_eff)):
31               print("&Delta;&epsilon;_p: "  ,evalf (Deltaepsilon_p )):
32               print("&Delta;&sigma;_p: "  ,evalf (Deltasigma_p )):
33               print("&epsilon;sm_&epsilon;cm"  ,evalf (epsilonsm_epsiloncm  )):
34               print("sr_max" ,evalf (sr_max )):
35          end if:
36          print("w_:",w_ ,"mm"):
37          print("[SLS cracks] Crack width u.c.:"   ,uc_SLS  ):
38          return  uc_SLS :
39      end proc:
40
41  end module:
```

E.5 Maple: Reinforcement properties module

```
> ReinforcementProp := proc(ϕstir := 16, Sstir := 300)
  cnom := 55 :
  cappb := 90 :
  cappt := 85 :

  Asb := 25133 :
  ϕsb := 40 :
  ysb := cappb + (3· ϕsb + 40 + 40)/2 + ϕstir :
      # The average of the three layers (and the transverse bars in between)

  Ast := 3272 :
  ϕst := 25 :
  yst := cappt + ϕstir + evalf(ϕst/2) :
  return [cnom, cappb, cappt, Asb, ysb, ϕsb, Ast, yst, ϕst, ϕstir, Sstir]
  end proc:
```

E.6 Maple: Solve ODE module

```
> SolveODE := proc( )
  local DE1, DE2, DE3, DE4, DE5, sol1;
  DE1 := EI * (diff(w1(x), x$4)) = q_total + piecewise(x_s1 - 1.41 ≥ x > 0, qP_R3, x_s1
      - 1.41 ≤ x < 0.361, -qP_R1);
  DE2 := EI * (diff(w2(x), x$4)) = q_total + piecewise(x_s1 - 1.41 > x > 0.361, qP_R3, x_s1
      - 1.41 ≤ x < 0.790, -qP_R1);
  DE3 := EI * (diff(w3(x), x$4)) = q_total + q_floor + piecewise(x_s1 - 1.41 > x, qP_R3,
      x_s1 - 1.41 < x < x_s2 - 1.41, -qP_R1, x ≥ x_s2 - 1.41, qP_R2);
  DE4 := EI * (diff(w4(x), x$4)) = q_total + q_floor + piecewise(12.909 < x < x_s2 - 1.41,
      -qP_R1, 15.909 > x ≥ x_s2 - 1.41, qP_R2);
  DE5 := EI * (diff(w5(x), x$4)) = q_total + q_floor ;
  sol1 := dsolve({DE1, DE2, DE3, DE4, DE5}, {w1(x), w2(x), w3(x), w4(x), w5(x)}) :
  return sol1;
  end proc:
```

E.7 Maple: Main Optimization module

▶ **Module imports**

Load combinations

```
> #This matrix is used to reduce the selfweight load matrix. The load matrix will be adjusted to automatically do this.
```

$$Loads_SW_Reduction := \begin{bmatrix} 0 \\ (1.75-h)\cdot 23\cdot 25 \\ 0 \\ 0 \\ 0 \\ 0 \\ 0 \\ 0 \\ 0 \\ 0 \\ 0 \\ -\frac{0.781^2}{2}\cdot((1.75-h)\cdot 23\cdot 25) \\ 0.781\cdot(1.75-h)\cdot 23\cdot 25 \\ 0 \end{bmatrix} :$$

$$> Loads_Matrix_Selfweight := \begin{bmatrix} 1006 \\ 0 \\ -3098 \\ 8187 \\ 0 \\ 0 \\ 0 \\ 0 \\ 0 \\ 0 \\ 0 \\ -307 \\ 786 \\ 0 \end{bmatrix} - Loads_SW_Reduction :$$

$$> Loads_Matrix_SLS_1_3 := \begin{bmatrix} 0 \\ 3381 \\ -10377 \\ 2530 \\ -17314 \\ 0 \\ -5151 \\ -5151 \\ -1768 \\ 0 \\ -1384 \\ -7196 \\ 8023 \\ -4167 \end{bmatrix} + Loads_Matrix_Selfweight :$$

```
> Loads_Matrix_ULS_3_12 := [0, 6127, −35405, 7590, −27282, 0, −12713.8, −12713.8, −3552, 0, −2600, −14932, 16172, −6438.8] + Loads_Matrix_Selfweight·1.2 :
```

Normal forces, calculated as described in the thesis.

```
> N_SLS := [737.450741813196, 518.845388018623, 518.845388018623, 205.934391874275, 387.108304917753] :
  N_ULS := [1159.339534, 937.5259061, 937.5259061, 397.5829022, 677.5307283] :
> springs := [2549.75·1000, 311.08·1000, 942.29·1000, 939.83·1000, 10.78·1000, 311.17·1000, 262.32·1000, 272.18·1000] :
```

INPUT

```
> h_start := 1.75 : L1_start := 11 : L1_stop := 18.1 : Ap := 4500 :
  ReinforcementProperties := ReinforcementProp(16, 300) : #First value represents the stirrup diameter, the second the c.t.c distance
> ytop := CalcY(ReinforcementProperties)[1]; ybot := CalcY(ReinforcementProperties)[2];
> LoadCombSLS := Loads_Matrix_SLS_1_3 :
> LoadCombULS := Loads_Matrix_ULS_3_12 :
> LoadCombSW := Loads_Matrix_Selfweight :
> LoadCombinations := Array([LoadCombSLS, LoadCombULS, LoadCombSW]) :
> kVA := springs[1] : kVB := springs[2] : kVC := springs[3] : kVD := springs[4] :
> h_list := Array(1..300) : h_opt := Array(1..300) :
> L1_list := Array(1..300) : L1_opt := Array(1..300) :
```

Solve the ODE

```
> solutionODE := SolveODE( ) : assign(solutionODE) :
> w1 := w1(x) : w2 := w2(x) : w3 := w3(x) : w4 := w4(x) : w5 := w5(x) :
  phi1 := −(diff(w1, x)) : phi2 := −(diff(w2, x)) : phi3 := −(diff(w3, x)) : phi4 := −(diff(w4, x)) : phi5 := −(diff(w5, x)) :
  kappa1 := (diff(phi1, x)) : kappa2 := (diff(phi2, x)) : kappa3 := (diff(phi3, x)) : kappa4 := (diff(phi4, x)) : kappa5 := (diff(phi5, x)) :
  M1 := EI·kappa1 : M2 := EI·kappa2 : M3 := EI·kappa3 : M4 := EI·kappa4 : M5 := EI·kappa5 :
  V1 := diff(M1, x) : V2 := diff(M2, x) : V3 := diff(M3, x) : V4 := diff(M4, x) : V5 := diff(M5, x) :
> x := 0 : eq1 := M1 = MA + MP_1 − MP_q3 + Mp_kink1 + MP_PV1 : eq2 := V1 = kVA * w1 − FVA − P_V1 − P_Vq3 − p_kink1 :
  x := 0.361 : eq3 := ϕ1 = ϕ2 : eq4 := w1 = w2 : eq5 := M1 = M2 + MB : eq6 := kVB * w1 − FVB = −(V1) + (V2) :
  x := 0.79 : eq7 := M2 = M3 : eq8 := V2 = V3 : eq9 := ϕ2 = ϕ3 : eq10 := w2 = w3 :
  x := 12.909 : eq11 := phi3 = phi4 : eq12 := w3 = w4 : eq13 := M3 = M4 + MC : eq14 := kVC * w3 − FVC = −(V3) + (V4) :
  x := x_2 − 1.41 : eq15 := ϕ4 = ϕ5 : eq16 := w4 = w5 : eq17 := M4 = M5 : eq18 := −p_kink2 = −(V4) + (V5) :
  x := 15.909 : eq19 := M5 = MD + MP_2 + MP_PV2 : eq20 := V5 = −kVD * w5 + FVD + P_V2 :
  x := 'x':
```

Creating Element arrays to be used in the loop

```
> ElementBounds := [[0, 0.361], [0.361, 0.790], [0.790, 12.909], [12.909, x_2 − 1.41], [x_2 − 1.41, 15.909]] :
> Moments := [M1, M2, M3, M4, M5] :
> ShearForces := [V1, V2, V3, V4, V5] :
```

MAIN LOOP

```
> h := h_start : L1 := L1_start :
  PrestrProps := Array(1..300) : # 300 here is an arbitrary high number, to ensure the array is large enough to store all data.

  #Store the moments
  MaxMoments_SLS := Array(1..300, 1..5) :
  MaxMoments_SLS_coord := Array(1..300, 1..5) :
  MaxMoments_ULS := Array(1..300, 1..5) :
  MaxMoments_ULS_coord := Array(1..300, 1..5) :

  #Store the moments
  MaxShear_ULS := Array(1..300, 1..5) :
  MaxShear_ULS_coord := Array(1..300, 1..5) :

  #Store moments for the selfweight case
  MaxMoments_SW := Array(1..300, 1..5) :
  MaxMoments_SW_coord := Array(1..300, 1..5) :
  MinMoments_SW := Array(1..300, 1..5) :
  MinMoments_SW_coord := Array(1..300, 1..5) :
```

```
ind := 1 :

################################Start of the main loop#####################################
while L1 ≤ L1_stop do
  print("L1:", L1) : print("h:", h) :
  EI := 12000·(1/12·23000·(h·1000)^3)·10^-6·10^-3 :
  #Determine the tendon path based on L1 and h
 PrestrProps[ind] := CalcPresPath(L1, h, ReinforcementProperties) :

  # Determing the loads that result form the path and prestressing force P_23m
 ploads := CalcPrestrLoads([PrestrProps[ind]], Ap) :
#=======================Calculate the governing ULS, SLS and SW combinations=======================
  for LoadComb in LoadCombinations do
    q_total := LoadComb[1] :
    q_floor := LoadComb[2] :
    MA := LoadComb[3] :
    FVA := LoadComb[4] :
    FHA := LoadComb[5] :
    MB := LoadComb[6] :
    FVB := LoadComb[7] :
    FHB := LoadComb[8] :
    MC := LoadComb[9] :
    FVC := LoadComb[10] :
    FHC := LoadComb[11] :
    MD := LoadComb[12] :
    FVD := LoadComb[13] :
    FHD := LoadComb[14] :

    if LoadComb = LoadCombSW then
    #Because at t=0 the laod is assumed to be at P_Max
    Pmax := 1/0.8 :
    else
    Pmax := 1 :
    end if:

     P_V1 := ploads[1]·Pmax :
    P_H1 := ploads[2]·Pmax :
    P_V2 := ploads[3]·Pmax :
    P_H2 := ploads[4]·Pmax :
    P_Vq3 := ploads[5]·Pmax :
    qP_R1 := ploads[6]·Pmax :
    qP_R2 := ploads[7]·Pmax :
    qP_R3 := ploads[8]·Pmax :
     MP_1 := ploads[9]·Pmax :
    MP_2 := ploads[10]·Pmax :
    MP_PV1 := ploads[11]·Pmax :
    MP_PV2 := ploads[12]·Pmax :
   MP_q3 := ploads[13]·Pmax :

     x_1 := PrestrProps[ind][11];
    x_2 := PrestrProps[ind][15];
    x_s1 := PrestrProps[ind][13];
    x_s2 := PrestrProps[ind][14];

   p_kink1 := ploads[14]·Pmax :
   p_kink2 := ploads[15]·Pmax :
   Mp_kink1 := p_kink1·(x_1 − 1.41) :

    # Solving the constants of the general solutions of the ODEs
    sol_constants := solve({eq1, eq2, eq3, eq4, eq5, eq6, eq7, eq8, eq9, eq10, eq11, eq12, eq13, eq14, eq15, eq16, eq17, eq18, eq19, eq20},
{_C1, _C2, _C3, _C4, _C5, _C6, _C7, _C8, _C9, _C10, _C11, _C12, _C13, _C14, _C15, _C16, _C17, _C18, _C19, _C20}) :
    assign(sol_constants) :

   #SLS LOADS----------------------------------------------------------------------------------------------------------------------------------------------------
   if LoadComb = LoadCombSLS then
      for i from 1 to 5 do
        MaxMoment := Maximize(Moments[i], x = ElementBounds[i][1]..ElementBounds[i][2]) :
        MaxMoments_SLS[ind, i] := MaxMoment[1] :
       MaxMoments_SLS_coord[ind, i] := MaxMoment[2][1] :
       end do:
     # Determine the maximum sagging moment within the model
      MaxMomTotal := max(MaxMoments_SLS[ind]) :
      max_index_M := Search(MaxMomTotal, MaxMoments_SLS[ind]) :

       print("The maximum sagging moment is [SLS]", MaxMomTotal, "at", MaxMoments_SLS_coord[ind, max_index_M]) :
```

```
    y_tendon := CalcTendonHeight(rhs(MaxMoments_SLS_coord[ind, max_index_M]) + 1.41, PrestrProps[ind]) :
    d_p_ := (h − (y_tendon + ybot)) · 1000 :


#ULS LOADS-----------------------------------------------------------------------------------------------------------------------------------------------------
--
elif LoadComb = LoadCombULS then
  for i from 1 to 5 do
    x := 'x':
    MaxMomentULS := Maximize(Moments[i], x = ElementBounds[i][1]..ElementBounds[i][2]) :
    MaxMoments_ULS[ind, i] := MaxMomentULS[1] :
    MaxMoments_ULS_coord[ind, i] := MaxMomentULS[2][1] :
    end do:

# Determine the maximum sagging moment within the model
  MaxMomTotalULS := max(MaxMoments_ULS[ind]) :
  max_index_Muls := Search(MaxMomTotalULS, MaxMoments_ULS[ind]) :
  print("The maximum sagging moment is [ULS]", MaxMomTotalULS, "at", MaxMoments_ULS_coord[ind, max_index_Muls]) :

  y_tendon_uls := CalcTendonHeight(rhs(MaxMoments_ULS_coord[ind, max_index_Muls]) + 1.41, PrestrProps[ind]) :
  d_p_M := (h − (y_tendon_uls + ybot)) · 1000 :

  # Shear force at 0.79
  x := 0.79 : M_check1 := M3/23 ; V_check1 := V3/23 ; x := 'x':

  y_tendon_V := CalcTendonHeight(0.79 + 1.41, PrestrProps[ind]) :
  d_p_V1 := (h − ( y_tendon_V + ybot)) · 1000 :
  xu_V1 := ULS_MRd:-MRdCheck(h · 1000, Ap, d_p_V1, N_ULS[2] · 1000, M_check1 · 1000 · 1000, ReinforcementProperties, false)[2] :


  print("The shear force V1 is [ULS]", V_check1, "at 0.79") :
  print("The moment force M1 is [ULS]", M_check1, "at 0.79") :
  print("xu_V1:", xu_V1) :

  # Shear force at 12.909
  x := 12.909 : M_check3 := M3/23 ; V_check3 := V3/23 ; M_check4 := M4/23 ; V_check4 := V4/23 ; x := 'x':

  y_tendon_V := CalcTendonHeight(12.909 + 1.41, PrestrProps[ind]) :
  d_p_V3 := (h − ( y_tendon_V + ybot)) · 1000 :
  xu_V3 := ULS_MRd:-MRdCheck(h · 1000, Ap, d_p_V3, N_ULS[2] · 1000, M_check3 · 1000 · 1000, ReinforcementProperties, false)[2] :

  xu_V4 := ULS_MRd:-MRdCheck(h · 1000, Ap, d_p_V3, N_ULS[3] · 1000, M_check4 · 1000 · 1000, ReinforcementProperties, false)[2] :


end if:
unassign('_C1', '_C2', '_C3', '_C4', '_C5', '_C6', '_C7', '_C8', '_C9', '_C10', '_C11', '_C12', '_C13', '_C14', '_C15', '_C16', '_C17', '_C18',
 '_C19', '_C20') :
end do:

#================================================================================== results: VEd max
and M max

 #Performing the resistance checks
  if ULS_Shear:-CheckShear(h · 1000, abs(V_check1 · 1000), N_ULS[2] · 1000, Ap, M_check1 · 1000 · 1000, d_p_V1,
ReinforcementProperties, xu_V1, false) < 1
 and ULS_Shear:-CheckShear(h · 1000, abs(V_check3 · 1000), N_ULS[2] · 1000, Ap, M_check3 · 1000 · 1000, d_p_V3,
ReinforcementProperties, xu_V3, false) < 1
 and ULS_Shear:-CheckShear(h · 1000, abs(V_check4 · 1000), N_ULS[3] · 1000, Ap, M_check4 · 1000 · 1000, d_p_V3,
ReinforcementProperties, xu_V4, false) < 1

  and SLS_CrackWidths:-SLSCheck(Ap, d_p_, h · 1000, (MaxMomTotal · 1000 · 1000)/23, N_SLS[max_index_M] · 1000,
ReinforcementProperties, false) < 1

  and ULS_MRd:-MRdCheck(h · 1000, Ap, d_p_M, N_ULS[max_index_Muls] · 1000, MaxMomTotalULS · 1000 · 1000/23,
ReinforcementProperties, false)[1] then

  OptimalSOL := L1, h :
  h_opt[ind] := h :
  L1_opt[ind] := L1 :

  print("------------------------------> All checks OK! <------------------------------") :
```

```
        h := h − 0.01 :
      else
      L1 := L1 + 0.1 :
      if ind = 1 then
        h_opt[ind] := h :
       L1_opt[ind] := L1 :
      else
      h_opt[ind] := h_opt[ind − 1] :
       L1_opt[ind] := L1_opt[ind − 1] :
       end if:
     end if:
  x ='x':
   h_list[ind] := h :
    L1_list[ind] := L1 :
   ind := ind + 1 :
     # Clearing the constants, which will be recalculated in the next iteration
     print("----------------------------------------------------------------------------------------------------------------------------------------------------------------
    ") :
 end do :
 ##########################################End of the main loop##########################################
```

(1)

E.8 Maple: SLS compression zone height calculation - Rectangular cross-section

```
> restart;
> with(RealDomain) :
> ε_st := ε_c·(x − d_st)/x :
> ε_sb := ε_c·(d_sb − x)/x :
> Δε_p := ε_c·(d_p − x)/x :
> N_c := (E_c·ε_c)·x·b·1/2 :
> N_st := ε_st·E_s·A_st :
> N_sb := ε_sb·E_s·A_sb :
> ΔN_p := ξ_1·Δε_p·E_p·A_p :
> M := (2000)·1000·1000 : N := (800)·1000 :
> A_p := 4500 : A_st := 3272 : A_sb := 25134 :
> d_p := 600 : d_st := 113.5 : d_sb := 994 :
> ξ_1 := 0.51335 :
> P_minf := 1200·A_p;
> φ := 1.4 :
> h := 1200 : b := 1000 :
> f_ck := 35 : f_cd := f_ck/1.5 :
> E_p := 195000 : E_s := 200000 : E_cm := 34000 : E_c := f_ck/(1.75·10^(−3)); E_c := E_cm/(1 + φ);
> eq1 := P_minf − N + ΔN_p − N_st − N_c + N_sb = 0 :
> eq2 := M = N_c·e_1 + N_st·e_2 − N_sb ·e_3 + N·(h/2) − P_minf·(h/2) − ΔN_p·e_4 :
> e_1 := h − x/3; e_2 := h − d_st; e_3 := h − d_sb; e_4 := h − d_p;
> sol1 := solve({eq1, eq2}, {x, ε_c});
```

E.9 Maple: SLS compression zone height calculation - Cross-section opening

```
> restart;
> with(RealDomain) :
> hf := 355 : #Top flange
  bopen := 400 : #Opening width
  c_a := 430 : #Centroidal axis of the cross-section
> ε_c2 := ε_c·(x − hf)/x :
> ε_st := ε_c·(x − d_st)/x :
> ε_sb := ε_c·(d_sb − x)/x :
> Δε_p := ε_c·(d_p − x)/x :
> N_c := (E_c·ε_c)·x·b·1/2 :
> N_c2 := (E_c·ε_c2)·(x − hf)·bopen·1/2 : # if xu > hft
> N_st := ε_st·E_s·A_st :
> N_sb := ε_sb·E_s·A_sb :
> ΔN_p := ξ_1·Δε_p·E_p·A_p :
> M := (233)·1000·1000 : N := (0)·1000 :
> A_p := 4500 : A_st := 25133 : A_sb := 3272 :
> d_p := 357.909 : d_st := 210 : d_sb := 772.5 :
> ξ_1 := 0.40585 :
> P_minf := A_p·1200 :
> φ := 1.4 :
> h := 890 : b := 1000 :
> f_ck := 35 : f_cd := f_ck/1.5 :
> E_p := 195000 : E_s := 200000 : E_cm := 34000 : E_c := f_ck/(1.75·10^−3); E_c := E_cm/(1 + φ);
> eq1 := P_minf − N + ΔN_p − N_st − N_c + N_c2 + N_sb = 0 :
> eq2 := M = N_c·e_1 + N_st·e_2 − N_sb·e_3 + N·(h − c_a) − P_minf·(h − c_a) − ΔN_p·e_4 − N_c2·e_5 :
> e_1 := h − x/3; e_2 := h − d_st; e_3 := h − d_sb; e_4 := h − d_p; e_5 := h − ((x − hf)/3 + hf);
> sol1 := solve({eq1, eq2}, {x, ε_c});
```

E.10 Maple: Tendon layout parameterization - Var 1/2

```
> restart;
> with(plots) :
> with(LinearAlgebra) :
> with(plottools) :
> with(VectorCalculus ) :
```

Calculating tendon paths, curved edge

```
> CalcY :=proc(props)
  #Calculating the minimum distance of the center of the tendon from respectively the top and bottom edge of the floor
  local ytop, ybot :
  ytop := 0.24765 + props[10]/1000 :
  ybot := 0.33765 + props[10]/1000 :
  return ytop, ybot :
  end proc:
```

Calculating the minimum radius

```
> CalcMinR1 :=proc(l1, hmax_)
  local M, V, x_abc, r :
  M := Matrix([[2·((18.1 − l1)/2), 2·hmax_, 1], [2·(18.1/2), 2·0, 1], [2·((18.1 + l1)/2), 2·hmax_, 1]]) :
  V := Matrix([[−((18.1 − l1)/2)^2 − hmax_^2], [−(18.1/2)^2 − 0^2], [−((18.1 + l1)/2)^2 − hmax_^2]]) :
  x_abc := LinearSolve(M, V, method='LU') :
  r := sqrt(x_abc[1]^2 + x_abc[2]^2 − x_abc[3]) :
  return r :
  end proc:
```

Circle 1

```
> CircleRad1 :=proc(l1, r1, hmax_)
  # Calculating the curve properties based on the length parameter L1, the radius r1 and the maximum height c
  # Returns the center of the circle and the y coordinate of the top edge of the tendon
  local xo1, yo1, yiii :
  xo1 := 18.1/2 :
  yo1 := r1 :
  yiii := hmax_ :
  return(xo1, yo1, yiii) :
  end proc:
```

Cricle 2

```
> CircleRad2 := proc(r1, r2, xo1, yo1, yiii)
  # Calculating the properties of transition curve 2 based on r1, r2 and the center of curve 1
  local b, c, a, xo2, yo2, d_, e, xv, yv, xs;

  b := (yo1 − yiii) + r2 :
  c := r1 + r2 :
  a := sqrt(c^2 − b^2) :
  xo2 := xo1 + a :
  yo2 := yo1 − b :
  d_ := 18.1 − xo2 :
  e := sqrt(r2^2 − d_^2) :
  xv := 18.1 : yv := yo2 + e :
  xs := xo1 + r1/(r1 + r2)·a :
  return(r2, xo2, yo2, xv, yv, xs) :
  end proc:
> CircleRad3 := proc(r1, r3, xo1, yo1, yiii)
  # Calculating the properties of transition curve 3 based on r1, r2 and the center of curve 1
  local b, c, a, xo3, yo3, d_, e, xi, yi, xs1;

  b := (yo1 − yiii) + r3 :
```

```
c := r1 + r3 :
a := sqrt(c^2 - b^2) :
xo3 := xo1 - a :
yo3 := yo1 - b :
d_ := xo3 :
e := sqrt(r3^2 - d_^2) :
xi := 0 : yi := yo3 + e :
xs1 := xo1 - r1/(r1 + r3)·a :
return(r3, xo3, yo3, xi, yi, xs1) :
end proc:
> CircleRad22 := proc(r1_, xo1_, yo1_, yiii_)
# Calculating the properties of transition curve 2 based on r1, and curve 1 properties
local yv, xv, eq1_, eq2_, eq3_, eq4_, r2_, xo2_, yo2_, xs_, ys_, sol3 :
yv := 0 :
xv := 18.1 :
yo2_ := yiii_ - r2_ :
eq1_ := (xs_ - xo1_)^2 + (ys_ - yo1_)^2 = r1_^2 :
eq2_ := (xs_ - xo2_)^2 + (ys_ - yo2_)^2 = r2_^2 :
eq3_ := (xv - xo2_)^2 + (yv - yo2_)^2 = r2_^2 :
eq4_ := r1_ + r2_ = sqrt((xo2_ - xo1_)^2 + (yo2_ - yo1_)^2) :

sol3 := solve({eq1_, eq2_, eq3_, eq4_}, {r2_, xo2_, xs_, ys_}) : assign(sol3[1]) :
yo2_ := yiii_ - r2_:
return(r2_, xo2_, yo2_)
end proc:
> CircleRad32 := proc(r1_, xo1_, yo1_, yiii_)
# Calculating the properties of transition curve 3 based on r1, and curve 1 properties
local yi, xi, eq1_, eq2_, eq3_, eq4_, r3_, xo3_, yo3_, xs1_, ys1_, sol3 :
yi := 0 :
xi := 0 :
yo3_ := yiii_ - r3_ :
eq1_ := (xo1_ - xs1_)^2 + (yo1_ - ys1_)^2 = r1_^2 :
eq2_ := (xs1_ - xo3_)^2 + (ys1_ - yo3_)^2 = r3_^2 :
eq3_ := (xo3_ - xi)^2 + (yo3_ - yi)^2 = r3_^2 :
eq4_ := r1_ + r3_ = sqrt((xo1_ - xo3_)^2 + (yo1_ - yo3_)^2) :

sol3 := solve({eq1_, eq2_, eq3_, eq4_}, {r3_, xo3_, xs1_, ys1_}) : assign(sol3[1]) :
yo3_ := yiii_ - r3_ :
return(r3_, xo3_, yo3_)
end proc:
```

Calculating the left linear segment

```
> CalcLeftLin := proc(r1_, xo1_, yo1_)
# Calculating the left linear segment
local a_1, b_1, c_1, Q1plus, Q1minus, P1minus, P1plus, yi_, xi_, x_1, y_1;

a_1 := (r1_^2 + 1) : b_1 := -2·r1_·xo1_ : c_1 := (xo1_)^2 - 1 :
Q1plus := (-b_1 + sqrt(b_1^2 - 4·a_1·c_1)) / (2·a_1) :
Q1minus := (-b_1 - sqrt(b_1^2 - 4·a_1·c_1)) / (2·a_1) :
P1minus := sqrt(1 - Q1minus^2) : P1plus := sqrt(1 - Q1plus^2) :
yi_ := yo1_ - P1minus·r1_ + Q1minus :
xi_ := xo1_ - Q1minus·r1_ - P1minus :
x_1 := evalf(P1minus) :
y_1 := r1_ - P1minus·r1_ :
return (xi_, yi_, x_1, y_1)
end proc:
> CalcRightLin := proc(r1_, xo1_, yo1_)
# Calculating the right linear segment
local a_2, b_2, c_2, Q2plus, Q2minus, P2minus, P2plus, yv_, xv_, x_2, y_2;

a_2 := (r1_^2 + 1) : b_2 := -2·r1_·xo1_ : c_2 := (xo1_)^2 - 1 :
Q2plus := (-b_2 + sqrt(b_2^2 - 4·a_2·c_2)) / (2·a_2) :
Q2minus := (-b_2 - sqrt(b_2^2 - 4·a_2·c_2)) / (2·a_2) :
P2minus := sqrt(1 - Q2minus^2) : P2plus := sqrt(1 - Q2plus^2) :
yv_ := yo1_ - P2minus·r1_ + Q2minus :
xv_ := xo1_ + Q2minus·r1_ + P2minus :
x_2 := 18.1 - P2minus;
y_2 := r1_ - P2minus·r1_ :
return (xv_, yv_, x_2, y_2)
end proc:
> CalcLeftLin2 := proc(r1_, xo1_, yo1_)
local a_1, b_1, c_1, Q1plus, Q1minus, P1minus, P1plus, yi_, xi_, x_1, y_1;
```

```
a_1 := (r1_^2 + 1) : b_1 := -2·r1_·xo1_ : c_1 := (xo1_)^2 - 1 :
Q1plus := (-b_1 + sqrt(b_1^2 - 4·a_1·c_1)) / (2·a_1) :
Q1minus := (-b_1 - sqrt(b_1^2 - 4·a_1·c_1)) / (2·a_1) :
P1minus := sqrt(1 - Q1minus^2) : P1plus := sqrt(1 - Q1plus^2) :
yi_ := yo1_ + P1minus·r1_ - Q1minus :
xi_ := xo1_ - Q1minus·r1_ - P1minus :
x_1 := evalf(P1minus) :
y_1 := yo1_ + P1minus·r1_:
return (xi_, yi_, x_1, y_1)
end proc:
```

Calculating based on length L1

```
> Calc_PropGreater181 :=proc(l1, h_, props)
  # Procedure that calculates the properties of the tendon when L1 is greater than 18.1
  local r1, r2, r3, Circ1, xo1, yo1, xo2, yo2, xo3, yo3, LeftLinSeg, x_i_, y_i_, x_1, y_1, RightLinSeg, xv_, yv_, x_2, y_2, x_s1, x_s2, ytop, ybot,
      hmax;

  ytop := CalcY(props)[1] : ybot := CalcY(props)[2] :
  hmax := h_ - ytop - ybot :

  r1 := CalcMinR1(l1, hmax) :
  r2 := 0 :
  r3 := 0 :

  Circ1 := CircleRad1(l1, r1, hmax) :
  xo1 := Circ1[1] :
  yo1 := Circ1[2] :
  xo2 := 0 :
  yo2 := 0 :
  xo3 := 0 :
  yo3 := 0 :

  LeftLinSeg := CalcLeftLin(r1, xo1, yo1) :
  x_i_ := LeftLinSeg[1] : y_i_ := LeftLinSeg[2] :
  x_1 := LeftLinSeg[3] : y_1 := LeftLinSeg[4] :

  RightLinSeg := CalcRightLin(r1, xo1, yo1) :
  xv_ := RightLinSeg[1] : yv_ := RightLinSeg[2] :
  x_2 := RightLinSeg[3] : y_2 := RightLinSeg[4] :
  x_s1 := x_1 :
  x_s2 := x_2 :
  return(xo1, yo1, xo2, yo2, xo3, yo3, r1, r2, r3, hmax, x_1, y_1, x_s1, x_s2, x_2, y_2, x_i_, y_i_, xv_, yv_, ytop, ybot, h_) :
  end proc:
> Calc_PropSec :=proc(l1, h_, props)
  # Procude that calculates the tendon layout properties in the case
  local ytop, ybot, hmax, r1, r2, r3, x_2, y_2, x_1, y_1, Circ1, xo1, yo1, xo2, yo2, xo3, yo3, x_i_, y_i_, xv_, yv_, eq1, eq2, eq3, sol2, eq1_3,
      eq2_3, eq3_3, sol3, x_s1, x_s2;

  ytop := CalcY(props)[1] : ybot := CalcY(props)[2] :

  hmax := h_ - ytop - ybot :

  r1 := CalcMinR1(l1, hmax);
  r2 := 0 :
  r3 := 0 :
  x_2 :='x_2':
  y_2 :='y_2':
  x_1 :='x_1':
  y_1 :='y_1':

  Circ1 := CircleRad1(l1, r1, hmax) :
  xo1 := Circ1[1] :
  yo1 := Circ1[2] :
  xo2 := 0 :
  yo2 := 0 :
  xo3 := 0 :
  yo3 := 0 :

  x_i_ := 0 :
  y_i_ := hmax :
  xv_ := 18.1 :
  yv_ := hmax :

  eq1 := (x_2 - xo1)^2 + (yo1 - y_2)^2 = r1^2 :
  eq2 := (xv_ - x_2)^2 + (yv_ - y_2)^2 = 1^2 :
  eq3 := x_2 < 18.1 :
```

```
sol2 := solve({eq1, eq2, eq3}, {x_2, y_2}); assign(sol2) :

 eq1_3 := (x_1 − xo1)^2 + (yo1 − y_1)^2 = r1^2 :
 eq2_3 := (x_i_ − x_1)^2 + (y_i_ − y_1)^2 = 1^2 :
 eq3_3 := x_1 < 18.1 :
sol3 := solve({eq1_3, eq2_3, eq3_3}, {x_1, y_1}); assign(sol3) :
 x_s1 := x_1 :
 x_s2 := x_2 :

 return(xo1, yo1, xo2, yo2, xo3, yo3, r1, r2, r3, hmax, x_1, y_1, x_s1, x_s2, x_2, y_2, x_i_, y_i_, xv_, yv_, ytop, ybot, h_) :
 end proc:
> Calc_PropMain := proc(l1, h_, props)
 local ytop, ybot, hmax, r1, r2, r3, Circ1, xo1, yo1, yiii, Circle2, xo2, yo2, yv, x_s2, Circle3, xo3, yo3, yi, x_s1, a_2, b_2, c_2, Q2plus,
     Q2minus, P2minus, P2plus, xv_, yv_, x_2, y_2, a_3, b_3, c_3, Q3plus, Q3minus, P3minus, P3plus, x_i_, y_i_, x_1, y_1, Circ2,
     Circle22, Circ3, LeftLinSeg, Circle32;

ytop := CalcY(props)[1] : ybot := CalcY(props)[2] :
hmax := h_ − ytop − ybot :

 # Initial curve properties, will be checked according to several conditions and changed accordingly
 r1 := CalcMinR1(l1, hmax);
 r2 := 3.5 :
 r3 := 3.5 :
 Circ1 := CircleRad1(l1, r1, hmax) :
 xo1 := Circ1[1] :
 yo1 := Circ1[2] :
 yiii := Circ1[3] :
 Circle2 := CircleRad2(r1, r2, xo1, yo1, yiii);
xo2 := Circle2[2] : yo2 := Circle2[3] : yv := Circle2[5] : x_s2 := Circle2[6] :
 Circle3 := CircleRad3(r1, r3, xo1, yo1, yiii);
xo3 := Circle3[2] : yo3 := Circle3[3] : yi := Circle3[5] : x_s1 := Circle3[6] :

 # Calculating the linear segment of the right transition curve 2
a_2 := (r2^2 + 1) : b_2 := −2·r2·(18.1 − xo2) : c_2 := (18.1 − xo2)^2 − 1 :
Q2plus := (−b_2 + sqrt(b_2^2 − 4·a_2·c_2)) / (2·a_2) :
Q2minus := (−b_2 − sqrt(b_2^2 − 4·a_2·c_2)) / (2·a_2) :
P2minus := sqrt(1 − Q2minus^2) : P2plus := sqrt(1 − Q2plus^2) :
xv_ := xo2 + (Q2minus)·r2 + P2minus :
yv_ := yo2 + P2minus·r2 − (Q2minus) :
x_2 := 18.1 − P2minus :
y_2 := P2minus·r2 + yo2 :

 # Calculating the linear segment of the left transition curve 3
a_3 := (r3^2 + 1) : b_3 := −2·r3·(xo3) : c_3 := (xo3)^2 − 1 :
 Q3plus := (−b_3 + sqrt(b_3^2 − 4·a_3·c_3)) / (2·a_3) :
Q3minus := (−b_3 − sqrt(b_3^2 − 4·a_3·c_3)) / (2·a_3) :
 P3minus := sqrt(1 − Q3minus^2) : P3plus := sqrt(1 − Q3plus^2) :
x_i_ := 0 :
y_i_ := yo3 + P3minus·r3 − (Q3minus) :
x_1 := P3minus :
y_1 := P3minus·r3 + yo3 :

 if (yv_ > hmax) then
 x_2 := (18.1 + l1)/2 :
 y_2 := hmax :
 r2 := 0 :
 xv_ := 18.1 :
 yv_ := hmax :
 x_s2 := x_2 :
 end if:

 if (y_i_ > hmax) then
 x_1 := (18.1 − l1)/2 :
 y_1 := hmax :
 r3 := 0 :
 x_i_ := 0 :
 y_i_ := hmax :
 x_s1 := x_1 :
 end if:

 if (yv < 0) or (Im(yv) > 0) then

     #This checks if the yv is below 0 and has to be fixed from this point, varying r2. The Imaginary part, is a check that when the circle
```

```
        with radius R2
    # equals 3.5 does not touch the edge of the floor anymore, the yv is no longer negative
    Circ2 := CircleRad22(r1, xo1, yo1, yiii) :
     r2 := Circ2[1] :
     xo2 := Circ2[2] :
     yo2 := Circ2[3] :
     a_2 := (r2^2 + 1) : b_2 := -2·r2·(18.1 - xo2) : c_2 := (18.1 - xo2)^2 - 1 :
    Q2plus := (-b_2 + sqrt(b_2^2 - 4· a_2·c_2)) / (2· a_2) :
    Q2minus := (-b_2 - sqrt(b_2^2 - 4· a_2·c_2)) / (2· a_2) :
    P2minus := sqrt(1 - Q2minus^2) : P2plus := sqrt(1 - Q2plus^2) :
    xv_ := xo2 + (Q2minus)·r2 + P2minus :
    yv_ := yo2 + P2minus·r2 - (Q2minus) :
    x_2 := 18.1 - P2minus :
    y_2 := P2minus·r2 + yo2 :
    Circle22 := CircleRad2(r1, r2, xo1, yo1, yiii); #xs can become imaginary in circrad22, therefore this method is used to calcualte x_s
     x_s2 := Circle22[6]
      end if:

     if (yi < 0) or (Im(yi) > 0) then

        #This checks if the yi is below 0 and has to be fixed from this point, varying r3. The Imaginary part, is a check that when the circle
        with radius R3
    #equals 3.5 does not touch the edge of the floor anymore, the yv is no longer negative
     Circ3 := CircleRad32(r1, xo1, yo1, yiii) :
     r3 := Circ3[1] :
     xo3 := Circ3[2] :
     yo3 := Circ3[3] :
     LeftLinSeg := CalcLeftLin2(r3, xo3, yo3) :
    x_i_ := LeftLinSeg[1] : y_i_ := LeftLinSeg[2] :
    x_1 := LeftLinSeg[3] : y_1 := LeftLinSeg[4] :
    Circle32 := CircleRad3(r1, r3, xo1, yo1, yiii); #xs can become imaginary in circrad32, therefore this method is used to calcualte x_s
     x_s1 := Circle32[6] :
      end if:

     if x_1 < 1 and y_i_ = hmax then
     return Calc_PropSec(l1, h_, props) :
     else
     return (xo1, yo1, xo2, yo2, xo3, yo3, r1, r2, r3, hmax, x_1, y_1, x_s1, x_s2, x_2, y_2, x_i_, y_i_, xv_, yv_, ytop, ybot, h_) :
     end if:
     end proc:
```

Plotting path

```
> CalcYIntersect :=proc(xo, yo, x_s, r_)
  # A procedure that calcualtes the specific angle theta on the circle at what point based on a point on that circle.
   local eq1, sol, y_s, theta_;
   eq1 := (x_s - xo)^2 + (y_s - yo)^2 = r_^2 :
  sol := solve({eq1, y_s < 2, y_s > 0}, {y_s}) :
   y_s := rhs(sol[1]) :

    theta_ := arctan((y_s - yo)/(x_s - xo)) :

   if x_s - xo < 0 then
      theta_ := theta_ + Pi :
   elif x_s - xo > 0 and y_s - yo < 0 then
      theta_ := theta_ + 2 * Pi :
   end if:
   return theta_ :
   end proc:
> PlotDiagram := proc(xo1, yo1, xo2, yo2, xo3, yo3, r1, r2, r3, hmax, x_1, y_1, x_s1, x_s2, x_2, y_2, x_i_, y_i_, xv_, yv_, ytop, ybot, h_, l1,
       x_t := -10, y_t := -10)
   # Procedure to plot the specific prestressing tendon layout

   local v1, v2, vs1, vs2, s1, s2, s3, s4, p_t, d1, d2, rectw, rectf, htop, hbot, hwall, theta1_1, theta1_2, theta3_1, theta3_2, theta2_1, theta2_2, c1,
        c2, c3, arr1, arr2, texarr, tex, diagram;

   v1 := line([x_1, -(1.75 - hmax)/2], [x_1, 1.75 - (1.75 - hmax)/2], linestyle = dot, color = red) :
   v2 := line([x_2, -(1.75 - hmax)/2], [x_2, 1.75 - (1.75 - hmax)/2], linestyle = dot, color = red) :
   vs1 := line([x_s1, -(1.75 - hmax)/2], [x_s1, 1.75 - (1.75 - hmax)/2], linestyle = dot, color = red) :
  vs2 := line([x_s2, -(1.75 - hmax)/2], [x_s2, 1.75 - (1.75 - hmax)/2], linestyle = dot, color = red) :

   s1 := point([1.41, -ybot - 0.15], color = black, symbol = circle, symbolsize = 15) :
```

```
s2 := point([1.771, -ybot - 0.15], color = black, symbol = circle, symbolsize = 15) :
s3 := point([14.319, -ybot - 0.15], color = black, symbol = circle, symbolsize = 15) :
s4 := point([17.319, -ybot - 0.15], color = black, symbol = circle, symbolsize = 15) :
p_t := point([x_t, y_t], color = red, symbol = solidbox , symbolsize = 10) :
d1 := line([0, y_i_], [x_1, y_1], thickness = 3) :
d2 := line([x_2, y_2], [xv_, yv_], thickness = 3) :
rectw := rectangle([0, -ybot], [2.2, 2], color = white) :
rectf := rectangle([2.2, -ybot], [18.1, hmax + ytop], color = white) :
htop := line([0, hmax], [18.1, hmax], color = black, linestyle = dot) :
hbot := line([0, 0], [18.1, 0], color = black, linestyle = dot) :
hwall := line([-0.5, 2], [2.7, 2], color = black, linestyle = dot) :

theta1_1 := CalcYIntersect(xo1, yo1, x_s1, r1) :
theta1_2 := CalcYIntersect(xo1, yo1, x_s2, r1) :
if r3 > 0 then
theta3_1 := CalcYIntersect(xo3, yo3, x_1, r3) :
theta3_2 := CalcYIntersect(xo3, yo3, x_s1, r3) :
else
theta3_1 := 0 :
theta3_2 := 0 :
end if:

if r2 > 0 then
theta2_1 := CalcYIntersect(xo2, yo2, x_s2, r2) :
theta2_2 := CalcYIntersect(xo2, yo2, x_2, r2) :
else
theta2_1 := 0 :
theta2_2 := 0 :
end if:

c1 := arc([xo1, yo1], r1, theta1_1 ..theta1_2, color = blue, thickness = [3]) :
c2 := arc([xo2, yo2], r2, theta2_1 ..theta2_2, color = red, thickness = [3]) :
c3 := arc([xo3, yo3], r3, theta3_1 ..theta3_2, color = red, thickness = [3]) :


arr1 := arrow([xo1 - l1/2, 1.8], [xo1 + l1/2, 1.8], 0.005, 0.1, 0.02, double_arrow) :
arr2 := arrow([xo1 + l1/2, 1.8], [xo1 - l1/2, 1.8], 0.005, 0.1, 0.02, double_arrow) :
texarr := textplot([xo1, 1.9 , cat("L1")], 'align' = 'above', 'font' = ["times", "roman", 14]) :

tex := textplot([9.05, -1.3 , cat("L1 = ", l1 , "m", " h = ", h_, "m")], 'align' = 'above', 'font' = ["times", "roman", 16]) :

diagram := display(c1, c2, c3, rectw, rectf, htop, hbot, hwall, s1, s2, s3, s4, p_t, d1, d2, tex, texarr, arr1, arr2, view = [-6..24, -2..2], scaling
    = constrained, size = [1400, 560], axes = none) :#-1,19
return diagram :
end proc:
> CalcTendonLength :=proc(xo1, yo1, xo2, yo2, xo3, yo3, r1, r2, r3, hmax, x_1, y_1, x_s1, x_s2, x_2, y_2, x_i_, y_i_, xv_, yv_, ytop, ybot, h_)
# Procedure to calculate the length of the tendon, used for the CO2 calculations.
local theta1_1, theta1_2, theta3_1, theta3_2, theta2_1, theta2_2, LC1, LC2, LC3, LD1, LD2;

theta1_1 := CalcYIntersect(xo1, yo1, x_s1, r1) :
theta1_2 := CalcYIntersect(xo1, yo1, x_s2, r1) :
if r3 > 0 then
theta3_1 := CalcYIntersect(xo3, yo3, x_1, r3) :
theta3_2 := CalcYIntersect(xo3, yo3, x_s1, r3) :
else
theta3_1 := 0 :
theta3_2 := 0 :
end if:

if r2 > 0 then
theta2_1 := CalcYIntersect(xo2, yo2, x_s2, r2) :
theta2_2 := CalcYIntersect(xo2, yo2, x_2, r2) :
else
theta2_1 := 0 :
theta2_2 := 0 :
end if:

LC1 := r1·(abs(theta1_1 - theta1_2));
LC2 := r2·(abs(theta2_1 - theta2_2));
LC3 := r3·(abs(theta3_1 - theta3_2));

LD1 := sqrt(x_1^2 + (y_i_ - y_1)^2) :
LD2 := sqrt((18.1 - x_2)^2 + (yv_ - y_2)^2) :
```

```
    return LC1 + LC2 + LC3 + LD1 + LD2 :
    end proc:
> CalcPresPath := proc(l1, h_, props)
  # The main procedure, called in the optimization to create the tendon properties.
  if (l1 > 18.1) then CalcPath := Calc_L1_18_1(l1, h_, props) :
   elif (0 ≤ l1 ≤ 18.1) then CalcPath := Calc_PropMain(l1, h_, props) :
  end if:
  return CalcPath :
  end proc:
Calculating the height of the tendon
> CalcTendonHeight :=proc(x_, xo1, yo1, xo2, yo2, xo3, yo3, r1, r2, r3, hmax, x_1, y_1, x_s1, x_s2, x_2, y_2, x_i_, y_i_, xv_, yv_, ytop, ybot,
      h_)
  # Procedure to calcualte the height of the tendon, given a certain location with coordinate x.
  # This is used to determine the tendon height at a specific location
  local solc1, y_c1, solc2, y_c2, solc3, y_c3, solr, y_r, soll, y_l, y_t;

  solc1 := solve((x_ − xo1)^2 + (y_c1 − yo1)^2 = r1^2, y_c1) :
  y_c1 := solc1[2] :
  solc2 := solve((x_ − xo2)^2 + (y_c2 − yo2)^2 = r2^2, y_c2) :
  y_c2 := solc2[1] :
   solc3 := solve((x_ − xo3)^2 + (y_c3 − yo3)^2 = r3^2, y_c3) :
  y_c3 := solc3[1] :
  solr := solve({y_2 = a_r·x_2 + b_r, yv_ = a_r·xv_ + b_r, y_r = a_r·x_ + b_r}, {a_r, b_r, y_r}) :
  y_r := rhs(solr[3]) :
  soll := solve({y_l = a_l·x_1 + b_l, y_i_ = a_l·x_i_ + b_l, y_l = a_l·x_ + b_l}, {a_l, b_l, y_l}) :
  y_l := rhs(soll[3]) :

  if x_ ≤ x_s1 and x_ < x_1 then
  y_t := y_l :
  elif x_ < x_s1 and x_ > x_1 then
  y_t := y_c3 :
   elif x_ > x_s1 and x_ > x_1 and x_ ≤ x_s2 and x_ ≤ x_2 then
 y_t := y_c1 :

  elif x_ > x_s2 and x_ < x_2 then
 y_t := y_c2 :

  elif x_ ≥ x_s2 and x_ ≥ x_2 then
 y_t := y_r :
  end if:

  return y_t
  end proc:
```

E.11 Maple: Tendon layout parameterization - Var 3

```
> restart;
> with(plots) :
> with(LinearAlgebra) :
> with(plottools) :
```

Calculating tendon paths, curved edge

```
> shift := 1.3 :
  shiftR := 0 :
> CalcY := proc(props)
  local ytop, ybot :
  ytop := 0.24765 + props[10]/1000 :
  ybot := 0.33765 + props[10]/1000 :
  return ytop, ybot :
  end proc:
```

Calculating the minimum radius

```
> CalcMinR1 := proc(l1, hmax_)
  local M, V, x_abc, r :
  M := [ 2·(0)        2·hmax_   1
         2·(l1/2)     2·0       1
         2·(l1)       2·hmax_   1 ] :
  V := [ -(0)^2 - hmax_^2
         -(l1/2)^2 - 0^2
         -(l1)^2 - hmax_^2 ] :
  x_abc := LinearSolve(M, V, method = 'LU') :
  r := sqrt(x_abc[1]^2 + x_abc[2]^2 - x_abc[3]) :
  return r :
  end proc:
```

Circle 1

```
> CircleRad1 := proc(l1, r1, hmax_)
  # Calculating the curve properties based on the length parameter L1, the radius r1 and the maximum height c
  # Returns the center of the circle and the y coordinate of the top edge of the tendon
  local xo1, yo1, yiii :

  xo1 := (18.1 + shift - shiftR)/2 :
  yo1 := r1 :
  yiii := hmax_ :
  return(xo1, yo1, yiii) :
  end proc:
```

Cricle 2

```
> CircleRad2 := proc(r1, r2, xo1, yo1, yiii)
  # Calculating the properties of transition curve 2 based on r1, r2 and the center of curve 1
  local b, c, a, xo2, yo2, d_, e, xv, yv, xs, xiv;

  b := (yo1 - yiii) + r2 :
  c := r1 + r2 :
  a := sqrt(c^2 - b^2) :
  xo2 := xo1 + a :
  yo2 := yo1 - b :
  xiv := xo1 + a :
  d_ := 18.1 - xo2 :
  e := sqrt(r2^2 - d_^2) :
  xv := 18.1 : yv := yo2 + e :
  xs := xo1 + r1/(r1 + r2)·a :
  return(r2, xo2, yo2, xv, yv, xs) :
  end proc:
> CircleRad3 := proc(r1, r3, xo1, yo1, yiii)
  # Calculating the properties of transition curve 3 based on r1, r2 and the center of curve 1
  local b, c, a, xo3, yo3, d_, e, xi, yi, xs1;

  b := (yo1 - yiii) + r3 :
  c := r1 + r3 :
  a := sqrt(c^2 - b^2) :
  xo3 := xo1 - a :
```

```
    yo3 := yo1 − b :
    d_ := xo3 :
    e := sqrt(r3^2 − d_^2) :
    xi := 0 : yi := yo3 + e :
    xs1 := xo1 − r1/(r1 + r3) · a :
    return(r3, xo3, yo3, xi, yi, xs1) :
    end proc:
> CircleRad22 := proc(r1_, xo1_, yo1_, yiii_)
  # Calculating the properties of transition curve 2 based on r1, and curve 1 properties
    local yv, xv, eq1_, eq2_, eq3_, eq4_, r2_, xo2_, yo2_, xs_, ys_, sol3 :

    yv := 0 :
    xv := 18.1 :
    yo2_ := yiii_ − r2_:
    eq1_ := (xs_ − xo1_)^2 + (ys_ − yo1_)^2 = r1_^2 :
    eq2_ := (xs_ − xo2_)^2 + (ys_ − yo2_)^2 = r2_^2 :
    eq3_ := (xv − xo2_)^2 + (yv − yo2_)^2 = r2_^2 :
    eq4_ := r1_ + r2_ = sqrt((xo2_ − xo1_)^2 + (yo2_ − yo1_)^2) :

    sol3 := solve({eq1_, eq2_, eq3_, eq4_}, {r2_, xo2_, xs_, ys_}) : assign(sol3[1]) :
    yo2_ := yiii_ − r2_ :
    return(r2_, xo2_, yo2_)
    end proc:
> CircleRad32 := proc(r1_, xo1_, yo1_, yiii_)
    # Calculating the properties of transition curve 3 based on r1, and curve 1 properties
    local yi, xi, eq1_, eq2_, eq3_, eq4_, r3_, xo3_, yo3_, xs1_, ys1_, sol3 :

    yi := yiii_ :
    xi := xo1_:
    yo3_ := yiii_ − r3_:
    eq1_ := (xo1_ − xs1_)^2 + (yo1_ − ys1_)^2 = r1_^2 :
    eq2_ := (xs1_ − xo3_)^2 + (ys1_ − yo3_)^2 = r3_^2 :
    eq3_ := (xo3_ − xi)^2 + (yo3_ − yi)^2 = r3_^2 :
    eq4_ := r1_ + r3_ = sqrt((xo1_ − xo3_)^2 + (yo1_ − yo3_)^2) :

    sol3 := solve({eq1_, eq2_, eq3_, eq4_}, {r3_, xo3_, xs1_, ys1_}) : assign(sol3[1]) :
    yo3_ := yiii_ − r3_:
    return(r3_, xo3_, yo3_)
    end proc:
> CircleRad12 := proc(r1_, r3_, xo3_, yo3_, yiii_)
    local yi, xi, eq1_, eq2_, eq3_, eq4_, eq5_, xo1_, yo1_, xs1_, ys1_, sol3 :

    yi := yiii_ :
    xi := shift :
    yo1_ := r1_:
    eq1_ := (xo1_ − xs1_)^2 + (yo1_ − ys1_)^2 = r1_^2 :
    eq2_ := (xs1_ − xo3_)^2 + (ys1_ − yo3_)^2 = r3_^2 :
    eq3_ := (xo3_ − xi)^2 + (yo3_ − yi)^2 = r3_^2 :
    eq4_ := r1_ + r3_ = sqrt((xo1_ − xo3_)^2 + (yo1_ − yo3_)^2) :
    eq5_ := xo1_ > 0 :

    sol3 := solve({eq1_, eq2_, eq3_, eq4_, eq5_}, {xo1_, xs1_, ys1_}) : assign(sol3[1]) :
    yo1_ := r1_:
    return(r1_, xo1_, yo1_)
    end proc:
```

Calculating the left linear segment

```
> CalcLeftLin := proc(r1_, xo1_, yo1_)
  # Calculating the left linear segment
    local a_1, b_1, c_1, Q1plus, Q1minus, P1minus, P1plus, yi_, xi_, x_1, y_1;

    a_1 := (r1_^2 + 1) : b_1 := −2·r1_·xo1_ : c_1 := (xo1_)^2 − 1 :
    Q1plus := (−b_1 + sqrt(b_1^2 − 4· a_1·c_1)) / (2· a_1) :
    Q1minus := (−b_1 − sqrt(b_1^2 − 4· a_1·c_1)) / (2· a_1) :
    P1minus := sqrt(1 − Q1minus^2) : P1plus := sqrt(1 − Q1plus^2) :
    yi_ := yo1_ − P1minus·r1_ + Q1minus :
    xi_ := xo1_ − Q1minus·r1_ − P1minus :
    x_1 := evalf(P1minus) :
    y_1 := r1_ − P1minus·r1_ :
    return (xi_, yi_, x_1, y_1)
    end proc:
> CalcLeftLin2 := proc(r1_, xo1_, yo1_)
```

```
# Calculating the left linear segment
local a_1, b_1, c_1, Q1plus, Q1minus, P1minus, P1plus, yi_, xi_, x_1, y_1;

a_1 := (r1_^2 + 1) : b_1 := -2·r1_·xo1_ : c_1 := (xo1_)^2 - 1 :
Q1plus := (-b_1 + sqrt(b_1^2 - 4·a_1·c_1)) / (2·a_1) :
Q1minus := (-b_1 - sqrt(b_1^2 - 4·a_1·c_1)) / (2·a_1) :
P1minus := sqrt(1 - Q1minus^2) : P1plus := sqrt(1 - Q1plus^2) :
yi_ := yo1_ + P1minus·r1_ - Q1minus :
xi_ := xo1_ - Q1minus·r1_ - P1minus :
x_1 := evalf(P1minus) :
y_1 := yo1_ + P1minus·r1_ :
return (xi_, yi_, x_1, y_1)
end proc:
> CalcRightLin := proc(r1_, xo1_, yo1_)
# Calculating the right linear segment
local a_2, b_2, c_2, Q2plus, Q2minus, P2minus, P2plus, yv_, xv_, x_2, y_2;

a_2 := (r1_^2 + 1) : b_2 := -2·r1_·xo1_ : c_2 := (xo1_)^2 - 1 :
Q2plus := (-b_2 + sqrt(b_2^2 - 4·a_2·c_2)) / (2·a_2) :
Q2minus := (-b_2 - sqrt(b_2^2 - 4·a_2·c_2)) / (2·a_2) :
P2minus := sqrt(1 - Q2minus^2) : P2plus := sqrt(1 - Q2plus^2) :
yv_ := yo1_ - P2minus·r1_ + Q2minus :
xv_ := xo1_ + Q2minus·r1_ + P2minus :
x_2 := 18.1 - P2minus;
y_2 := r1_ - P2minus·r1_ :
return (xv_, yv_, x_2, y_2)
end proc:
```

Calculating based on length L1

```
> Calc_PropMain := proc(l1, h_, props)
# Procedure to calculate the properties of the prestressing tendon layout
local ytop, ybot, hmax, r1, r2, r3, Circ1, xo1, yo1, yiii, Circle3, xo3, yo3, x_s1, distanceStart, Circle2, xo2, yo2, x_s2, a_2, b_2, c_2, Q2plus,
    Q2minus, P2minus, P2plus, xv_, yv_, x_2, y_2, x_i_, y_i_, x_1, y_1, eq1, eq2, eq3, sol2;

ytop := CalcY(props)[1] : ybot := CalcY(props)[2] :
hmax := h_ - ytop - ybot :

# Initial curve properties, will be checked according to several conditions and changed accordingly
r1 := CalcMinR1(l1, hmax);
r2 := 3.5 :
r3 := 3.5 :
Circ1 := CircleRad1(l1, r1, hmax) :
xo1 := Circ1[1] :
yo1 := Circ1[2] :
yiii := hmax :
Circle3 := CircleRad3(r1, r3, xo1, yo1, yiii);
xo3 := Circle3[2] : yo3 := Circle3[3] : x_s1 := Circle3[6] :

distanceStart := xo3 - shift :
xo3 := xo3 - distanceStart : #=shift
x_s1 := x_s1 - distanceStart :
xo1 := xo1 - distanceStart :

Circle2 := CircleRad2(r1, r2, xo1, yo1, yiii);
xo2 := Circle2[2] : yo2 := Circle2[3] : x_s2 := Circle2[6] :

# Calculating the linear segment of the right transition curve 2
a_2 := (r2^2 + 1) : b_2 := -2·r2·(18.1 - xo2) : c_2 := (18.1 - xo2)^2 - 1 :
Q2plus := (-b_2 + sqrt(b_2^2 - 4·a_2·c_2)) / (2·a_2) :
Q2minus := (-b_2 - sqrt(b_2^2 - 4·a_2·c_2)) / (2·a_2) :
P2minus := sqrt(1 - Q2minus^2) : P2plus := sqrt(1 - Q2plus^2) :
xv_ := xo2 + (Q2minus)·r2 + P2minus :
yv_ := yo2 + P2minus·r2 - (Q2minus) :

if (yv_ > hmax) then
x_2 := xo1 + l1/2 :
y_2 := hmax :
r2 := 0 :
xv_ := 18.1 :
yv_ := hmax :
x_s2 := x_2 :
else
xv_ := 18.1 : yv_ := hmax :
x_2 := xo2 : y_2 := hmax :
```

```
    end if:

    x_i_ := 0 : y_i_ := hmax :
    x_1 := xo3 : y_1 := hmax :

    if xo1 + l1/2 > 17.1 and yv_ = hmax then
    x_2 :='x_2': y_2 :='y_2':
    eq1 := (x_2 - xo1)^2 + (yo1 - y_2)^2 = r1^2 :
    eq2 := (xv_ - x_2)^2 + (yv_ - y_2)^2 = l^2 :
    eq3 := x_2 < 18.1 :
    sol2 := solve({eq1, eq2, eq3}, {x_2, y_2}); assign(sol2) :
    x_s2 := x_2 :
    end if:

    return (xo1, yo1, xo2, yo2, xo3, yo3, r1, r2, r3, hmax, x_1, y_1, x_s1, x_s2, x_2, y_2, x_i_, y_i_, xv_, yv_, ytop, ybot, h_) :
    end proc:
```

Plotting path

```
> CalcYIntersect := proc(xo, yo, x_s, r_)
  # A procedure that calcualtes the specific angle theta on the circle at what point based on a point on that circle.
  local eq1, sol, y_s, theta_;

  eq1 := (x_s - xo)^2 + (y_s - yo)^2 = r_^2 :
  sol := solve({eq1, y_s < 2, y_s > 0}, {y_s}) :
  y_s := rhs(sol[1]) :

  theta_ := arctan((y_s - yo)/(x_s - xo)) :

  if x_s - xo < 0 then
     theta_ := theta_ + Pi :
  elif x_s - xo > 0 and y_s - yo < 0 then
     theta_ := theta_ + 2 * Pi :
  end if:
  return theta_ :
  end proc:
> PlotDiagram := proc(xo1, yo1, xo2, yo2, xo3, yo3, r1, r2, r3, hmax, x_1, y_1, x_s1, x_s2, x_2, y_2, x_i_, y_i_, xv_, yv_, ytop, ybot, h_, l1,
      x_t := -10, y_t := -10)

   # Procedure to plot the specific prestressing tendon layout
  local v1, v2, vs1, vs2, s1, s2, s3, s4, p_t, d1, d2, rectw, rectf, htop, hbot, hwall, theta1_1, theta1_2, theta3_1, theta3_2, theta2_1, theta2_2, c1,
       c2, c3, arr1, arr2, texarr, tex, diagram;


  v1 := line([x_1, -(1.75 - hmax)/2], [x_1, 1.75 - (1.75 - hmax)/2], linestyle = dot, color = red) :
  v2 := line([x_2, -(1.75 - hmax)/2], [x_2, 1.75 - (1.75 - hmax)/2], linestyle = dot, color = red) :
  vs1 := line([x_s1, -(1.75 - hmax)/2], [x_s1, 1.75 - (1.75 - hmax)/2], linestyle = dot, color = red) :
  vs2 := line([x_s2, -(1.75 - hmax)/2], [x_s2, 1.75 - (1.75 - hmax)/2], linestyle = dot, color = red) :

  s1 := point([1.41, -ybot - 0.15], color = black, symbol = circle, symbolsize = 15) :
  s2 := point([1.771, -ybot - 0.15], color = black, symbol = circle, symbolsize = 15) :
  s3 := point([14.319, -ybot - 0.15], color = black, symbol = circle, symbolsize = 15) :
  s4 := point([17.319, -ybot - 0.15], color = black, symbol = circle, symbolsize = 15) :
  p_t := point([x_t, y_t], color = red, symbol = solidbox , symbolsize = 10) :
  d1 := line([0, y_i_], [x_1, y_1], thickness = 3) :
  d2 := line([x_2, y_2], [xv_, yv_], thickness = 3) :
  rectw := rectangle([0, -ybot], [2.2, 2], color = white) :
  rectf := rectangle([2.2, -ybot], [18.1, hmax + ytop], color = white) :
  htop := line([0, hmax], [18.1, hmax], color = black, linestyle = dot) :
  hbot := line([0, 0], [18.1, 0], color = black, linestyle = dot) :
  hwall := line([-0.5, 2], [2.7, 2], color = black, linestyle = dot) :


  theta1_1 := CalcYIntersect(xo1, yo1, x_s1, r1) :
  theta1_2 := CalcYIntersect(xo1, yo1, x_s2, r1) :
  if r3 > 0 then
  theta3_1 := CalcYIntersect(xo3, yo3, x_1, r3) :
  theta3_2 := CalcYIntersect(xo3, yo3, x_s1, r3) :
  else
  theta3_1 := 0 :
  theta3_2 := 0 :
```

```
end if:

if r2 > 0 then
 theta2_1 := CalcYIntersect(xo2, yo2, x_s2, r2) :
theta2_2 := CalcYIntersect(xo2, yo2, x_2, r2) :
else
theta2_1 := 0 :
theta2_2 := 0 :
end if:

c1 := arc([xo1, yo1], r1, theta1_1 ..theta1_2, color = blue, thickness = [3]) :
c2 := arc([xo2, yo2], r2, theta2_1 ..theta2_2, color = red, thickness = [3]) :
c3 := arc([xo3, yo3], r3, theta3_1 ..theta3_2, color = red, thickness = [3]) :

 arr1 := arrow([xo1 - l1/2, 1.8], [xo1 + l1/2, 1.8], 0.005, 0.1, 0.02, double_arrow) :
arr2 := arrow([xo1 + l1/2, 1.8], [xo1 - l1/2, 1.8], 0.005, 0.1, 0.02, double_arrow) :
texarr := textplot([xo1, 1.9 , cat("L1")], 'align' = 'above', 'font' = ["times", "roman", 14]) :

tex := textplot([9.05, -1.3 , cat("L1 = ", l1 , "m", " h = ", h_, "m")], 'align' = 'above', 'font' = ["times", "roman", 16]) :

diagram := display(c1, c2, c3, rectw, rectf, htop, hbot, hwall, s1, s2, s3, s4, p_t, d1, d2, tex, texarr, arr1, arr2, view = [-1 ..19, -2 ..2], scaling
    = constrained, size = [1000, 400], axes = none) :
return diagram :
end proc:
> CalcTendonLength := proc(xo1, yo1, xo2, yo2, xo3, yo3, r1, r2, r3, hmax, x_1, y_1, x_s1, x_s2, x_2, y_2, x_i_, y_i_, xv_, yv_, ytop, ybot, h_)
# Procedure to calculate the length of the tendon, used for the CO2 calculations.
local theta1_1, theta1_2, theta3_1, theta3_2, theta2_1, theta2_2, LC1, LC2, LC3, LD1, LD2;

 theta1_1 := CalcYIntersect(xo1, yo1, x_s1, r1) :
theta1_2 := CalcYIntersect(xo1, yo1, x_s2, r1) :
if r3 > 0 then
theta3_1 := CalcYIntersect(xo3, yo3, x_1, r3) :
theta3_2 := CalcYIntersect(xo3, yo3, x_s1, r3) :
else
theta3_1 := 0 :
theta3_2 := 0 :
end if:

if r2 > 0 then
 theta2_1 := CalcYIntersect(xo2, yo2, x_s2, r2) :
theta2_2 := CalcYIntersect(xo2, yo2, x_2, r2) :
else
theta2_1 := 0 :
theta2_2 := 0 :
end if:

LC1 := r1·(abs(theta1_1 - theta1_2));
LC2 := r2·(abs(theta2_1 - theta2_2));
LC3 := r3·(abs(theta3_1 - theta3_2));

 LD1 := sqrt(x_1^2 + (y_i_ - y_1)^2) :
 LD2 := sqrt((18.1 - x_2)^2 + (yv_ - y_2)^2) :

 return LC1 + LC2 + LC3 + LD1 + LD2 :
 end proc:
> CalcPresPath := proc(l1, h_, props)
 # The main procedure, called in the optimization to create the tendon properties.
  if (0 ≤ l1 ≤ 18.1 - shift - shiftR) then CalcPath := Calc_PropMain(l1, h_, props) :
 end if:
 return CalcPath :
 end proc:
Calculating the height of the tendon
> CalcTendonHeight := proc(x_, xo1, yo1, xo2, yo2, xo3, yo3, r1, r2, r3, hmax, x_1, y_1, x_s1, x_s2, x_2, y_2, x_i_, y_i_, xv_, yv_, ytop, ybot,
    h_)
 # Procedure to calcualte the height of the tendon, given a certain location with coordinate x.
  # This is used to determine the tendon height at a specific location
 local solc1, y_c1, solc2, y_c2, solc3, y_c3, solr, y_r, soll, y_l, y_t;
  solc1 := solve((x_ - xo1)^2 + (y_c1 - yo1)^2 = r1^2, y_c1) :
  y_c1 := solc1[2] :
  solc2 := solve((x_ - xo2)^2 + (y_c2 - yo2)^2 = r2^2, y_c2) :
  y_c2 := solc2[1] :
   solc3 := solve((x_ - xo3)^2 + (y_c3 - yo3)^2 = r3^2, y_c3) :
  y_c3 := solc3[1] :
  solr := solve({y_2 = a_r·x_2 + b_r, yv_ = a_r·xv_ + b_r, y_r = a_r·x_ + b_r}, {a_r, b_r, y_r}) :
```

```
y_r := rhs(solr[3]) :
soll := solve({y_1 = a_l·x_1 + b_l, y_i_ = a_l·x_i_ + b_l, y_l = a_l·x_ + b_l}, {a_l, b_l, y_l}) :
y_l := rhs(soll[3]) :

if x_ ≤ x_s1 and x_ < x_1 then
y_t := y_l :
elif x_ < x_s1 and x_ > x_1 then
y_t := y_c3 :
elif x_ > x_s1 and x_ > x_1 and x_ < x_s2 and x_ < x_2 then
y_t := y_c1 :

elif x_ > x_s2 and x_ < x_2 then
y_t := y_c2 :

elif x_ ≥ x_s2 and x_ ≥ x_2 then
y_t := y_r :
end if:

return y_t
end proc:
```

F Carbon calculations

F.1 Carbon calculations

F.1.1 Variant reference

length	15,90	m	
height	1,64	m	
n prestressing	-		
11.859,44	**kg CO2 per meter**		
Total carbon emissions:			
Reinforcement - Y			
Top	3.272,00	mm2	3.272
Bot	25.133,00	mm2	25.133
Total area	0,028	m2	
Total volume	0,452	m3	
Density	7.850,00	kg/m3	
Weight	3.545,37	kg	
	1,02	kg CO2 eq per kg	
	3.616,28	**kg CO2**	
Reinforcement - X			
phi bot 1	32	150	85.250
phi bot 2	40	1.050	19.029
phi top 1	25	150	52.033
Top	52.032,63	mm2	
Bot	104.279,33	mm2	
Area	0,16	m2	
Volume	0,16	m3	
Density	7.850,00	kg/m3	
Weight	1.227,05	kg	
	1,02	kg CO2 eq per kg	
	1.251,59	**kg CO2**	
Stirrups			
phi	16,00	300,00	
legs	4,00		
Area per leg	201,06	mm2	
Vertical	62.445.814	mm3	
Horizontal	9.590.654	mm3	
Total	0,07	m3	
Density	7.850,00	kg/m3	
Weight	565,49	kg	
	1,02	kg CO2 eq per kg	
	576,80	**kg CO2**	
Prestressing			
Area one cable	2.250,00	mm2	
n cables	-		
Total area	-	mm2	
Total length	-	m	
Volume	-	m3	
Density	7.850,00	kg/m3	
Weight	-	kg	
	1,83	kg CO2 eq per kg	
	-	**kg CO2**	
Concrete			
width	1,00	m	
height	1,64	m	
Area	**1,61**	**m2**	
Volume	**25,40**	**m3**	
	252,59	kg CO2 eq per m3	
	6.414,78	**kg CO2**	
Cover top	85,00		
Cover bot	90,00		

F.1.2 Variant 1

length	15,90	m		length	15,90	m		length	15,90	m	
height	1,57	m		height	1,47	m		height	1,32	m	
n prestressing	1			n prestressing	2			n prestressing	3		
12.132,30	**kg CO2 per meter**			**12.273,17**	**kg CO2 per meter**			**12.196,55**	**kg CO2 per meter**		
Total carbon emissions:				**Total carbon emissions:**				**Total carbon emissions:**			
Reinforcement - Y				**Reinforcement - Y**				**Reinforcement - Y**			
Top	3.272,00	mm2		Top	3.272,00	mm2		Top	3.272,00	mm2	
Bot	25.133,00	mm2		Bot	25.133,00	mm2		Bot	25.133,00	mm2	
Area	0,03	m2		Area	0,03	m2		Area	0,03	m2	
Volume	0,45	m3		Volume	0,45	m3		Volume	0,45	m3	
Density	7.850,00	kg/m3		Density	7.850,00	kg/m3		Density	7.850,00	kg/m3	
Weight	3.545,37	kg		Weight	3.545,37	kg		Weight	3.545,37	kg	
	1,02	kg CO2 eq per kg			1,02	kg CO2 eq per kg			1,02	kg CO2 eq per kg	
	3.616,28	**kg CO2**			**3.616,28**	**kg CO2**			**3.616,28**	**kg CO2**	
Reinforcement - X				**Reinforcement - X**				**Reinforcement - X**			
phi bot 1	32	150	85.250	phi bot 1	32	150	85.250	phi bot 1	32	150	85.250
phi bot 2	40	1.050	19.029	phi bot 2	40	1.050	19.029	phi bot 2	40	1.050	19.029
phi top 1	25	150	52.033	phi top 1	25	150	52.033	phi top 1	25	150	52.033
Top	52.032,63	mm2		Top	52.032,63	mm2		Top	52.032,63	mm2	
Bot	104.279,33	mm2		Bot	104.279,33	mm2		Bot	104.279,33	mm2	
Area	0,16	m2		Area	0,16	m2		Area	0,16	m2	
Volume	0,16	m3		Volume	0,16	m3		Volume	0,16	m3	
Density	7.850,00	kg/m3		Density	7.850,00	kg/m3		Density	7.850,00	kg/m3	
Weight	1.227,05	kg		Weight	1.227,05	kg		Weight	1.227,05	kg	
	1,02	kg CO2 eq per kg			1,02	kg CO2 eq per kg			1,02	kg CO2 eq per kg	
	1.251,59	**kg CO2**			**1.251,59**	**kg CO2**			**1.251,59**	**kg CO2**	
Stirrups				**Stirrups**				**Stirrups**			
phi	16,00	300,00		phi	16,00	300,00		phi	16,00	300,00	
legs	4,00			legs	4,00			legs	4,00		
Area per leg	201,06	mm2		Area per leg	201,06	mm2		Area per leg	201,06	mm2	
Vertical	59.462.055	mm3		Vertical	55.199.542	mm3		Vertical	48.805.773	mm3	
Horizontal	9.590.654	mm3		Horizontal	9.590.654	mm3		Horizontal	9.590.654	mm3	
Total	0,07	m3		Total	0,06	m3		Total	0,06	m3	
Density	7.850,00	kg/m3		Density	7.850,00	kg/m3		Density	7.850,00	kg/m3	
Weight	542,06	kg		Weight	508,60	kg		Weight	458,41	kg	
	1,02	kg CO2 eq per kg			1,02	kg CO2 eq per kg			1,02	kg CO2 eq per kg	
	552,91	**kg CO2**			**518,78**	**kg CO2**			**467,58**	**kg CO2**	
Prestressing				**Prestressing**				**Prestressing**			
Area one cable	2.250,00	mm2		Area one cable	2.250,00	mm2		Area one cable	2.250,00	mm2	
n cables	1,00			n cables	2,00			n cables	3,00		
Total area	2.250,00	mm2		Total area	4.500,00	mm2		Total area	6.750,00	mm2	
Total length	18,18	m		Total length	18,15	m		Total length	18,14	m	
Volume	0,04	m3		Volume	0,08	m3		Volume	0,12	m3	
Density	7.850,00	kg/m3		Density	7.850,00	kg/m3		Density	7.850,00	kg/m3	
Weight	321,02	kg		Weight	641,15	kg		Weight	961,19	kg	
	1,83	kg CO2 eq per kg			1,83	kg CO2 eq per kg			1,83	kg CO2 eq per kg	
	587,46	**kg CO2**			**1.173,30**	**kg CO2**			**1.758,98**	**kg CO2**	
Concrete				**Concrete**				**Concrete**			
width	1,00	m		width	1,00	m		width	1,00	m	
height	1,57	m		height	1,47	m		height	1,32	m	
Area	**1,54**	**m2**		**Area**	**1,44**	**m2**		**Area**	**1,29**	**m2**	
Volume	**24,25**	**m3**		**Volume**	**22,62**	**m3**		**Volume**	**20,20**	**m3**	
	252,59	kg CO2 eq per m3			252,59	kg CO2 eq per m3			252,59	kg CO2 eq per m3	
	6.124,07	**kg CO2**			**5.713,23**	**kg CO2**			**5.102,12**	**kg CO2**	
Cover top	85,00			Cover top	85,00			Cover top	85,00		
Cover bot	90,00			Cover bot	90,00			Cover bot	90,00		

length	15,90	m		
height	1,20	m		
n prestressing	4			
12.249,69	**kg CO2 per meter**			
Total carbon emissions:				
Reinforcement - Y				
Top	3.272,00	mm2		
Bot	25.133,00	mm2		
Area	0,03	m2		
Volume	0,45	m3		
Density	7.850,00	kg/m3		
Weight	3.545,37	kg		
	1,02	kg CO2 eq per kg		
	3.616,28	**kg CO2**		
Reinforcement - X				
phi bot 1	32	150	85.250	
phi bot 2	40	1.050	19.029	
phi top 1	25	150	52.033	
Top	52.032,63	mm2		
Bot	104.279,33	mm2		
Area	0,16	m2		
Volume	0,16	m3		
Density	7.850,00	kg/m3		
Weight	1.227,05	kg		
	1,02	kg CO2 eq per kg		
	1.251,59	**kg CO2**		
Stirrups				
phi	16,00	300,00		
legs	4,00			
Area per leg	201,06	mm2		
Vertical	43.690.757	mm3		
Horizontal	9.590.654	mm3		
Total	0,05	m3		
Density	7.850,00	kg/m3		
Weight	418,26	kg		
	1,02	kg CO2 eq per kg		
	426,62	**kg CO2**		
Prestressing				
Area one cable	2.250,00	mm2		
n cables	4,00			
Total area	9.000,00	mm2		
Total length	18,13	m		
Volume	0,16	m3		
Density	7.850,00	kg/m3		
Weight	1.280,88	kg		
	1,83	kg CO2 eq per kg		
	2.344,02	**kg CO2**		
Concrete				
width	1,00	m		
height	1,20	m		
Area	**1,17**	**m2**		
Volume	**18,26**	**m3**		
	252,59	kg CO2 eq per m3		
	4.611,18	**kg CO2**		
Cover top	85,00			
Cover bot	90,00			

F.1.3 Variant 2

length	15,90	m		length	15,90	m		length	15,90	m		length	15,90	m	
height	1,33	m		height	1,21	m		height	1,09	m		height	1,11	m	
n prestressing	1			n prestressing	2			n prestressing	3			n prestressing	4		
11.089,25	**kg CO2 per meter**			**11.144,30**	**kg CO2 per meter**			**11.195,85**	**kg CO2 per meter**			**11.858,49**	**kg CO2 per meter**		
Total carbon emissions:				**Total carbon emissions:**				**Total carbon emissions:**				**Total carbon emissions:**			
Reinforcement - Y				**Reinforcement - Y**				**Reinforcement - Y**				**Reinforcement - Y**			
Top	3.272,00	mm2		Top	3.272,00	mm2		Top	3.272,00	mm2		Top	3.272,00	mm2	
Bot	25.133,00	mm2		Bot	25.133,00	mm2		Bot	25.133,00	mm2		Bot	25.133,00	mm2	
Area	0,03	m2		Area	0,03	m2		Area	0,03	m2		Area	0,03	m2	
Volume	0,45	m3		Volume	0,45	m3		Volume	0,45	m3		Volume	0,45	m3	
Density	7.850,00	kg/m3		Density	7.850,00	kg/m3		Density	7.850,00	kg/m3		Density	7.850,00	kg/m3	
Weight	3.545,37	kg		Weight	3.545,37	kg		Weight	3.545,37	kg		Weight	3.545,37	kg	
	1,02	kg CO2 eq per kg			1,02	kg CO2 eq per kg			1,02	kg CO2 eq per kg			1,02	kg CO2 eq per kg	
	3.616,28	**kg CO2**			**3.616,28**	**kg CO2**			**3.616,28**	**kg CO2**			**3.616,28**	**kg CO2**	
Reinforcement - X				**Reinforcement - X**				**Reinforcement - X**				**Reinforcement - X**			
phi bot 1	32	150	85.250	phi bot 1	32	150	85.250	phi bot 1	32	150	85.250	phi bot 1	32	150	85.250
phi bot 2	40	1.050	19.029	phi bot 2	40	1.050	19.029	phi bot 2	40	1.050	19.029	phi bot 2	40	1.050	19.029
phi top 1	25	150	52.033	phi top 1	25	150	52.033	phi top 1	25	150	52.033	phi top 1	25	150	52.033
Top	52.032,63	mm2		Top	52.032,63	mm2		Top	52.032,63	mm2		Top	52.032,63	mm2	
Bot	104.279,33	mm2		Bot	104.279,33	mm2		Bot	104.279,33	mm2		Bot	104.279,33	mm2	
Area	0,16	m2		Area	0,16	m2		Area	0,16	m2		Area	0,16	m2	
Volume	0,16	m3		Volume	0,16	m3		Volume	0,16	m3		Volume	0,16	m3	
Density	7.850,00	kg/m3		Density	7.850,00	kg/m3		Density	7.850,00	kg/m3		Density	7.850,00	kg/m3	
Weight	1.227,05	kg		Weight	1.227,05	kg		Weight	1.227,05	kg		Weight	1.227,05	kg	
	1,02	kg CO2 eq per kg			1,02	kg CO2 eq per kg			1,02	kg CO2 eq per kg			1,02	kg CO2 eq per kg	
	1.251,59	**kg CO2**			**1.251,59**	**kg CO2**			**1.251,59**	**kg CO2**			**1.251,59**	**kg CO2**	
Stirrups				**Stirrups**				**Stirrups**				**Stirrups**			
phi	16,00	300,00		phi	16,00	300,00		phi	16,00	300,00		phi	16,00	300,00	
legs	4,00			legs	4,00			legs	4,00			legs	4,00		
Area per leg	201,06	mm2		Area per leg	201,06	mm2		Area per leg	201,06	mm2		Area per leg	201,06	mm2	
Vertical	49.232.024	mm3		Vertical	44.117.009	mm3		Vertical	39.001.993	mm3		Vertical	39.854.496	mm3	
Horizontal	9.590.654	mm3		Horizontal	9.590.654	mm3		Horizontal	9.590.654	mm3		Horizontal	9.590.654	mm3	
Total	0,06	m3		Total	0,05	m3		Total	0,05	m3		Total	0,05	m3	
Density	7.850,00	kg/m3		Density	7.850,00	kg/m3		Density	7.850,00	kg/m3		Density	7.850,00	kg/m3	
Weight	461,76	kg		Weight	421,61	kg		Weight	381,45	kg		Weight	388,14	kg	
	1,02	kg CO2 eq per kg			1,02	kg CO2 eq per kg			1,02	kg CO2 eq per kg			1,02	kg CO2 eq per kg	
	470,99	**kg CO2**			**430,04**	**kg CO2**			**389,08**	**kg CO2**			**395,91**	**kg CO2**	
Prestressing				**Prestressing**				**Prestressing**				**Prestressing**			
Area one cable	2.250,00	mm2		Area one cable	2.250,00	mm2		Area one cable	2.250,00	mm2		Area one cable	2.250,00	mm2	
n cables	1,00			n cables	2,00			n cables	3,00			n cables	4,00		
Total area	2.250,00	mm2		Total area	4.500,00	mm2		Total area	6.750,00	mm2		Total area	9.000,00	mm2	
Total length	18,18	m		Total length	18,17	m		Total length	18,13	m		Total length	18,13	m	
Volume	0,04	m3		Volume	0,08	m3		Volume	0,12	m3		Volume	0,16	m3	
Density	7.850,00	kg/m3		Density	7.850,00	kg/m3		Density	7.850,00	kg/m3		Density	7.850,00	kg/m3	
Weight	321,10	kg		Weight	641,86	kg		Weight	960,66	kg		Weight	1.280,88	kg	
	1,83	kg CO2 eq per kg			1,83	kg CO2 eq per kg			1,83	kg CO2 eq per kg			1,83	kg CO2 eq per kg	
	587,62	**kg CO2**			**1.174,60**	**kg CO2**			**1.758,01**	**kg CO2**			**2.344,02**	**kg CO2**	
Concrete				**Concrete**				**Concrete**				**Concrete**			
width	1,00	m		width	1,00	m		width	1,00	m		width	1,00	m	
height	1,33	m		height	1,21	m		height	1,09	m		height	1,11	m	
Area	**1,30**	**m2**		**Area**	**1,18**	**m2**		**Area**	**1,06**	**m2**		**Area**	**1,08**	**m2**	
Volume	**20,44**	**m3**		**Volume**	**18,50**	**m3**		**Volume**	**16,55**	**m3**		**Volume**	**16,83**	**m3**	
	252,59	kg CO2 eq per m3			252,59	kg CO2 eq per m3			252,59	kg CO2 eq per m3			252,59	kg CO2 eq per m3	
	5.162,77	**kg CO2**			**4.671,80**	**kg CO2**			**4.180,89**	**kg CO2**			**4.250,69**	**kg CO2**	
Cover top	85,00			Cover top	85,00			Cover top	85,00			Cover top	85,00		
Cover bot	90,00			Cover bot	90,00			Cover bot	90,00			Cover bot	90,00		

F.1.4 Variant 3

length	15,9	m		length	15,9	m		length	15,9	m	
height	1,25	m		height	1,06	m		height	1,04	m	
n prestressing	1			n prestressing	2			n prestressing	3		
10.741,51	**kg CO2 per meter**			**10.490,38**	**kg CO2 per meter**			**10.978,52**	**kg CO2 per meter**		
Total carbon emissions:				**Total carbon emissions:**				**Total carbon emissions:**			
Reinforcement - Y				**Reinforcement - Y**				**Reinforcement - Y**			
Top	3.272,00	mm2		Top	3.272,00	mm2		Top	3.272,00	mm2	
Bot	25.133,00	mm2		Bot	25.133,00	mm2		Bot	25.133,00	mm2	
Area	0,03	m2		Area	0,03	m2		Area	0,03	m2	
Volume	0,45	m3		Volume	0,45	m3		Volume	0,45	m3	
Density	7.850,00	kg/m3		Density	7.850,00	kg/m3		Density	7.850,00	kg/m3	
Weight	3.545,37	kg		Weight	3.545,37	kg		Weight	3.545,37	kg	
	1,02	kg CO2 eq per kg			1,02	kg CO2 eq per kg			1,02	kg CO2 eq per kg	
	3.616,28	**kg CO2**			**3.616,28**	**kg CO2**			**3.616,28**	**kg CO2**	
Reinforcement - X				**Reinforcement - X**				**Reinforcement - X**			
phi bot 1	32	150	85.250	phi bot 1	32	150	85.250	phi bot 1	32	150	85.250
phi bot 2	40	1.050	19.029	phi bot 2	40	1.050	19.029	phi bot 2	40	1.050	19.029
phi top 1	25	150	52.033	phi top 1	25	150	52.033	phi top 1	25	150	52.033
Top	52.032,63	mm2		Top	52.032,63	mm2		Top	52.032,63	mm2	
Bot	104.279,33	mm2		Bot	104.279,33	mm2		Bot	104.279,33	mm2	
Area	0,16	m2		Area	0,16	m2		Area	0,16	m2	
Volume	0,16	m3		Volume	0,16	m3		Volume	0,16	m3	
Density	7.850,00	kg/m3		Density	7.850,00	kg/m3		Density	7.850,00	kg/m3	
Weight	1.227,05	kg		Weight	1.227,05	kg		Weight	1.227,05	kg	
	1,02	kg CO2 eq per kg			1,02	kg CO2 eq per kg			1,02	kg CO2 eq per kg	
	1.251,59	**kg CO2**			**1.251,59**	**kg CO2**			**1.251,59**	**kg CO2**	
Stirrups				**Stirrups**				**Stirrups**			
phi	16,00	300,00		phi	16,00	300,00		phi	16,00	300,00	
legs	4,00			legs	4,00			legs	4,00		
Area per leg	201,06	mm2		Area per leg	201,06	mm2		Area per leg	201,06	mm2	
Vertical	45.822.014	mm3		Vertical	37.723.239	mm3		Vertical	36.870.737	mm3	
Horizontal	9.590.654	mm3		Horizontal	9.590.654	mm3		Horizontal	9.590.654	mm3	
Total	0,06	m3		Total	0,05	m3		Total	0,05	m3	
Density	7.850,00	kg/m3		Density	7.850,00	kg/m3		Density	7.850,00	kg/m3	
Weight	434,99	kg		Weight	371,41	kg		Weight	364,72	kg	
	1,02	kg CO2 eq per kg			1,02	kg CO2 eq per kg			1,02	kg CO2 eq per kg	
	443,69	**kg CO2**			**378,84**	**kg CO2**			**372,02**	**kg CO2**	
Prestressing				**Prestressing**				**Prestressing**			
Area one cable	2.250,00	mm2		Area one cable	2.250,00	mm2		Area one cable	2.250,00	mm2	
n cables	1,00			n cables	2,00			n cables	3,00		
Total area	2.250,00	mm2		Total area	4.500,00	mm2		Total area	6.750,00	mm2	
Total length	18,18	m		Total length	18,14	m		Total length	18,13	m	
Volume	0,04	m3		Volume	0,08	m3		Volume	0,12	m3	
Density	7.850,00	kg/m3		Density	7.850,00	kg/m3		Density	7.850,00	kg/m3	
Weight	321,10	kg		Weight	640,80	kg		Weight	960,66	kg	
	1,83	kg CO2 eq per kg			1,83	kg CO2 eq per kg			1,83	kg CO2 eq per kg	
	587,62	**kg CO2**			**1.172,66**	**kg CO2**			**1.758,01**	**kg CO2**	
Concrete				**Concrete**				**Concrete**			
width	1,00	m		width	1,00	m		width	1,00	m	
height	1,25	m		height	1,06	m		height	1,04	m	
Area	**1,22**	**m2**		**Area**	**1,03**	**m2**		**Area**	**1,01**	**m2**	
Volume	**19,17**	**m3**		**Volume**	**16,12**	**m3**		**Volume**	**15,76**	**m3**	
	252,59	kg CO2 eq per m3			252,59	kg CO2 eq per m3			252,59	kg CO2 eq per m3	
	4.842	**kg CO2**			**4.071**	**kg CO2**			**3.981**	**kg CO2**	
Cover top	85			Cover top	85			Cover top	85		
Cover bot	90			Cover bot	90			Cover bot	90		

length	15,9	m	
height	1,12	m	
n prestressing	4		
11.901,95	**kg CO2 per meter**		
Total carbon emissions:			
Reinforcement - Y			
Top	3.272,00	mm2	
Bot	25.133,00	mm2	
Area	0,03	m2	
Volume	0,45	m3	
Density	7.850,00	kg/m3	
Weight	3.545,37	kg	
	1,02	kg CO2 eq per kg	
	3.616,28	**kg CO2**	
Reinforcement - X			
phi bot 1	32	150	85.250
phi bot 2	40	1.050	19.029
phi top 1	25	150	52.033
Top	52.032,63	mm2	
Bot	104.279,33	mm2	
Area	0,16	m2	
Volume	0,16	m3	
Density	7.850,00	kg/m3	
Weight	1.227,05	kg	
	1,02	kg CO2 eq per kg	
	1.251,59	**kg CO2**	
Stirrups			
phi	16,00	300,00	
legs	4,00		
Area per leg	201,06	mm2	
Vertical	40.280.747	mm3	
Horizontal	9.590.654	mm3	
Total	0,05	m3	
Density	7.850,00	kg/m3	
Weight	391,49	kg	
	1,02	kg CO2 eq per kg	
	399,32	**kg CO2**	
Prestressing			
Area one cable	2.250,00	mm2	
n cables	4,00		
Total area	9.000,00	mm2	
Total length	18,13	m	
Volume	0,16	m3	
Density	7.850,00	kg/m3	
Weight	1.280,88	kg	
	1,83	kg CO2 eq per kg	
	2.344,02	**kg CO2**	
Concrete			
width	1,00	m	
height	1,12	m	
Area	**1,09**	**m2**	
Volume	**16,99**	**m3**	
	252,59	kg CO2 eq per m3	
	4.291	**kg CO2**	
Cover top	85		
Cover bot	90		

F.1.5 Final variant - $\phi 20 - 250mm$

length	15,9	m	
height	0,89	m	
n prestress	2		
9.853	**kg CO2 per meter**		
Total carbon emissions:			
Reinforcement - Y			
Top	3272	mm2	
Bot	25133	mm2	
Area	0,028	m2	
Volume	0,452	m3	
Density	7850,0	kg/m3	
Weight	3545,4	kg	
	1,02	kg CO2 eq per kg	
	3.616	**kg CO2**	
Reinforcement - X			
phi bot 1	32	150	85.250
phi bot 2	40	1050	19.029
phi top 1	25	150	52.033
Top	52.033	mm2	
Bot	104.279	mm2	
Area	0,156	m2	
Volume	0,156	m3	
Density	7850,0	kg/m3	
Weight	1227,0	kg	
	1,02	kg CO2 eq per kg	
	1.252	**kg CO2**	
Stirrups			
phi	16	300	
legs	4		
Area per le	201	mm2	
Vertical	18.976.225	mm3	
Horizontal	5.971.539	mm3	
Total	0,0249	m3	
Density	7850	kg/m3	
Weight	195,8	kg	
	1,02	kg CO2 eq per kg	
	200	**kg CO2**	
Prestressing			
Area one c	2250	mm2	
n cables	2		
Total area	4500	mm2	
Total lengt	18,12	m	
Volume	0,08154	m3	
Density	7850	kg/m3	
Weight	640,089	kg	
	1,83	kg CO2 eq per kg	
	1.171	**kg CO2**	
Concrete			
width	1	m	
height	0,89	m	
Area	**0,86**	**m2**	
Volume	**13,41**	**m3**	
	252,59	kg CO2 eq per m3	
	3.387	**kg CO2**	
Cover top	85	mm	
Cover bot	90	mm	
Stirrups additional			
length	6	m	
phi	20	250	
legs	4		
Area per le	314	mm2	
Vertical	21.563.892	mm3	
Horizontal	6.785.840	mm3	
Total	0,0283	m3	
Density	7850	kg/m3	
Weight	222,5	kg	
	1,02	kg CO2 eq per kg	
	227	**kg CO2**	

F.1.6 Final variant - Cross-section

length	15,9	m		
height	0,89	m		
hopen	0,345	m		
bopen	0,4	m		
n prestress	2			
9.504	**kg CO2 per meter**			
Total carbon emissions:				
Reinforcement - Y				
Top	3272	mm2		
Bot	25133	mm2		
Area	0,028	m2		
Volume	0,452	m3		
Density	7850,0	kg/m3		
Weight	3545,4	kg		
	1,02	kg CO2 eq per kg		
	3.616	**kg CO2**		
Reinforcement - X				
phi bot 1	32		150	85.250
phi bot 2	40		1050	19.029
phi top 1	25		150	52.033
Top	52.033	mm2		
Bot	104.279	mm2		
Area	0,156	m2		
Volume	0,156	m3		
Density	7850,0	kg/m3		
Weight	1227,0	kg		
	1,02	kg CO2 eq per kg		
	1.252	**kg CO2**		
Stirrups				
phi	16		300	
legs	4			
Area per le	201	mm2		
Vertical	18.976.225	mm3		
Horizontal	5.971.539	mm3		
Total	0,0249	m3		
Density	7850	kg/m3		
Weight	195,8	kg		
	1,02	kg CO2 eq per kg		
	200	**kg CO2**		
Prestressing				
Area one c	2250	mm2		
n cables	2			
Total area	4500	mm2		
Total lengt	18,12	m		
Volume	0,08154	m3		
Density	7850	kg/m3		
Weight	640,089	kg		
	1,83	kg CO2 eq per kg		
	1.171	**kg CO2**		
Concrete				
width	1	m		
height	0,89	m		
Area	**0,72**	**m2**		
Volume	**11,22**	**m3**		
	252,59	kg CO2 eq per m3		
	2.834	**kg CO2**		
Cover top	85	mm		
Cover bot	90	mm		
Stirrups additional				
length	6	m		
phi	20		300	
legs	4			
Area per le	314	mm2		
Vertical	17.969.910	mm3		
Horizontal	5.654.867	mm3		
Total	0,0236	m3		
Density	7850	kg/m3		
Weight	185,5	kg		
	1,02	kg CO2 eq per kg		
	189	**kg CO2**		
EPS Formwork				
Area	0,138	m2		
Volume	2,194	m3		
Emb. Carb.	110,136	kg CO2eq		
Density	20,00	kg/m3		
Weight	43,88	kg		
	242	**kg CO2**		

F.1.7 Discussion variant

length	15,9	m	
height	1,523	m	
n prestressing	0		
11.350,88	**kg CO2 per meter**		
Total carbon emissions:			
Reinforcement - Y			
Top	3.272,00	mm2	
Bot	25.133,00	mm2	
Area	0,03	m2	
Volume	0,45	m3	
Density	7.850,00	kg/m3	
Weight	3.545,37	kg	
	1,02	kg CO2 eq per kg	
	3.616,28	**kg CO2**	
Reinforcement - X			
phi bot 1	32	150	85.250
phi bot 2	40	1.050	19.029
phi top 1	25	150	52.033
Top	52.032,63	mm2	
Bot	104.279,33	mm2	
Area	0,16	m2	
Volume	0,16	m3	
Density	7.850,00	kg/m3	
Weight	1.227,05	kg	
	1,02	kg CO2 eq per kg	
	1.251,59	**kg CO2**	
Stirrups			
phi	16,00	300,00	
legs	4,00		
Area per leg	201,06	mm2	
Vertical	57.458.674	mm3	
Horizontal	9.590.654	mm3	
Total	0,07	m3	
Density	7.850,00	kg/m3	
Weight	526,34	kg	
	1,02	kg CO2 eq per kg	
	536,86	**kg CO2**	
Prestressing			
Area one cable	2.250,00	mm2	
n cables	-		
Total area	-	mm2	
Total length	-	m	
Volume	-	m3	
Density	7.850,00	kg/m3	
Weight	-	kg	
	1,83	kg CO2 eq per kg	
	-	**kg CO2**	
Concrete			
width	1,00	m	
height	1,52	m	
Area	**1,49**	**m2**	
Volume	**23,54**	**m3**	
	252,59	kg CO2 eq per m3	
	5.946	**kg CO2**	
Cover top	85		
Cover bot	90		

G Verifications

To verify that the Maple model works accordingly, several verifications have been performed.

G.1 Model verification

The maple calculations have been verified using Technosoft [SOURCE]. First the results of the two governing loads combinations are shown below. For the bending moments and shear forces four cross-sections have been checked. Namely the start of the floor, the location with the highest sagging moment in the largest span and the two foundation piles (supports C and D of the analytical model).

G.1.1 Results

Table 60: SLS Bending moments

Cross-section	**1**	**2**	**3**	**4**	
Maple	4.775	87.226	10.343	-7.503	kNm
Technosoft	4.778	87.224	10.385	-7.504	kNm

Table 61: ULS Bending moments

Cross-section	**1**	**2**	**3**	**4**	
Maple	9.300	134.506	12.270	-15.300	kNm
Technosoft	9.300	134.512	12.493	-15.301	kNm

Table 62: ULS Shear forces

Cross-section	**1**	**2**	**3**	**4**	
Maple	45.928	0	-42.954	-20.191	kN
Technosoft	45.930	0	-42.957	-20.192	kN

For the deformations the same locations have been checked, the only change being the second check is now at the location of the largest deformation.

Table 63: SLS Deformations

Cross-section	**1**	**2**	**3**	**4**	
Maple	14.7	33.6	28.5	22.7	mm
Technosoft	14.7	33.6	28.5	22.7	mm

The normal forces as calculated in section 4.4 are also verified using the results of the Technosoft model.

Table 64: SLS Normal forces in each element

	Element 1	**Element 2**	**Element 3**	
Maple	16.961	11.933	4.736	kN
Technosoft	16.959	11.871	4.697	kN

Table 65: ULS Normal forces in each element

	Element 1	**Element 2**	**Element 3**	
Maple	26.665	21.563	9.144	kN
Technosoft	26.661	21.451	9.072	kN

G.1.2 Technosoft and Maple output

Royal HaskoningDHV Blad1

Technosoft Raamwerken release 6.82 27 mrt 2025

Project.....: SIF 2 Quay Wall
Onderdeel....: Verification ULS 3.12

Resultaten staaf:1-3 B.G:3 ULS 3.12

Geometrie



Momenten 1e orde

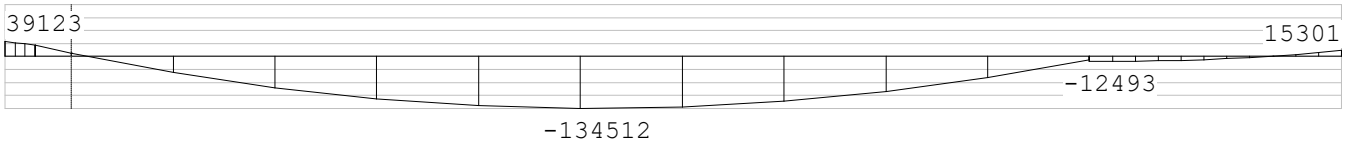

Dwarskrachten 1e orde

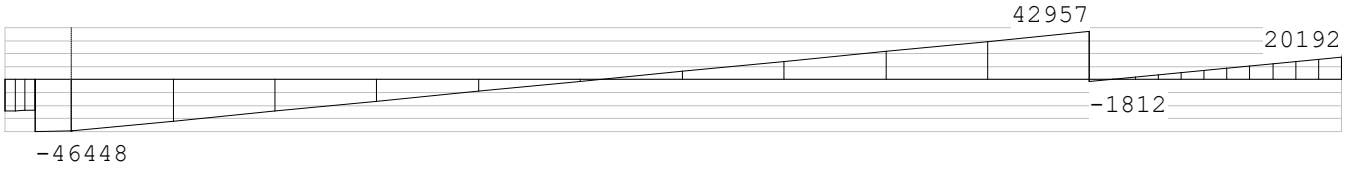

Normaalkrachten 1e orde

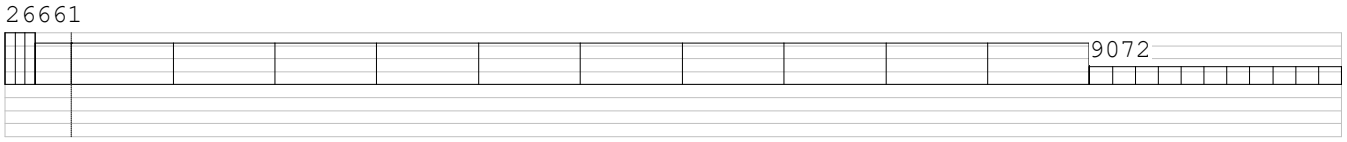

Verplaatsingen 1e orde

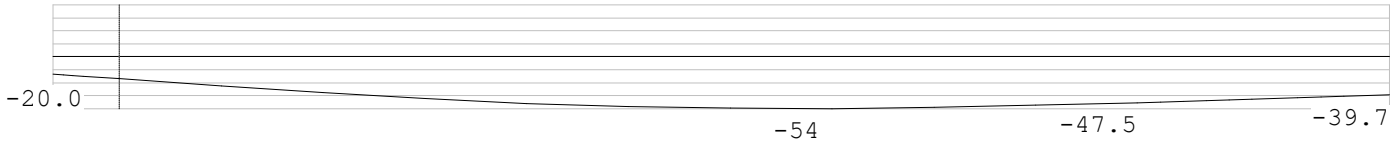

Resultaten van staaf:2 op pos:0.429

Momenten	9299,70
Dwarskr.	-45930,03
Normaalkr.	21450,58
Verpl.[mm]	-22,71

Profiel	B*H 23000*1750
E-modulus	12000
Oppervlak	4.025e+07
I_y	1.02721e+13

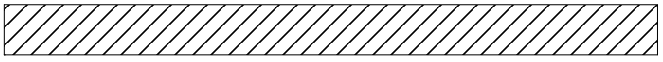

Royal HaskoningDHV Blad2

Technosoft Raamwerken release 6.82 27 mrt 2025

Project.....: SIF 2 Quay Wall
Onderdeel....: Verification SLS 1.3

Resultaten staaf:1-3 B.G:1 SLS 1.3

Geometrie



Momenten 1e orde

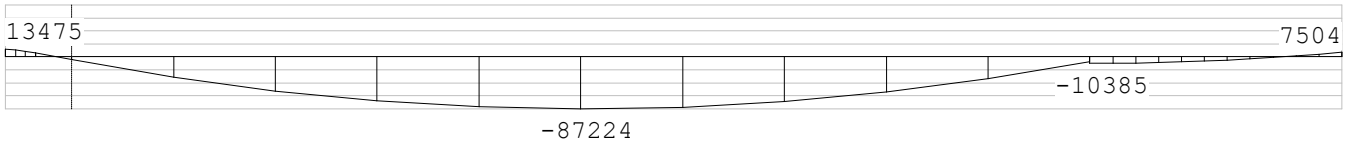

Dwarskrachten 1e orde



Normaalkrachten 1e orde

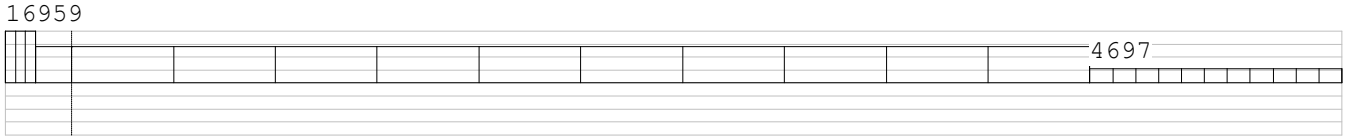

Verplaatsingen 1e orde

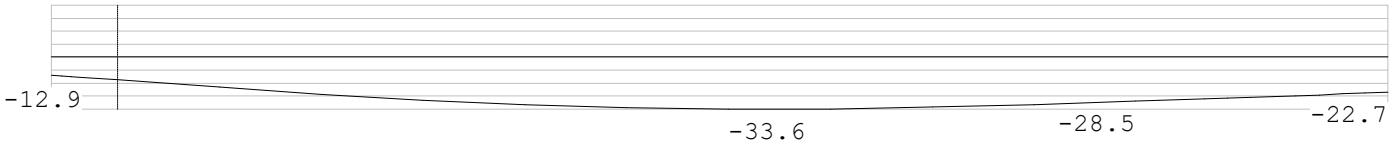

Resultaten van staaf:2 op pos:0.429

Momenten	-4774,78
Dwarskr.	-26896,32
Normaalkr.	11871,47
Verpl.[mm]	-14,69

Profiel	B*H 23000*1750
E-modulus	12000
Oppervlak	4.025e+07
I_y	1.02721e+13

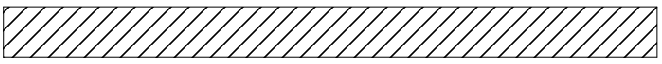

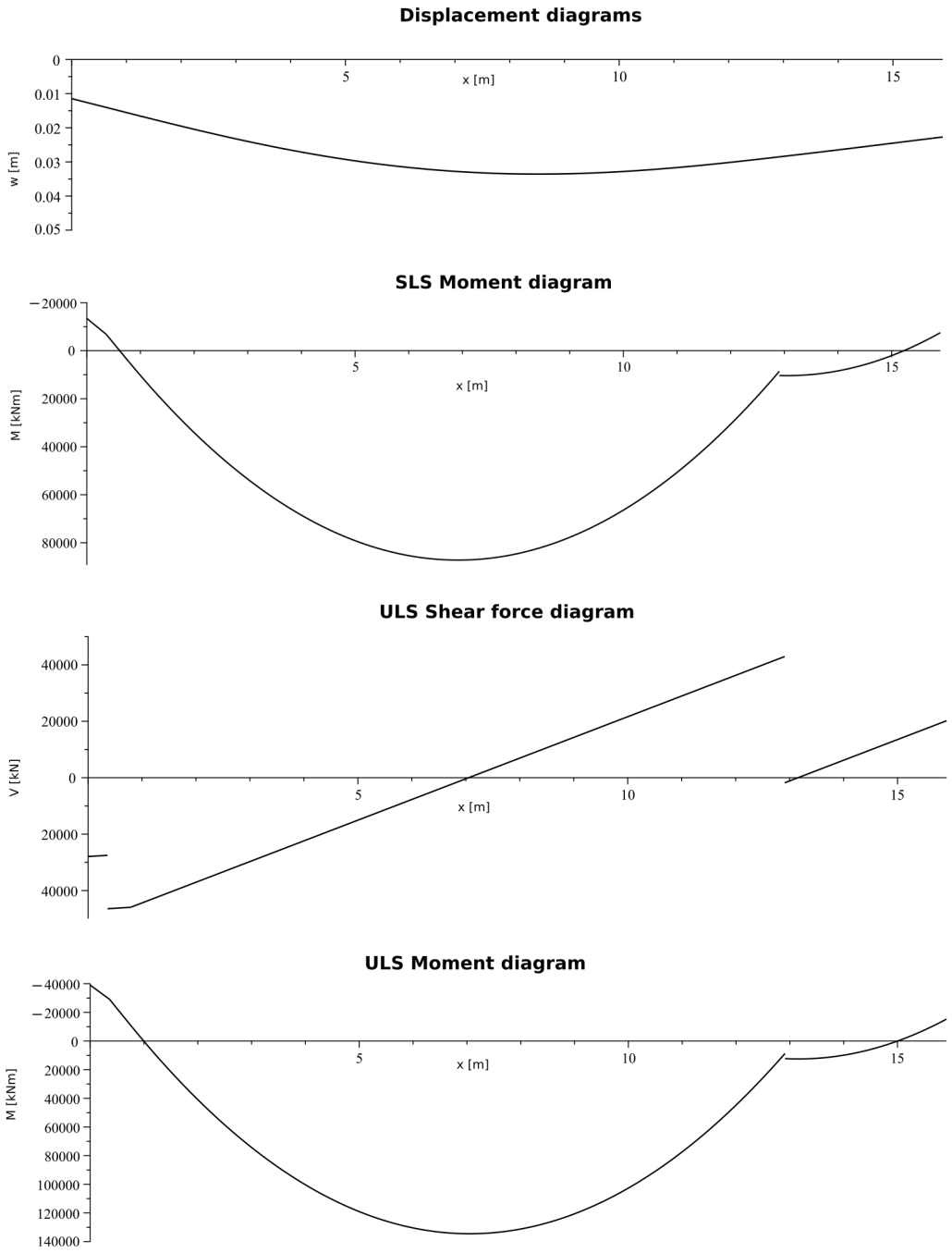

Figure 91: Analysis force diagrams

G.2 Resistance check modules

Verifications of the resistance check modules have been performed. The modules have been verified with manual calculations (using Excel sheets). The calculations of both are shown in Appendix 6.3 and 6.3.

G.2.1 Verification inputs

Three verifications have been performed for every check. The first one with a positive bending moment and two prestressing tendons, the second is the same, but with a negative bending moment and the third one a positive bending moment but without prestressing.

Table 66: ULS MRd verification inputs

Verification	**1**	**2**	**3**	
h	1.200	1.400	1.600	mm
$\mathbf{A_p}$	4.500	4.500	0	mm^2
$\mathbf{d_p}$	600	600	0	mm
$\mathbf{N_{Ed}}$	800	800	1.000	kN
$\mathbf{M_{Ed}}$	2.000	-2.500	3.000	kNm

Table 67: ULS VRd verification inputs

Verification	**1**	**2**	**3**	
h	1.200	1.400	1.600	mm
$\mathbf{A_p}$	4.500	4.500	0	mm^2
$\mathbf{d_p}$	600	600	0	mm
$\mathbf{N_{Ed}}$	800	800	1.000	kN
$\mathbf{V_{Ed}}$	2.000	2.000	2.000	kNm
$\mathbf{M_{Ed}}$	+	-	+	kNm
$\mathbf{x_u}$	500	300	200	mm

Table 68: SLS Crack widths verification inputs

Verification	**1**	**2**	**3**	
h	1.200	1.400	1.600	mm
$\mathbf{A_p}$	4.500	4.500	0	mm^2
$\mathbf{d_p}$	600	600	0	mm
N	800	800	800	kN
M	2.000	-2.500	1.500	kNm

G.2.2 Results

Table 69: Resistance verification unity checks results

Verification	**1**		**2**		**3**	
	Maple	**Manual**	**Maple**	**Manual**	**Maple**	**Manual**
MRd	0,25	0,25	0,91	0,91	0,24	0,24
VRd	1,51	1,51	1,54	1,54	1,11	1,11
SLS	0,17	0,17	0,50	0,50	0,31	0,31

G.2.3 Manual and Maple outputs

```
> restart :
>
      read("C:/Users/927585/OneDrive − Royal HaskoningDHV/Thesis/Content/Calculations/Maple/Final/ResistanceChecks/SLS_CrackWidth -
      final - 2025-03-09.mpl") :
> read("C:/Users/927585/OneDrive − Royal HaskoningDHV/Thesis/Content/Calculations/Maple/Final/ResistanceChecks/ULS_ShearResistance -
      final - 2025-03-09.mpl") :

> read("C:/Users/927585/OneDrive − Royal HaskoningDHV/Thesis/Content/Calculations/Maple/Final/Relieving platform properties.mpl") :
> read("C:/Users/927585/OneDrive − Royal HaskoningDHV/Thesis/Content/Calculations/Maple/Final/Prestressing forces - final - 2025-03-09.
      mpl") :
> read("C:/Users/927585/OneDrive − Royal HaskoningDHV/Thesis/Content/Calculations/Maple/Final/ResistanceChecks/ULS_BendingMoments
      - final - 2025-03-09.mpl") :
```

Verification 1

```
> h := 1200 : # mm
  Ap := 4500 : # mm2
  dp_ := 600 : # mm
  N_ULS := 800 : # kN
  M_ULS := 2000 : # kNm
  ReinforcementProperties := ReinforcementProp( ) :
>  ULS_MRd:-MRdCheck(h, Ap, dp_, N_ULS·1000, M_ULS·1000·1000, ReinforcementProperties, false) :
                                "MRd:", 8.100116295 × 10^9, "kN"
                    "[ULS MRd] bending moment resistance, u.c.:", 0.2469100353   (1)

> V := 1200 : #kN
  x := 500 : # mm (compression zone height)
> ULS_Shear:-CheckShear(h, V·1000, N_ULS·1000, Ap, 1, dp_, ReinforcementProperties, x, false) :
                    "[ULS VRd,c] Without reinforcement u.c.:", 0.9055075079
                    "[ULS VRd,s] With reinforcement u.c.:", 0.9911173838   (2)

>  N_SLS := 800 : # kN
  M_SLS := 2000 : # kNm
> SLS_CrackWidths:-SLSCheck(Ap, dp_, h, (M_SLS·1000·1000), N_SLS·1000, ReinforcementProperties, false) :
                                "w_:", 0.05636533385, "mm"
                    "[SLS cracks] Crack width u.c.:", 0.1722274090   (3)
```

Verification 2

```
> h := 1400 : # mm
  Ap := 4500 : # mm2
  dp_ := 600 : # mm
  N_ULS := 800 : # kN
  M_ULS := −2500 : # kNm
  ReinforcementProperties := ReinforcementProp( ) :
>  ULS_MRd:-MRdCheck(h, Ap, dp_, N_ULS·1000, M_ULS·1000·1000, ReinforcementProperties, false) :
                                "MRd:", 5.243998055 × 10^9, "kN"
                    "[ULS MRd] bending moment resistance, u.c.:", 0.4767354934   (4)

> V := 2000 : #kN
  x := 300 : # mm (compression zone height)
> ULS_Shear:-CheckShear(h, V·1000, N_ULS·1000, Ap, −1, dp_, ReinforcementProperties, x, false) :
                    "[ULS VRd,c] Without shear reinforcement u.c.:", 1.963073463
                    "[ULS VRd,s] With shear reinforcement u.c.:", 1.535721352   (5)

>  N_SLS := 800 : # kN
  M_SLS := −2500 : # kNm
> SLS_CrackWidths:-SLSCheck(Ap, dp_, h, (M_SLS·1000·1000), N_SLS·1000, ReinforcementProperties, false) :
                                "w_:", 0.1701640873, "mm"
                    "[SLS cracks] Crack width u.c.:", 0.5004826097   (6)
```

Verification 3

```
> h := 1600 : # mm
  Ap := 0 : # mm2
  dp_ := 0 : # mm
  N_ULS := 1000 : # kN
  M_ULS := 3000 : # kNm
  ReinforcementProperties := ReinforcementProp( ) :
>  ULS_MRd:-MRdCheck(h, Ap, dp_, N_ULS·1000, M_ULS·1000·1000, ReinforcementProperties, false) :
                                "MRd:", 1.266509576 × 10^10, "kN"
                    "[ULS MRd] bending moment resistance, u.c.:", 0.2368714818   (7)

> V := 2000 : #kN
  x := 200 : # mm (compression zone height)
> ULS_Shear:-CheckShear(h, V·1000, N_ULS·1000, Ap, 1, dp_, ReinforcementProperties, x, false) :
                    "[ULS VRd,c] Without shear reinforcement u.c.:", 2.539524286
                    "[ULS VRd,s] With shear reinforcement u.c.:", 1.106970587   (8)
```

ULS: Bending moment resistance 1 - Verifications

Inputs

Cross-section analysed	x	0,790	[m]
Cross-section height	h	1200	[mm]
Tendons amount	n	2	[-]
Prestressing tendon area	A_p	4500	[mm^2]
Prestressing tendon depth	d_p	600	[mm]
Normal force	Ned	800.000	[N]
Bending moment	Med	2.000	[kNm]

Reinforcement

Shear reinforcement diameter	ϕ	16	[mm]
Shear reinforcement distance	s	300	[mm]
Top reinforcement area	Ast	3272	[mm^2]
Top reinforcement depth	dst	113,5	[mm]
Bottom reinforcement area	Asb	25133	[mm^2]
Bottom reinforcement depth	dsb	994	[mm]

Prestressing design



Prestressing stress per tendon (t = ∞)	$\sigma_{pm\infty}$	1200	[N/mm^2]
Total prestressing force (t = ∞)	$P_{m\infty}$	5.400.000	[N]

Material properties

Concrete

Characteristic compressive strength	fck	35	[N/mm^2]
Design compressive strength	fcd	23,33	[N/mm^2]
Concrete strain at failure	εuk	-0,0035	[-]
	α	0,75	[-]
	β	0,39	[-]

Reinforcement steel

Yield strength	fyd	435	[N/mm^2]
	Es	200000	

Prestressing steel

E-modulus	E_p	195000	[N/mm^2]
Yield strength	f_{pk}	1860	[N/mm^2]
	$f_{p0,1k}$		[N/mm^2]
	f_{pd}	1522	[N/mm^2]
Assumed prestr. stress at failure	σ_{pu}	1522	[N/mm^2]

Compression zone height

Compression zone height	xu	**664,186169**	[mm]	= ([Asb * fyd] + [Ap * (fpd - σpu)] + [σpu * Ap] - [Ned] - [Ast * fyd]) / (α * fcd * b)) + dx
dx for horizontal force equilibrium	dx	-225	[mm]	

Strains

Total prestressing tendon strain	εp	0,00581561	[-]	= εp,∞ + Δεp
	Δεp	-0,00033824	[-]	= εuk (dp/xu - 1)
	$\varepsilon_{pm\infty}$	0,00615385	[-]	= σpm∞ / Ep
	εst	-0,0029019	[-]	= ((xu - dst)/xu) * εuk
	εsb	0,00173799	[-]	= ((dst - xu)/xu) * εuk

Stresses

Actual prestressing stress	σp	1134,044	[N/mm^2]
Top reinforcement stress	σst	-435	[N/mm^2]
Top reinforcement stress	σsb	347,597845	[N/mm^2]

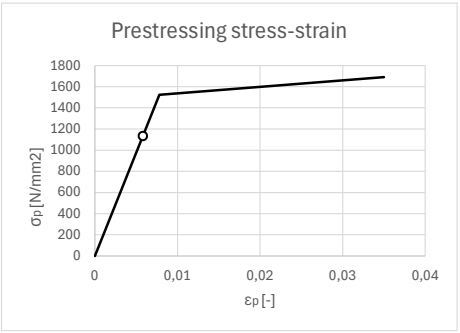

Forces

Force in the concrete	Nc	-11.621.598	[N]	= α * xu * fcd * 1000
Force in the top reinforcement	Nst	-1.423.320	[N]	= Ast * σst
Force in the bot. reinforcement	Nsb	8.736.177	[N]	= Asb * σsb
Additional force prestr. tendon	ΔNp	-296.802	[N]	= Ap * (σp - σpm∞)

Horizontal force equilibrium

-5.543 → OK

Eccentricities

Concrete	=	ec	341	[mm]	= h/2 - β*xu
Top reinforcement	=	est	487	[mm]	= h/2 - dst
Bottom reinforcement	=	esb	-394	[mm]	= dsb - h/2
Prestressing tendon	=	esp	0	[mm]	= dp - h/2

Results

Effective depth steel	deff		[mm]	
Rotational capacity check		-		
Bending moment resistance	MRd	8.097	[kNm]	
	u.c.	0,25	→	OK

ULS: Bending moment resistance 2 - Verifications

Inputs

Cross-section analysed	x	6,500	[m]
Cross-section height	h	1400	[mm]
Tendons amount	n	2	[-]
Prestressing tendon area	A_p	4500	[mm^2]
Prestressing tendon depth	d_p	800	[mm]
Normal force	Ned	800.000	[N]
Bending moment	Med	2.500 (-)	[kNm]

Reinforcement

Shear reinforcement diameter	ϕ	16	[mm]
Shear reinforcement distance	s	300	[mm]
Top reinforcement area	Ast	25133	[mm^2]
Top reinforcement depth	dst	206	[mm]
Bottom reinforcement area	Asb	3272	[mm^2]
Bottom reinforcement depth	dsb	1286,5	[mm]

Prestressing design



Prestressing stress per tendon (t = ∞)	$\sigma_{pm\infty}$	1200	[N/mm^2]
Total prestressing force (t = ∞)	$P_{m\infty}$	5.400.000	[N]

Material properties

Concrete

Characteristic compressive strength	fck	35	[N/mm^2]
Design compressive strength	fcd	23,33	[N/mm^2]
Concrete strain at failure	εuk	-0,0035	[-]
	α	0,75	[-]
	β	0,39	[-]

Reinforcement steel

Yield strength	fyd	435	[N/mm^2]
	Es	200000	

Prestressing steel

E-modulus	E_p	195000	[N/mm^2]
Yield strength	f_{pk}	1860	[N/mm^2]
	$f_{p0,1k}$		[N/mm^2]
	f_{pd}	1522	[N/mm^2]
Assumed prestr. stress at failure	σ_{pu}	1522	[N/mm^2]

Compression zone height

Compression zone height	x_u	**252,22689**	[mm]	= ([A_{sb} * f_{yd}] + [A_p * (f_{pd} - σ_{pu})] + [σ_{pu} * A_p] - [N_{ed}] - [A_{st} * f_{yd}]) / (α * f_{cd} * b)) + dx
dx for horizontal force equilibrium	dx	450	[mm]	

Strains

Total prestressing tendon strain	εp	0,01375496	[-]	= $\varepsilon_{p,\infty}$ + $\Delta\varepsilon_p$
	$\Delta\varepsilon_p$	0,00760112	[-]	= ε_{uk} (d_p/x_u - 1)
	$\varepsilon_{pm\infty}$	0,00615385	[-]	= $\sigma_{pm\infty}$ / E_p
	εst	-0,00064146	[-]	= ((xu - dst)/xu) * εuk
	εsb	0,01435198	[-]	= ((dst - xu)/xu) * εuk

Stresses

Actual prestressing stress	σ_p	1558,99958	[N/mm^2]
Top reinforcement stress	σst	-128,292518	[N/mm^2]
Top reinforcement stress	σsb	435	[N/mm^2]

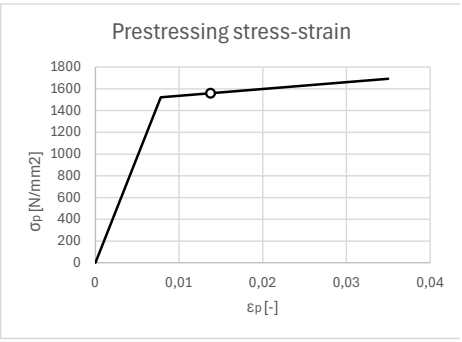

Forces

Force in the concrete	N_c	-4.413.340	[N]	= α * x_u * f_{cd} * 1000	
Force in the top reinforcement	N_{st}	-3.224.376	[N]	= Ast * σst	
Force in the bot. reinforcement	N_{sb}	1.423.320	[N]	= Asb * σsb	
Additional force prestr. tendon	ΔN_p	1.615.498	[N]	= Ap * (σ_p - $\sigma_{pm\infty}$)	

Horizontal force equilibrium

1.102 → OK

Eccentricities

Concrete	=	ec	602	[mm]	= h/2 - β*xu
Top reinforcement	=	est	494	[mm]	= h/2 - dst
Bottom reinforcement	=	esb	-587	[mm]	= dsb - h/2
Prestressing tendon	=	esp	-100	[mm]	= dp - h/2

Results

Effective depth steel	d_{eff}		[mm]	
Rotational capacity check		-		
Bending moment resistance	M_{Rd}	5.244	[kNm]	
	u.c.	0,48	→	OK

ULS: Bending moment resistance 3 - Verifications

Inputs

Cross-section analysed	x	12,597	[m]
Cross-section height	h	1600	[mm]
Tendons amount	n	0	[-]
Prestressing tendon area	A_p	-	[mm^2]
Prestressing tendon depth	d_p	0	[mm]
Normal force	Ned	1.000.000	[N]
Bending moment	Med	3.000	[kNm]

Reinforcement

Shear reinforcement diameter	ϕ	16	[mm]
Shear reinforcement distance	s	300	[mm]
Top reinforcement area	Ast	3272	[mm^2]
Top reinforcement depth	dst	113,5	[mm]
Bottom reinforcement area	Asb	25133	[mm^2]
Bottom reinforcement depth	dsb	1394	[mm]

Compression zone height

Compression zone height	x_u	**486,3**	[mm]
dx for horizontal force equilibrium	dx	0	[mm]

Strains

Total prestressing tendon strain	εp	0,00265385	[-]	= εp,∞ + Δεp
	$\Delta\varepsilon_p$	-0,0035	[-]	= ε_{uk} (d_p/x_u - 1)
	$\varepsilon_{pm\infty}$	0,00615385	[-]	= $\sigma_{pm\infty}$ / E_p
	εst	-0,00268317	[-]	= ((xu - dst)/xu) * εuk
	εsb	0,00653231	[-]	= ((dst - xu)/xu) * εuk

Stresses

Actual prestressing stress	σp	517,5	[N/mm^2]
Top reinforcement stress	σst	-435	[N/mm^2]
Top reinforcement stress	σsb	435	[N/mm^2]

Prestressing design



Prestressing stress per tendon (t = ∞)	$\sigma_{pm\infty}$	1200	[N/mm^2]
Total prestressing force (t = ∞)	$P_{m\infty}$	-	[N]

Material properties

Concrete

Characteristic compressive strength	fck	35	[N/mm^2]
Design compressive strength	fcd	23,33	[N/mm^2]
Concrete strain at failure	εuk	-0,0035	[-]
	α	0,75	[-]
	β	0,39	[-]

Reinforcement steel

Yield strength	fyd	435	[N/mm^2]
	Es	200000	

Prestressing steel

E-modulus	E_p	195000	[N/mm^2]
Yield strength	f_{pk}	1860	[N/mm^2]
	$f_{p0,1k}$		[N/mm^2]
	f_{pd}	1522	[N/mm^2]
Assumed prestr. stress at failure	σ_{pu}	1522	[N/mm^2]

= ([Asb * fyd] + [Ap * (fpd - σpu)] + [σpu * Ap] - [Ned] - [Ast * fyd]) / (α * fcd * b)) + dx

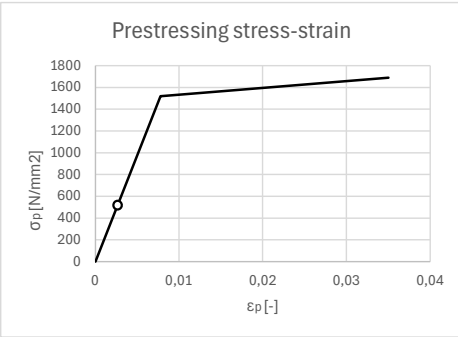

Forces

Force in the concrete	Nc	-8.509.535	[N]	= α * xu * fcd * 1000
Force in the top reinforcement	Nst	-1.423.320	[N]	= Ast * σst
Force in the bot. reinforcement	Nsb	10.932.855	[N]	= Asb * σsb
Additional force prestr. tendon	ΔNp	-	[N]	= Ap * (σp - σpm∞)

Horizontal force equilibrium

- → OK

Eccentricities

Concrete	=	ec	610	[mm]	= h/2 - β*xu
Top reinforcement	=	est	687	[mm]	= h/2 - dst
Bottom reinforcement	=	esb	-594	[mm]	= dsb - h/2
Prestressing tendon	=	esp	800	[mm]	= dp - h/2

Results

Effective depth steel	deff		[mm]	
Rotational capacity check		-		
Bending moment resistance	MRd	12.665	[kNm]	
	u.c.	0,24	→	OK

ULS: Shear force resistance 1 - **Verifications**

Inputs

Cross-section analysed	x	0,998	[m]
Cross-section height	h	1200	[mm]
Tendons amount	n	2	[-]
Prestressing tendon area	A_p	**4500**	[mm^2]
Prestressing tendon depth	d_p	600	[mm]
Normal force	Ned	800.000	[N]
Bending moment	Med	1	[kNm]
Shear force	Ved	1.200.000	[N]

Location check



Prestressing stress per tendon (t = ∞)	$\sigma_{pm\infty}$	1200	[N/mm^2]
Total prestressing force (t = ∞)	$P_{m\infty}$	5.400.000	[N]

Reinforcement

Shear reinforcement diameter	ϕ	16	[mm]
Shear reinforcement distance	s	300	[mm]
Top reinforcement area	Ast	3272	[mm^2]
Top reinforcement depth	dst	113,5	[mm]
Bottom reinforcement area	Asb	25133	[mm^2]
Bottom reinforcement depth	dsb	994	[mm]

Material properties

Concrete

Characteristic compressive strength	fck	35	[N/mm^2]
Design compressive strength	fcd	23,33	[N/mm^2]

Reinforcement steel

Yield strength	fyd	435	[N/mm^2]

	xu	**500**	[mm]

Without shear reinforcement [NEN-EN 1992-1-1]

	A_{sl}	25133	[mm^2]	
	d_{sl}	994	[mm]	
Check if dp is within the tensile zone			→	Yes
	A_p	4500	[mm]	
	d_{eff}	934,16806	[mm]	
	ρ_l	0,0317		
	k_1	0,15		
	$C_{Rd,c}$	0,12		
	σ_{cp}	3,833	< 0,2 f_{cd}	4,666667 N/mm2
	k	1,463	< 2.0	
	v_{min}	0,94	[N/mm^2]	
	v_{Rdc}	1,42	[N/mm^2]	
	V_{min}	879.332	[N]	u.c. 1,36
	V_{Rdc}	1.325.224	[N]	u.c. 0,91

With shear reinforcement [NEN-EN 1992-1-1]

Area shear reinforcement	A_{sw}	804,2	[mm^2]	
Stirrup diameter	ϕ_{stir}	16	[mm]	
	s	300	[mm]	
Assumed as z = 0,9 * d_{eff}	z	841	[mm]	
	θ	39	[deg]	
	v1	0,516		
	αcw	1,16		
	$V_{Rd,s}$	1.210.755	[N]	u.c. 0,99
	$V_{Rd,max}$	5.764.053	[N]	u.c. 0,21

ULS: Shear force resistance 2 - Verifications

Inputs

Cross-section analysed	x	12,257	[m]
Cross-section height	h	1400	[mm]
Tendons amount	n	2	[-]
Prestressing tendon area	A_p	**4500**	[mm²]
Prestressing tendon depth	d_p	800	[mm]
Normal force	Ned	800.000	[N]
Bending moment	Med	-1	[kNm]
Shear force	Ved	2.000.000	[N]

Prestressing design



Prestressing stress per tendon (t = ∞)	$\sigma_{pm\infty}$	1200	[N/mm²]
Total prestressing force (t = ∞)	$P_{m\infty}$	5.400.000	[N]

Reinforcement

Shear reinforcement diameter	ϕ	16	[mm]
Shear reinforcement distance	s	300	[mm]
Top reinforcement area	Ast	3272	[mm²]
Top reinforcement depth	dst	113,5	[mm]
Bottom reinforcement area	Asb	25133	[mm²]
Bottom reinforcement depth	dsb	1194	[mm]

Material properties

Concrete

Characteristic compressive strength	fck	35	[N/mm²]
Design compressive strength	fcd	23,33	[N/mm²]

Reinforcement steel

Yield strength	fyd	435	[N/mm²]

	xu	**300,0**	[mm]

Without shear reinforcement [NEN-EN 1992-1-1]

	A_{sl}	3272	[mm²]		
	d_{sl}	1286,5	[mm]		
Check if dp is within the tensile zone			→	Yes	(since the moment is negative, dp = h - dp)
	A_p	4500	[mm]		
	d_{eff}	1004,8157	[mm]		
	ρ_l	0,0077			
	k_1	0,15			
	$C_{Rd,c}$	0,12			
	σ_{cp}	3,286	< 0,2 f_{cd}	4,666667	N/mm2
	k	1,446	< 2.0		
	v_{min}	0,85	[N/mm²]		
	v_{Rdc}	1,01	[N/mm²]		
	V_{min}	857.060	[N]	u.c.	2,33
	V_{Rdc}	1.018.811	[N]	u.c.	1,96

With shear reinforcement [NEN-EN 1992-1-1]

Area shear reinforcement	A_{sw}	804,2	[mm²]		
Stirrup diameter	ϕ_{stir}	16	[mm]		
	s	300	[mm]		
Assumed as z = 0,9 * d_{eff}	z	904	[mm]		
	θ	39	[deg]		
	v1	0,516			
	αcw	1,14			
	$V_{Rd,s}$	1.302.320	[N]	u.c.	1,54
	$V_{Rd,max}$	6.074.990	[N]	u.c.	0,33

ULS: Shear force resistance 3	-	**Verifications**					
Inputs				**Prestressing design**			
Cross-section analysed	x	13,561	[m]				
Cross-section height	h	**1600**	[mm]				
Tendons amount	n	**0**	[-]				
Prestressing tendon area	A_p	**0**	[mm^2]				
Prestressing tendon depth	d_p	**0**	[mm]	Prestressing stress per tendon (t = ∞)	$\sigma_{pm\infty}$	1200	[N/mm^2]
Normal force	Ned	**1.000.000**	[N]	Total prestressing force (t = ∞)	$P_{m\infty}$	-	[N]
Bending moment	Med	**1**	[kNm]				
Shear force	Ved	**2.000.000**	[N]				
Reinforcement				**Material properties**			
Shear reinforcement diameter	ϕ	**16**	[mm]	**Concrete**			
Shear reinforcement distance	s	**300**	[mm]	Characteristic compressive strength	fck	35	[N/mm^2]
Top reinforcement area	Ast	**3272**	[mm^2]	Design compressive strength	fcd	23,33	[N/mm^2]
Top reinforcement depth	dst	**113,5**	[mm]	**Reinforcement steel**			
Bottom reinforcement area	Asb	**25133**	[mm^2]	Yield strength	fyd	435	[N/mm^2]
Bottom reinforcement depth	dsb	**1394**	[mm]				

	xu	**200,0**	[mm]		
Without shear reinforcement [NEN-EN 1992-1-1]					
	A_{sl}	25133	[mm^2]		
	d_{sl}	1394	[mm]		
Check if dp is within the tensile zone			→	No	
	A_p	0	[mm]		
	d_{eff}	1394	[mm]		
	ρ_l	0,0180			
	k_1	0,15			
	$C_{Rd,c}$	0,12			
	σ_{cp}	-0,625	< 0,2 f_{cd}	4,666667 N/mm2	
	k	1,379	< 2.0		
	v_{min}	0,24	[N/mm^2]		
	v_{Rdc}	0,56	[N/mm^2]		
	V_{min}	336.623	[N]	u.c. 5,94	
	V_{Rdc}	787.549	[N]	u.c. 2,54	
With shear reinforcement [NEN-EN 1992-1-1]					
Area shear reinforcement	A_{sw}	804,2	[mm^2]		
Stirrup diameter	ϕ_{stir}	16	[mm]		
	s	300	[mm]		
Assumed as z = 0,9 * d_{eff}	z	1.255	[mm]		
	θ	39	[deg]		
	v1	0,516			
	αcw	0,97			
	$V_{Rd,s}$	1.806.733	[N]	u.c. 1,11	
	$V_{Rd,ma}$	7.189.764	[N]	u.c. 0,28	

SLS: Crack width control 1 - **Verifications**

Inputs

Cross-section analysed	x	6,09	[m]
Cross-section height	h	1200	[mm]
Tendons amount	n	2	[-]
Prestressing tendon area (total)	A_p	4.500	[mm²]
Prestressing tendon depth	d_p	600,00	[mm]
Normal force	N	800	[kN]
Bending moment	M	2000,00	[kNm]

Reinforcement

Shear reinforcement diameter	ϕ	16	[mm]
Shear reinforcement distance	s	300	[mm]
Top reinforcement area	Ast	3272	[mm²]
Top reinforcement depth	dst	113,5	[mm]
	ϕst	25	[mm]
Bottom reinforcement area	Asb	25133	[mm²]
Bottom reinforcement depth	dsb	994	[mm]
	ϕsb	40	[mm]
	ξ	0,5	
	ξ1	0,51336	
		$=\sqrt{\xi * \varphi_s/\varphi_p}$	
	kx	1,64	

Prestressing design



Prestressing stress per tendon (t = ∞)	$\sigma_{pm\infty}$	1200	[N/mm²]
Total prestressing force (t = ∞)	$P_{m\infty}$	5.400.000	[N]
Tendon area (per tendon)	Ap	2250	[mm²]
Tendon equivalent diameter	ϕ	75,89	[mm]

Material properties

Concrete

Characteristic compressive strength	fck	35	[N/mm²]
Design compressive strength	fcd	23,33	[N/mm²]
E-modulus	E_{cm}	34000	[N/mm²]
E-modulus (= Ecm/ (1+1,4))	E_c	14.166,7	[N/mm²]
Concrete strain at failure	εuk	0,0035	[-]
Tensile strength	fctm	3,2	[N/mm²]

Reinforcement steel

Yield strength	fyd	435	[N/mm²]
E-modulus	E_s	200000	[N/mm²]

Prestressing steel

E-modulus	E_p	195000	[N/mm²]

Strains

Top reinforcement strain	εst	0,00303	[-]	= εc * ((x-dst)/x)
Bottom reinforcement strain	εsb	0,00061	[-]	= εc * ((dsb-x)/x)
Prestressing strain (due to bending)	Δεp	-0,00102	[-]	= εc * ((dp-x)/x)

Forces

Force in the concrete	N_c	= Ec*εc*x*b*1/2	[N]	
Force in the top reinforcement	N_{st}	= εst*Es*Ast	[N]	
Force in the bot. reinforcement	N_{sb}	= εsb*Es*Asb	[N]	
Additional force prestr. tendon	ΔN_p	= ξ1*Δεp*Ep*Ap	[N]	

Eccentricities

Concrete	ec	= 1750 - x/3	[mm]	= h - x/3
Top reinforcement	est	1087	[mm]	= h - dst
Bottom reinforcement	esb	206	[mm]	= h - dsb
Prestressing tendon	ep	600	[mm]	= h - dp
Pminf	epm∞	600	[mm]	= h/2
Normal force	eN	600	[mm]	= h/2

Compression zone height and concrete strain

Compression zone height	xu	846	[mm]	
Concrete top edge strain	εc	0,0007913	[-]	

Effective reinforcement

Effective height	hc,eff	117,95	[mm]	= min(2,5*(h-d) ; (h-x)/3 ; h/2)
Effective area	Aceff	117948,35	[mm²]	
Effective reinforcement	**ρp,eff**	0,2130848		

Crack widths (EN 1992-1-1 7.3.4 equation 7.8)

Concrete cover	c	106	[mm]		
	$s_{r,max}$	392,31	[mm]	= k3*c + k1*k2*k4*(ϕ/ρp,eff)	k1 = 0,8 k2=0,5 k3 = 3,4 k4 = 0,425
	αe	5,8824		= Es/Ecm	NEN-EN 1992-1-1 NA
Depth lowest reinforcement bar	d	1070	[mm]		
Strain bottom reinforcement	εsb	0,0002	[-]		kt = 0,4 (long term)
Stress bottom reinforcement	σsb	41,8686	[N/mm²]		
εsm - εcm		0,00014	[-]		
Crack width	wmax	0,056	[mm]	= sr,max * (εsm - εcm)	
wmax < 0,342 (= 0,2 * kx)	u.c.	0,17	→	OK	

SLS: Crack width control 2 - **Verifications**

Inputs

Cross-section analysed	x	6,09	[m]	
Cross-section height	h	1400	[mm]	
Tendons amount	n	2	[-]	
Prestressing tendon area (total)	A_p	4.500	[mm²]	
Prestressing tendon depth	d_p	800,00	[mm]	
Normal force	N	800	[kN]	
Bending moment	M	2500,00	(-) [kNm]	

Reinforcement

Shear reinforcement diameter	ϕ	16	[mm]	
Shear reinforcement distance	s	300	[mm]	
Top reinforcement area	Ast	25133	[mm²]	
Top reinforcement depth	dst	206	[mm]	
	ϕst	40	[mm]	
Bottom reinforcement area	Asb	3272	[mm²]	
Bottom reinforcement depth	dsb	1286,5	[mm]	
	ϕsb	25	[mm]	
	ξ	0,5		
	ξ1	0,40585		
		$=\sqrt{\xi * \varphi_s/\varphi_p}$		
	kx	1,70		

Prestressing design



Prestressing stress per tendon (t = ∞)	$\sigma_{pm\infty}$	1200	[N/mm²]	
Total prestressing force (t = ∞)	$P_{m\infty}$	5.400.000	[N]	
Tendon area (per tendon)	Ap	2250	[mm²]	
Tendon equivalent diameter	ϕ	75,89	[mm]	

Material properties

Concrete

Characteristic compressive strength	fck	35	[N/mm²]	
Design compressive strength	fcd	23,33	[N/mm²]	
E-modulus	E_{cm}	34000	[N/mm²]	
E-modulus (= Ecm/ (1+1,4))	E_c	14.166,7	[N/mm²]	
Concrete strain at failure	εuk	0,0035	[-]	
Tensile strength	fctm	3,2	[N/mm²]	

Reinforcement steel

Yield strength	fyd	435	[N/mm²]	
E-modulus	E_s	200000	[N/mm²]	

Prestressing steel

E-modulus	E_p	195000	[N/mm²]	

Strains

Top reinforcement strain	εst	0,00250	[-]	= εc * ((x-dst)/x)
Bottom reinforcement strain	εsb	0,00275	[-]	= εc * ((dsb-x)/x)
Prestressing strain (due to bending)	Δεp	0,00038	[-]	= εc * ((dp-x)/x)

Forces

Force in the concrete	N_c	= Ec*εc*x*b*1/2	[N]	
Force in the top reinforcement	N_{st}	= εst*Es*Ast	[N]	
Force in the bot. reinforcement	N_{sb}	= εsb*Es*Asb	[N]	
Additional force prestr. tendon	ΔN_p	= ξ1*Δεp*Ep*Ap	[N]	

Eccentricities

Concrete	ec	= 1750 - x/3	[mm]	= h - x/3
Top reinforcement	est	1194	[mm]	= h - dst
Bottom reinforcement	esb	114	[mm]	= h - dsb
Prestressing tendon	ep	600	[mm]	= h - dp
Pminf	epm∞	700	[mm]	= h/2
Normal force	eN	700	[mm]	= h/2

Compression zone height and concrete strain

Compression zone height	xu	721	[mm]	
Concrete top edge strain	εc	0,0005648	[-]	

Effective reinforcement

Effective height	hc,eff	226,38	[mm]	= min(2,5*(h-d) ; (h-x)/3 ; h/2)
Effective area	Aceff	226376,63	[mm²]	
Effective reinforcement	$\rho_{p,eff}$	0,0144538		

Crack widths (EN 1992-1-1 7.3.4 equation 7.8)

Concrete cover	c	101	[mm]		
	$s_{r,max}$	637,44	[mm]	= k3*c + k1*k2*k4*(ϕ/ρp,eff)	k1 = 0,8 k2=0,5 k3 = 3,4 k4 = 0,425
	αe	5,8824		= Es/Ecm	NEN-EN 1992-1-1 NA
Depth lowest reinforcement bar	d	1286,5	[mm]		
Strain bottom reinforcement	εsb	0,0004	[-]		kt = 0,4 (long term)
Stress bottom reinforcement	σsb	88,6417	[N/mm²]		
εsm - εcm		0,00027	[-]		
Crack width	wmax	0,170	[mm]	= sr,max * (εsm - εcm)	
wmax < 0,342 (= 0,2 * kx)	u.c.	0,50	→	OK	

SLS: Crack width control 3 - Verifications

Inputs

Cross-section analysed	x	6,09	[m]
Cross-section height	h	1600	[mm]
Tendons amount	n	0	[-]
Prestressing tendon area (total)	A_p	-	[mm²]
Prestressing tendon depth	d_p	0,00	[mm]
Normal force	N	800	[kN]
Bending moment	M	1500	[kNm]

Reinforcement

Shear reinforcement diameter	ϕ	16	[mm]
Shear reinforcement distance	s	300	[mm]
Top reinforcement area	Ast	3272	[mm²]
Top reinforcement depth	dst	113,5	[mm]
	ϕst	25	[mm]
Bottom reinforcement area	Asb	25133	[mm²]
Bottom reinforcement depth	dsb	1394	[mm]
	ϕsb	40	[mm]
	ξ	0,5	
	ξ1	0,51336	
		$=\sqrt{\xi * \varphi_s/\varphi_p}$	
	kx	1,64	

Prestressing design



Prestressing stress per tendon (t = ∞)	$\sigma_{pm\infty}$	1200	[N/mm²]
Total prestressing force (t = ∞)	$P_{m\infty}$	-	[N]
Tendon area (per tendon)	Ap	2250	[mm²]
Tendon equivalent diameter	ϕ	75,89	[mm]

Material properties

Concrete

Characteristic compressive strength	fck	35	[N/mm²]
Design compressive strength	fcd	23,33	[N/mm²]
E-modulus	E_{cm}	34000	[N/mm²]
E-modulus (= Ecm/ (1+1,4))	E_c	14.166,7	[N/mm²]
Concrete strain at failure	εuk	0,0035	[-]
Tensile strength	fctm	3,2	[N/mm²]

Reinforcement steel

Yield strength	fyd	435	[N/mm²]
E-modulus	E_s	200000	[N/mm²]

Prestressing steel

E-modulus	E_p	195000	[N/mm²]

Strains

Top reinforcement strain	εst	0,00274	[-]	= εc * ((x-dst)/x)
Bottom reinforcement strain	εsb	0,00578	[-]	= εc * ((dsb-x)/x)
Prestressing strain (due to bending)	Δεp	-0,00350	[-]	= εc * ((dp-x)/x)

Forces

Force in the concrete	Nc	= Ec*εc*x*b*1/2	[N]	
Force in the top reinforcement	Nst	= εst*Es*Ast	[N]	
Force in the bot. reinforcement	Nsb	= εsb*Es*Asb	[N]	
Additional force prestr. tendon	ΔNp	= ξ1*Δεp*Ep*Ap	[N]	

Eccentricities

Concrete	ec	= 1750 - x/3	[mm]	= h - x/3
Top reinforcement	est	1487	[mm]	= h - dst
Bottom reinforcement	esb	206	[mm]	= h - dsb
Prestressing tendon	ep	1600	[mm]	= h - dp
Pminf	epm∞	800	[mm]	= h/2
Normal force	eN	800	[mm]	= h/2

Compression zone height and concrete strain

Compression zone height	xu	526	[mm]	
Concrete top edge strain	εc	0,0001972	[-]	

Effective reinforcement

Effective height	hc,eff	358,01	[mm]	= min(2,5*(h-d) ; (h-x)/3 ; h/2)
Effective area	Aceff	358011,88	[mm²]	
Effective reinforcement	ρp,eff	0,0702016		

Crack widths (EN 1992-1-1 7.3.4 equation 7.8)

Concrete cover	c	106	[mm]		
	sr,max	457,26	[mm]	= k3*c + k1*k2*k4*(ϕ/ρp,eff)	k1 = 0,8 k2=0,5 k3 = 3,4 k4 = 0,425
	αe	5,8824		= Es/Ecm	NEN-EN 1992-1-1 NA
Depth lowest reinforcement bar	d	1470	[mm]		
Strain bottom reinforcement	εsb	0,0004	[-]		kt = 0,4 (long term)
Stress bottom reinforcement	σsb	70,7805	[N/mm²]		
εsm - εcm		0,00023	[-]		
Crack width	wmax	0,103	[mm]	= sr,max * (εsm - εcm)	
wmax < 0,342 (= 0,2 * kx)	u.c.	0,31	→	OK	

H Calculations

H.1 Chapter 4: Analytical results

H.1.1 Section 4.4 - Analytical results

ULS: Bending moment resistance 1 - **Original (analytical loads)**

Inputs

Cross-section analysed	x	7,05	[m]
Cross-section height	h	1750	[mm]
Tendons amount	n	0	[-]
Prestressing tendon area	A_p	0	[mm^2]
Prestressing tendon depth	d_p	0	[mm]
Normal force	Ned	938000	[N]
Bending moment	Med	5848	[kNm]

Reinforcement

Shear reinforcement diameter	ϕ	16	[mm]
Shear reinforcement distance	s	300	[mm]
Top reinforcement area	Ast	3272	[mm^2]
Top reinforcement depth	dst	113,5	[mm]
Bottom reinforcement area	Asb	25133	[mm^2]
Bottom reinforcement depth	dsb	1544	[mm]

Floor design

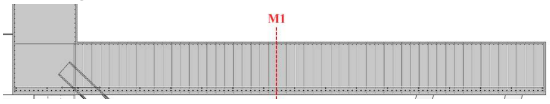

Prestressing stress per tendon (t = ∞)	$\sigma_{pm\infty}$	0	[N/mm^2]
Total prestressing force (t = ∞)	$P_{m\infty}$	-	[N]

Material properties

Concrete

Characteristic compressive strength	fck	35	[N/mm^2]
Design compressive strength	fcd	23,33	[N/mm^2]
Concrete strain at failure	εuk	-0,0035	[-]
	α	0,75	[-]
	β	0,39	[-]

Reinforcement steel

Yield strength	fyd	435	[N/mm^2]
	Es	200000	

Prestressing steel

E-modulus	E_p	195000	[N/mm^2]
Yield strength	f_{pk}	1860	[N/mm^2]
	$f_{p0,1k}$		[N/mm^2]
	f_{pd}	1522	[N/mm^2]
Assumed prestr. stress at failure	σ_{pu}	1522	[N/mm^2]

Compression zone height

Compression zone height	x_u	**489,871982**	[mm]	= ([Asb * fyd] + [Ap * (fpd - σpu)] + [σpu * Ap] - [Ned] - [Ast * fyd]) / (α * fcd * b)) + dx
dx for horizontal force equilibrium	dx	0	[mm]	

Strains

Total prestressing tendon strain	εp	0	[-]	= εp,∞ + Δεp
	Δεp	0	[-]	= εuk (dp/xu - 1)
	$\varepsilon_{pm\infty}$	0	[-]	= σpm∞ / Ep
	εst	-0,00268907	[-]	= ((xu - dst)/xu) * εuk
	εsb	0,00753145	[-]	= ((xu - dsb)/xu) * εuk

Stresses

Actual prestressing stress	σp	0	[N/mm^2]
Top reinforcement stress	σst	-435	[N/mm^2]
Top reinforcement stress	σsb	435	[N/mm^2]

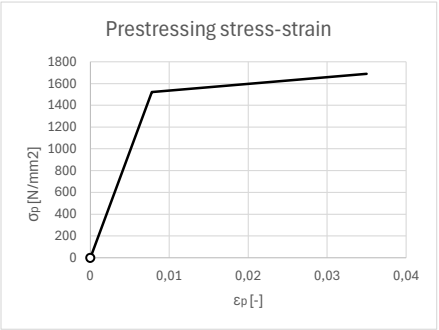

Forces

Horizontal force equilibrium

Force in the concrete		Nc	-8.571.535	[N]	= α * xu * fcd * 1000	-	→ OK
Force in the top reinforcement		Nst	-1.423.320	[N]	= Ast * σst		
Force in the bot. reinforcement		Nsb	10.932.855	[N]	= Asb * σsb		
Additional force prestr. tendon		ΔNp	-	[N]	= Ap * (σp - σpm∞)		

Eccentricities

Concrete	=	ec	684	[mm]	= h/2 - β*xu
Top reinforcement	=	est	762	[mm]	= h/2 - dst
Bottom reinforcement	=	esb	-669	[mm]	= h/2 - dsb
Prestressing tendon	=	esp	0	[mm]	= h/2 -dp

Results

Effective depth steel	deff		[mm]	
Rotational capacity check		OK		xu/deff < ((fpk/1.1) -σpm∞) * Ap + fyd*Asb) / (Ap + Asb)
Bending moment resistance	MRd	14.260	[kNm]	
	u.c.	0,41	→	OK

ULS: Bending moment resistance 2 - **Original (analytical loads)**

Inputs

Cross-section analysed	x	15,597	[m]	
Cross-section height	h	1750	[mm]	
Tendons amount	n	0	[-]	
Prestressing tendon area	A_p	0	[mm^2]	
Prestressing tendon depth	d_p	0	[mm]	
Normal force	Ned	398.000	[N]	
Bending moment	Med	406,9	(-) [kNm]	

Reinforcement

Shear reinforcement diameter	ϕ	16	[mm]	
Shear reinforcement distance	s	300	[mm]	
Top reinforcement area	Ast	25134	[mm^2]	
Top reinforcement depth	dst	206	[mm]	
Bottom reinforcement area	Asb	3272	[mm^2]	
Bottom reinforcement depth	dsb	1636,5	[mm]	

Floor design

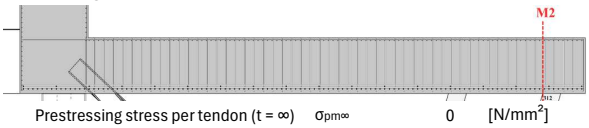

Prestressing stress per tendon (t = ∞)	$\sigma_{pm\infty}$	0	[N/mm^2]
Total prestressing force (t = ∞)	$P_{m\infty}$	-	[N]

Material properties

Concrete

Characteristic compressive strength	fck	35	[N/mm^2]
Design compressive strength	fcd	23,33	[N/mm^2]
Concrete strain at failure	εuk	-0,0035	[-]
	α	0,75	[-]
	β	0,39	[-]

Reinforcement steel

Yield strength	fyd	435	[N/mm^2]
	Es	200000	

Prestressing steel

E-modulus	E_p	195000	[N/mm^2]
Yield strength	f_{pk}	1860	[N/mm^2]
	$f_{p0,1k}$		[N/mm^2]
	f_{pd}	1522	[N/mm^2]
Assumed prestr. stress at failure	σ_{pu}	1522	[N/mm^2]

Compression zone height

Compression zone height	xu	**183,249446**	[mm]	= ([Asb * fyd] + [Ap * (fpd - σpu)] + [σpu * Ap] - [Ned] - [Ast * fyd]) / (α * fcd * b)) + dx
dx for horizontal force equilibrium	dx	749,5	[mm]	

Strains

Total prestressing tendon strain	εp	0	[-]	= εp,∞ + Δεp
	Δεp	0	[-]	= εuk (dp/xu - 1)
	εpm∞	0	[-]	= σpm∞ / Ep
	εst	0,00043453	[-]	= ((xu - dst)/xu) * εuk
	εsb	0,02775657	[-]	= ((dst - xu)/xu) * εuk

Stresses

Actual prestressing stress	σp	0	[N/mm^2]
Top reinforcement stress	σst	86,9055175	[N/mm^2]
Top reinforcement stress	σsb	435	[N/mm^2]

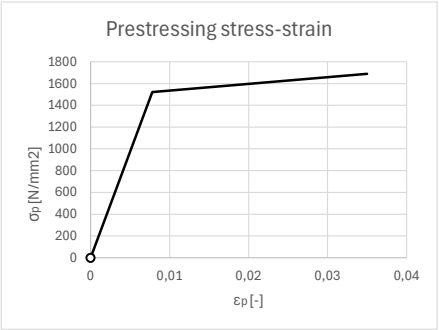

Forces

Force in the concrete	Nc	-3.206.407	[N]	= α * xu * fcd * 1000
Force in the top reinforcement	Nst	2.184.283	[N]	= Ast * σst
Force in the bot. reinforcement	Nsb	1.423.320	[N]	= Asb * σsb
Additional force prestr. tendon	ΔNp	-	[N]	= Ap * (σp - σpm∞)

Horizontal force equilibrium

3.196 → OK

Eccentricities

Concrete	=	ec	804	[mm]	= h/2 - β*xu
Top reinforcement	=	est	669	[mm]	= h/2 - dst
Bottom reinforcement	=	esb	-762	[mm]	= h/2 - dsb
Prestressing tendon	=	esp	875	[mm]	= h/2 -dp

Results

Effective depth steel	deff		[mm]	
Rotational capacity check		-		
Bending moment resistance	MRd	2.199	[kNm]	
	u.c.	0,19	→	OK

ULS: Shear force resistance 1 - **Original (analytical loads)**

Inputs

Cross-section analysed	x	0,998	[m]
Cross-section height	h	1.750	[mm]
Tendons amount	n	0	[-]
Prestressing tendon area	A_p	0	[mm^2]
Prestressing tendon depth	d_p	0	[mm]
Normal force	Ned	938.000	[N]
Bending moment	Med	808	[kNm]
Bending moment	Ved	1.792.800	[N]

Prestressing design

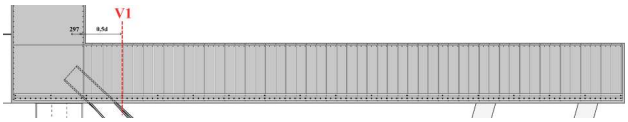

Prestressing stress per tendon (t = ∞)	$\sigma_{pm\infty}$	0	[N/mm^2]
Total prestressing force (t = ∞)	$P_{m\infty}$	-	[N]

Reinforcement

Shear reinforcement diameter	ϕ	16	[mm]
Shear reinforcement distance	s	300	[mm]
Top reinforcement area	Ast	3.272	[mm^2]
Top reinforcement depth	dst	114	[mm]
Bottom reinforcement area	Asb	25.133	[mm^2]
Bottom reinforcement depth	dsb	1.544	[mm]

Material properties

Concrete

Characteristic compressive strength	fck	35	[N/mm^2]
Design compressive strength	fcd	23,33	[N/mm^2]

Reinforcement steel

Yield strength	fyd	435	[N/mm^2]

	xu	-	[mm]		
Without shear reinforcement [NEN-EN 1992-1-1]					
	A_{sl}	25133	[mm^2]		
	d_{sl}	1544	[mm]		
Check if dp is within the tensile zone			→	No	
	A_p	0	[mm]		
	d_{eff}	1544	[mm]		
	ρ_l	0,0163			
	k_1	0,15			
	$C_{Rd,c}$	0,12			
	σ_{cp}	-0,536	< 0,2 f_{cd}	4,666667	N/mm2
	k	1,360	< 2.0		
	v_{min}	0,25	[N/mm^2]		
	v_{Rdc}	0,55	[N/mm^2]		
	V_{min}	382.869	[N]	u.c.	4,68
	V_{Rdc}	845.389	[N]	u.c.	2,12
With shear reinforcement [NEN-EN 1992-1-1]					
Area shear reinforcement	A_{sw}	804,2	[mm^2]		
Stirrup diameter	ϕ_{stir}	16	[mm]		
	s	300	[mm]		
Assumed as z = 0,9 * d_{eff}	z	1.390	[mm]		
	θ	39	[deg]		
	v1	0,516			
	αcw	0,98			
	$V_{Rd,s}$	2.001.144	[N]	u.c.	0,90
	$V_{Rd,max}$	7.994.622	[N]	u.c.	0,22

ULS: Shear force resistance 3 - **Original (analytical loads)**

Inputs

Cross-section analysed	x	12,909	[m]
Cross-section height	h	1750	[mm]
Tendons amount	n	0	[-]
Prestressing tendon area	A_p	0	[mm^2]
Prestressing tendon depth	d_p	0	[mm]
Normal force	Ned	938.000	[N]
Bending moment	Med	2216,0	[kNm]
Bending moment	Ved	1.521.936	[N]

Reinforcement

Shear reinforcement diameter	ϕ	16	[mm]
Shear reinforcement distance	s	300	[mm]
Top reinforcement area	Ast	3272	[mm^2]
Top reinforcement depth	dst	113,5	[mm]
Bottom reinforcement area	Asb	25133	[mm^2]
Bottom reinforcement depth	dsb	1544	[mm]

Prestressing design

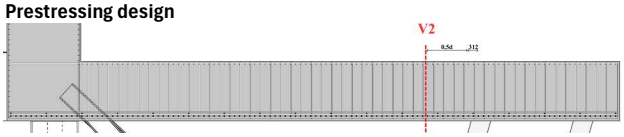

Prestressing stress per tendon (t = ∞)	$\sigma_{pm\infty}$	0	[N/mm^2]
Total prestressing force (t = ∞)	$P_{m\infty}$	-	[N]

Material properties

Concrete

Characteristic compressive strength	fck	35	[N/mm^2]
Design compressive strength	fcd	23,33	[N/mm^2]

Reinforcement steel

Yield strength	fyd	435	[N/mm^2]

	xu	-	[mm]		
Without shear reinforcement [NEN-EN 1992-1-1]					
	A_{sl}	25133	[mm^2]		
	d_{sl}	1544	[mm]		
Check if dp is within the tensile zone			→	No	
	A_p	0	[mm]		
	d_{eff}	1544	[mm]		
	ρ_l	0,0163			
	k_1	0,15			
	$C_{Rd,c}$	0,12			
	σ_{cp}	-0,536	< 0,2 f_{cd}	4,666667	N/mm2
	k	1,360	< 2.0		
	v_{min}	0,25	[N/mm^2]		
	v_{Rdc}	0,55	[N/mm^2]		
	V_{min}	382.869	[N]	u.c.	3,98
	V_{Rdc}	845.389	[N]	u.c.	1,80
With shear reinforcement [NEN-EN 1992-1-1]					
Area shear reinforcement	A_{sw}	804,2	[mm^2]		
Stirrup diameter	ϕ_{stir}	16	[mm]		
	s	300	[mm]		
Assumed as z = 0,9 * d_{eff}	z	1.390	[mm]		
	θ	39	[deg]		
	v1	0,516			
	αcw	0,98			
	$V_{Rd,s}$	2.001.144	[N]	u.c.	0,76
	$V_{Rd,ma}$	7.994.622	[N]	u.c.	0,19

SLS: Crack width control - **Original (analytical loads)**

Inputs

Cross-section analysed	x	6,92	[m]
Cross-section height	h	1750	[mm]
Tendons amount	n	0	[-]
Prestressing tendon area (total)	A_p	0	[mm^2]
Prestressing tendon depth	d_p	0	[mm]
Normal force	N	519	[kN]
Bending moment	M	3792,5	[kNm]

Reinforcement

Shear reinforcement diameter	ϕ	16	[mm]
Shear reinforcement distance	s	300	[mm]
Top reinforcement area	Ast	3272	[mm^2]
Top reinforcement depth	dst	113,5	[mm]
	ϕst	25	[mm]
Bottom reinforcement area	Asb	25133	[mm^2]
Bottom reinforcement depth	dsb	1544	[mm]
	ϕsb	40	[mm]
	ξ	0,5	
	ξ1	0,51336	
		$=\sqrt{\xi * \varphi_s/\varphi_p}$	
	kx	1,64	

Prestressing design

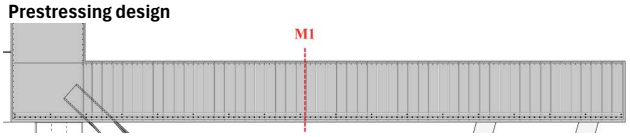

Prestressing stress per tendon (t = ∞)	$\sigma_{pm\infty}$	1200	[N/mm^2]
Total prestressing force (t = ∞)	$P_{m\infty}$	-	[N]
Tendon area (per tendon)	Ap	2250	[mm^2]
Tendon equivalent diameter	ϕ	75,89	[mm]

Material properties

Concrete

Characteristic compressive strength	fck	35	[N/mm^2]
Design compressive strength	fcd	23,33	[N/mm^2]
E-modulus	E_{cm}	34000	[N/mm^2]
E-modulus (= Ecm/ (1+ϕ))	E_c	14166,67	[N/mm^2]
Concrete strain at failure	εuk	0,0035	[-]
Tensile strength	fctm	3,2	[N/mm^2]

Reinforcement steel

Yield strength	fyd	435	[N/mm^2]
E-modulus	E_s	200000	[N/mm^2]

Prestressing steel

E-modulus	E_p	195000	[N/mm^2]

Strains

Top reinforcement strain	εst	0,00291	[-]	= ε_c * ((x-d_{st})/x)
Bottom reinforcement strain	εsb	0,00447	[-]	= ε_c * ((d_{sb}-x)/x)
Prestressing strain (due to bending)	$\Delta\varepsilon_p$	-0,00350	[-]	= ε_c * ((d_p-x)/x)

Forces

Force in the concrete	N_c	= E_c*ε_c*x*b*1/2	[N]	
Force in the top reinforcement	N_{st}	= ε_{st}*E_s*A_{st}	[N]	
Force in the bot. reinforcement	N_{sb}	= ε_{sb}*E_s*A_{sb}	[N]	
Additional force prestr. tendon	ΔN_p	= ξ_1*$\Delta\varepsilon_p$*E_p*A_p	[N]	

Eccentricities

Concrete	ec	= 1750 - x/3	[mm]	= h - x/3
Top reinforcement	est	1637	[mm]	= h - dst
Bottom reinforcement	esb	206	[mm]	= h - dsb
Prestressing tendon	ep	1750	[mm]	= h - dp
Pminf	epm∞	875	[mm]	= h/2
Normal force	eN	875	[mm]	= h/2

Compression zone height and concrete strain

Compression zone height	x_u	678	[mm]
Concrete top edge strain	ε_c	0,000485	[-]

Effective reinforcement

Effective height	hc,eff	357,33	[mm]	= min(2,5*(h-d) ; (h-x)/3 ; h/2)
Effective area	Aceff	357333,33	[mm^2]	
Effective reinforcement	$\rho_{p,eff}$	0,0703349		

Crack widths (EN 1992-1-1 7.3.4 equation 7.8)

Concrete cover	c	106	[mm]	
	$s_{r,max}$	457,0803	[mm]	= k3*c + k1*k2*k4*(ϕ/$\rho_{p,eff}$)
	α_e	5,8824		= E_s/E_{cm}
Depth lowest reinforcement bar	d	1.624	[mm]	
Strain bottom reinforcement	ε_{sb}	0,00068	[-]	
Stress bottom reinforcement	σ_{sb}	135,4491	[N/mm^2]	
ε_{sm} - ε_{cm}		0,0005486	[-]	
Crack width	wmax	0,251	[mm]	= $s_{r,max}$ * (ε_{sm} - ε_{cm})
wmax < 0,31 (= 0,2 * k_x)	u.c.	0,76	→	OK

k1 = 0,8 k2=0,5 k3 = 3,4 k4 = 0,
according to the NEN-EN 1992

kt = 0,4 (long term)

SLS: Crack width control - **Original (analytical loads)**

Inputs

Cross-section analysed	x	15,909	[m]	
Cross-section height	h	1.750	[mm]	
Tendons amount	n	0	[-]	
Prestressing tendon area (total)	A_p	0	[mm²]	
Prestressing tendon depth	d_p	0	[mm]	
Normal force	N	206	[kN]	
Bending moment	M	165,5	(-) [kNm]	

Reinforcement

Shear reinforcement diameter	ϕ	16	[mm]
Shear reinforcement distance	s	300	[mm]
Top reinforcement area	Ast	25134	[mm²]
Top reinforcement depth	dst	206	[mm]
	ϕst	40	[mm]
Bottom reinforcement area	Asb	3272	[mm²]
Bottom reinforcement depth	dsb	1.637	[mm]
	ϕsb	25	[mm]
	ξ	0,5	
	ξ1	0,40585	
		$=\sqrt{\xi * \varphi_s/\varphi_p}$	
	kx	1,7	

Prestressing design

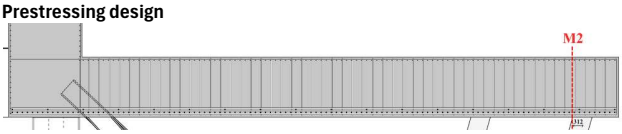

Prestressing stress per tendon (t = ∞)	$\sigma_{pm\infty}$	1200	[N/mm²]
Total prestressing force (t = ∞)	$P_{m\infty}$	-	[N]
Tendon area (per tendon)	Ap	2250	[mm²]
Tendon equivalent diameter	ϕ	75,89	[mm]

Material properties

Concrete

Characteristic compressive strength	fck	35	[N/mm²]
Design compressive strength	fcd	23,33	[N/mm²]
E-modulus	E_{cm}	34000	[N/mm²]
E-modulus (= Ecm/ (1+ϕ))	E_c	14166,67	[N/mm²]
Concrete strain at failure	εuk	0,0035	[-]
Tensile strength	fctm	3,2	[N/mm²]

Reinforcement steel

Yield strength	fyd	435	[N/mm²]
E-modulus	E_s	200000	[N/mm²]

Prestressing steel

E-modulus	E_p	195000	[N/mm²]

Strains

Top reinforcement strain	εst	-0,00080	[-]	= ε_c * ((x-d_{st})/x)
Bottom reinforcement strain	εsb	0,03065	[-]	= ε_c * ((d_{sb}-x)/x)
Prestressing strain (due to bending)	Δεp	-0,00350	[-]	= ε_c * ((d_p-x)/x)

Forces

Force in the concrete	Nc	= Ec*εc*x*b*1/2	[N]	
Force in the top reinforcement	Nst	= εst*Es*Ast	[N]	
Force in the bot. reinforcement	Nsb	= εsb*Es*Asb	[N]	
Additional force prestr. tendon	ΔNp	= ξ1*Δεp*Ep*Ap	[N]	

Eccentricities

Concrete	ec	= 1750 - x/3	[mm]	= h - x/3
Top reinforcement	est	1544	[mm]	= h - dst
Bottom reinforcement	esb	114	[mm]	= h - dsb
Prestressing tendon	ep	1750	[mm]	= h - dp
Pminf	epm∞	875	[mm]	= h/2
Normal force	eN	875	[mm]	= h/2

Compression zone height and concrete strain

Compression zone height	xu	168	[mm]	
Concrete top edge strain	εc	3,618E-05	[-]	

Effective reinforcement

Effective height	hc,eff	283,75	[mm]	= min(2,5*(h-d) ; (h-x)/3 ; h/2)
Effective area	Aceff	283750	[mm²]	
Effective reinforcement	ρp,eff	0,0115313		

Crack widths (EN 1992-1-1 7.3.4 equation 7.8)

Concrete cover (longitudinal)	c	101	[mm]		
	$s_{r,max}$	711,9628	[mm]	= k3*c + k1*k2*k4*(ϕ/ρp,eff)	
	αe	5,8824		= Es/Ecm	k1 = 0,8 k2=0,5 k3 = 3,4 k4 = 0,
Depth lowest reinforcement bar	d	1.637	[mm]		according to the NEN-EN 1992·
Strain bottom reinforcement	εsb	0,00032	[-]		
Stress bottom reinforcement	σsb	63,3829	[N/mm²]		kt = 0,4 (long term)
εsm - εcm		0,0001901	[-]		
Crack width	wmax	0,135	[mm]	= $s_{r,max}$ * (εsm - εcm)	
wmax < 0,34 (= 0,2 * kx)	u.c.	0,40	→	OK	

H.2 Chapter 6: Optimized results

H.2.1 Section 6.3 - Increased shear resistance

ULS: Bending moment resistance 1 - 6.3 Prestressed + Shear

Inputs

Cross-section analysed	x	0,790	[m]
Cross-section height	h	890	[mm]
Tendons amount	n	2	[-]
Prestressing tendon area	A_p	4500	[mm^2]
Prestressing tendon depth	d_p	309,9	[mm]
Normal force	Ned	938.000	[N]
Bending moment shift: 378	Med	526	[kNm]

Reinforcement

Shear reinforcement diameter	ϕ	20	[mm]
Shear reinforcement distance	s	250	[mm]
Top reinforcement area	Ast	3272	[mm^2]
Top reinforcement depth	dst	117,5	[mm]
Bottom reinforcement area	Asb	25133	[mm^2]
Bottom reinforcement depth	dsb	680	[mm]

Prestressing design

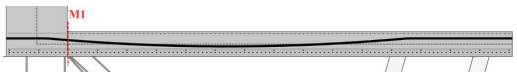

Prestressing stress per tendon (t = ∞)	$\sigma_{pm\infty}$	1200	[N/mm^2]
Total prestressing force (t = ∞)	$P_{m\infty}$	5.400.000	[N]

Material properties

Concrete

Characteristic compressive strength	fck	35	[N/mm^2]
Design compressive strength	fcd	23,33	[N/mm^2]
Concrete strain at failure	εuk	-0,0035	[-]
	α	0,75	[-]
	β	0,39	[-]

Reinforcement steel

Yield strength	fyd	435	[N/mm^2]
	Es	200000	

Prestressing steel

E-modulus	E_p	195000	[N/mm^2]
Yield strength	f_{pk}	1860	[N/mm^2]
	$f_{p0,1k}$		[N/mm^2]
	f_{pd}	1522	[N/mm^2]
Assumed prestr. stress at failure	σ_{pu}	1522	[N/mm^2]

Compression zone height

Compression zone height	x_u	**492,299328**	[mm]	= ([A_{sb} * f_{yd}] + [A_p * (f_{pd} - σ_{pu})] + [σ_{pu} * A_p] - [N_{ed}] - [A_{st} * f_{yd}]) / (α * f_{cd} * b)) + dx
dx for horizontal force equilibrium	dx	-389	[mm]	

Strains

Total prestressing tendon strain	εp	0,00485708	[-]	= $\varepsilon_{p,\infty}$ + Δεp
	Δεp	-0,00129677	[-]	= ε_{uk} (d_p/x_u - 1)
	$\varepsilon_{pm\infty}$	0,00615385	[-]	= $\sigma_{pm\infty}$ / E_p
	εst	-0,00266463	[-]	= ((xu - dst)/xu) * εuk
	εsb	0,00133446	[-]	= ((dst - xu)/xu) * εuk

Stresses

Actual prestressing stress	σp	947,130385	[N/mm^2]
Top reinforcement stress	σst	-435	[N/mm^2]
Top reinforcement stress	σsb	266,891427	[N/mm^2]

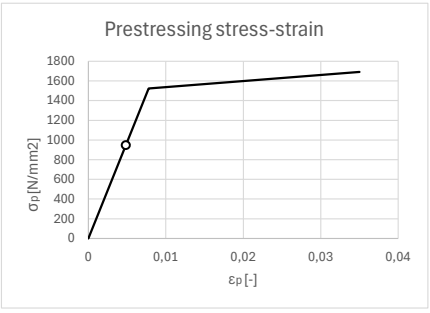

Forces

Force in the concrete	N_c	-8.614.008	[N]	= α * x_u * f_{cd} * 1000
Force in the top reinforcement	N_{st}	-1.423.320	[N]	= A_{st} * σst
Force in the bot. reinforcement	N_{sb}	6.707.782	[N]	= A_{sb} * σsb
Additional force prestr. tendon	ΔN_p	-1.137.913	[N]	= A_p * (σ_p - $\sigma_{pm\infty}$)

Horizontal force equilibrium

-5.459 → OK

Eccentricities

Concrete	=	ec	253	[mm]	= h/2 - β*x_u
Top reinforcement	=	est	328	[mm]	= h/2 - dst
Bottom reinforcement	=	esb	-235	[mm]	= h/2 - dsb
Prestressing tendon	=	esp	135	[mm]	= h/2 -d_p

Results

Effective depth steel	deff		[mm]	
Rotational capacity check		-		
Bending moment resistance	M_{Rd}	4.376	[kNm]	
	u.c.	0,12	→	OK

ULS: Bending moment resistance 2 - 6.3 Prestressed + Shear

Inputs

Cross-section analysed	x	6,500	[m]
Cross-section height	h	890	[mm]
Tendons amount	n	2	[-]
Prestressing tendon area	A_p	4500	[mm²]
Prestressing tendon depth	d_p	532,35	[mm]
Normal force	Ned	938.000	[N]
Bending moment	Med	3.635	[kNm]

Reinforcement

Shear reinforcement diameter	ϕ	16	[mm]
Shear reinforcement distance	s	300	[mm]
Top reinforcement area	Ast	3272	[mm²]
Top reinforcement depth	dst	117,5	[mm]
Bottom reinforcement area	Asb	25133	[mm²]
Bottom reinforcement depth	dsb	680	[mm]

Prestressing design

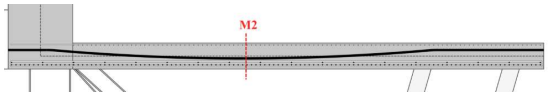

Prestressing stress per tendon (t = ∞)	$\sigma_{pm\infty}$	1200	[N/mm²]
Total prestressing force (t = ∞)	$P_{m\infty}$	5.400.000	[N]

Material properties

Concrete

Characteristic compressive strength	fck	35	[N/mm²]
Design compressive strength	fcd	23,33	[N/mm²]
Concrete strain at failure	εuk	-0,0035	[-]
	α	0,75	[-]
	β	0,39	[-]

Reinforcement steel

Yield strength	fyd	435	[N/mm²]
	Es	200000	

Prestressing steel

E-modulus	E_p	195000	[N/mm²]
Yield strength	f_{pk}	1860	[N/mm²]
	$f_{p0,1k}$		[N/mm²]
	f_{pd}	1522	[N/mm²]
Assumed prestr. stress at failure	σ_{pu}	1522	[N/mm²]

Compression zone height

Compression zone height	x_u	511,299328	[mm]	= ([Asb * fyd] + [Ap * (fpd - σpu)] + [σpu * Ap] - [Ned] - [Ast * fyd]) / (α * fcd * b)) + dx
dx for horizontal force equilibrium	dx	-370	[mm]	

Strains

Total prestressing tendon strain	εp	0,00629794	[-]	= εp,∞ + Δεp
	Δεp	0,0001441	[-]	= εuk (dp/xu - 1)
	$\varepsilon_{pm\infty}$	0,00615385	[-]	= σpm∞ / Ep
	εst	-0,00269568	[-]	= ((xu - dst)/xu) * εuk
	εsb	0,00115481	[-]	= ((dst - xu)/xu) * εuk

Stresses

Actual prestressing stress	σp	1228,09916	[N/mm²]
Top reinforcement stress	σst	-435	[N/mm²]
Top reinforcement stress	σsb	230,96152	[N/mm²]

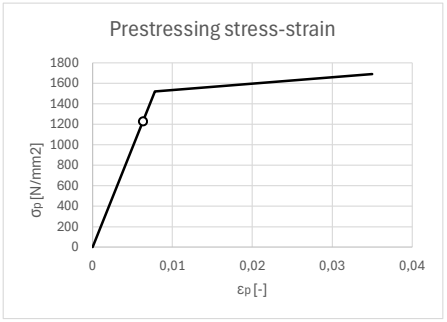

Forces

Force in the concrete	Nc	-8.946.460	[N]	= α * xu * fcd * 1000
Force in the top reinforcement	Nst	-1.423.320	[N]	= Ast * σst
Force in the bot. reinforcement	Nsb	5.804.756	[N]	= Asb * σsb
Additional force prestr. tendon	ΔNp	126.446	[N]	= Ap * (σp - σpm∞)

Eccentricities

Concrete	=	ec	246	[mm]	= h/2 - β*xu
Top reinforcement	=	est	328	[mm]	= h/2 - dst
Bottom reinforcement	=	esb	-235	[mm]	= h/2 - dsb
Prestressing tendon	=	esp	-87	[mm]	= h/2 -dp

Results

Effective depth steel	deff	658	[mm]
Rotational capacity check		NOT OK	
Bending moment resistance	MRd	4.038	[kNm]
	u.c.	0,90	→ OK

Horizontal force equilibrium

23.422 → OK

Rotational capacity → NOT OK

f = ((fpk/1.1) -σpm∞) * Ap + fyd*Asb) / (Ap + Asb)

f	443	
xu/deff	0,778	
	<	
	0,530	= 500 /(500 + f)

xu/deff < ((fpk/1.1) -σpm∞) * Ap + fyd*Asb) / (Ap + Asb)

ULS: Bending moment resistance 2 - **6.3 Prestressed + Shear**

Inputs				
Cross-section analysed	x	6,550	[m]	
Cross-section height	h	890	[mm]	
Tendons amount	n	0	[-]	Removed 2 prestressing tendons
Prestressing tendon area	A_p	0	[mm²]	
Prestressing tendon depth	d_p	512	[mm]	
Normal force	Ned	938000	[N]	
Bending moment	Med	4.195	[kNm]	
Reinforcement				
Shear reinforcement diameter	ϕ	16	[mm]	
Shear reinforcement distance	s	300	[mm]	
Top reinforcement area	Ast	3272	[mm²]	
Top reinforcement depth	dst	117,5	[mm]	
Bottom reinforcement area	Asb	20107	[mm²]	Removed 4 reinforcement bars
Bottom reinforcement depth	dsb	688	[mm]	

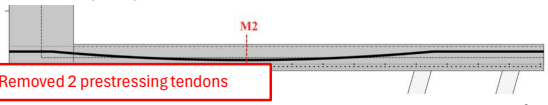

Prestressing design

Prestressing stress per tendon (t = ∞)	$\sigma_{pm\infty}$	1200	[N/mm²]
Total prestressing force (t = ∞)	$P_{m\infty}$	-	[N]

Material properties

Concrete

Characteristic compressive strength	fck	35	[N/mm²]
Design compressive strength	fcd	23,33	[N/mm²]
Concrete strain at failure	εuk	-0,0035	[-]
	α	0,75	[-]
	β	0,39	[-]

Reinforcement steel

Yield strength	fyd	435	[N/mm²]
	Es	200000	

Prestressing steel

E-modulus	E_p	195000	[N/mm²]
Yield strength	f_{pk}	1860	[N/mm²]
	$f_{p0,1k}$		[N/mm²]
	f_{pd}	1522	[N/mm²]
Assumed prestr. stress at failure	σ_{pu}	1522	[N/mm²]

Compression zone height				
Compression zone height	xu	364,93331	[mm]	= ([Asb * fyd] + [Ap * (fpd - σpu)] + [σpu * Ap] - [Ned] - [Ast * fyd]) / (α * fcd * b)) + dx
dx for horizontal force equilibrium	dx	0	[mm]	
Strains				
Total prestressing tendon strain	εp	0,00756041	[-]	= εp,∞ + Δεp
	Δεp	0,00140657	[-]	= εuk (dp/xu - 1)
	εpm∞	0,00615385	[-]	= σpm∞ / Ep
	εst	-0,00237308	[-]	= ((xu - dst)/xu) * εuk
	εsb	0,00309847	[-]	= ((dst - xu)/xu) * εuk
Stresses				
Actual prestressing stress	σp	1474,2803	[N/mm²]	
Top reinforcement stress	σst	-435	[N/mm²]	
Top reinforcement stress	σsb	435	[N/mm²]	

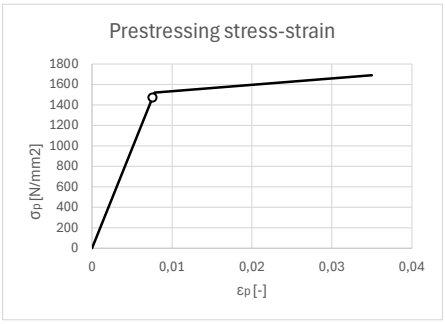

Forces					**Horizontal force equilibrium**
Force in the concrete	Nc	-6.385.421	[N]	= α * xu * fcd * 1000	0,00 → OK
Force in the top reinforcement	Nst	-1.423.320	[N]	= Ast * σst	
Force in the bot. reinforcement	Nsb	8.746.741	[N]	= Asb * σsb	
Additional force prestr. tendon	ΔNp	-	[N]	= Ap * (σp - σpm∞)	
Eccentricities					
Concrete =	ec	303	[mm]	= h/2 - β*xu	**Rotational capacity** → OK
Top reinforcement =	est	328	[mm]	= h/2 - dst	f = ((fpk/1.1) -σpm∞) * Ap + fyd*Asb) / (Ap + Asb)
Bottom reinforcement =	esb	-243	[mm]	= h/2 - dsb	f 435
Prestressing tendon =	esp	-67	[mm]	= h/2 -dp	xu/deff 0,530
Results					<
Effective depth steel	deff	688	[mm]		0,535 = 500 /(500 + f)
Rotational capacity check		OK		xu/deff < ((fpk/1.1) -σpm∞) * Ap + fyd*Asb) / (Ap + Asb)	
Bending moment resistance	MRd	4.524	[kNm]		
	u.c.	0,93	→	OK	

ULS: Bending moment resistance 3 - 6.3 Prestressed + Shear

Inputs

Cross-section analysed	x	12,597	[m]
Cross-section height	h	890	[mm]
Tendons amount	n	2	[-]
Prestressing tendon area	A_p	4.500	[mm^2]
Prestressing tendon depth	d_p	612,6	[mm]
Normal force	Ned	938.000	[N]
Bending moment	Med	438 (-)	[kNm]

Reinforcement

Shear reinforcement diameter	ϕ	20	[mm]
Shear reinforcement distance	s	250	[mm]
Top reinforcement area	Ast	25.133	[mm^2]
Top reinforcement depth	dst	210	[mm]
Bottom reinforcement area	Asb	3.272	[mm^2]
Bottom reinforcement depth	dsb	772,5	[mm]

Compression zone height

Compression zone height	x_u	**253,3**	[mm]
dx for horizontal force equilibrium	dx	459	[mm]

Strains

Total prestressing tendon strain	εp	0,01111717	[-]	= εp,∞ + Δεp
	Δεp	0,00496333	[-]	= εuk (d_p/x_u - 1)
	εpm∞	0,00615385	[-]	= σpm∞ / Ep
	εst	-0,00059876	[-]	= ((xu - dst)/xu) * εuk
	εsb	0,00717241	[-]	= ((dst - xu)/xu) * εuk

Stresses

Actual prestressing stress	σp	1542,61039	[N/mm^2]
Top reinforcement stress	σst	-119,752223	[N/mm^2]
Top reinforcement stress	σsb	435	[N/mm^2]

Prestressing design



Prestressing stress per tendon (t = ∞)	σpm∞	1200	[N/mm^2]
Total prestressing force (t = ∞)	Pm∞	5.400.000	[N]

Material properties

Concrete

Characteristic compressive strength	fck	35	[N/mm^2]
Design compressive strength	fcd	23,33	[N/mm^2]
Concrete strain at failure	εuk	-0,0035	[-]
	α	0,75	[-]
	β	0,39	[-]

Reinforcement steel

Yield strength	fyd	435	[N/mm^2]
	Es	200000	

Prestressing steel

E-modulus	Ep	195000	[N/mm^2]
Yield strength	fpk	1860	[N/mm^2]
	fp0,1k		[N/mm^2]
	fpd	1522	[N/mm^2]
Assumed prestr. stress at failure	σpu	1522	[N/mm^2]

= ([Asb * fyd] + [Ap * (fpd - σpu)] + [σpu * Ap] - [Ned] - [Ast * fyd]) / (α * fcd * b)) + dx

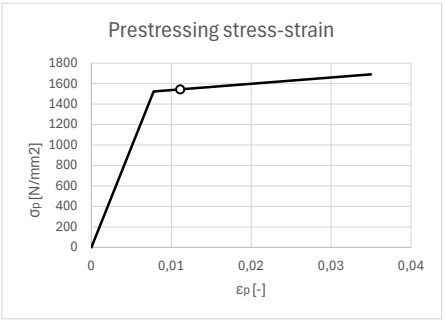

Forces

Force in the concrete	Nc	-4.432.818	[N]	= α * xu * fcd * 1000
Force in the top reinforcement	Nst	-3.009.733	[N]	= Ast * σst
Force in the bot. reinforcement	Nsb	1.423.320	[N]	= Asb * σsb
Additional force prestr. tendon	ΔNp	1.541.747	[N]	= Ap * (σp - σpm∞)

Horizontal force equilibrium

-15.483 → OK

Eccentricities

Concrete	=	ec	346	[mm]	= h/2 - β*xu
Top reinforcement	=	est	235	[mm]	= h/2 - dst
Bottom reinforcement	=	esb	-328	[mm]	= h/2 - dsb
Prestressing tendon	=	esp	-168	[mm]	= h/2 -dp

Results

Effective depth steel	deff		[mm]	
Rotational capacity check		-		
Bending moment resistance	MRd	2.966	[kNm]	
	u.c.	0,15	→	OK

ULS: Bending moment resistance 4 - 6.3 Prestressed + Shear

Inputs

Cross-section analysed	x	13,221	[m]	
Cross-section height	h	890	[mm]	
Tendons amount	n	2	[-]	
Prestressing tendon area	A_p	4.500	[mm^2]	
Prestressing tendon depth	d_p	642,35	[mm]	
Normal force	Ned	398.000	[N]	
Bending moment	Med	457	(-) [kNm]	

Reinforcement

Shear reinforcement diameter	ϕ	20	[mm]	
Shear reinforcement distance	s	250	[mm]	
Top reinforcement area	Ast	25.133	[mm^2]	
Top reinforcement depth	dst	210	[mm]	
Bottom reinforcement area	Asb	3.272	[mm^2]	
Bottom reinforcement depth	dsb	772,5	[mm]	

Compression zone height

Compression zone height	x_u	**260,2016**	[mm]	= ([A_{sb} * f_{yd}] + [A_p * (f_{pd} - σ_{pu})] + [σ_{pu} * A_p] - [N_{ed}] - [A_{st} * f_{yd}]) / (α * f_{cd} * b)) + dx
dx for horizontal force equilibrium	dx	435	[mm]	

Strains

Total prestressing tendon strain	εp	0,01129417	[-]	= εp,∞ + Δεp
	Δεp	0,00514032	[-]	= εuk (d_p/x_u - 1)
	εpm∞	0,00615385	[-]	= σpm∞ / Ep
	εst	-0,00067527	[-]	= ((xu - dst)/xu) * εuk
	εsb	0,00689098	[-]	= ((dst - xu)/xu) * εuk

Stresses

Actual prestressing stress	σp	1543,71007	[N/mm^2]
Top reinforcement stress	σst	-135,053436	[N/mm^2]
Top reinforcement stress	σsb	435	[N/mm^2]

Prestressing design

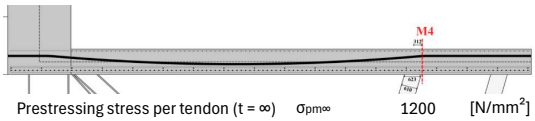

Prestressing stress per tendon (t = ∞)	σpm∞	1200	[N/mm^2]
Total prestressing force (t = ∞)	Pm∞	5.400.000	[N]

Material properties

Concrete

Characteristic compressive strength	fck	35	[N/mm^2]
Design compressive strength	fcd	23,33	[N/mm^2]
Concrete strain at failure	εuk	-0,0035	[-]
	α	0,75	[-]
	β	0,39	[-]

Reinforcement steel

Yield strength	fyd	435	[N/mm^2]
	Es	200000	

Prestressing steel

E-modulus	Ep	195000	[N/mm^2]
Yield strength	fpk	1860	[N/mm^2]
	$f_{p0,1k}$		[N/mm^2]
	fpd	1522	[N/mm^2]
Assumed prestr. stress at failure	σpu	1522	[N/mm^2]

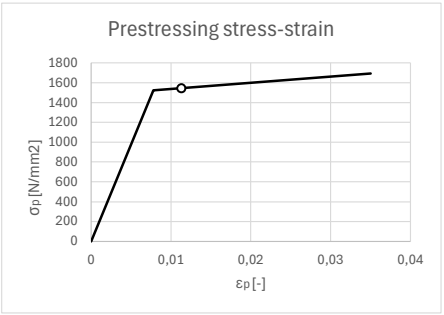

Forces

Force in the concrete	Nc	-4.552.878	[N]	= α * x_u * f_{cd} * 1000
Force in the top reinforcement	Nst	-3.394.298	[N]	= A_{st} * σst
Force in the bot. reinforcement	Nsb	1.423.320	[N]	= A_{sb} * σsb
Additional force prestr. tendon	ΔNp	1.546.695	[N]	= A_p * (σp - σpm∞)

Horizontal force equilibrium

24.840 → OK

Eccentricities

Concrete	=	ec	344	[mm]	= h/2 - β*x_u
Top reinforcement	=	est	235	[mm]	= h/2 - d_{st}
Bottom reinforcement	=	esb	-328	[mm]	= h/2 - d_{sb}
Prestressing tendon	=	esp	-197	[mm]	= h/2 -d_p

Results

Effective depth steel	deff		[mm]	
Rotational capacity check		-		
Bending moment resistance	MRd	3.133	[kNm]	
	u.c.	0,15	→	OK

ULS: Shear force resistance 1 - 6.3 Prestressed + Shear

Inputs				**Location check**			
Cross-section analysed	x	0,998	[m]	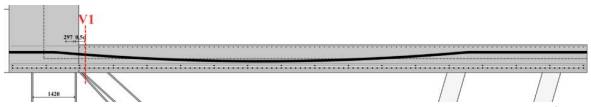			
Cross-section height	h	890	[mm]				
Tendons amount	n	2	[-]				
Prestressing tendon area	A_p	**4500**	[mm²]				
Prestressing tendon depth	d_p	325,85	[mm]	Prestressing stress per tendon (t = ∞)	$\sigma_{pm\infty}$	1200	[N/mm²]
Normal force	Ned	938.000	[N]	Total prestressing force (t = ∞)	$P_{m\infty}$	5.400.000	[N]
Bending moment	Med	312	[kNm]				
Shear force	Ved	1.207.000	[N]				
Reinforcement				**Material properties**			
Shear reinforcement diameter	ϕ	20	[mm]	**Concrete**			
Shear reinforcement distance	s	250	[mm]	Characteristic compressive strength	fck	35	[N/mm²]
Top reinforcement area	Ast	3272	[mm²]	Design compressive strength	fcd	23,33	[N/mm²]
Top reinforcement depth	dst	117,5	[mm]	**Reinforcement steel**			
Bottom reinforcement area	Asb	25133	[mm²]	Yield strength	fyd	435	[N/mm²]
Bottom reinforcement depth	dsb	680	[mm]				

	xu	**494**	[mm]		
Without shear reinforcement [NEN-EN 1992-1-1]					
	A_{sl}	25133	[mm²]		
	d_{sl}	680	[mm]		
Check if dp is within the tensile zone			→	No	
	A_p	0	[mm]		
	d_{eff}	680	[mm]		
	ρ_l	0,0370			
	k_1	0,15			
	$C_{Rd,c}$	0,12			
	σ_{cp}	4,667	< 0,2 f_{cd}	4,666667	N/mm2
	k	1,542	< 2.0		
	v_{min}	1,10	[N/mm²]		
	v_{Rdc}	1,64	[N/mm²]		
	V_{min}	745.696	[N]	u.c.	1,62
	V_{Rdc}	1.112.504	[N]	u.c.	1,08
With shear reinforcement [NEN-EN 1992-1-1]					
Area shear reinforcement	A_{sw}	1256,6	[mm²]		
Stirrup diameter	ϕ_{stir}	20	[mm]		
	s	250	[mm]		
Assumed as z = 0,9 * d_{eff}	z	612	[mm]		
	θ	39	[deg]		
	v1	0,516			
	αcw	1,20			
	$V_{Rd,s}$	1.652.499	[N]	u.c.	0,73
	$V_{Rd,max}$	4.324.477	[N]	u.c.	0,28

ULS: Shear force resistance 2 - **6.3 Prestressed + Shear**

Inputs

Cross-section analysed	x	12,257	[m]
Cross-section height	h	890	[mm]
Tendons amount	n	2	[-]
Prestressing tendon area	A_p	**4500**	[mm^2]
Prestressing tendon depth	d_p	305,053	[mm]
Normal force	Ned	938.000	[N]
Bending moment	Med	3,85	[kNm]
Shear force	Ved	1.262.000	[N]

Prestressing design

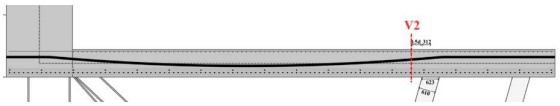

Prestressing stress per tendon (t = ∞)	$\sigma_{pm\infty}$	1200	[N/mm^2]
Total prestressing force (t = ∞)	$P_{m\infty}$	5.400.000	[N]

Reinforcement

Shear reinforcement diameter	ϕ	20	[mm]
Shear reinforcement distance	s	250	[mm]
Top reinforcement area	Ast	3272	[mm^2]
Top reinforcement depth	dst	117,5	[mm]
Bottom reinforcement area	Asb	25133	[mm^2]
Bottom reinforcement depth	dsb	680	[mm]

Material properties

Concrete

Characteristic compressive strength	fck	35	[N/mm^2]
Design compressive strength	fcd	23,33	[N/mm^2]

Reinforcement steel

Yield strength	fyd	435	[N/mm^2]

	xu	**491,3**	[mm]		
Without shear reinforcement [NEN-EN 1992-1-1]					
	A_{sl}	25133	[mm^2]		
	d_{sl}	680	[mm]		
Check if dp is within the tensile zone			→	No	
	A_p	0	[mm]		
	d_{eff}	680	[mm]		
	ρ_l	0,0370			
	k_1	0,15			
	$C_{Rd,c}$	0,12			
	σ_{cp}	4,667	< 0,2 f_{cd}	4,666667	N/mm2
	k	1,542	< 2.0		
	v_{min}	1,10	[N/mm^2]		
	v_{Rdc}	1,64	[N/mm^2]		
	V_{min}	745.696	[N]	u.c.	1,69
	V_{Rdc}	1.112.504	[N]	u.c.	1,13
With shear reinforcement [NEN-EN 1992-1-1]					
Area shear reinforcement	A_{sw}	1256,6	[mm^2]		
Stirrup diameter	ϕ_{stir}	20	[mm]		
	s	250	[mm]		
Assumed as z = 0,9 * d_{eff}	z	612	[mm]		
	θ	39	[deg]		
	v1	0,516			
	αcw	1,20			
	$V_{Rd,s}$	1.652.499	[N]	u.c.	0,76
	$V_{Rd,ma}$	4.324.477	[N]	u.c.	0,29

ULS: Shear force resistance 3 - 6.3 Prestressed + Shear

Inputs

Cross-section analysed	x	13,561	[m]
Cross-section height	h	890	[mm]
Tendons amount	n	2	[-]
Prestressing tendon area	A_p	**4500**	[mm^2]
Prestressing tendon depth	d_p	642,35	[mm]
Normal force	Ned	398.000	[N]
Bending moment	Med	-230,9	[kNm]
Shear force	Ved	616.300	[N]

Prestressing design



Prestressing stress per tendon (t = ∞)	$\sigma_{pm\infty}$	1200	[N/mm^2]
Total prestressing force (t = ∞)	$P_{m\infty}$	5.400.000	[N]

Reinforcement

Shear reinforcement diameter	ϕ	20	[mm]
Shear reinforcement distance	s	250	[mm]
Top reinforcement area	Ast	3272	[mm^2]
Top reinforcement depth	dst	117,5	[mm]
Bottom reinforcement area	Asb	25133	[mm^2]
Bottom reinforcement depth	dsb	680	[mm]

Material properties

Concrete

Characteristic compressive strength	fck	35	[N/mm^2]
Design compressive strength	fcd	23,33	[N/mm^2]

Reinforcement steel

Yield strength	fyd	435	[N/mm^2]

	xu	**260,0**	[mm]		
Without shear reinforcement [NEN-EN 1992-1-1]					
	A_{sl}	3272	[mm^2]		
	d_{sl}	772,5	[mm]		
Check if dp is within the tensile zone			→	Yes	(since the moment is negative, dp = h - dp)
	A_p	4500	[mm]		
	d_{eff}	697,14295	[mm]		
	ρ_l	0,0111			
	k_1	0,15			
	$C_{Rd,c}$	0,12			
	σ_{cp}	4,667	< 0,2 f_{cd}	4,666667	N/mm2
	k	1,536	< 2.0		
	v_{min}	1,09	[N/mm^2]		
	v_{Rdc}	1,33	[N/mm^2]		
	V_{min}	762.693	[N]	u.c.	0,81
	V_{Rdc}	923.725	[N]	u.c.	0,67
With shear reinforcement [NEN-EN 1992-1-1]					
Area shear reinforcement	A_{sw}	1256,6	[mm^2]		
Stirrup diameter	ϕ_{stir}	20	[mm]		
	s	250	[mm]		
Assumed as z = 0,9 * d_{eff}	z	627	[mm]		
	θ	39	[deg]		
	v1	0,516			
	αcw	1,20			
	$V_{Rd,s}$	1.694.159	[N]	u.c.	0,36
	$V_{Rd,max}$	4.433.498	[N]	u.c.	0,14

SLS: Crack width control t=0 - 6.3 Prestressed + Shear

Inputs				**Prestressing design**				
Cross-section analysed	x	6,71	[m]	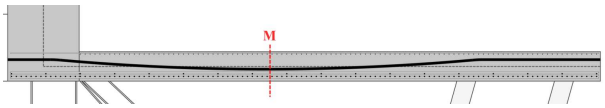				
Cross-section height	h	890	[mm]					
Tendons amount	n	2	[-]					
Prestressing tendon area (total)	A_p	4.500	[mm²]	Prestressing stress per tendon (t = ∞)	$\sigma_{pm\infty}$	1428,48	[N/mm²]	
Prestressing tendon depth	d_p	532,00	[mm]	Total prestressing force (t = ∞)	$P_{m\infty}$	6.428.160	[N]	
Normal force	N	519	[kN]	Tendon area (per tendon)	Ap	2250	[mm²]	
Bending moment	M	-337,78	[kNm]	Tendon equivalent diameter	ϕ	75,89	[mm]	
Reinforcement								
Shear reinforcement diameter	ϕ	20	[mm]					
Shear reinforcement distance	s	300	[mm]	**Material properties**				
Top reinforcement area	Ast	25133	[mm²]	**Concrete**				
Top reinforcement depth	dst	210	[mm]	Characteristic compressive strength	fck	35	[N/mm²]	
	ϕst	40	[mm]	Design compressive strength	fcd	23,33	[N/mm²]	
Bottom reinforcement area	Asb	3272	[mm²]	E-modulus	E_{cm}	34000	[N/mm²]	
Bottom reinforcement depth	dsb	772,5	[mm]	E-modulus (= Ecm/ (1+1,4))	E_c	14.166,7	[N/mm²]	
	ϕsb	25	[mm]	Concrete strain at failure	εuk	0,0035	[-]	
	ξ	0,5		Tensile strength	fctm	3,2	[N/mm²]	
	ξ1	0,40585		**Reinforcement steel**				
	$=\sqrt{\xi * \varphi_s/\varphi_p}$			Yield strength	fyd	435	[N/mm²]	
				E-modulus	E_s	200000	[N/mm²]	
	kx	1,78		**Prestressing steel**				
				E-modulus	E_p	195000	[N/mm²]	

Strains				
Top reinforcement strain	εst	0,00297	[-]	= εc * ((x-dst)/x)
Bottom reinforcement strain	εsb	-0,00155	[-]	= εc * ((dsb-x)/x)
Prestressing strain (due to bending)	Δεp	-0,00215	[-]	= εc * ((dp-x)/x)
Forces				
Force in the concrete	Nc	= Ec*εc*x*b*1/2	[N]	
Force in the top reinforcement	Nst	= εst*Es*Ast	[N]	
Force in the bot. reinforcement	Nsb	= εsb*Es*Asb	[N]	
Additional force prestr. tendon	ΔNp	= ξ1*Δεp*Ep*Ap	[N]	
Eccentricities				
Concrete	ec	= 1750 - x/3	[mm]	= h - x/3
Top reinforcement	est	680	[mm]	= h - dst
Bottom reinforcement	esb	118	[mm]	= h - dsb
Prestressing tendon	ep	358	[mm]	= h - dp
Pminf	epm∞	445	[mm]	= h/2
Normal force	eN	445	[mm]	= h/2
Compression zone height and concrete strain				
Compression zone height	xe	1.384	[mm]	
Concrete top edge strain	εc	0,0004396	[-]	
Effective reinforcement				
Effective height	hc,eff	-164,67	[mm]	= min(2,5*(h-d) ; (h-x)/3 ; h/2)
Effective area	Aceff	-164666,7	[mm²]	
Effective reinforcement	ρp,eff	-0,01987		
Crack widths (EN 1992-1-1 7.3.4 equation 7.8)				
Concrete cover	c	105	[mm]	
	sr,max	143,1145	[mm]	= k3*c + k1*k2*k4*(ϕ/ρp,eff)
	αe	5,8824		= Es/Ecm
Depth lowest reinforcement bar	d	772,5	[mm]	
Strain bottom reinforcement	εsb	-0,0002	[-]	
Stress bottom reinforcement	σsb	-38,8445	[N/mm²]	
εsm - εcm		0,0001	[-]	
Crack width	wmax	Uncracked	[mm]	= sr,max * (εsm - εcm)
wmax < 0,356 (= 0,2 * kx)	u.c.	Uncracked	→	OK

k1 = 0,8 k2=0,5 k3 = 3,4 k4 = 0,42
according to the NEN-EN 1992-1

kt = 0,4 (long term)

SLS: Crack width control t=∞ - 6.3 Prestressed + Shear

Inputs				**Prestressing design**			
Cross-section analysed	x	6,09	[m]	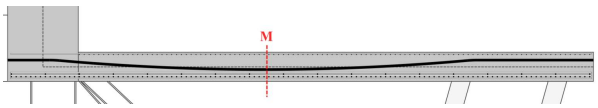			
Cross-section height	h	890	[mm]				
Tendons amount	n	2	[-]				
Prestressing tendon area (total)	A_p	4.500	[mm²]				
Prestressing tendon depth	d_p	531,22	[mm]	Prestressing stress per tendon (t = ∞)	$\sigma_{pm\infty}$	1200	[N/mm²]
Normal force	N	519	[kN]	Total prestressing force (t = ∞)	$P_{m\infty}$	5.400.000	[N]
Bending moment	M	2076,10	[kNm]	Tendon area (per tendon)	Ap	2250	[mm²]
Reinforcement				Tendon equivalent diameter	ϕ	75,89	[mm]
Shear reinforcement diameter	ϕ	16	[mm]				
Shear reinforcement distance	s	300	[mm]	**Material properties**			
Top reinforcement area	Ast	3272	[mm²]	**Concrete**			
Top reinforcement depth	dst	117,5	[mm]	Characteristic compressive strength	fck	35	[N/mm²]
	ϕst	25	[mm]	Design compressive strength	fcd	23,33	[N/mm²]
Bottom reinforcement area	Asb	25133	[mm²]	E-modulus	Ecm	34000	[N/mm²]
Bottom reinforcement depth	dsb	680	[mm]	E-modulus (= Ecm/ (1+1,4))	Ec	14.166,7	[N/mm²]
	ϕsb	40	[mm]	Concrete strain at failure	εuk	0,0035	[-]
	ξ	0,5		Tensile strength	fctm	3,2	[N/mm²]
	ξ1	0,51336		**Reinforcement steel**			
		$=\sqrt{\xi * \varphi_s/\varphi_p}$		Yield strength	fyd	435	[N/mm²]
				E-modulus	Es	200000	[N/mm²]
	kx	1,71		**Prestressing steel**			
				E-modulus	Ep	195000	[N/mm²]

Strains				
Top reinforcement strain	εst	0,00276	[-]	= εc * ((x-dst)/x)
Bottom reinforcement strain	εsb	0,00076	[-]	= εc * ((dsb-x)/x)
Prestressing strain (due to bending)	Δεp	-0,00017	[-]	= εc * ((dp-x)/x)
Forces				
Force in the concrete	Nc	= Ec*εc*x*b*1/2	[N]	
Force in the top reinforcement	Nst	= εst*Es*Ast	[N]	
Force in the bot. reinforcement	Nsb	= εsb*Es*Asb	[N]	
Additional force prestr. tendon	ΔNp	= ξ1*Δεp*Ep*Ap	[N]	
Eccentricities				
Concrete	ec	= 1750 - x/3	[mm]	= h - x/3
Top reinforcement	est	773	[mm]	= h - dst
Bottom reinforcement	esb	210	[mm]	= h - dsb
Prestressing tendon	ep	359	[mm]	= h - dp
Pminf	epm∞	445	[mm]	= h/2
Normal force	eN	445	[mm]	= h/2
Compression zone height and concrete strain				
Compression zone height	xe	559	[mm]	
Concrete top edge strain	εc	0,0014338	[-]	
Effective reinforcement				
Effective height	hc,eff	110,45	[mm]	= min(2,5*(h-d) ; (h-x)/3 ; h/2)
Effective area	Aceff	110448,57	[mm²]	
Effective reinforcement	ρp,eff	0,2275539		
Crack widths (EN 1992-1-1 7.3.4 equation 7.8)				
Concrete cover	c	110	[mm]	
	sr,max	403,8830	[mm]	= k3*c + k1*k2*k4*(ϕ/ρp,eff)
	αe	5,8824		= Es/Ecm
Depth lowest reinforcement bar	d	760	[mm]	
Strain bottom reinforcement	εsb	0,0005	[-]	
Stress bottom reinforcement	σsb	103,3534	[N/mm²]	
εsm - εcm		0,0005	[-]	
Crack width	wmax	0,182	[mm]	= sr,max * (εsm - εcm)
wmax < 0,342 (= 0,2 * kx)	u.c.	0,53	→	OK

k1 = 0,8 k2=0,5 k3 = 3,4 k4 = 0,42
according to the NEN-EN 1992-1

kt = 0,4 (long term)

H.2.2 Section 6.4 - Final variant

ULS: Bending moment resistance 1 - **6.4 Prestressed + Shear + Opening**

Inputs

Cross-section analysed	x	0,79	[m]	
Cross-section height	h	890	[mm]	
Tendons amount	n	2	[-]	
Prestressing tendon area	A_p	4.500	[mm²]	
Prestressing tendon depth	d_p	309,9	[mm]	
Normal force	Ned	938.000	[N]	
Bending moment shift: 378	Med	496,7	[kNm]	

Reinforcement

Shear reinforcement diameter	ϕ	20	[mm]	
Shear reinforcement distance	s	300	[mm]	
Top reinforcement area	Ast	3272	[mm²]	
Top reinforcement depth	dst	118	[mm]	
Bottom reinforcement area	Asb	25133	[mm²]	
Bottom reinforcement depth	dsb	680	[mm]	
	b_{open}	0,4	[m]	
	h_{open}	0,345	[m]	
	h_{fb}	0,355	[m]	
	yc_op	0,0825	[m]	
	c.a.	0,4601	[m]	
	hf (top	0,19	[m]	

Compression zone height

	x_u	**513,3**	[mm]	
Compression zone height	x_u	881,3	[mm]	= ([A_{sb} * f_{yd}] + [A_p * (f_{pd} - σ_{pu})] + [σ_{pu} * A_p] - [N_{ed}] - [A_{st} * f_{yd}]) / (α * f_{cd} * b)) + dx
Compression zone height xu>hft	x_u	1.218,7	[mm]	
dx for horizontal force equilibrium	dx	-368	[mm]	$= \frac{-\eta f_{cd} h_f b_{eff} + \eta f_{cd} h_f b_w - N_{Ed} - A_{st} f_{yd} + A_{sb} f_{yd} + A_p f_{pd}}{\eta f_{cd} \lambda b_w}$

Strains

Total prestressing tendon strain	εp	0,004766941	[-]	= εp,∞ + Δεp
	Δεp	-0,00138691	[-]	= εuk (d_p/x_u - 1)
	$\varepsilon_{pm\infty}$	0,006153846	[-]	= $\sigma_{pm\infty}$ / E_p
	εst	-0,0026954	[-]	= ((xu - dst)/xu) * εuk
	εsb	0,001136671	[-]	= ((dst - xu)/xu) * εuk

Stresses

Actual prestressing stress	σp	929,5534321	[N/mm²]
Top reinforcement stress	σst	-435	[N/mm²]
Top reinforcement stress	σsb	227,3341569	[N/mm²]

Forces

Force in the concrete	N_{c1}	-4.432.700	[N]	= η * f_{cd} * h_f * b_{eff}
	N_{c2}	-3.088.511	[N]	= η * f_{cd} * (λxu - h_f) * b_w
Force in the top reinforcement	N_{st}	-1.423.320	[N]	= A_{st} * σst
Force in the bot. reinforcement	N_{sb}	5.713.589	[N]	= A_{sb} * σsb
Additional force prestr. tendon	ΔNp	-1.217.010	[N]	= A_p * (σp - $\sigma_{pm\infty}$)

Eccentricities

Concrete 1	=	ec1	365	[mm]	= c.a. - 0,5*hft
Concrete 2	=	ec2	159,8	[mm]	= c.a. - ((λxu - hft)/2 + hft)
Top reinforcement	=	est	342	[mm]	= c.a. - dst
Bottom reinforcement	=	esb	-220	[mm]	= c.a. - dsb
Prestressing tendon	=	esp	150	[mm]	= c.a. - dp

Results

Effective depth steel	deff	680	[mm]
Rotational capacity check		-	
Bending moment resistance	M_{Rd}	4.038	[kNm]
	u.c.	0,12	→ OK

Prestressing design

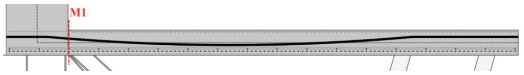

Prestressing stress per tendon (t = ∞)	$\sigma_{pm\infty}$	1200	[N/mm²]
Total prestressing force (t = ∞)	$P_{m\infty}$	5.400.000	[N]

Material properties

Concrete

Characteristic compressive strength	fck	35	[N/mm²]
Design compressive strength	fcd	23,33	[N/mm²]
Concrete strain at failure	εuk	-0,0035	[-]
	α	0,75	[-]
	β	0,39	[-]

Reinforcement steel

Yield strength	fyd	435	[N/mm²]
	Es	200000	

Prestressing steel

E-modulus	E_p	195000	[N/mm²]
Yield strength	f_{pk}	1860	[N/mm²]
	$f_{p0,1k}$		[N/mm²]
	f_{pd}	1522	[N/mm²]
Assumed prestr. stress at failure	σ_{pu}	1522	[N/mm²]

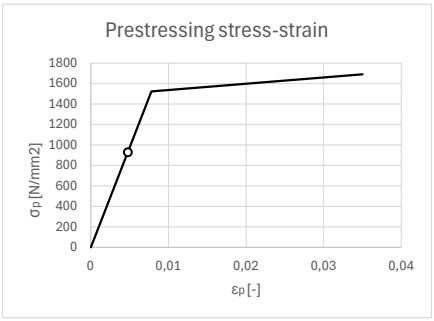

Horizontal force equilibrium

14.049 → OK

ULS: Bending moment resistance 2 - **6.4 Prestressed + Shear + Opening**

Inputs

Cross-section analysed	x	6,49	[m]
Cross-section height	h	890	[mm]
Tendons amount	n	2	[-]
Prestressing tendon area	A_p	4.500	[mm²]
Prestressing tendon depth	d_p	532,35	[mm]
Normal force	Ned	938.000	[N]
Bending moment	Med	3.534	[kNm]

Reinforcement

Shear reinforcement diameter	ϕ	20	[mm]
Shear reinforcement distance	s	300	[mm]
Top reinforcement area	Ast	3272	[mm²]
Top reinforcement depth	dst	118	[mm]
Bottom reinforcement area	Asb	25133	[mm²]
Bottom reinforcement depth	dsb	680	[mm]
	b_{open}	0,4	[m]
	h_{open}	0,345	[m]
	h_{ft}	0,355	[m]
	yc_op	0,0825	[m]
	c.a.	0,4601	[m]
	hf (top	0,19	[m]

Compression zone height

	x_u	**535,7**	[mm]	
Compression zone height	x_u	881,3	[mm]	= ([A_{sb} * f_{yd}] + [A_p * (f_{pd} - σ_{pu})] + [σ_{pu} * A_p] - [Ned] - [A_{st} * f_{yd}]) / (α * f_{cd} * b)) + dx
Compression zone height xu>h_{ft}	x_u	1.218,7	[mm]	$= \frac{-\eta f_{cd} h_f b_{eff} + \eta f_{cd} h_f b_w - N_{Ed} - A_{st} f_{yd} + A_{sb} f_{yd} + A_p f_{pd}}{\eta f_{cd} \lambda b_w}$
dx for horizontal force equilibrium	dx	-683	[mm]	

Strains

Total prestressing tendon strain	εp	0,006131979	[-]	= $\varepsilon_{p,\infty} + \Delta\varepsilon_p$
	$\Delta\varepsilon_p$	-2,1867E-05	[-]	= ε_{uk} (d_p/x_u - 1)
	$\varepsilon_{pm\infty}$	0,006153846	[-]	= $\sigma_{pm\infty}$ / E_p
	εst	-0,00272904	[-]	= ((xu - dst)/xu) * εuk
	εsb	0,000942811	[-]	= ((dst - xu)/xu) * εuk

Stresses

Actual prestressing stress	σ_p	1195,735952	[N/mm²]	
Top reinforcement stress	σst	-435	[N/mm²]	
Top reinforcement stress	σsb	188,5622242	[N/mm²]	

Forces

Force in the concrete	N_{c1}	-4.432.700	[N]	= η * f_{cd} * h_f * b_{eff}
	N_{c2}	-3.339.328	[N]	= η * f_{cd} * (λxu - h_f) * b_w
Force in the top reinforcement	N_{st}	-1.423.320	[N]	= A_{st} * σ_{st}
Force in the bot. reinforcement	N_{sb}	4.739.134	[N]	= A_{sb} * σ_{sb}
Additional force prestr. tendon	ΔN_p	-19.188	[N]	= A_p * (σ_p - $\sigma_{pm\infty}$)

Eccentricities

Concrete 1	=	ec1	365	[mm]	= c.a. - 0,5*h_{ft}
Concrete 2	=	ec2	150,9	[mm]	= c.a. - ((λxu - h_f)/2 + h_f)
Top reinforcement	=	est	342	[mm]	= c.a. - dst
Bottom reinforcement	=	esb	-220	[mm]	= c.a. - dsb
Prestressing tendon	=	esp	-72	[mm]	= c.a. - dp

Results

Effective depth steel	deff	680	[mm]
Rotational capacity check		NOT OK	
Bending moment resistance	M_{Rd}	3.650	[kNm]
	u.c.	0,97	→ OK

Prestressing design

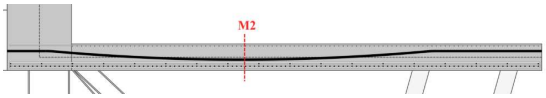

Prestressing stress per tendon (t = ∞)	$\sigma_{pm\infty}$	1200	[N/mm²]
Total prestressing force (t = ∞)	$P_{m\infty}$	5.400.000	[N]

Material properties

Concrete

Characteristic compressive strength	fck	35	[N/mm²]
Design compressive strength	fcd	23,33	[N/mm²]
Concrete strain at failure	εuk	-0,0035	[-]
	α	0,75	[-]
	β	0,39	[-]

Reinforcement steel

Yield strength	fyd	435	[N/mm²]
	Es	200000	

Prestressing steel

E-modulus	E_p	195000	[N/mm²]
Yield strength	f_{pk}	1860	[N/mm²]
	$f_{p0,1k}$		[N/mm²]
	f_{pd}	1522	[N/mm²]
Assumed prestr. stress at failure	σ_{pu}	1522	[N/mm²]

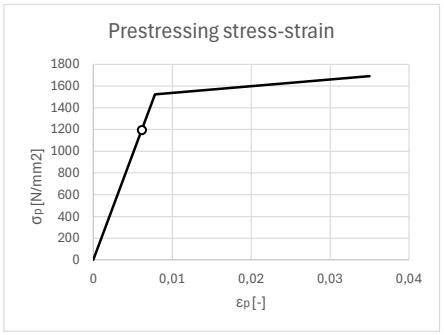

Horizontal force equilibrium

-13.402 → OK

Rotational capacity → NOT OK

f = ((fpk/1.1) -σpm∞) * Ap + fyd*Asb) / (Ap + Asb)

f	443	
xu/deff	0,788	
	<	
	0,530	= 500 /(500 + f)

xu/deff < ((fpk/1.1) -σpm∞) * Ap + fyd*Asb) / (Ap + Asb)

ULS: Bending moment resistance - **6.4 Prestressed + Shear + Opening**

Inputs

Cross-section analysed	x	6,5	[m]	
Cross-section height	h	890	[mm]	
Tendons amount	n	0	[-]	Removed 2 prestressing tendons
Prestressing tendon area	A_p	0	[mm²]	
Prestressing tendon depth	d_p	0	[mm]	
Normal force	Ned	938000	[N]	
Bending moment	Med	4095,2	[kNm]	

Reinforcement

Shear reinforcement diameter	ϕ	20	[mm]	
Shear reinforcement distance	s	300	[mm]	
Top reinforcement area	Ast	3272	[mm²]	
Top reinforcement depth	dst	118	[mm]	
Bottom reinforcement area	Asb	18850	[mm²]	
Bottom reinforcement depth	dsb	680	[mm]	Removed 5 reinforcement bars
		5		
	b_{open}	0,4	[m]	
	h_{open}	0,345	[m]	
	h_{ft}	0,355	[m]	
	yc_op	0,0825	[m]	
	c.a.	0,46014	[m]	
	hf (top	0,19	[m]	

Compression zone height

	xu	363,0	[mm]	
Compression zone height	xu	333,7	[mm]	= ([Asb * fyd] + [Ap * (fpd - σpu)] + [σpu * Ap] - [Ned] - [Ast * fyd]) / (α * fcd * b)) + dx
Compression zone height xu>hf	xu	363,0	[mm]	
dx for horizontal force equilibrium	dx	0	[mm]	$= \frac{-\eta f_{cd} h_f b_{eff} + \eta f_{cd} h_f b_w - N_{Ed} - A_{st} f_{yd} + A_{sb} f_{yd} + A_p f_{pd}}{\eta f_{cd} \lambda b_w}$

Strains

Total prestressing tendon strain	εp	0	[-]	= εp,∞ + Δεp
	Δεp	-0,0035	[-]	= εuk (dp/xu - 1)
	εpm∞	0,006153846	[-]	= σpm∞ / Ep
	εst	-0,0023623	[-]	= ((xu - dst)/xu) * εuk
	εsb	0,003056252	[-]	= ((xu - dsb)/xu) * εuk

Stresses

Actual prestressing stress	σp	0	[N/mm²]
Top reinforcement stress	σst	-435	[N/mm²]
Top reinforcement stress	σsb	435	[N/mm²]

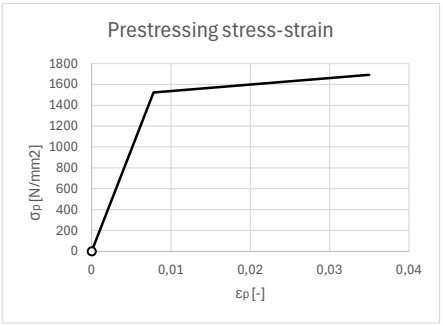

Forces

Force in the concrete	N_{c1}	-4.432.700	[N]	= η * fcd * hf * beff
	N_{c2}	-1.405.537	[N]	= η * fcd * (λxu - hf) * bw
Force in the top reinforcement	Nst	-1.423.320	[N]	= Ast * σst
Force in the bot. reinforcement	Nsb	8.199.557	[N]	= Asb * σsb
Additional force prestr. tendon	ΔNp	-	[N]	= Ap * (σp - σpm∞)

Horizontal force equilibrium

-0 → OK

Eccentricities

Concrete 1	=	ec1	365	[mm]	= c.a. - 0,5*hft
Concrete 1	=	ec2	219,9	[mm]	= c.a. - ((λxu - hft)/2 + hft)
Top reinforcement	=	est	342	[mm]	= c.a. - dst
Bottom reinforcement	=	esb	-220	[mm]	= c.a. - dsb
Prestressing tendon	=	esp	460	[mm]	= c.a. - dp

Rotational capacity → OK

f = ((fpk/1.1) -σpm∞) * Ap + fyd*Asb) / (Ap + Asb)

f	435
xu/deff	0,534
	<
	0,535 = 500 /(500 + f)

Results

Effective depth steel	deff	680	[mm]	
Rotational capacity check		OK		xu/deff < ((fpk/1.1) -σpm∞) * Ap + fyd*Asb) / (Ap + Asb)
Bending moment resistance	MRd	4.217	[kNm]	
	u.c.	0,97	→	OK

ULS: Bending moment resistance 3 - **6.4 Prestressed + Shear + Opening**

Inputs

Cross-section analysed	x	12,597	[m]	
Cross-section height	h	890	[mm]	
Tendons amount	n	2	[-]	
Prestressing tendon area	A_p	4.500	[mm²]	
Prestressing tendon depth	d_p	612,60	[mm]	
Normal force	Ned	938.000	[N]	
Bending moment	Med	477,3	(-) [kNm]	

Reinforcement

Shear reinforcement diameter	ϕ	20	[mm]	
Shear reinforcement distance	s	300	[mm]	
Top reinforcement area	Ast	25133	[mm²]	
Top reinforcement depth	dst	210	[mm]	
Bottom reinforcement area	Asb	3272	[mm²]	
Bottom reinforcement depth	dsb	772,5	[mm]	
	b_{open}	0,4	[m]	
	h_{open}	0,345	[m]	
	$h_{ft,b}$	0,19	[m]	
	yc_open	0,0825	[m]	
	c.a.	0,4299	[m]	
	hf (top)	0,355	[m]	

Compression zone height

	x_u	**253,3**	[mm]	
Compression zone height	x_u	-205,7	[mm]	= ([Asb * fyd] + [Ap * (fpd - σpu)] + [σpu * Ap] - [Ned] - [Ast * fyd]) / (α * fcd * b)) + dx
Compression zone height xu>hft	x_u	-617,2	[mm]	
dx for horizontal force equilibrium	dx	459	[mm]	$= \frac{-\eta f_{cd} h_f b_{eff} + \eta f_{cd} h_f b_w - N_{Ed} - A_{st} f_{yd} + A_{sb} f_{yd} + A_p f_{pd}}{\eta f_{cd} \lambda b_w}$

Strains

Total prestressing tendon strain	εp	0,0111	[-]	= εp,∞ + Δεp
	Δεp	0,0050	[-]	= εuk (dp/xu - 1)
	$\varepsilon_{pm\infty}$	0,0062	[-]	= σpm∞ / Ep
	εst	-0,0006	[-]	= ((xu - dst)/xu) * εuk
	εsb	0,0072	[-]	= ((dst - xu)/xu) * εuk

Stresses

Actual prestressing stress	σp	1542,6	[N/mm²]
Top reinforcement stress	σst	-119,8	[N/mm²]
Top reinforcement stress	σsb	435	[N/mm²]

Forces

Force in the concrete	N_{c1}	-4.432.818	[N]	α * xu * fcd * 1000
	N_{c2}	-	[N]	
Force in the top reinforcement	Nst	-3.009.733	[N]	= Ast * σst
Force in the bot. reinforcement	Nsb	1.423.320	[N]	= Asb * σsb
Additional force prestr. tendon	ΔNp	1.541.747	[N]	= Ap * (σp - σpm∞)

Eccentricities

Concrete 1	=	ec1	331	[mm]	= c.a. - β*xu
Concrete 2	=	ec2	0,0	[mm]	
Top reinforcement	=	est	220	[mm]	= c.a. - dst
Bottom reinforcement	=	esb	-343	[mm]	= c.a. - dsb
Prestressing tendon	=	esp	-183	[mm]	= c.a. - dp

Results

Effective depth steel	deff	679,92	[mm]	
Rotational capacity check		-		
Bending moment resistance	M_{Rd}	2.899	[kNm]	
	u.c.	0,16	→	OK

Prestressing design

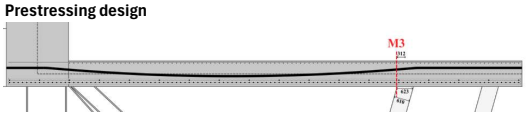

Prestressing stress per tendon (t = ∞)	σpm∞	1200	[N/mm²]
Total prestressing force (t = ∞)	Pm∞	5.400.000	[N]

Material properties

Concrete

Characteristic compressive strength	fck	35	[N/mm²]
Design compressive strength	fcd	23,33	[N/mm²]
Concrete strain at failure	εuk	-0,0035	[-]
	α	0,75	[-]
	β	0,39	[-]

Reinforcement steel

Yield strength	fyd	435	[N/mm²]
	Es	200000	

Prestressing steel

E-modulus	Ep	195000	[N/mm²]
Yield strength	fpk	1860	[N/mm²]
	$f_{p0,1k}$		[N/mm²]
	fpd	1522	[N/mm²]
Assumed prestr. stress at failure	σpu	1522	[N/mm²]

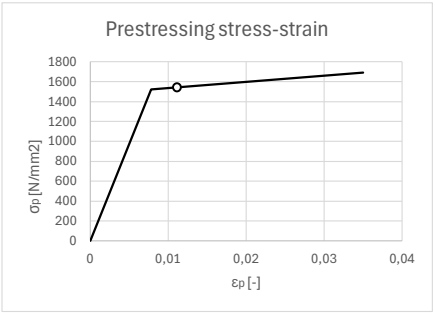

Horizontal force equilibrium

-15.483 → OK

ULS: Bending moment resistance 4 - **6.4 Prestressed + Shear + Opening**

Inputs

Cross-section analysed	x	13,221	[m]	
Cross-section height	h	890	[mm]	
Tendons amount	n	2	[-]	
Prestressing tendon area	A_p	4.500	[mm²]	
Prestressing tendon depth	d_p	642,35	[mm]	
Normal force	Ned	398.000	[N]	
Bending moment	Med	487,7	(-) [kNm]	

Reinforcement

Shear reinforcement diameter	ϕ	20	[mm]	
Shear reinforcement distance	s	300	[mm]	
Top reinforcement area	Ast	25133	[mm²]	
Top reinforcement depth	dst	210	[mm]	
Bottom reinforcement area	Asb	3272	[mm²]	
Bottom reinforcement depth	dsb	772,5	[mm]	
	b_{open}	0,4	[m]	
	h_{open}	0,345	[m]	
	h_{ft}	0,19	[m]	
	yc_op	0,0825	[m]	
	c.a.	0,4299	[m]	
	hf (top	0,355	[m]	

Compression zone height

	x_u	**260,2**	[mm]	
Compression zone height	x_u	-174,8	[mm]	= ([Asb * fyd] + [Ap * (fpd - σpu)] + [σpu * Ap] - [Ned] - [Ast * fyd]) / (α * fcd * b)) + dx
Compression zone height xu>hft	x_u	-569,0	[mm]	
dx for horizontal force equilibrium	dx	435	[mm]	$= \frac{-\eta f_{cd} h_f b_{eff} + \eta f_{cd} h_f b_w - N_{Ed} - A_{st} f_{yd} + A_{sb} f_{yd} + A_p f_{pd}}{\eta f_{cd} \lambda b_w}$

Strains

Total prestressing tendon strain	εp	0,0113	[-]	= εp,∞ + Δεp
	Δεp	0,0051	[-]	= εuk (dp/xu - 1)
	εpm∞	0,0062	[-]	= σpm∞ / Ep
	εst	-0,0007	[-]	= ((xu - dst)/xu) * εuk
	εsb	0,0069	[-]	= ((dst - xu)/xu) * εuk

Stresses

Actual prestressing stress	σp	1543,7	[N/mm²]
Top reinforcement stress	σst	-135,1	[N/mm²]
Top reinforcement stress	σsb	435	[N/mm²]

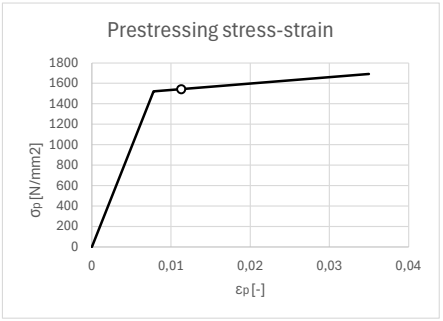

Forces

Force in the concrete	N_{c1}	-4.552.878	[N]	α * xu * fcd * 1000
	N_{c2}	-	[N]	
Force in the top reinforcement	N_{st}	-3.394.298	[N]	= Ast * σst
Force in the bot. reinforcement	N_{sb}	1.423.320	[N]	= Asb * σsb
Additional force prestr. tendon	ΔN_p	1.546.695	[N]	= Ap * (σp - σpm∞)

Horizontal force equilibrium

24.840 → OK

Eccentricities

Concrete 1	=	ec1	328	[mm]	= c.a. - β*xu
Concrete 2	=	ec2	0,0	[mm]	
Top reinforcement	=	est	220	[mm]	= c.a. - dst
Bottom reinforcement	=	esb	-343	[mm]	= c.a. - dsb
Prestressing tendon	=	esp	-212	[mm]	= c.a. - dp

Results

Effective depth steel	d_{eff}	697,14	[mm]	
Rotational capacity check		-		
Bending moment resistance	M_{Rd}	3.058	[kNm]	
	u.c.	0,16	→	OK

Prestressing design



Prestressing stress per tendon (t = ∞)	$\sigma_{pm\infty}$	1200	[N/mm²]
Total prestressing force (t = ∞)	$P_{m\infty}$	5.400.000	[N]

Material properties

Concrete

Characteristic compressive strength	fck	35	[N/mm²]
Design compressive strength	fcd	23,33	[N/mm²]
Concrete strain at failure	εuk	-0,0035	[-]
	α	0,75	[-]
	β	0,39	[-]

Reinforcement steel

Yield strength	fyd	435	[N/mm²]
	Es	200000	

Prestressing steel

E-modulus	E_p	195000	[N/mm²]
Yield strength	f_{pk}	1860	[N/mm²]
	$f_{p0,1k}$		[N/mm²]
	f_{pd}	1522	[N/mm²]
Assumed prestr. stress at failure	σpu	1522	[N/mm²]

ULS: Shear force resistance 1 - **6.4 Prestressed + Shear + Opening**

Inputs

Cross-section analysed	x	0,998	[m]	
Cross-section height	h	**890**	[mm]	
Tendons amount	n	**2**	[-]	
Prestressing tendon area	A_p	**4500**	[mm²]	
Prestressing tendon depth	d_p	**325,80**	[mm]	
Normal force	Ned	**938.000**	[N]	
Bending moment	Med	**287**	[kNm]	
Shear force	Ved	**1.182.000**	[N]	

Prestressing design

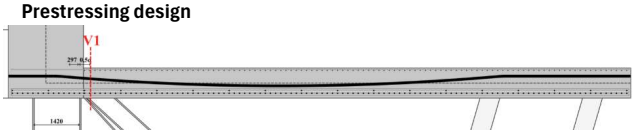

Prestressing stress per tendon (t = ∞)	$\sigma_{pm\infty}$	1200	[N/mm²]
Total prestressing force (t = ∞)	$P_{m\infty}$	5.400.000	[N]
	Φ_{duct}	86,20	[mm]

Reinforcement

Shear reinforcement diameter	ϕ	**20**	[mm]
Shear reinforcement distance	s	**300**	[mm]
Top reinforcement area	Ast	**3.272**	[mm²]
Top reinforcement depth	dst	**117,5**	[mm]
Bottom reinforcement area	Asb	**25.134**	[mm²]
Bottom reinforcement depth	dsb	**680**	[mm]

Material properties

Concrete

Characteristic compressive strength	fck	35	[N/mm²]
Design compressive strength	fcd	23,33	[N/mm²]

Reinforcement steel

Yield strength	fyd	435	[N/mm²]

	b_{open}	**0,4**	[m]	
	h_{open}	**0,345**	[m]	
	h_{fb}	0,355	[m]	
	yc_ope	0,0825	[m]	
	c.a.	0,460	[m]	
	hf (top	0,19	[m]	
	bw	0,5138	[m]	--> bw - 0,5Σϕ
	xu	**515,3**	[mm]	

Without shear reinforcement [NEN-EN 1992-1-1]

	A_{sl}	25134	[mm²]	
	d_{sl}	680	[mm]	
Check if dp is within the tensile zone			→	No
	A_p	0	[mm]	
	d_{eff}	680	[mm]	
	ρ_l	0,0719		
	k_1	0,15		
	$C_{Rd,c}$	0,12		
	σ_{cp}	4,667	< 0,2 f_{cd}	4,666667 N/mm2
	k	1,542	< 2.0	
	v_{min}	1,10	[N/mm²]	
	v_{Rdc}	1,87	[N/mm²]	
	V_{min}	383.139	[N]	u.c. 3,09
	V_{Rdc}	652.891	[N]	u.c. 1,81

With shear reinforcement [NEN-EN 1992-1-1]

Area shear reinforcement	A_{sw}	1256,6	[mm²]	
Stirrup diameter	ϕ_{stir}	20	[mm]	
	s	300	[mm]	
Assumed as z = 0,9 * d_{eff}	z	612	[mm]	
	θ	39	[deg]	
	v1	0,516		
	αcw	1,20		
	$V_{Rd,s}$	1.377.083	[N]	u.c. 0,86
	$V_{Rd,max}$	2.221.916	[N]	u.c. 0,53

ULS: Shear force resistance 2 - 6.4 Prestressed + Shear + Opening

Inputs				**Prestressing design**			
Cross-section analysed	x	12,257	[m]	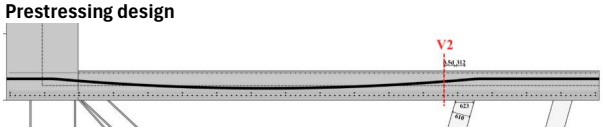			
Cross-section height	h	890	[mm]				
Tendons amount	n	2	[-]				
Prestressing tendon area	A_p	**4500**	[mm²]				
Prestressing tendon depth	d_p	585	[mm]	Prestressing stress per tendon (t = ∞)	$\sigma_{pm\infty}$	1200	[N/mm²]
Normal force	Ned	938.000	[N]	Total prestressing force (t = ∞)	$P_{m\infty}$	5.400.000	[N]
Bending moment	Med	-43	[kNm]		Φ_{duct}	86,20	[mm]
Shear force	Ved	1.240.600	[N]				
Reinforcement				**Material properties**			
Shear reinforcement diameter	ϕ	20	[mm]	**Concrete**			
Shear reinforcement distance	s	300	[mm]	Characteristic compressive strength	fck	35	[N/mm²]
Top reinforcement area	Ast	3272	[mm²]	Design compressive strength	fcd	23,33	[N/mm²]
Top reinforcement depth	dst	117,5	[mm]	**Reinforcement steel**			
Bottom reinforcement area	Asb	25133	[mm²]	Yield strength	fyd	435	[N/mm²]
Bottom reinforcement depth	dsb	680	[mm]				

	b_{open}	**0,4**	[m]	
	h_{open}	**0,345**	[m]	
	h_{fb}	0,355	[m]	
	yc_ope	0,0825	[m]	
	c.a.	0,460	[m]	
	hf (top	0,19	[m]	
	bw	0,5138	[m]	ϕduct ≤ bw /8 --> bw,nom = bw
	xu	**253,3**	[mm]	

Without shear reinforcement [NEN-EN 1992-1-1]

	A_{sl}	3272	[mm²]		
	d_{sl}	772,5	[mm]		
Check if dp is within the tensile zone			→	Yes	(since the moment is negative, dp = h - dp)
	A_p	4500	[mm]		
	d_{eff}	663,93721	[mm]		
	ρ_l	0,0228			
	k_1	0,15			
	$C_{Rd,c}$	0,12			
	σ_{cp}	4,667	< 0,2 f_{cd}	4,666667	N/mm2
	k	1,549	< 2.0		
	v_{min}	1,10	[N/mm²]		
	v_{Rdc}	1,50	[N/mm²]		
	V_{min}	374.947	[N]	u.c.	3,31
	V_{Rdc}	511.692	[N]	u.c.	2,42

With shear reinforcement [NEN-EN 1992-1-1]

Area shear reinforcement	A_{sw}	1256,6	[mm²]		
Stirrup diameter	ϕ_{stir}	20	[mm]		
	s	300	[mm]		
Assumed as z = 0,9 * d_{eff}	z	598	[mm]		
	θ	39	[deg]		
	v1	0,516			
	αcw	1,20			
	$V_{Rd,s}$	1.344.554	[N]	u.c.	0,92
	$V_{Rd,max}$	2.169.431	[N]	u.c.	0,57

ULS: Shear force resistance 3 - **6.4 Prestressed + Shear + Opening**

Inputs

Cross-section analysed	x	13,561	[m]
Cross-section height	h	**890**	[mm]
Tendons amount	n	**2**	[-]
Prestressing tendon area	A_p	**4.500**	[mm^2]
Prestressing tendon depth	d_p	**642,35**	[mm]
Normal force	Ned	**398.000**	[N]
Bending moment	Med	**-258,8**	[kNm]
Shear force	Ved	**624.000**	[N]

Prestressing design

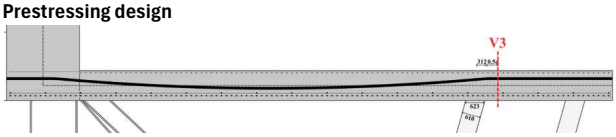

Prestressing stress per tendon (t = ∞)	$\sigma_{pm\infty}$	1200	[N/mm^2]
Total prestressing force (t = ∞)	$P_{m\infty}$	5.400.000	[N]
	Φ_{duct}	86,20	[mm]

Reinforcement

Shear reinforcement diameter	ϕ	**20**	[mm]
Shear reinforcement distance	s	**300**	[mm]
Top reinforcement area	Ast	**3272**	[mm^2]
Top reinforcement depth	dst	**117,5**	[mm]
Bottom reinforcement area	Asb	**25133**	[mm^2]
Bottom reinforcement depth	dsb	**680**	[mm]

Material properties

Concrete

Characteristic compressive strength	fck	35	[N/mm^2]
Design compressive strength	fcd	23,33	[N/mm^2]

Reinforcement steel

Yield strength	fyd	435	[N/mm^2]

	b_{open}	**0,4**	[m]	
	h_{open}	**0,345**	[m]	
	h_{fb}	0,355	[m]	
	yc_ope	0,0825	[m]	
	c.a.	0,460	[m]	
	hf (top	0,19	[m]	
	bw	0,5138	[m]	ϕduct ≤ bw /8 --> bw,nom = bw
	xu	**260,2**	[mm]	

Without shear reinforcement [NEN-EN 1992-1-1]

	A_{sl}	3272	[mm^2]		
	d_{sl}	772,5	[mm]		
Check if dp is within the tensile zone			→	Yes	(since the moment is negative, dp = h - dp)
	A_p	4500	[mm]		
	d_{eff}	697,14295	[mm]		
	ρ_l	0,0217			
	k_1	0,15			
	$C_{Rd,c}$	0,12			
	σ_{cp}	4,667	< 0,2 f_{cd}	4,666667	N/mm2
	k	1,536	< 2.0		
	v_{min}	1,09	[N/mm^2]		
	v_{Rdc}	1,48	[N/mm^2]		
	V_{min}	391.872	[N]	u.c.	1,59
	V_{Rdc}	530.251	[N]	u.c.	1,18

With shear reinforcement [NEN-EN 1992-1-1]

Area shear reinforcement	A_{sw}	1256,6	[mm^2]		
Stirrup diameter	ϕ_{stir}	20	[mm]		
	s	300	[mm]		
Assumed as z = 0,9 * d_{eff}	z	627	[mm]		
	θ	39	[deg]		
	v1	0,516			
	αcw	1,20			
	$V_{Rd,s}$	1.411.799	[N]	u.c.	0,44
	$V_{Rd,max}$	2.277.931	[N]	u.c.	0,27

SW: Crack width control t = 0 - **6.4 Prestressed + Shear + Opening**

Inputs				**Prestressing design**				
Cross-section analysed	x	6,91	[m]	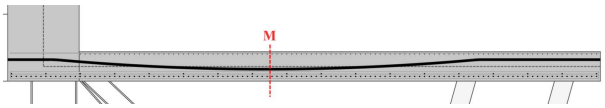				
Cross-section height	h	890	[mm]					
Tendons amount	n	2	[-]					
Prestressing tendon area (total)	A_p	4500	[mm²]	Prestressing stress per tendon (t = ∞)	$\sigma_{pm\infty}$	1428,48	[N/mm²]	
Prestressing tendon depth	d_p	359	[mm]	Total prestressing force (t = ∞)	$P_{m\infty}$	6.428.160	[N]	
Normal force	N	0	[kN]	Tendon area (per tendon)	Ap	2250	[mm²]	
Bending moment	M	-233,06	[kNm]	Tendon equivalent diameter	ϕ	75,89	[mm]	
Reinforcement								
Shear reinforcement diameter	ϕ	20	[mm]					
Shear reinforcement distance	s	300	[mm]	**Material properties**				
Top reinforcement area	Ast	25133	[mm²]	**Concrete**				
Top reinforcement depth	dst	210	[mm]	Characteristic compressive strength	fck	35	[N/mm²]	
	ϕst	40	[mm]	Design compressive strength	fcd	23,33	[N/mm²]	
Bottom reinforcement area	Asb	3272	[mm²]	E-modulus	E_{cm}	34000	[N/mm²]	
Bottom reinforcement depth	dsb	772,5	[mm]	E-modulus (= Ecm/ (1+ϕ))	E_c	14166,67	[N/mm²]	
	ϕsb	25	[mm]	Concrete strain at failure	εuk	0,0035	[-]	
	ξ	0,5		Tensile strength	fctm	3,2	[N/mm²]	
	ξ1	0,40585		**Reinforcement steel**				
		$=\sqrt{\xi * \varphi_s/\varphi_p}$		Yield strength	fyd	435	[N/mm²]	
				E-modulus	E_s	200000	[N/mm²]	
	kx	1,7		**Prestressing steel**				
				E-modulus	E_p	195000	[N/mm²]	
Strains								
Top reinforcement strain	εst	0,00305	[-]	= εc * ((x-dst)/x)	**Cross section**			
Bottom reinforcement strain	εsb	-0,00186	[-]	= εc * ((dsb-x)/x)	b_{open}	0,4	[m]	
Prestressing strain (due to bending)	Δεp	-0,00274	[-]	= εc * ((dp-x)/x)	h_{open}	0,35	[m]	
Forces					h_{ft}	0,19	[m]	
Force in the concrete	Nc	= Ec*εc*x*b*1/2	[N]		y_{c_oper}	0,0825	[m]	
Force in the top reinforcement	Nst	= εst*Es*Ast	[N]		c.a.	0,4299	[m]	
Force in the bot. reinforcement	Nsb	= εsb*Es*Asb	[N]		h_{ft}	0,355	[m]	
Additional force prestr. tendon	ΔNp	= ξ1*Δεp*Ep*Ap	[N]					
Eccentricities								
Concrete	ec	= 1750 - x/3	[mm]	= h - x/3				
Top reinforcement	est	680	[mm]	= h - dst				
Bottom reinforcement	esb	118	[mm]	= h - dsb				
Prestressing tendon	ep	531	[mm]	= h - dp				
Pminf	epm∞	445	[mm]	= h - c.a.				
Normal force	eN	445	[mm]	= h - c.a.				
Compression zone height and concrete strain								
Compression zone height	xu	1.647	[mm]					
Concrete top edge strain	εc	0,0004657	[-]					
Effective reinforcement								
Effective height	hc,eff	-252,17	[mm]	= min(2,5*(h-d) ; (h-x)/3 ; h/2)				
Effective area	Aceff	-252.167	[mm²]	=hc,eff * 1000				
Effective reinforcement	ρp,eff	-0,0130						
Crack widths (EN 1992-1-1 7.3.4 equation 7.8)								
Concrete cover	c	105	[mm]					
	sr,max	29,46	[mm]	= k3*c + k1*k2*k4*(ϕ/ρp,eff)				
	αe	5,88		= Es/Ecm	k1 = 0,8 k2=0,5 k3 = 3,4 k4 = 0,425			
Depth lowest reinforcement bar	d	772,5	[mm]		NEN-EN 1992-1-1 NA			
Strain bottom reinforcement	εsb	-0,0002	[-]					
Stress bottom reinforcement	σsb	-49,44	[N/mm²]		kt = 0,4 (long term)			
εsm - εcm		0,0002	[-]					
Crack width	wmax	Uncracked	[mm]	= sr,max * (εsm - εcm)				
wmax < 0,2 [section 6.4.1]	u.c.	Uncracked	→	OK				

SLS: Crack width control t = ∞ - **6.4 Prestressed + Shear + Opening**

Inputs

Cross-section analysed	x	6,06	[m]
Cross-section height	h	890	[mm]
Tendons amount	n	2	[-]
Prestressing tendon area (total)	A_p	4500	[mm²]
Prestressing tendon depth	d_p	531	[mm]
Normal force	N	519	[kN]
Bending moment	M	1997,07	[kNm]

Reinforcement

Shear reinforcement diameter	ϕ	20	[mm]
Shear reinforcement distance	s	300	[mm]
Top reinforcement area	Ast	3272	[mm²]
Top reinforcement depth	dst	117,5	[mm]
	ϕst	25	[mm]
Bottom reinforcement area	Asb	25133	[mm²]
Bottom reinforcement depth	dsb	680	[mm]
	ϕsb	40	[mm]
	ξ	0,5	
	ξ1	0,51336	
		$=\sqrt{\xi * \varphi_s/\varphi_p}$	
	kx	-	

Prestressing design

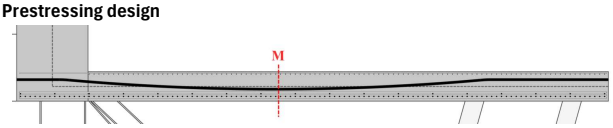

Prestressing stress per tendon (t = ∞)	$\sigma_{pm\infty}$	1200	[N/mm²]
Total prestressing force (t = ∞)	$P_{m\infty}$	5.400.000	[N]
Tendon area (per tendon)	Ap	2250	[mm²]
Tendon equivalent diameter	ϕ	75,89	[mm]

Material properties

Concrete

Characteristic compressive strength	fck	35	[N/mm²]
Design compressive strength	fcd	23,33	[N/mm²]
E-modulus	E_{cm}	34000	[N/mm²]
E-modulus (= Ecm/ (1+ϕ))	E_c	14166,67	[N/mm²]
Concrete strain at failure	εuk	0,0035	[-]
Tensile strength	fctm	3,2	[N/mm²]

Reinforcement steel

Yield strength	fyd	435	[N/mm²]
E-modulus	E_s	200000	[N/mm²]

Prestressing steel

E-modulus	E_p	195000	[N/mm²]

Strains

Top reinforcement strain	εst	0,00281	[-]	= εc * ((x-dst)/x)
Bottom reinforcement strain	εsb	0,00051	[-]	= εc * ((dsb-x)/x)
Prestressing strain (due to bending)	Δεp	-0,00037	[-]	= εc * ((dp-x)/x)

Forces

Force in the concrete	Nc	= Ec*εc*x*b*1/2	[N]	
Force in the top reinforcement	Nst	= εst*Es*Ast	[N]	
Force in the bot. reinforcement	Nsb	= εsb*Es*Asb	[N]	
Additional force prestr. tendon	ΔNp	= ξ1*Δεp*Ep*Ap	[N]	

Eccentricities

Concrete	ec	= 1750 - x/3	[mm]	= h - x/3
Top reinforcement	est	773	[mm]	= h - dst
Bottom reinforcement	esb	210	[mm]	= h - dsb
Prestressing tendon	ep	359	[mm]	= h - dp
Pminf	epm∞	445	[mm]	= h - c.a.
Normal force	eN	445	[mm]	= h - c.a.

Compression zone height and concrete strain

Compression zone height	xu	593	[mm]	
Concrete top edge strain	εc	0,001496	[-]	

Effective reinforcement

Effective height	hc,eff	98,92	[mm]	= min(2,5*(h-d) ; (h-x)/3 ; h/2)
Effective area	Aceff	98.920	[mm²]	=hc,eff * 1000
Effective reinforcement	ρp,eff	0,2541		

Crack widths (EN 1992-1-1 7.3.4 equation 7.8)

Concrete cover	c	110	[mm]	
	Sr,max	400,7639	[mm]	= k3*c + k1*k2*k4*(ϕ/ρp,eff)
	αe	5,8824		= Es/Ecm
Depth lowest reinforcement bar	d	760	[mm]	
Strain bottom reinforcement	εsb	0,0004	[-]	
Stress bottom reinforcement	σsb	84,1311	[N/mm²]	
εsm - εcm		0,0004	[-]	
Crack width	wmax	0,143	[mm]	= Sr,max * (εsm - εcm)
wmax < 0,2 [section 6.4.1]	u.c.	0,72	→	OK

Cross section

b_{open}	0,4	[m]
h_{open}	0,345	[m]
h_{fb}	0,355	[m]
y_{c_oper}	0,0825	[m]
c.a.	0,4601	[m]
h_{ft}	0,19	[m]

k1 = 0,8 k2=0,5 k3 = 3,4 k4 = 0,425
NEN-EN 1992-1-1 NA

kt = 0,4 (long term)

H.3 Chapter 8: Discussion

H.3.1 Section 8.1 - Smaller crack angle

ULS: Shear force resistance 2 - 9.1 Discussion shear angle (Prestressed + Shear + Opening)

Inputs

Cross-section analysed	x	12,257	[m]
Cross-section height	h	890	[mm]
Tendons amount	n	2	[-]
Prestressing tendon area	A_p	4500	[mm²]
Prestressing tendon depth	d_p	585	[mm]
Normal force	Ned	938.000	[N]
Bending moment	Med	-43	[kNm]
Shear force	Ved	1.240.600	[N]

Prestressing design

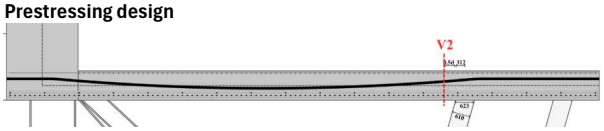

Prestressing stress per tendon (t = ∞)	$\sigma_{pm\infty}$	1200	[N/mm²]
Total prestressing force (t = ∞)	$P_{m\infty}$	5.400.000	[N]
	Φ_{duct}	86,20	[mm]

Reinforcement

Shear reinforcement diameter	ϕ	20	[mm]
Shear reinforcement distance	s	300	[mm]
Top reinforcement area	Ast	3272	[mm²]
Top reinforcement depth	dst	117,5	[mm]
Bottom reinforcement area	Asb	25133	[mm²]
Bottom reinforcement depth	dsb	680	[mm]

Material properties

Concrete

Characteristic compressive strength	fck	35	[N/mm²]
Design compressive strength	fcd	23,33	[N/mm²]

Reinforcement steel

Yield strength	fyd	435	[N/mm²]

	b_{open}	**0,4**	[m]
	h_{open}	**0,345**	[m]
	h_{fb}	0,355	[m]
	yc_ope	0,0825	[m]
	c.a.	0,460	[m]
	hf (top	0,19	[m]
	bw	0,5138	[m]
	xu	**253,3**	[mm]

ϕduct ≤ bw /8 --> bw,nom = bw

Without shear reinforcement [NEN-EN 1992-1-1]

	A_{sl}	3272	[mm²]	
	d_{sl}	772,5	[mm]	
Check if dp is within the tensile zone			→	Yes (since the moment is negative, dp = h - dp)
	A_p	4500	[mm]	
	d_{eff}	663,93721	[mm]	
	ρ_l	0,0228		
	k_1	0,15		
	$C_{Rd,c}$	0,12		
	σ_{cp}	4,667	< 0,2 f_{cd}	4,666667 N/mm2
	k	1,549	< 2.0	
	v_{min}	1,10	[N/mm²]	
	v_{Rdc}	1,50	[N/mm²]	
	V_{min}	374.947	[N]	u.c. 3,31
	V_{Rdc}	511.692	[N]	u.c. 2,42

With shear reinforcement [NEN-EN 1992-1-1]

Area shear reinforcement	A_{sw}	1256,6	[mm²]	
Stirrup diameter	ϕ_{stir}	20	[mm]	
	s	300	[mm]	
Assumed as z = 0,9 * d_{eff}	z	598	[mm]	
	θ	30	[deg]	
	v1	0,516		
	αcw	1,20		
	$V_{Rd,s}$	1.885.854	[N]	u.c. 0,66
	$V_{Rd,max}$	1.920.755	[N]	u.c. 0,65

The VRd,s using an angle of 39 degrees: 1.344.554 [N] --> 40% increase